राष्ट्र की सेवा में परमाणु
भा प अ कें
BARC
ATOMS IN THE SERVICE OF THE NATION

TECHNOLOGIES FOR
NEW INDIA @ 75
आजादी का अमृत महोत्सव

NLS - 30

DAE-BRNS
National Laser Symposium
(NLS-30)

BOOK OF ABSTRACTS

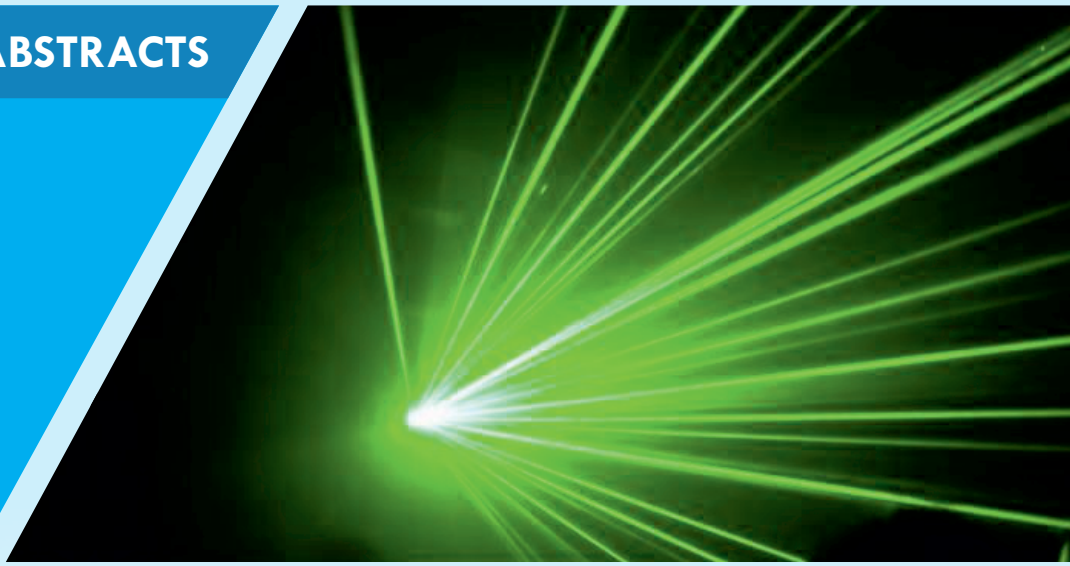

January 19 - 22, 2022

Organized at

Bhabha Atomic Research Centre

Mumbai-400085, Maharashtra, India

DAE – BRNS
National Laser Symposium
NLS - 30

DAE – BRNS
National Laser Symposium
NLS - 30

January 19 – 22, 2022

BOOK OF ABSTRACTS

In collaboration with

Indian Laser Association

Organized by

Bhabha Atomic Research Centre
Department of Atomic Energy
Mumbai – 400085, Maharashtra, India

Published by Bhabha Atomic Research Centre (BARC), Mumbai
Title: DAE-BRNS National Laser Symposium (NLS-30)-Book of Abstracts
Edition : January, 2022
Copies : 150
Pages : 180
Cover-page design : Dr V S Rawat
Printed at : Sharda stationery & Xerox , Govandi, Mumbai - 88
For pivate circulation only
Not to be sale

PREFACE

Symposia undoubtedly are the lifeline of a scientific community where exchange of information, dissemination of knowledge and germination of new ideas takes place. The DAE-BRNS National Laser Symposium (NLS), now three decades old, is one such symposium that binds the laser community in India. The 30th edition of this Symposium i.e. NLS-30 is being organized by the Beam Technology Development Group of Bhabha Atomic Research Centre at the DAE convention Centre, Anushaktinagar, Mumbai during January 19-22, 2022. That it coincides with the celebration of '*Azadi Ka Amrit Mahotsav*' this year brings great cheer. The symposium will be conducted in a hybrid mode with in-person participation of the local delegates and virtual participation by the outstation delegates.

Ever since the NLS was held for the first time at IIT Madras in 1992, it has been growing both in size and stature. Although the pandemic succeeded in casting its shadow, receiving close to two hundred contributory papers and fifteen Ph. D dissertations, speaks volumes of the unabated enthusiasm in the research fraternity.NLS-30 will be inaugurated by Prof. S. Ramakrishnan, Director, Tata Institute of Fundamental Research an academician and astute Condensed Matter Physicist himself. Dr. A. K. Mohanty, Director, Bhabha Atomic Research Centre has kindly agreed to preside over the Inauguration function. Keynote address on "Extreme science with extreme light" will be delivered by Dr. G. Ravindra Kumar, Distinguished Professor and Chair, Department of Nuclear and Atomic Physics, TIFR.
The symposium will have 14 regular scientific sessions besides the concluding session. A total of 25 invited talks will be delivered by researchers drawn from both India and abroad, comprising of a perfect blend of experience and enthusiasm. The contributory papers will be presented topic wise, orally, in parallel sessions spread over three days in addition to being displayed online over the entire duration of the symposium. Thesis presentation and an Industrial session on lasers and related products by industrial representatives will form an important component of the symposium. A special evening talk on the very topical subject "fs light channelling and the laser lightening rod project" is scheduled to be delivered by Dr. Aurelien Houard of Ecole Polytechnique, Paris, France.

The symposium will be preceded by two short tutorial courses, viz., "Laser based measuring instruments: Technology and Applications" and "Photonics materials for lasers, biomedical and sensor applications", that would be conducted online by Indian Laser Association (ILA) on January 17-18, 2022. ILA, like last year, will organize a virtual exhibition of lasers and laser related products during the symposium.

We express our sincere gratitude to all the authors who have enthusiastically responded to our call for submission of papers and all the scientific committee members and reviewers for judging the submitted papers over a short period. Thanks also to all the invited speakers for agreeing to take time out of their busy schedule to participate in NLS-30 and share some of their exciting scientific results.

We also thank all the members of National Advisory Committee and the Symposium Organising Committee for their valuable suggestions, guidance and support. We are

thankful to DAE-BRNS for the financial support and the industrial delegates for their active participation in the Symposium.

On behalf of the Symposium Organising Committee and the Local Organising Committee, we wish all the delegates a very fruitful and inspiring interaction time during NLS-30.

Archana Sharma, Chairperson SOC
Martin Mascarenhas, Co-Chairman
J. Padma Nilaya, Convener
Nitin Kawade, Co-convener
G. Sridhar, Secretary
M. L. shah, Secretary

CONTENTS

NLS – 30 COMMITTEE

NATIONAL ADVISORY COMMITTEE

Vyas K N BARC, Mumbai
Avhanta Venu Gopal, NPL, New Delhi
Bhawalkar D D, Indore
Chaturvedi S, IPT, Gandhinagar
Das B K, IRDE, Dehradun
Grover R B, BRNS, Mumbai
Gupta P D, Indore
Mishra S K, CGCRI Kolkata
Naik P A, BITS-PIlani, Goa
Nakhe S V, RRCAT, Indore
Nath, A. K., IIT, Kharagpur
Nayak J, CHESS, DRDO Hyderabad
Rao D N, UoH, Hyderabad
Mohanty A K, BARC, Mumbai
Ravindra Kumar G, TIFR, Mumbai
Sharma S K, NPCIL, Mumbai
Singh B P, IIT, Mumbai
Som S VECC Kolkata
Sood A K, IISc, Bengaluru
Sriram V K, LEOS, Benguluru
Srivastava H B, LASTEC, Delhi
Vasudeva Rao P R, HBNI Mumbai
Vekat Raman B, IGCAR, Kalpakkam
Vinayak S, SSPL DRDO New Delhi
Sharma Archana, BARC, Mumbai

SYMPOSIUM ORGANIZING COMMITTEE

Sharma Archana, Chairperson
Padma Nilaya J, Convener
Sridhar G, Secretary (Scientific)
Saxena P, General Secretary, ILA
Bindra K S, RRCAT, Indore
Bisht P B, IIT, Chennai
Bhatt R B, AFFF,NRB, Tarapur
Datta A, IIT Mumbai
Datta P K, IIT, Kharagpur
Dalal D K, ATC, BRNS
Dixit S K, RRCAT, Indore
Das S K , G M Univ., Sambalpur
John R, IIT, Hyderabad
Joseph Joby, IIT, Delhi
Khare Alika, IIT, Guwahati
Krishnamurthy, M., TIFR, Mumbai
Kundu S, BARC, Mumbai
Mascarenhas M L, Co-Chairman
Kawade N O, Co-Convener
Shah M L, Secretary (Organizing)
Kundu T, IIT, Mumbai
Majumder S K , RRCAT, Indore
Mishra H, BHU, Varanas
Mishra S R, RRCAT, Indore
Moorthy Babu, S., AU, Chennai
Nakhate S G, BARC, Mumbai
Rapol U D, IISER Pune
Ray A K, BARC, Mumbai
Santhosh C, MIT, Manipal
Sinha Sucharita, BARC, Mumbai
Tata B V R, UoH, Hyderabad
Singh B, RRCAT, Indore
Udupa D, BARC, Mumbai
Vas Dev, BARC, Mumbai

LOCAL ORGANIZING COMMITTEE

Nilaya J P, Convener
Kawade N O, Co - Convener
Sridhar G, Secretary (Scientific)
Shah M L, Secretary (Organizing)
Saxena P, General Secretary, ILA

Agrawal P K, RRCAT, Indore
Agrawalla S K, BARC Mumbai
Baruah S, BARC, Mumbai
Bhale D, BARC, Mumbai
Das D R, BARC, Mumbai
Das R C, BARC, Mumba
Dikshit B, BARC, Mumbai
Ghosh A, BARC, Mumbai
Joshi M J, BARC, Mumbai
Kumar A, BARC, Tarapur
Kundu S, BARC, Mumbai
Mishra K K, BARC, Mumbai
Nayak A S, BARC, Mumbai
Pradhan S, BARC, Mumbai
Prabhala A, BARC, Mumbai
Rana Paramjit, BARC, Mumbai
Rao S, BARC, Mumbai
Rath A D, BARC, Mumbai
Rawat A S, BARC, Mumbai
Rawat V S, BARC, Mumbai
Sahoo A C, BARC, Mumbai
Sahoo S P, BARC, Mumbai
Sahu G K, BARC, Mumbai
Sethi S, BARC, Mumbai
Singh D K, BARC, Mumbai
Shah R, BARC, Mumbai
Thomas J, BARC, Mumbai

SUB COMMITTEE

Scientific	Dr. S G Nakhate Mr. S Kundu
Accounts	Dr. R C Das Dr. A Ghosh
Registration & Reception	Ms. Anupama Prabhala Dr. A Kumar
Publication/Printing	Dr. V S Rawat Dr. S Pradhan
Posters Sessions	Dr. B Dikshit Dr. S. Rao
Technical Exhibition (Ila)	Dr. B Dikshit Dr. S Rao
Transport and Accomodation	Dr. P Rana Sh. S.P Sahoo
Venu Management	Sh. T B Pal Dr. P K Mandal

Web & It Management	Dr. M L Shah Sh. Mandar Joshi
Medical	Sh. K. K. Mishra Dr. A U Seema

SCIENTIFIC PROGRAM SCHEDULE

DAY 1: WEDNESDAY, JANUARY 19, 2022

Session 1	**Inaugural session**	
09:30 – 11:15	**Welcome Address:** Convener, NLS-30 **Presedential Address:** Chairman, NLS-30 and Director, BARC **Chief Guest Address:** Prof. S Ramakrishnan, Director TIFR, Mumbai **ILA Activity:** President, ILA or Director, RRCAT **Keynote :** Dr. G Ravindra Kumar, TIFR, Mumbai "Extreme Science with Extreme Light" Inauguration of industrial exhibition **Vote of Thanks:** Secretary, NLS-30	
11:15 – 12.00	Director's High Tea	
Session 2	**Ultrafast Lasers and Application**	
12:00 – 12:30	Prof. Danailov Miltcho Elettra, Trieste, Italy *"Ultrafast Laser systems at the FERMI Free Electron Laser Facility"*	IT-01
12:30 – 13:00	Dr Kamaraju Natarajan IISER, Kolkata *"Ultrafast electrons and quasiparticles dynamics in photo-excited condensed matter systems probed through femtosecond and THz pulses"*	IT-02
13:00 – 14:00	Lunch break	
Session 3	**Oral Presentation of Paper**	OPP - 1
14:00 – 16:30 (150 Min)	**Parallel Sessions**	OPP-1
16:30 – 16:45	Tea / Coffee break	
Session 4	**Plasmonic and Photonics**	
16:45 – 17:15	Dr. Ravi Pant IISER, Thiruvananthapuram *"Translation ofIR combs fromdeep UV to NIR wavelength region using higher-harmonic generation in a silica nanowire"*	IT-03
17:15 – 17:45	Dr. Nithyanandan IIT Hyderabad *"Recent advances in dissipative soliton dynamics in Ultra-fast fiber laser systems"*	IT-04
17:45 – 18:15	Dr Mool C Gupta University of Verginia *"High Power Laser Applications in Photonic Devices"*	IT-05
18:15 – 19:00	Tea / Coffee break	
19:00 – 20:00 Evening Talk	Dr. Aurelien Houard Insta Paris, Paris "fs light channeling the lightning laser rod"	SET – 1

DAY 2: THURSDAY, JANUARY 20, 2022

Session 5	**Advance Laser Technologies and Applications**	
09:30 – 10:00	Dr B N upadhyaya RRCAT, Indore *"Recent Developments on High Power CW Fiber Lasers at RRCAT"*	IT-06
10:00 – 10:30	Prof. Kazuo Tanaka ELI-NP, Japan *"New scientific landscape with 10 PW (10^{16}W) laser beams at A:I-NP"*	IT-07
10:30 – 11:00	Prof. Sivarama Krishnan IIT Madras *"Photoelectron imaging and multi-coincidence spectroscopy of doped quantum fluid He nanodroplets with extreme ultraviolet photons"*	IT-08
11:00 – 11:15	Tea / Coffee break	
Session 6	**Lasers Materials and Devices**	
11:15 – 11:45	Prof. C Jagadish Australian Nat. Univ., Canberra *"Semiconductor Nanostructures for Optoelectronics Applications"*	IT-09
11:45 – 12:15	Dr. Shobha Shukla IIT Mumbai *"Additive manufacturing of sub-wavelength resolved 2D/3D free standing micro/nanostructures"*	IT-10
12:15 – 12:45	Dr. Jitendra Kumar RRCAT, Indore *"Technology Development and Applications of Fiber Bragg Grating Sensors"*	IT-11
12:45 – 13:30	Lunch break	
Session 7	**Oral Presentation of Paper**	OPP- 2
13:30-16:00 (150 Min)	**Parallel Sessions**	
16:00-16:15	Tea / Coffee break	
Session 8	**Quantum and Atom Optics**	
16:15 – 16:45	Prof. Urbasi Sinha RRI Bangaluru "Photonic Quantum Science and Technologies"	IT-12
16:45 – 17:15	Dr. M V Suryanarayana BARC, Vizag *"Challenges in Atomic Vapor Laser Isotope Separation of Lutetium"*	IT-13
17:15 – 17:45	Dr. S P Ram RRCAT, Indore *"Trapping and Manipulating Cold Atoms Using Magnetic and Laser Fields"*	IT-14
17:45 – 18:00	Tea / Coffee break	
18:00 – 19:00	**ILA General Body Meeting**	

DAY 3: FRIDAY, JANUARY 21, 2022

Session 9	**Laser Spectroscopy and Applications**	
09:30 – 10:00	Prof. Jagdish Singh Mississippi Univ, Starkville, USA *"Laser Induced Breakdown Spectroscopy: Application to Nuclear waste Management"*	IT-15
10:00 – 10:30	Prof. Naresh Patwari IIT, Mumbai *"Intermolecular Coulombic Decay in Molecular Clusters"*	IT-16
10:30 – 11:00	Dr.Anil K Singh BARC, Mumbai *"Enrichment of Isotopes by Laser Isotope Separation (LIS) Technique for Nuclear Medicine"*	IT-17
11:00 – 11:15	Tea / Coffee break	
Session 10	**Laser Based Instrumentation**	
11:15 – 11:45	Prof. Ashis Banerjee Univ Of Washington "Towards Precise Patterning of Microstructures Using Optical Tweezers"	IT – 18
11:45- 12:15	Dr. Naveen K Nischal IIT Patna *"Image Encryption through Structured Light"*	IT – 19
12:15 – 12:45	Dr Amit Rav BARC, Mumbai *"Characterization and Utilization of VISAR in Shock Wave Experiments"*	IT – 20
12:45 – 13:45	Lunch break	
Session 11	**Oral Presentation of Paper**	
13:45 – 16:00 135 Min	**Parallel Sessions**	OPP - 3
16:00 – 16:15	Tea / Coffee break	
16:15 – 17:15	**Industrail Presentations** **6 Speakers**	
17:15 – 17:30	Tea / Coffee break	
Session 12	**Non – Linear Optics**	
17:30 – 18:00	Prof. Pratima Sen DAVV, Indore *"Nonlinear Optics : From infancy to blooming youth"*	IT -21
18: 00 – 18:30	Dr. Someswara Rao BARC, Mumbai *"Development of single mode high repetition rate visible optical parametric oscillators and its spectroscopic application"*	IT - 22

DAY 4: SATURDAY, JANUARY 22, 2022

Session 13	**Thesis Presentations**	
09:00 – 11:30	**Parallel Sessions**	TH – 1 To TH - 15
11:30 – 11:45	Tea / Coffee break	
Session 14	**Applications of Lasers in Chemistry Biology and Materials**	
11:45 – 12:15	Prof. Ranjani Vishwanatha JNCASR Bangaluru *"Magneto-optical Effects in Doped Quantum Dots"*	IT-23
12:00 – 12:30	Dr. Sunita Kedia BARC, Mumbai *"Enhanced Functionality of Metallic Biomaterials using Pulsed Lasers"*	IT-24
12:30 – 13:15	Dr Khageswar Sahu RRCAT, Indore "Antimicrobial Phototherapy: A new frontier in fight against antibiotic resistant bacteria and newly emerging infectious microorganisms"	IT – 25
13:15 – 14:15	Lunch break	
Session 15	**Award and Closing Ceremony**	
14:15 – 15:30	*Award Presentations, Feedback and Vote of thanks*	

KEYNOTE ADDRESS

Extreme Science with Extreme Light

G Ravindra Kumar
Tata Institute of Fundamental Research, Mumbai
grk@tifr.res.in; www.tifr.res.in/~uphill

Our universe is predominantly a hot and dense place, contrary to the gentle environment we experience on the surface of the earth. Stars and their violent explosions in the sky as well as the volcanoes erupting from deep within the earth are ready testimonies to this fact. In recent times, such extreme states containing high energy density have been created and studied in the laboratory focusing 'extreme light' namely, high peak power, ultrashort pulsed laser light, to micron spatial scales. As laser technology marches on inexorably to higher and higher powers, we can expect to simulate such matter better and better in lab experiments and learn more about the complex interactions and dynamics in such systems. At the same time, we can exploit the rich emissions of high energy photons and material particles from such matter to fashion novel, table top sources of radiation for a variety of applications in science, technology and medicine [1 and the references therein].

This talk will attempt to describe some of the physics of dense, hot matter, with reference to experiments performed at TIFR – creation of gigantic magnetic pulses (100s of megagauss), ultrafast plasma dynamics, passage of relativistic electrons through dense, hot matter and its consequences in terms of MeV ion production, ultrafast hard x-ray emission *etc.* [2-8]. The emphasis will be on conveying the broad scope of the field as well as some pointers to the future.

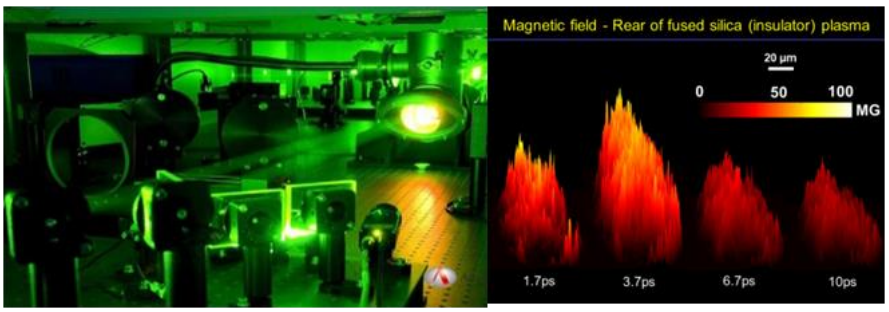

The 150 terawatt, femtosecond laser system at TIFR (Right) A spatially resolved, ultrafast evolution of Megagauss magnetic pulse, measured.

[Gerard Mourou and Donna Strickland won half the Nobel prize in physics in 2018 for the invention of chirped pulse amplification that made ultrahigh power laser, femtosecond laser pulses. The most powerful, ultrashort pulse laser emitting 10 petawatt, 25 femtosecond pulses was inaugurated in Nov 2020 at the 'Extreme Light Infrastructure- Nuclear Physics' in Romania..]

Two dimensional, sub-picosecond motion a plasma created on a solid surface by 25 femtosecond pulse at ~10^{19}Wcm^{-2} (Ref. 7).

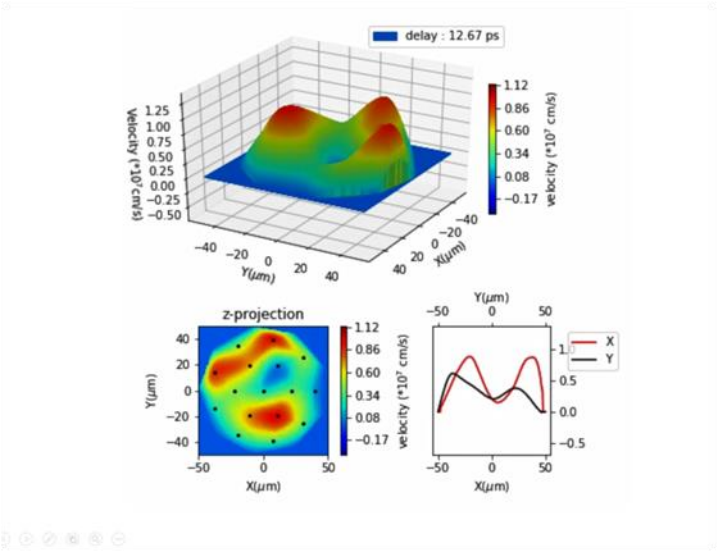

REFERENCES

1. S.V. Bulanov *et al.*, *Plasma Physics Reports*, **2015**, 41, 1
2. G. Chatterjee et al., *Phys. Rev. Lett.* **2012**, 108, 235005
3. M. Shaikh *et al.*, *Phys. Rev. Lett.* **2018**,120, 065001
4. S. Mondal *et al.*, *Proc. Natl. Acad. Sci. (USA)* **2012**, 109, 8011
5. S. Mondal *et al.*, *Phys. Rev. Lett.* **2010**, 105, 105002
6. A. Adak *et al.*, *Phys. Rev.Lett.* **2015**, 114, 115001
7. K. Jana *et al.*, *Phys. Rev. Res.* **2021**, 3, 033034
8. G. Chatterjee *et al.*, *Nat. Commun.* **2017**, 8,15970; A. Das et al., *Phys. Rev. Res.* **2020**, 3, 033405

EVENING TALK

FEMTOSECOND LASER FILAMENTATION IN THE ATMOSPHERE FOR REMOTE LASER APPLICATIONS AND THE LASER LIGHTNING ROD PROJECT

*Aurelien HOUARD, LOA, ENSTA Paris, CNRS, Ecole polytechnique, Institut polytechnique de Paris, 91762 Palaiseau, France,*E-mail: aurelien.houard@ensta-paris.fr at http://llr-fet.eu/*

Abstract: I will discuss different applications based on the formation of intense light strings called laser filament in the atmosphere. In particular I will focus on theLaser Lightning Rod (LLR) project, which aims atinitiatingupward lightning discharges through filamentation of a high-repetition-rate terawatt laser

Laser filamentation is a nonlinear phenomenon observed during propagation of ultrashort laser pulses in transparent media, when their peak power exceeds a critical power (a few Gigawatts in air at 800 nm). It results in the self-contraction of the beam, maintaining a very high intensity in a thin channel of almost constant radius over many Rayleigh lengths, and leaving a plasma channel in the wake of the laser pulse [1]. This spectacular effect can be obtained at a long distance (kilometer range) allowing the future development of numerous remote applications requiring high laser intensity [2]. In the last decade femtosecond filaments has proved to be a powerful tool to control electric discharges in atmospheric air [3], to generate acoustics waves and optical waveguide through hydrodynamic effects [4], to produce supercontinuum in the visible range [5], UV lasing from excited Nitrogen [6] or to create a clear channel for laser telecommunication though fog[7].

.

Fig. 1. Photography of the LLR experiment on Mont Saentis in July 2021.

Controlling lightning is a long-time dream of mankind.Along with the rapid evolution of the laser technologies, the idea to develop lighting protection based on filamentation of high-power ultrashort lasers has recently emerged [8-9]. Started in 2017, the goal of the Laser Lightning Rod (LLR) project is to investigate a new type of lightning protection based on the use of upward lightning discharges initiated through a high-repetition-rate multi-terawatt laser. Funded under the European research program Horizon 2020, the project is a collaboration between LOA, Université de Genève, EPFL, HES-SO, as well as laser company Trumpf Scientific Lasers, and Ariane group [10].

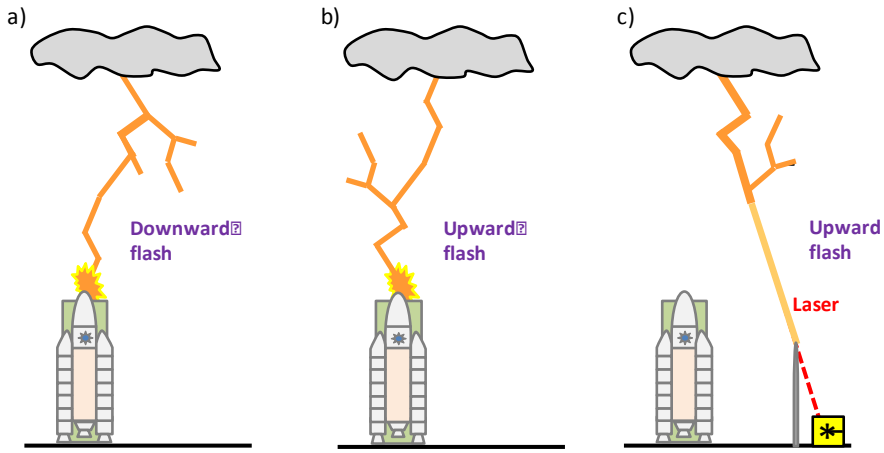

Fig. 2. The laser lightning as a protective device: a) Downward lightning to victim; b) upward lightning; c) upward lightning facilitated by laser filamentation discharges the cloud and protects the potential victim.

The feasibility of the novel technique is based on recent research providing new insights into the mechanism responsible for the guiding of electrical discharges by laser filaments [11], on cutting-edge high power laser technology [12] and on the availability of the uniquely suitable Säntis lightning measurement station in Northeastern Switzerland, located at an altitude of 2 500 meter [13].A low-density channel created by a1 J, 1 kHz, pulsed laser will operate by promoting the initiation of upward discharges to preemptively transfer cloud charges to the ground (see Fig. 2).

In this talk I will review recent developments in the field of femtosecond laser filamentation in the atmosphere, in particular in the frame of the Laser Lightning Rod project [8].

References

[1] A. Couairon, A. Mysyrowicz, "Femtosecond filamentation in transparent media," Physics Reports **441**, 47 (2007).
[2] M. Durand *et al.*, "Kilometer range filamentation," Opt. Express 2**1**, 26836 (2013).
[3] B. Forestier, *et al.*, "Triggering, guiding and deviation of long air spark discharges with femtosecond laser filament," AIP Advances **2**, 012151 (2012).
[4] N. Jhajj, E. W. Rosenthal, R. Birnbaum, J.K. Wahlstrand, and H.M. Milchberg, Demonstration of long-lived high power opticalwaveguides in air, Phys. Rev. X **4**, 011027 (2014).
[5] J. Kasparian *et al.* "White light filaments for atmospheric analysis," Science **301**, 61 (2003).
[6] G. Point, *et al.*, Lasing of ambient air with microjoule pulse energy pumped by a multi terawatt IR femtosecond laser, Opt. Lett. **39**, 1725 (2014)

[7] G. Schimmel, T. Produit, D. Mongin, J. Kasparian, and J.-P. Wolf, « Free space publication laser telecommunication through fog, » Optica **5**, 1338 (2018).
[8] X.M. Zhao, J.C. Diels, C.Y. Wang, and J.M. Elizondo, "Femtosecond ultraviolet laser pulse induced lightning discharges in gases," IEEE J. Quantum Electron. **31**, 599 (1995).
[9] J.-P. Wolf, "Short-pulse lasers for weather control," Reports on Progress in Physics **81**, 026001 (2018).
[10] T. Produit, P. Walch, C. Herkommer, A. Mostajabi, M. Moret, U. Andral, A. Sunjerga, M. Azadifar, Y.-B. André, B. Mahieu, W. Haas, B. Esmiller, G. Fournier, P. Krötz, T. Metzger, K. Michel, A. Mysyrowicz, M. Rubinstein, F. Rachidi, J. Kasparian, J.-P. Wolf, A. Houard, The Laser Lightning Rod project, The European Physical Journal Applied Physics **93**, 10504 (2021).
[11] A. Houard, *et al.* "Study of filamentation with a high power high repetition rate ps laser at 1.03 µm," Opt. Express **24**, 7437 (2016).
[12] C. Herkommer, *et al.*,Ultrafast thin-disk multipass amplifier with 720 mJ operating at kilohertz repetition rate for applications in atmospheric research, Optics Express **28**, 30164 (2020).
[13] A. Mostajabi*et al.*, "Simultaneous records of current and 380-km distant electric field of a bipolar lightning flash," 2017 International Symposium on Lightning Protection (XIV SIPDA), Natal, 2017, pp. 183-187

INVITED TALKS

IT-1. ULTRAFAST LASER SYSTEMS AT THE FERMI FREE ELECTRON LASER FACILITY

Prof. *M.B.Danailov, P.Cinquegrana, A.Demidovich, G.Kurdi, I.Nikolov, P. Sigalotti, P.Susnjar, [1] Elettra-Sincrotrone Trieste, Area Science Park, Trieste, Italy*

An important trend in Extreme UV (EUV) and Soft X-ray Free Electron Laser (FEL) development in the last years has become the use of seeding by an external laser, aimed to improve the coherence and stability of the generated pulses. Based on the High-Gain Harmonic Generation (HGHG) seeding scheme,FERMI was the first FEL facility where external seeding was implemented. The initially planned FERMI wavelength ranges of 40-100 nm in single-cascade (FEL-1) and 10-40 nm in double-cascade fresh-bunch mode (FEL-2) have been largely extended and now the facility provides users with EUV/Soft X-ray tunable light spanning the ranges 17-110 nm (FEL1) and 4-20 nm (FEL2).

There are two main ultrafast laser systems integrated in the free electron laser, namely the photoinjector laser (PIL) and the Seed Laser (SL),both of utmost importance for reaching the desired FEL parameters. The PIL provides deep-UV laser pulses generating the initial electron bunch in a Copper-based photoinjector. The same laser system is also used as a source of the infrared pulses of the Laser Heater (LH) setup used to suppress the growth of micro-bunching instabilities during the acceleration process.

At FERMI the bunch is accelerated to energy of up to 1.5 GeV, compressed to a few-hundred femtoseconds, and then sent to one of the two undulatorchains for generating the desired EUV/Soft-X ray pulses. Instead of starting from incoherent spontaneous emission noise, like in the commonly used at other facilities SASE scheme, the FEL emission is initiated by the well-defined modulation of a pre-bunched electron beam. To obtain this modulation, the accelerated electron bunch interacts with a sufficiently strong seed pulse in a short modulator undulator resonant at the seed pulse wavelength. The resulting electron beam energy modulation is transformed into bunching at the harmonics of the seed wavelength λ by subsequently sending the electron beam through a dispersive section. Finally, the microbunchedelectrons propagate through a chain of radiator undulators tuned at the *n*-th harmonic of the seed wavelength and emit highly coherent FEL pulses at a wavelength λ/n .

In this talk we present the current design and foreseen upgrades of the above mentioned main laser systems. Particular attention is dedicated to the Seed Laser. The originalrelatively simple version of this system has seen continuous development and upgrades to meet the increasing challenges to the quality and flexibility of the seed pulses. Thedevelopment of the unique FERMI pump-probe scheme based on a Seed-laser derived pulse delivered to the end-stations for pump-probe experiments, allowed taking a full advantage of the intrinsic to the seeding scheme tight synchronization of the FEL pulse to the seed. This scheme provided nearly jitter-free pump/probe pulse-pairs and has been anadditional driver for constant improvement and increase of the complexity of the seed laser. We describe the layout of the main system, including details on the HGHG seeding dedicated part. Timing synchronization, online diagnostics and feedbacks are essential for the successful user operation of the facility and

are also briefly addressed. In the last part of the talk we also describe the ongoing upgrade of the seed for implementing a new seeding scheme, namely Echo-Enabled Harmonic Generation (EEHG) which promises further improvement of the FERMI performance, and in particular an advancement of the generated photon energy into the water window.

IT-2. ULTRAFAST ELECTRONS AND QUASIPARTICLES DYNAMICS IN PHOTO-EXCITED CONDENSED MATTER SYSTEMS PROBED THROUGH FEMTOSECOND AND THZ PULSES

Dr. N. Kamaraju, Indian Institute of Science Education Research Kolkata, ***Email****:nkamaraju@iiserkol.ac.in*

Ultrashort pulses with pulse widths of ~50 femtosecond pulses of electromagnetic radiation offer multitude ways to maneuver and also probe the elementary and quasi particle excitations of condensed matter systems. Understanding of the underlying physics upon excitation of femtosecond pulses on a semiconductor for example still is very much important in the development of photonics and spintronics as alternatives to traditional electronics, crossing the boundaries of physics, materials science, and electrical engineering. Here in the talk, I will present some of the recent results from our laboratorydemonstrating this capability to understand the effect of carrier density on the electron-phonon coupling in wide band gap semiconductor nanoparticles and single crystals of topological insulator systems using ultrafast and THz spectroscopies.

IT-3. TRANSLATION OF IR COMBS FROMDEEP UV TO NIR WAVELENGTH REGION USING HIGHER-HARMONIC GENERATION IN A SILICA NANOWIRE

Dr. Ravi Pant, IISER, Thiruvananthapuram, Kerala, India

A frequency comb consists of equally spaced narrow linewidth spectral components. The advent of combs,which have been described as a “newmeasuring stick” [1],has revolutionized the way we measure things, be it time,length, or spectrum of gases. The simple idea of using the spectral response of a pulse train, whichconsists of equally spaced frequencies (frequency comb), for spectroscopy was mootedby Theodor W.Hänsch in late 1970’s [2,3]. However, it took the development of photonic crystal fiber (PCF) [4]and demonstration of an octave spanning supercontinuum that led to the 2005 Nobel Prize winningwork of John L Hall [5] and Theodor W Hänsch in the area of frequency combs [6]. Since then thefield of frequency combs has exploded and theirapplication to frequency metrology [6], optical atomicclocks [7], frequency synthesis [8], femtosecond pulse generation [10], arbitrary waveformgeneration [11] and sensing [12] has beenexplored. Many of these applications require frequency combs in the deep UV to NIR wavelength region. Frequency combs in the visible are typically generated using the mode-locked lasers in the visible wavelength region or through harmonic generation of Ti: Sapphire lasers. These mode-locked lasers are typically bulky, require cooling and have

a large footprint. Applications such as single photon spectroscopy [13], quantum memories will benefit from low power visible combs in a compact platform.

In this talk, we present a brief overview of frequency combs and their applications. Limitations in realizing compact frequency combs in the visiblewavelength region are discussed. We presentthe simultaneous generation of frequency combs at 260 nm (deep UV), 520 nm (visible), and NIR (780 nm) through second-, third and sixth-harmonic generation of a 1560 nm mode-locked laser in a 10 mm long silica nanowire [14]. We discuss the role of dispersion engineering for phase matching the pump mode to higher-order modes at the harmonic frequencies and pulse compression in the nanowire for enhancing the efficiency of the harmonic generation. Even though silica does not have even-order nonlinearities due to its centrosymmetric nature, second-harmonic generation has been observed in silica fibers and nanowires due to the surface induced nonlinearities and the photogalvanic effect, and in periodically poled silica fibers. We exploit second- and third-harmonic generation in a silica nanowire of diameter ~ 900 nm to achieve translation of 1560 nm frequency combs to NIR and visible. The deep UV signal is obtained using the second-harmonic generation of the third-harmonic signal. The work allows single-photon spectroscopy of gases and single ions using a compact platform that enables trapping of atoms and molecules in the evanescent field of the nanowire for enhanced light-matter interaction.

References:

1. https://www.nobelprize.org/uploads/2018/06/popular-physicsprize2005.pdf
2. Phys. Rev. Lett. 38, 760–764 (1977).
3. Phys. Rev. Lett. 40, 847–850 (1978).
4. Science 299, 358-362 (2003).
5. Science Vol. 288, 635-639 (2000).
6. Nature 416 (6877), 233(2002).
7. Reviews of Modern Physics 87, 637-701 (2015).
8. Physical Review Letters 84, 5102-5105 (2000). presented.

IT-4. RECENT ADVANCES IN DISSIPATIVE SOLITON DYNAMICS IN ULTRAFAST FIBER LASER SYSTEMS

Dr. Nithyanandan Kanagaraj, IITHyderabad, Kandi - 502284

The talk would be broadly divided into two parts aimed at attracting both the novice as well as the experienced laser scientists. In the first phase, I would introduce to the broader audience the concept of dissipative soliton and the ultrafast fiber laser systems. I wouldparticularly highlight the associated nonlinear dynamics of the propagating laser pulse in the cavity and convince why the fiber laser is an elegant testbed to explore many novel complex yet intriguing nonlinear dynamics. While discussing, I also review and highlight the few of the classical NLD in fiber laser systems. In the second phase of the talk, I would introduce some of the ultrafast measurement techniques with a particular emphasize on the dispersive Fourier Transform (DFT) technique and its unique capabilities in the real-time shot-to-shot characterization. Moving on, I will briefly review our recent results on dissipative soliton dynamics in ultrafast fiber laser systems, aimed at bringing parallel to the famous concept of matter-soliton analogy. A soliton is a pulsed waveform that maintains its shape as it travels. If multiple solitons travel in a medium, their mutual attraction can cause them to form bound states that can be seen as “molecules.” Courtesy to ultrafast real-time characterization, I explain our discoveries of complex soliton molecular complexesshowin in the **Fig.1** and also resolve both

temporally and spectrally the build-up ofsome complex pattern formation in the fiber lasers system, such as chaotic pulse bunches, noise-like pulses, rogue waves, soliton liquid, soliton gases etc. Finally, I summarize the talk with some of the applications along with the ongoing research and the potential future scope going forwardin this exciting field.

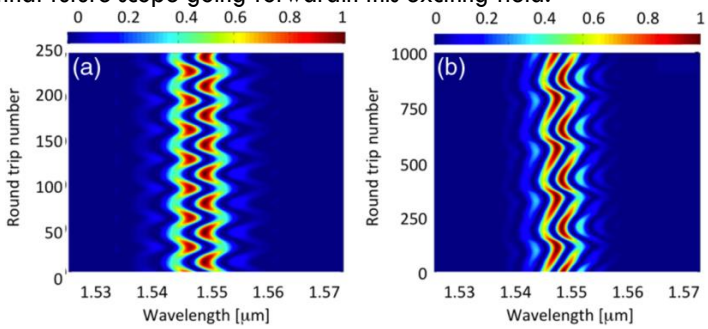

(a) Vibrating Soliton Molecule **(b)** Evolving Phase Soliton molecule

Figure. 1 *Internal motion in bi-soliton molecule.*

References

1. *Ph. Grelu and N. Akhmediev, Nat. Photonics 6, 84 (2012).*
2. *K. Kurupa, K. Nithyanandan, Andra, PT.Dinda, P. Grelu, PRL. 118, 243901 (2017).*
3. *ZQ Wang, K Nithyanandan, A Coillet, P Tchofo-Dinda, P Grelu, Nature communications 10 (1), 1-11 (2019)*
4. *K Krupa, K Nithyanandan, P Grelu Optica 4 (10), 1239-1244 (2017)*

IT-5. HIGH POWER LASER APPLICATIONS IN PHOTONIC DEVICES

Dr. Mool C Gupta, Department of Electrical & Computer Engr., University of Virginia, Charlottesville, VA 22904

Introduction : Lasers are attractive for photonic devices as they provide energy through a non-contact process, the beam can be focused to microns in size, energy can be provided continuously, or in pulse mode, the light wavelength can be tuned to a specific material requirement, and they can generate high energy density for heating, melting and ablation. Lasers have been used for the fabrication of photonic devices such as photovoltaic, thermo photovoltaic, photodetectors, focal plane arrays, micro-optical components, etc. Lasers can be used for direct laser patterning, sintering of nano/micro particles for thin films, thermal annealing, crystallization, surface microtexturing for controlling light absorption and reflection, etc. Lasers are also being investigated for use in the advanced manufacturing of photonic devices such as solar cells. Next, we provide some specific examples of laser applications in photonic devices.

Lasers in photovoltaics: A large number of research papers have been published on the use of high-power lasers for the fabrication of photovoltaic devices [1]. The use of lasers has been pursued in the fabrication of light trapping structures, surface passivation, doping, crystallization, patterning, thermal annealing, and controlling the surface light emission for solar cell devices [2,3]. Figure 1 shows a scanning electron microscope (SEM) image of a laser microtextured silicon surface. The microtexture can be used for efficient light trapping to enhance light absorption for photovoltaic devices and thermophotovoltaic devices. The laser microtextured surface can also be used to control the water wetting properties allowing the fabrication of superhydrophobic surfaces [4,5]. High power lasers have also been used for

patterning of interdigitated back contact heterojunction solar cells, and crystallization of amorphous silicon for tunnel oxide passivated contact TOPCon solar cells.

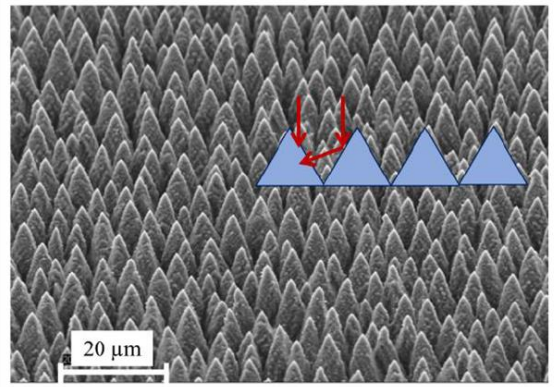

Fig. 1. SEM image of laser microtextured silicon surface for light trapping [Reprinted from ref. [6], with permission from Wiley, Progress in Photovoltaics Research].

Lasers in photodetection and imaging: High power lasers can be used to sinter nano/micro articles to form thin films of semiconductor materials like Ge, SiGe, and PbSe, etc., [7,8]. Ge thin films can be used to fabricate near-infrared detectors, and PbSe thin films are used for mid-infrared detection. Figure 2 shows a cross-section of PbSe thin film fabricated by the laser sintering process. Similarly, Ge [9] and SiGe [10] thin films were fabricated by a laser sintering process. SiGe thin film was used for high-temperature thermoelectric applications. The laser sintering method allows the fabrication of thick (several microns) polycrystalline semiconductor films on various substrates.

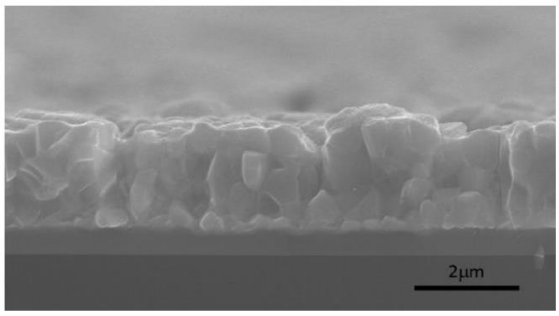

Fig. 2. SEM cross section image of laser sintered PbSe thin film [Reprinted from reference [7], with permission from Elsevier, Journal of Alloys & Compounds].

Lasers for micro-optical component fabrication

High power lasers can be used to fabricate planar optical lens using the optical diffraction phenomena. Optical diffraction gratings can also be written on various substrates using a direct laser writing process. Figure 3 shows a scanning electron microscope image of a photon sieve fabricated by laser ablation of 50 nm silver thin film on a glass substrate. The laser ablation was carried out using a 50 ns pulse width Nd: YAG fiber laser. The focal length of the lens was 40 cm, and the full width at half maximum (FWHM) of the focused spot was 45 microns. The lasers of wavelength 1064 nm from a fiber laser were focused to a spot diameter of

approximately 35 μ m. Laser ablation can be used to fabricate microlenses and diffraction gratings on various substrates. Both planoconvex and planoconcave lenses have been fabricated using a laser ablation process.

In summary, we show various applications of high-power lasers for photonic device fabrication, such as photovoltaics, photodetectors, micro-optical components, etc.

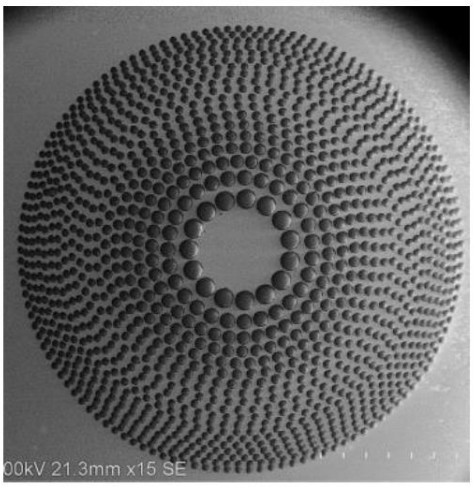

Fig. 3. SEM image of laser fabricated photon sieve [Reprinted from reference [11], Optics Express].

V. References

1. M. C. Gupta, "Laser-Induced Surface Modification for Photovoltaic Device Applications," Handbook of Laser Micro-and Nano-Engineering, pg. 829-856, Springer, 2020. (Book chapter)
2. M. C. Gupta, L. V. Zhigilei, M. He, Z. Sun "Generation and Annealing of Crystalline Disorder in Laser Processing of Silicon," Handbook of Laser Micro-and Nano-Engineering, pg. 797-827, Springer, 2020. (Book chapter)
3. M. C. Gupta and D. E. Carlson. Laser Processing of Materials for Renewable Energy Applications. MRS Energy & Sustainability, 2, 2015 (Invited review article).
4. A. Chakraborty, A. T. Mulroney, and M. C. Gupta, Superhydrophobic Surfaces by Microtexturing: A Critical Review, Reviews of Adhesion and Adhesives, 9, 35-64 (2021). (Review article).
5. M. C. Gupta, A. Mulroney, Ice Adhesion and Anti-Icing Using Microtextured Surfaces, Ice Adhesion: Mechanism, Measurement, and Mitigation, Chapter 13, 389-415, Wiley, 2020. (Book chapter).
6. B. K. Nayak, V. V. Iyengar, and M. C. Gupta, "Efficient Light Trapping in Silicon Solar Cells by Ultrafast-laser-induced Self-assembled Micro/nano Structures", Progress in Photovoltaics: Research and Applications, Vol.19, 631-639 (2011).
7. Joel T. Harrison, Elisa Pantoja, Moon-Hyung Jang, Mool C. Gupta, Laser Sintered PbSe Semiconductor Thin Films for Mid-IR Applications using Nanocrystals, 849, 156537 (2020).
8. M. C. Gupta, J. T. Harrison, and M. T. Islam, Photoconductive PbSe Thin Films for Infrared Imaging, Materials Advances, Royal Society of Chemistry (RSC) Materials Advances, 2, 3133-3160 (2021) (Invited review article).

9. Md. T. Islam and M. C. Gupta, Synthesis, Structural, Optical, and Electrical Properties of Continuous Wave and Pulse Laser Sintered Thick Ge Films, Semiconductor Science and Technology, (under review).
10. K. Xie, and M. C. Gupta, High-Temperature Thermoelectric Energy Conversion Devices Using Si- Ge Thick Films Prepared by Laser Sintering of Nano/Micro Particles, IEEE Transactions on Electron Devices, 67, 2113-2119 (2020).
11. M. N. Julian, D. G. MacDonnell, and M. C. Gupta, Fabrication of Photon Sieves by Laser Ablation and Optical Properties, Optics Express, Vol. 25, pp. 31528-31538, (2017).

IT-6. RECENT DEVELOPMENTS ON HIGH POWER CW FIBER LASERS AT RRCAT

Dr. B N Upadhyaya, Laser Technology Division, Raja Ramanna Centre for Advanced Technology, Indore, India, ***E-mail:*** *bnand@rrcat.gov.in*

Monolithic fiber lasers are the state-of-the-art of new generation solid state lasers and are now well established for industrial, medical and defence applications. Fiber lasers offer several advantages over bulk solid state lasers such as efficient heat dissipation due to large surface area to volume ratio, higher conversion efficiency, diffraction-limited beam quality, long life of maintenance free operation and no risk of misalignment due to in-built fiber Bragg grating mirrors. High power continuous wave (CW) fiber lasers with multi-kW output power and nearly diffracted-limited beam quality have been reported by several researchers worldwide[1-3]. Laser configurations used for generation of high output power from fiber lasers are: (a) oscillator configuration, (b) master oscillator power amplifier (MOPA) configuration, and (c) amplification of seed signal from laser diodes[4]. Generation of high power CW and pulsed output from fiber lasers is done by pumping with high power laser diodes and splicing the gain fiber with different fiber laser components together. Although it seems to be an easy task, but, there are several technological challenges in the development of high power fiber lasers. Selection of fiber laser components is a critical issue in development of monolithic fiber laser systems,which includes selection of high power fiber coupled pump diode and its wavelength, compatible input pump fibers, high power handling pump combiner, doped fiber core and inner clad size and fiber Bragg gratings.Major challenges faced in high power fiber laser development are minimization of splice loss, selection of pump configuration, reliable recoating at different splice joints, removal of leakage pump power, and efficient removal of heat load from thin polymer coated double-clad fibers. Several physical phenomena such as self-pulsing, fiber fuse effect, transverse mode instabilities, optical damage, photodarkening, stimulated Raman scattering (SRS), stimulated Brillouin scattering (SBS), self-phase modulation (SPM) and four wave mixing (FWM) also pose limitations in the generation of high output power from fiber lasers[4].

In view of increasing applications of high power fiber lasers, Raja Ramanna Centre for Advanced Technology (RRCAT) is also pursuing research and development on high power Yb-doped, Er-doped, Er:Yb co-doped and Tm-doped CW and pulsed fiber lasers since past several years. In this direction, development of up to 1kW of single transverse mode monolithic Yb-doped CW fiber laser at 1080 nm, 100 W of CW output power at eye-safe wavelength of 1940 nm from Tm-doped fiber and50 W of Er-doped CW fiber laser at 1600 nm has been carried out. Figure 1(a) shows a schematic of in-house developed monolithic 1kW single transverse mode Yb-doped CW fiber laser at 1080 nm and Fig. 1(b) variation of output power as a function of input pump power showing a slope efficiency of ~74.4%. An engineered

version of 500 W of Yb-doped CW fiber laser based on indigenously developed fiber laser engine has also been developed for cutting, welding and laser additive manufacturing applications and is being utilized for these applications[5-6].

Thulium-doped fiber lasers (TDFL) provide emission in the wavelength region of 1850-2100 nm, and are known as 'eye-safe' due to high absorption of this wavelength region in water, which prevents damage of retina. Laser generation at 1940 nm wavelength is particularly important due to water absorption peak at 1940 nm and water being main constituent of biological tissues results in strong absorption and substantial heating of small areas of biological tissues. Lasers at 1940 nm have become ideal source for surgical procedures since very precise cutting of biological tissues can be achieved and bleeding during the process of laser cutting is also suppressed by coagulation. Tm-doped fibers can be easily pumped using readily available 793 nm laser diodes, but due to higher quantum defect, theoretical limit for efficiency is ~41%. However, due to cross-relaxation process, two excited Tm-ions can be obtained for one pump photon and much higher efficiencies as compared to theoretical value can be achieved. In this direction, development of more than 100 W of CW output power at 1940 nm from an all-fiber oscillator configuration has been carried out with an optical-to-optical conversion efficiency of ~45%.

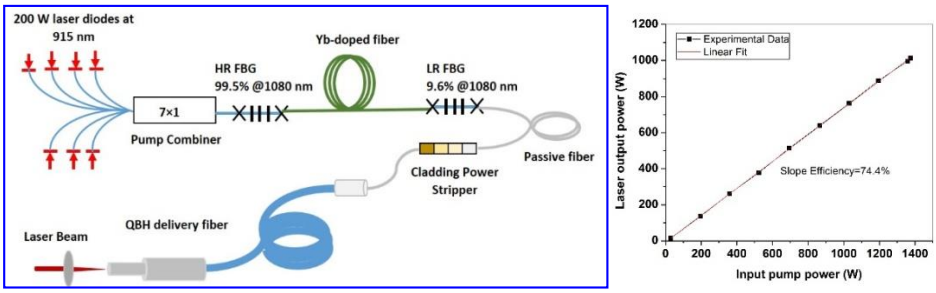

(a) *(b)*

Fig. 1: (a) Schematic of in-house developed monolithic 1 kW single transverse mode Yb-doped CW fiber laser, and (b) variation of laser output power vs input pump power.

Further, Er-doped fiber (EDF) lasers emitting in the spectral range of 1500-1700 nm are attractive for many applications including free space communication, LIDAR, sensing, target illumination, directed energy, etc. Generation of high output power from EDF laser is challenging due to higher quantum defect and lower allowable Er^{3+}-ion concentration in EDF to avoid clustering effects, which results in manufacturing of less efficient double-clad fibers. Out of the several approaches used to increase the laser efficiency near 1550 nm wavelength, the simplest and the most efficient approach is clad-pumping of EDFswith commercially available low cost 976 nm pump diodes. In this direction, development of 50 W of CW output power from an all-fiber Yb-free EDF laser using master oscillator power amplifier (MOPA) configuration by pumping with 976 nm pump diodes with a slope efficiency of ~24% has been carried out. This talk will cover details of development of different high power CW fiber lasers at RRCAT along with challenges and limitations encountered during these developments.

Acknowledgements: Author is thankful to Shri S. V. Nakhe, Director, RRCAT, Dr. K. S. Bindra, Head, Laser Technology Division and all the team members of Industrial Lasers & Applications Lab, RRCAT for their continuous support and encouragement for fiber laser development activity at RRCAT.

References:

1. URL: <http://www.ipgphotonics.com>.
2. Wang et al., *Proc. of SPIE* 11260, Fiber Lasers XVII: Technology and systems, 1126022 (2020).
3. Baolai Yang et al., *Laser Phys. Lett.*, 15, 075106 (2018).
4. Michalis N. Zervas and Christophe A. Codemard, *IEEE J. of Selected Topics in Quantum. Electron.*, 20, 0904123 (2014).
5. Pushkar Misra et al., *DAE-BRNS National Laser Symposium (NLS-27)*, Dec. 3-6, 2018 Indore, India.
6. Avdhesh Kumar et al., *DAE-BRNS National Laser Symposium (NLS-29)*, 12-15 Feb. 2021, Indore, India.

IT-7. NEW SCIENTIFIC LANDSCAPE WITH 10 PW (10^{16} W) LASER BEAMS AT ELI-NP

Prof. Kazuo Tanaka, ELI-NP, cientific Director, ELI-NPReatorului No. 30, Magurele-Bucharest, 077125 Romania

After ESFRI (The European Strategy Forum on Research Infrastructure) selected a proposal of creating the state of art laser-based institutes in Romania, Hungary and Czech, the construction fund had been received in 2012 and ELI-NP has started the entire construction of the institute since then as one of the three ELI pillars.

ELI-NP (Extreme Light Infrastructure: Nuclear Physics), located at 10km south of Bucharest in Romania, has concentrated on the implementation of 2 beams of 10 PW (230J output energy with 23 fsec laser pulse width) and is successful for the implementation. Recent live performance on Nov. 17, 2020 demonstrated the 10 PW laser shots for 10 minutes every 1 minute witnessed by 230 Zoom participants from all over the world with also the presence of Prof G Mourou and Prof D Strickland, the Nobel Laureate in 2018.

Commissioning experiments have already started at 100 TW and 1 PW laser output experimental stations. The commissioning experiments were intended to test the laser system performance and our readiness to conduct the experiments. The successful electron acceleration results show a good control of electron spectra up to 300 MeV either with a mono energetic or broad band spectra. Further upgrade of this electron acceleration is being conducted at 1 PW laser output. Series of commissioning experiments are planned such as measuring the maximum energies of electrons and ions accelerated using various acceleration schemes such as laser wake field acceleration and testing a new plasma mirror scheme using thin liquid crysital foil.

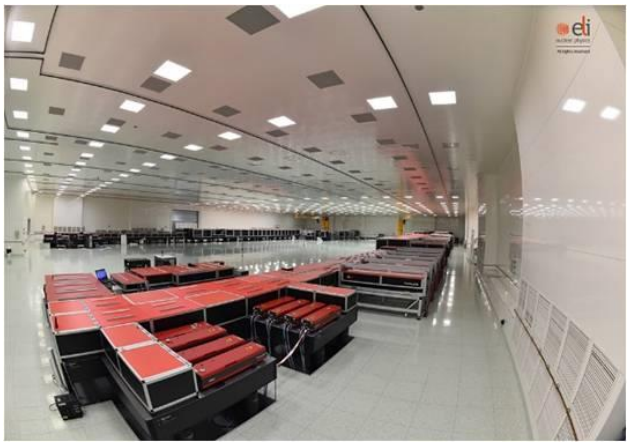

Figure 1 High power laser system that can deliver 100 TW, 1PW, and 10 PW at 2 laser arms sit in 100x70m clean room

Then user experiments will follow the commissioning. The users from all over the world may be able to submit their proposals soon in 2022. 78 letters of intent (preliminary version of the proposal) have been submitted already at the first user workshop in 2019. The proposals will be scientifically evaluated by the third party committee for the allocation of the laser machine times.

The 10 PW experimental stations will be activated soonin 2022 and will be available for the user experiments in 2023. The user access has been tested with the early and commissioning experiments and will be formulated coherently with the IMPULSE project guided by ELI-DC. The IMPULSE project is considered to be a ramp up of the three ELI pillars to become virtually connected laser institute in Europe.

Reference

Current Status and Highlights of the ELI-NP Research Program, KA Tanaka, KM Spohr, D Balabanski, S Balascuta, L Capponi, M Cernaianu, M Cuciuc, A Cucoanes, I Dancus, A Dhal, B Diaconescu, D Doria, P Genuche, D Ghita, S Kisyov, V Nasgtasa, F Ong, F Rotaru, D Sangwan, P-A Sonderstrom, D Stutman, G Suliman, O Tesieanu, L Tudor, N Tsoneva, C Ur, D Ursescu, and NV Zamfir, Matter and Rad. Extrems, **5**, 024402 (2020).

IT-8. PHOTOELECTRON IMAGING AND MULTI-COINCIDENCE SPECTROSCOPY OF DOPED QUANTUM FLUID HE NANODROPLETS WITH EXTREME ULTRAVIOLET PHOTONS

Sivarama Krishnan[1], Suddhasattwa Mandal[2], Vandana Sharma[3], and Marcel Mudrich [1]Department of Physics and QuCenDiEM group, Indian Institute of Technology Madras, Chennai 600036, India , [2]Department of Physics, Indian Institute of Science Education and Research, Pune 411008, India, [3]Department of Physics, Indian Institute of Technology Hyderabad, Kandi, Telangana 502285, India, 4 Department of Physics and Astronomy, Aarhus University, 8000 Aarhus C, Denmark., *Email:srkrishnan@iitm.ac.in*

The In this talk we will present results from our set of research campaigns over the last few years to study atomic aggregates in quantum fluid He nanodroplets by EUV photoelectron and photoion imaging using synchrotrons and free-electron laser pulses. The unique place of He nanodroplets as personal nanocryostats for small atomic systems embedded in or attached to them is well justified by the studies. Not only does this provide an opportunities to cool and form aggregates of dopant atoms of molecules, the He host itself upon electronic excitation turns out be an important player in the quantum dynamics that ensues. From process such as Penning- and charge-transfer ionization of dopants in He nanodroplets to correlated dynamics in the form of inter-atomic Coulomb decay (ICD) and electron transfer mediated decay (ETMD), this system serves as a versatile candidate for investigations of quantum dynamics of few and many particle quantum systems. We will motivate this by sharing the results of our recent and ongoing experiments on this system at the Elettra synchrotron in a coherent international collaboration.

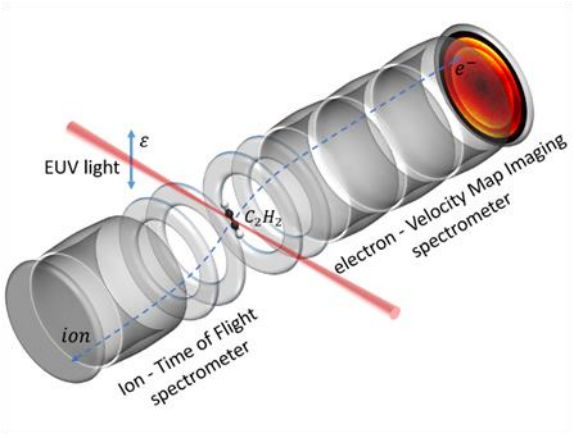

Figure 1Velocity map imaging (VMI) to image photoelectrons with simultaneous coincidence measurement of photoion spectrometry: This spectrometer along with the data acquisition system tags each photoelectron with its parent ion(s). Photoelectrons are projected from the volume where the target beam with doped He nanodroplets interacts with EUV photons onto a position sensitive detector – which is a microchannel plate (MCP) with a delay line anode. The arrival of the photoelectron at the detector starts the clock setting the zero of time for measuring the time of flight of a parent photoion in the ion – time of flight spectrometer operated in tandem

Keywords: Helium nanodroplets, quantum fluid, extreme ultraviolet spectroscopy, synchrotrons, electron-ion coincidence spectroscopy, Penning ionization, interatomic Coulombic decay, electron-transfer mediated decay..

IT-9. SEMICONDUCTOR NANOSTRUCTURES FOR OPTOELECTRONICS APPLICATIONS

Professor Chennupati Jagadish, AC, MNAE, (US), FAA, FTSE, FTWAS, FNAI, FNA, NAE, FASc, FAPAS, FEurASc, FNASc, Research School of Physics, The Australian National University, Canberra, ACT 2601, Australia, Email: c.jagadish@ieee.org

Semiconductors have played an important role in the development of information and communications technology, solar cells, solid state lighting. Nanowires are considered as building blocks for the next generation electronics and optoelectronics. In this talk, I will present the results on optoelectronic devices such as lasers/LEDs, photodetectors and Neuro-electrodes. Future prospects of the semiconductor nanowires will be discussed.

IT-10. ADDITIVE MANUFACTURING OF SUB-WAVELENGTH RESOLVED 2D/3D FREE STANDING MICRO/NANOSTRUCTURES

*Dr. Shobha Shukla, Nanostructures Engineering and Modeling Laboratory, Department of Metallurgical Engineering and Materials Science, Indian Institute of Technology Bombay, Mumbai 400076, MH, India, [2]Nanostructures Engineering and Modeling Laboratory, Department of Metallurgical Engineering and Materials Science, Indian Institute of Technology Bombay-Monash Research Academy, Mumbai 400076, MH, India, *sshukla@iitb.ac.in*

Abstract

Active/passive polymeric micro/nanostructures with predefined architecture and functional attributes have been explored towards specific applications, and have resulted in rapid progress of several technologies including fields like nanophotonics [1,2], anticounter feiting [3], plasmonics [4] and metamaterials [5] among others. Fabrication offunctional structures are achieved *via* doping active ingredients such as magnetic /plasmonic nanoparticles/precursors, carbon/semiconductor nanomaterials, dyes etc. to the photocurable resin used for polymerization. Additive manufacturing technologies such as continuous liquid interface production, stereo-lithography, digital light processing and two-photon lithography are implemented towards realization of these structures for rapid prototyping. Further, these technologies offer controllable chemical, mechanical, and optical properties of the final construct. Two-photon lithography is preferred over other techniques due to its unmatched precision and capability to generate sub-wavelength resolved three-dimensionalstructures in a single exposure step.

Two-photon lithography is based on non-linear laser-matter interaction to induce photo-polymerization. Such phenomenaare dependent on the square of the intensity of illumination and higher-order susceptibilities of the materials. Such excitations are achieved only in spatially localized volumes, limited to the focal plane of the specimen by spatiotemporal compression of photons in the material. These excitations when applied to photopolymers, enable pin-point polymerization within the focal volume and result in the generation of basic building blocks know as voxels. These polymerized voxels exhibit volumes of the order of few femto-liters; and by traversing the sample/focal point, a series of such voxels are added to generate a micro/nanostructure with predefined structural attribute. The photo-patternable resins used here, are transparent to the illumination wavelength, and hence the regions outside the focal plane remain unaffected, resulting in sub-diffraction limited resolutions. Due to its capabilities of generation of sub-wavelength resolved three-dimensional constructs in single-exposure step, this technique has witnessed rapid progress over last two decades. However, limited availability of two-photon active resins has introduced a bottleneck in growth of this technology. Design, synthesis and formulationof such resins involve complex and time-consuming

processes, so there is a need to develop a material system with good non-linear activity and efficient two-photon polymerization sensitivity.

In this pursuit, we have formulated a two-photon polymerizable resin, wherein we have implemented two-photon active carbon dots as a photo initiator, and demonstrated fabrication of optically active structures with resolutions as good as 250 nm using a 800 nm excitation.[6]. Systematic studies and the characterization of the fabricated structures revealed that resin as well as the polymerized structures exhibits good non-linear activity. Furthermore, the emissive properties of the carbon dots have been exploited towards non-invasive characterization of the polymerized structures via fluorescent imaging with high contrast. The printing performances were found to be at par with the state of the art linewidths reported in this field. Combining the structural resolution and the printing performance, we can state that the formulated resinis expected to facilitate the growth of this technology to its true potential.

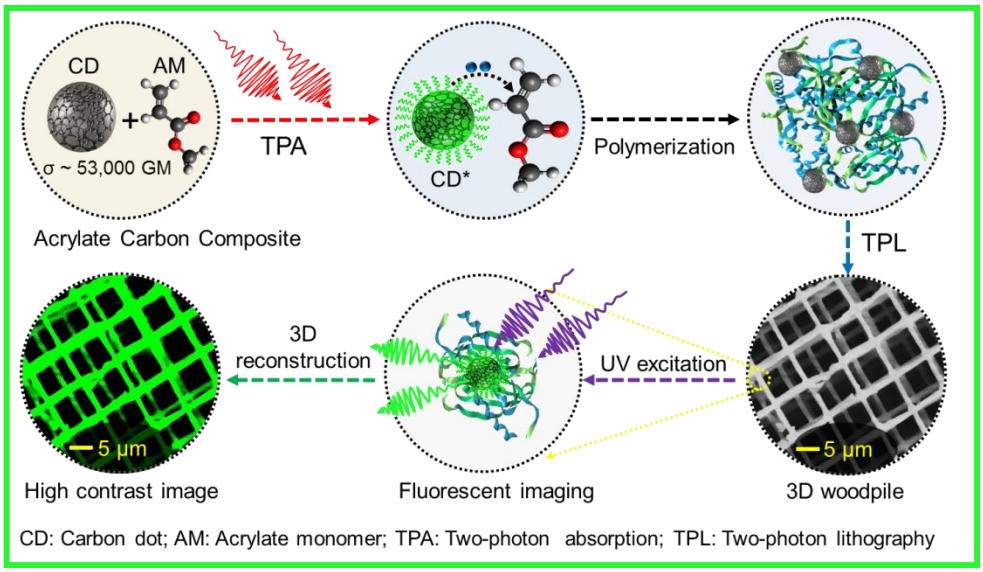

Figure 1: Schematice representation of quantum dots sensitized photopolymeric systems. Jaiswal et al ACS Nano 2021[6]

Refernces:

[1] R. P. Chaudhary, A. Jaiswal, G. Ummethala, S. R. Hawal, S. Saxena, S. Shukla, *Addit. Manuf.***2017**, *16*, 30.

[2] G. Ummethala, A. Jaiswal, R. P. Chaudhary, S. Hawal, S. Saxena, S. Shukla, *Polymer (Guildf).***2017**, *117*, 364.

[3] "Two-photon Lithography of Cloaked Fluorescent Microstructures for Anti-counterfeiting Applications," can be found under https://www.osapublishing.org/abstract.cfm?uri=LAC-2021-JTu1A.49, **n.d.**

[4] R. P. Chaudhary, G. Ummethala, A. Jaiswal, S. Hawal, S. Saxena, S. Shukla, *RSC Adv.***2016**, *6*, 113457.

[5] A. Jaiswal, S. Rani, G. P. Singh, M. Hassan, A. Nasrin, V. G. Gomes, S. Saxena, S. Shukla, *Mater. Today Phys.***2021**, *20*, 100434.

[6] A. Jaiswal, S. Rani, G. P. Singh, M. Hassan, A. Nasrin, V. G. Gomes, S. Saxena, S. Shukla, *ACS Nano***2021**, acsnano.1c01083.

IT-11. TECHNOLOGY DEVELOPMENT AND APPLICATIONS OF FIBER BRAGG GRATING SENSORS

Dr. Jitendra Kumar, Fibre Grating Lab, Fibre Sensors and Optical Spectroscopy Section, Raja Ramanna Centre for Advanced Technology, Indore,E-mail: jkmadaan@rrcat.gov.in

Fiber Bragg grating (FBG) sensors are one of the most exciting developments in the field of sensors in recent years. FBG sensors have a number of distinguishing advantages over conventional fiber or non-fiber sensors. This includes high spatial resolution, single point as well as distributed sensing capabilities, high sensitivity, fast response time, accessing the difficult & remote locations and capability to work in harsh environment including high EMI (electromagnetic interference). The conventional temperature or strain sensors in high EMI, nuclear radiation, chemical and industrial environment are likely to malfunction, transform or drift, in long run due to intense interaction with extreme environment. In such difficult situations, FBG sensors provide an alternative approach for measurement of different parameters including temperature, strain, pressure, vibrations, force etc. FBG sensors prove to be one of the most promising candidates for fibre-optic smart structures.FBG represents a periodic modulation of the refractive index (RI) in a fiber core over a fixed length. This RI modulation is imprinted in photosensitive fiber core by exposing it to the CW/ns pulses UV interference pattern or by fs pulses (IR & UV) in non-photosensitive fiber, of submicron period. The pitch, strength of RI modulation and grating length decide the spectral and reflection/transmission characteristics of a FBG.In RRCAT, a FBG fabrication facility is established. It is based on highly coherent, high repetition rate (~ 5.6 kHz) UV pulses at 255 nm, obtained from second harmonic (SH) of copper vapour laser (CVL). FBGs, fabricated using this facility, have been successfully tested for various applications, like temperature sensing, strain sensing, chemical sensing etc. The facility is being used for various in-house research and development work. The facility is also available to Indian industries and research institutes through incubation centre RRCAT (IC-RRCAT) for customised FBG fabrication on chargeable basis.This talk presents the design, development and deployment of FBG sensors for a few challenging applications such as temperature measurement in acidic & high radiation and high EMI environments and strain measurement in Indian railway safety equipment. FBG sensors are developed for temperature measurements and characterized for online monitoring in the nuclear fuel recycling unit of the Fuel Fabrication (FF) -Integrated Nuclear Recycle Plant (INRP) at BARC, Tarapur. The conventional thermocouple, used in a microwave furnace, locally distorts the electromagnetic field, conduct heat away from the sample, induce temperature instabilities and microwave breakdown resulting in arcing. This may leads to serious measurement errors. So, the challenges for the temperature sensor include capability to operate at high microwave power (~ 6 kW), high radiation field at the sensor location (~ 200 mR/h), high temperature (800 °C) with measurement accuracy (±1°C) and acidic environment (HNO_3). Reliable and accurate temperature measurement helped to precisely control the process and to avoid the spill over of Uranium, Plutonium Nitrate solution in the microwave heated process chamber. RRCAT fabricated FBG has been successfully used by M/s Lab to Market, IIScBengaluru for the development of 'Wheel Impact Load Detection (WILD)' system pertaining to Railway safety. The whole system consisted of FBGs fixed on the side of railways track and online FBG strain monitoring system (located in the control room) as the train travels on the track. The wheel deformation i.e. flat wheel led to change in the strain pattern as experienced by the FBG. Different level of wheel flatness led to different strain response as recoded by FBGs. This is very important development pertaining to railway safety. It is anticipated that FBG sensor systems will be widely commercialized and applied in the near future due to the maturity of

economical production of FBGs and the availability of cost effective interrogation system and multiplexing technique.

IT-12. PHOTONIC QUANTUM SCIENCE AND TECHNOLOGIES

 *Dr. Urbasi Sinha, RRI, Bangaluru*

Quantum mechanics is a cornerstone of modern physics. Just as the 19th century was called the Machine Age and the 20th century the Information Age, the 21st century promises to go down in history as the Quantum Age. Quantum Computing promises unprecedented speed in solving certain classes of problems while Quantum Cryptography promises unconditional security in communications. In this talk, I will discuss the world of single and entangled photons and also discuss ongoing work towards quantum computing, quantum information and quantum cryptography in our Quantum Information and Computing lab at the Raman Research Institute, Bengaluru.

I will end with our broad vision for the future, which includes establishment of long distance secure quantum communications in India and beyond involving satellite based, fibre based as well as integrated photonics based approaches towards the global quantum internet.

http://www.rri.res.in/quic/

IT-13. CHALLENGES IN ATOMIC VAPOR LASER ISOTOPE SEPARATION OF LUTETIUM

 *Dr. M V Suryanarayana, Bhabha Atomic Research Centre, Visakhapatnam, Andhra Pradesh, India, email: suryam@barc.gov.in*

Abstract: Atomic Vapor Laser Separation of Lanthanides is more complex than actinides due to small isotope shifts, atomic hyperfine structure and number of constituent isotopes. This necessitates utilization of narrow-band lasers, tighter control of Doppler broadening. All the atomic and system parameters have strong influence on the degree of enrichment and production rates. Thus arriving at optimum conditions through experimental work would be a long and arduous task. It is possible to accurately describe laser-atom interactions in a multi-step photoionization process through density-matrix formalism. Through appropriate modelling, it is possible to understand the laser-atom interactions in the realistic laser isotope separation scenario and predict degree of enrichment and production rate with variation in the system parameters. This is illustrated with an example of ^{177}Lu laser isotope separation.

Introduction: Invention of lasers in 1960 has brought new possibilities in atomic spectroscopy. Its unique features such high monochromaticity and intensity allowed researchers to study subtle variations in the atomic spectra of various isotopes of the same element. Most of the studies during 1970-80 were oriented towards understanding origin of such variations in the atomic spectra. It has also been realised during this period that it is possible to efficiently separate

isotopes of the same element using these subtle variations in the atomic spectra through multi-step photoionization process using lasers. Due to its foreseeable application in the separation of actinides (primarily Uranium and Plutonium) a lot time, energy, funds were invested on developing the basic building blocks such as high energy-high repetition rate pulsed tunable lasers and large scale evaporators for the separation of actinides in gas phase. These initiatives led to a new field known as Atomic Vapor Laser Isotope Separation (AVLIS). Two well known laboratories Lawrence Livermore National Laboratory, USA and Kurchatov Institute, Russia have made considerable progress in successful demonstration of large scale separation of minor isotope of Uranium. The technology developed during this period had also been used for the separation Plutonium isotope.
Apart from the actinides, there is also a requirement of separation of isotopes in other areas. For example ^{169}Yb (produced by irradiation of enriched ^{168}Yb) is found to be highly useful for thin metal industrial gamma radiography. In medicine, there is also a requirement for the production of carrier free medical isotopes for in-situ cancer therapy. Among the several medical isotopes used for cancer therapy, ^{177}Lu has unique properties. This radioisotope is produced by the irradiation of ^{176}Lu parent isotope. ^{177}Lu radioactive isotope thus produced has a half-life of 6.65 days and decays to ^{177}Hf through medium energy □-decay. The daughter nuclide ^{177}Hf decays by producing low energy □-photons. Since the characteristics being very ideal for therapeutics and diagnostics (known as theranostic property), ^{177}Lu isotope is in high demand.

^{177}Lu medical isotope can be produced by neutron irradiation in a nuclear reactor of either enriched ^{176}Yb (Yb-route) or enriched ^{176}Lu (Lu-route). Lu-route is a preferred choice due to high thermal neutron absorption cross section of ^{176}Lu (□ = 2090 b) over ^{176}Yb (□ =2.85 b). Kurchatov Institute, Russia has extensively worked on the enrichment of Lu and Yb isotopes. Vast majority of the chelating agents can be used when the isotopic purity of ^{177}Lu exceeds 60% which is important for the treatment of several types of tumours.
Unlike laser isotope separation of actinides, isotope separation of lanthanides is extremely complex. Among them primary reasons are the isotope shift and hyperfine spectrum. Isotope shift of an atomic transition is influenced by both field shift (arises due to size and shape of nuclei) and mass shift (arises due to mass difference). Unlike the case of actinides, lanthanides have small field and mass shifts resulting in small isotope shifts. Since lanthanum being an odd nuclei, the constituent isotopes lanthanum have complex atomic hyperfine spectrum. This necessitates utilization of narrow-band lasers, tighter control of Doppler broadening of atomic systems. Further; power, pulse width, delay between pulses, atomic number densities all influence the degree of enrichment and production rates of the AVLIS process. However it is nearly impossible arrive at optimum conditions for achieving high efficiency and selectivity of the isotope process as all the system parameters have complex interplay.
We have developed a quantum mechanical model which accurately describes laser-atom interactions in the realistic system environment for the laser isotope separation process. Such methods have been successfully employed by the other laboratories in deriving optimum process conditions.

It is possible to produce carrier free ^{177}Lu through AVLIS process wherein first the natural Lu is irradiated in a thermal reactor followed by isotope separation of ^{177}Lu from the irradiated isotope mixture (^{175}Lu, ^{176}Lu, ^{177}Lu and ^{177m}Lu) . In this presentation, effect of atomic and system parameters on the laser isotope separation of ^{177}Lu isotope will be discussed.

IT-14. TRAPPING AND MANIPULATING COLD ATOMS USING MAGNETIC AND LASER FIELDS

Dr. S P Ram, RRCAT, Indore, Email: spram@rrcat.gov.in

Trapping[1-5] of cold atoms is useful for several applications starting from precision measurements to achieving the real manifestation of quantum mechanics *i.e.* Bose-Einstein condensation. Though the atoms are neutral, the Zeeman effect due to magnetic field and the AC-Stark effect due to laser fields experienced by atoms are being exploited to trap them. In this talk, trapping of laser cooled atoms using magnetic, radio-frequency (rf), optical fields will be discussed.

In the magnetic trap front, trapping of atoms using quadrupole trap and quadrupole Ioffe configuration (QUIC) trap will be discussed. A recently proposed method to trap and manipulate atoms using rf-dressed traps, which are generated by superposition of static and time varying magnetic field (rf field), will also be presented. The rf-dressed traps are able to generate some novel trapping geometries such as double well, ring, arc, etc. Time averaged adiabatic potential traps (TAAP) further extend the capability of rf-dressed traps. Various trapping geometries for ^{87}Rb atoms investigated using the TAAP scheme will be presented.

Further, in the optical dipole trap (ODT) front, the loading of ^{87}Rb atoms in a trap generated by a focused laser beam output will be discussed. In the presence of the ODT beam, the energy levels of the atoms get modified due to AC-Stark shift. This results in a modification in the absorption cross section due a probe beam. The relevance of AC-Stark shift in the optical dipole trap to measure the number of atoms using absorption probe imaging in the ODT will be brought out.

References:

1. S. R. Mishra, S. P. Ram, S. K. Tiwari and H. S. Rawat, *Pramana-J. Phys.* **88**, 59 (2017).
2. S. P. Ram, S. R. Mishra, S. K. Tiwari, and H. S. Rawat, *J. Korean Phys. Soc.,* **65**, 462 (2014).
3. S. Sarkar, S. P. Ram, V. B. Tiwari and S. R. Mishra, *Eur. Phys. J. D*, **75**, 281 (2021) and references therein.
4. A. Chakraborty, S. R. Mishra, S. P. Ram, S. K. Tiwari, and H. S. Rawat, *J. Phys. B: At., Mol. Opt. Phys.,* **49**, 075304 (2016).
5. K. Bhardwaj, S. P. Ram, S. Singh, V. B. Tiwari and S. R. Mishra, *Physica Scripta*, **96**, 015405 (2021) and references therein.

IT-15. FIBER LASER INDUCED BREAKDOWN SPECTROSCOPY: APPLICATION TO NUCLEAR WASTE MANAGEMENT

Dr. Jagdish P. Singh,Seong Yong Oh,Krishna K.Ayyalasomayajula and Fang Yu Yueh, Institute for Clean Energy Technology and Department of Physics and Astronomy, MississippiStateUniversity, Starkville, MS39759, USA, *E-mail: jagdishpsingh@gmail.com*

Laser induced breakdown spectroscopy (LIBS) is the spectroscopic method which analyzes the elemental composition in a laser-produced plasma plume which is produced by a focused high pulse energy laser beam[1].Strong electric field of laser pulse and pulse-duration induce the ablation, atomization, ionization and excitation of the sample. The spectral information which reflects the existence of the characteristic atom in the sample can be obtained from these optical emission spectra. LIBS is suitable for rapid on-line elemental analysis of any material phase and has proved its value in obtaining analytical atomic emission spectra directly from solid, liquid, and gaseous samples.LIBS is a fast qualitative analysis technique that has been used on a variety of samples such as polluted soils, Mars surface, alloy, glass, explosive, tissues, etc. In some solid samples, LIBS has demonstrated an accuracy of 3-6% for elements with a concentration greater than 1 wt% and an accuracy of 5-10% or better for minor elements depending on their concentration.

Recently, LIBS technique has been popular because of its intrinsic advantages and the significant developments of instrument (broadband spectrometer with high resolution and intensified charge coupled device). Conjugation with the optical fiber, minimal sample preparation, and quick on-line elemental analysis are the distinguishable marks of the LIBS probe, which make it practicable to apply in the inaccessible place.

Vitrification of liquid radioactive wastes is an essential task in nuclear industries, facilitating the safe handling and long-term storage of radioactive waste.Analytic tools are necessary for analyzing the sludge prior to and during the vitrification process of the liquid radioactive wastes. The LIBS technique has been applied for the analysis of glass, glass melts and glass batch. The aim of this paper is to explore the possibility of applying LIBS as a remote and the near real-time analytical tool that can be used to analyze liquid radioactive wastes during the vitrification process.The main issues to be resolved with LIBS analysis of liquid samples are poor detection sensitivity and precision. Because water can quench the laser plasma and suppresses the LIBS signal, poor sensitivity may result. Large standard deviations for LIBS liquid data are due to the laser induced shock wave caused turbulence on the liquid surface. Slurry samples contain a large amount of water and large particle sizes. The effects of water content and particle sizes on LIBS measurement will also need to be studied to determine best data analysis method. To evaluate the figure of merit of direct slurry measurement with LIBS, two DWPF simulant slurry samples with different acid levels from SRNL were used in the study. The test results with these slurry samples showed that the splattering and surface cavitationresult in large signal fluctuation.To improve LIBS' reproducibility and detection limits for slurry measurements, various experimental parameters which can affect LIBS' analytical figure of merit were studied. The study has shown that by using the appropriate slurry sample handling systems, optimum experimental parameters and some data processing techniques,reasonable accuracy and precision for the major elements can be achieved. However, further work on improving signal sensitivity and data reproducibility is needed.

This paper examines the experimental conditions associated with the laser induced breakdown spectroscopy (LIBS) analysis of slurriesto achieve better measurement precision. Various experimental configurations and sampling methods were tested. We found that using a pickup lens to direct couple the signal to the optical fiber aligned 45° with laser beam can improve LIBS signal about 5-10 times as compared to the standard backward detection method.Sample preparation procedures that can produce same thickness of samples for analysis have been developed based on a spin coating method. For this method, a drop of slurry was placed on the glass substrate. The slurry is then coated on the substrate via a spin coater machine. The thickness of the sample layered on the substrates is dependent upon the weight, original water content in the sample and the type of substrates. Different substrates for the sample preparation method have been evaluated. It was determined the double-sided tape attached to a glass slide gave reproducible thickness for the samples and LIBS results without

contribution/ interference from the glass substrate. Four calibration samples and an unknown were prepared by adjusting the base simulant composition for SRS Tank 8F sludge simulant. LIBS data of the calibration sample were taken to develop a calibration curve for specific slurry constituents such as Fe, Al, Ni, Ca, and Si. Various data processing techniques have been evaluated to develop these calibration curves. The concentration of the various elements from the unknown are measured and compared with inductively coupled plasma (ICP) data to evaluate the quantitative measurement capability of the LIBS techniques.

References:

Laser Induced Breakdown Spectroscopy, Edited by Jagdish P Singh and Surya N Thakur, Elsevier, 2020.

IT-16. INTERMOLECULAR COULOMBIC DECAY IN MOLECULAR CLUSTERS

Namitha Brijit Bejoy and G. Naresh Patwari, Department of Chemistry Indian Institute of Technology Bombay, Mumbai 400076 India, E-mail: naresh@chem.iitb.ac.in

Intermolecular coulombic decay (ICD) is an efficient and fast charge migration process following the ionization of the inner electrons.[1] The ICD process can be described with respect to a hetero-dimer A···B interacting via intermolecular forces (such as hydrogen bonding) as the following. If the adiabatic ionization energy (AIE) of A is greater than that of B, and if the ionization of A is achieved, the electron ejection occurs from B instead of the initially excited (ionized) molecule A.[2] The excess energy, which is the difference between the AIEs of A and B, can lead to doubly ionizing B or fragmentation of B and other reactive pathways. The ICD process, as described above, is much more efficient than the excitation energy transfer process as the acceptor state lies in the continuum. It has been recently reported that the ICD processes can be relevant in a number of chemical and biological systems interacting with a variety of radiation sources.[3]

The hydrogen-bonded complexes of 2,6-difluorophenylacetylene (DFPHA) with dimethylamine (DMA) and trimethylamine (TMA) were investigated using one-colour resonant two photon process with 4.43 eV photons, with excitation centred on the $S_0 \rightarrow S_1$ electronic transition of DFPHA. In this particular case, the AIE of DFPHA (9.11 eV) is higher than the two-photon energy of 8.86 eV. However, the hydrogen-bonded partners of DFPHA, the DMA and TMA have AIEs of 8.32 and 7.82 eV, respectively, which is lower than experimentally available energy of 8.86 eV. Even though the resonant two-photon excitation is centred on the DFPHA chromophore, results in the formation of DMA/TMA cations. The infrared spectra recorded using IR-UV double-resonance spectroscopic method, while monitoring the DMA/TMA cation channel, indicates formation of hydrogen-bonded complexes, which is shown in Figure 1.[4]

Further, the amine cations were created following resonantly enhanced ionization of the binary complex with the excitation based on the DFPHA chromophore. The amine cations were collected using ion-optics which focused the ions on to a microchannel plate (MCP) detector coupled to a phosphor screen. The voltages on the lenses were adjusted such that the fragments with the same recoil velocity in the plane perpendicular to the flight direction are focused to the same point on the detector. The entire ion cloud was selectively detected by applying an 80 ns voltage pulse to the MCP detector and the ensuing secondary electrons scintillate on the phosphor screen which was recorded by a CMOS camera. The images of amine cations were

acquired both in the raw (20,000 laser shots) and centroiding (50,000 laser shots) modes and were Quadrant symmetrized. Abel inversion was carried out by Basis Set Expansion method (BASEX)[5] to extract the kinetic energy spectrum of the fragment kinetic energy distribution of the fragment ions (both DMA and TMA cations).

Using combination of spectroscopic and ion imaging techniques, the ICD process following resonant two-photon excitation of weak hydrogen-bonded complexes of fluorophenylacetylene and alkyl amines at modest energies (around 4.4 eV) was demonstrated. Significantly, the kinetic energy release was found to be independent of the initial geometry as the structural isomers converge on to the same asymptote. The present set of experiments demonstrate that the presence of chromophores that absorb in the near UV region can under appropriate conditions result in the ICD process, and are likely to be relevant in the biological milieu in addition to the production of secondary electrons.

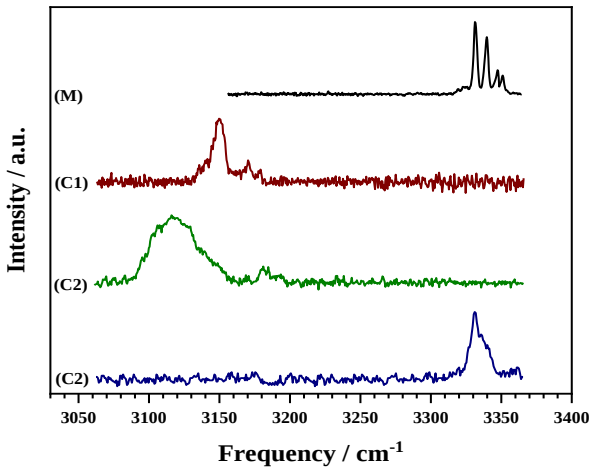

Figure 1. *IR-UV double resonance spectra of the DFPHA monomer (M) and its complexes DMA (C1) and TMA (C2 and C3). Based on these spectra, the structures of the complexes have been assigned to hydrogen bonding.*

.References

1 T. Jahnke, U. Hergenhahn, B. Winter, R. Dörner, U. Frühling, P. V Demekhin, K. Gokhberg, L. S. Cederbaum, A. Ehresmann, A. Knie and A. Dreuw, Interatomic and Intermolecular Coulombic Decay, *Chem. Rev.*, 2020, **120**, 11295–11369.

2 A. C. LaForge, M. Shcherbinin, F. Stienkemeier, R. Richter, R. Moshammer, T. Pfeifer and M. Mudrich, Highly efficient double ionization of mixed alkali dimers by intermolecular Coulombic decay, *Nat. Phys.*, 2019, **15**, 247–250.

3 B. Boudaïffa, P. Cloutier, D. Hunting, M. A. Huels and L. Sanche, Resonant formation of DNA strand breaks by low-energy (3 to 20 eV) electrons, *Science* 2000, **287**, 1658–1660.

4 S. I. Mondal, A. Dey, S. Sen, G. N. Patwari and D. Ghosh, Spectroscopic and ab initio investigation of 2,6-difluorophenylacetylene–amine complexes: coexistence of C–H···N and lone-pair···π complexes and intermolecular coulombic decay, *Phys. Chem. Chem. Phys.*, 2015, **17**, 434–443.

5 S. Marggi Poullain, D. V. Chicharro, J. González-Vázquez, L. Rubio-Lago and L. Bañares, A velocity map imaging study of the photodissociation of the methyl iodide cation, *Phys. Chem. Chem. Phys.*, 2017, **19**, 7886–7896.

IT-17. ENRICHMENT OF ISOTOPES BY LASER ISOTOPE SEPARATION (LIS) TECHNIQUE FOR NUCLEAR MEDICINE

Dr. A K Singh, BARC, Mumbai Email: anilks@barc.gov.in

The Nuclear medicine has grown worldwide during last few decades and playing important role in diagnostic and therapeutic applications. These are specialized medicines containing small quantity of radioisotopes. To meet specific performance of the nuclear medicine, high enrichment of radioisotopes is needed. There exist various techniques for enrichment of isotopes depending upon their properties.

One of the techniques used for enrichment is Laser Isotope Separation (LIS) which offers very high separation factor, and thus high enrichment in comparison to other techniques, in a single step. In addition to high selectivity, this technique has potential to enrich middle isotope of an element having many isotopes. LIS process utilizes the small difference in energy levels of different isotopes for selective photo-ionization of desired isotope through multistep photo-excitation process. Thereafter, the generated photo-ions are collected on suitable collector plates using electric field. A LIS facility can be broadly divided into two parts namely– (i) Laser facility & (ii) vapor generation, photo-ionization & processing facility. Laser facility is heart of any LIS facility which requires to meet several stringent characteristics to get targeted enrichment level with efficient utilization of atomic vapor. For example, laser must have high average power, precise wavelengths, high pulse repetition rate (several kHz), short pulse duration (comparable or shorter than the lifetime of the energy levels involved), narrow linewidth, excellent wavelength and linewidth stability, good beam quality etc. All these properties along with high efficiency are easily obtained in the pulsed dye lasers which make them an attractive for the LIS process. Therefore, we have developed narrow linewdith dye laser facility with the aim to demonstrate enrichment of stable isotopes which are used as precursors for medical radioisotopes.

We have targeted enrichment of ^{176}Yb and ^{176}Lu isotopes which are used as precursor to produce radioisotope ^{177}Lu. ^{177}Lu is one of the most important isotopes which is playing pivotal role in therapeutic application and its applications are growing with time. ^{177}Lu is produced by neutron activation of either highly enriched ^{176}Lu (≥60%) or ^{176}Yb (≥95%) in nuclear reactors. ^{177}Lu production by irradiating ^{176}Lu and ^{176}Yb are known as direct and indirect route, respectively. Both the routes have their own merits and demerits. Direct route of ^{177}Lu production offers high yield with low specific activity. On the other hand, indirect route produces no carrier added (NCA) ^{177}Lu which has very high specific activity. However, this route has low yield of ^{177}Lu production due to poor neutron absorption cross-section of ^{176}Yb isotope. In addition, enrichment of ^{168}Yb and^{174}Yb isotopes are being also targeted because it can be done in the same enrichment facility used for ^{176}Yb by simply changing wavelengths and power levels. Also, these isotopes are used as precursors for producing ^{169}Yb and ^{175}Yb which also find application in nuclear medicine. ^{169}Yb, apart from being used in nuclear medicine is also widely used in industry for non-destructive testing (NDT).

Recently, we have demonstrated enrichment of ^{176}Yb, ^{174}Yb and ^{168}Yb isotopes up to ~97.8% , ~98.5% and ~15% respectively from their natural abundances of ~12.76%, ~31.8% and ~0.13% using LIS process. The achieved throughput for these enriched isotopes are 6 mg/hr, 3.5 mg/hr and 0.04 mg/hr, respectively. Development of lasers and spectroscopic

investigation for enrichment of ^{176}Lu using in house developed photoionization scheme have been also completed. Characterization of Lutetium atomic vapor source is under progress.

In this talk, some of our results related to development of laser facility for LIS along with enrichment results on^{176}Yb, ^{174}Yb and ^{168}Yb will be presented. In addition, spectroscopy investigation results on ^{176}Lu will also be presented. At the end, future perspective of our LIS program for enrichment of medical isotopes will be briefly summarized.

IT-18. TOWARDS PRECISE PATTERNING OF MICROSTRUCTURES USING OPTICAL TWEEZERS

Prof. Ashis Barerjee, University of Washington, Washington

Optical (laser) tweezers provide precise multiplexing capabilities at the micro scale with independent control of up to a hundred objects in three dimensions using a dynamically reconfigurable hologram. It also provides tremendous versatility in terms of the types of objects that can be trapped, moved, and positioned in a stable manner. However, much of its use has been limited to concurrent manipulation of just a few objects for biophysical studies or directed assembly of simple structures using manual or tele-operated control.

In this talk, I will present some recent advances in developing real-time imaging, modeling, and planning methods for automated patterning of microstructures comprising colloidal particles or cells. Specifically, a combination of traditional edge and contour detection methods and state-of the-art deep learning-based semantic segmentation methods is designed to detect heterogeneous objects that may be aggregated together. A stochastic Langevin dynamics model is developed to estimate the states (locations) of the detected objects, which are then fed to a hybrid framework consisting of the D* Lite algorithm layered on top of a model predictive controller to plan stable and collision-free trajectories of the objects.

Experiments with silica and polystyrene beads of varying sizes and human endothelial cells in a variety of fluid media show promising performances. The patterned microstructures are expected to form the building blocks of engineered tissues or granular media with enhanced functional.

IT-19. IMAGE ENCRYPTION THROUGH STRUCTURED LIGHT

Dr. Naveen K. Nishchal, Department of Physics, Indian Institute of Technology Patna, Bihta, Patna-801 106, INDIA, E-mail: nkn@iitp.ac.in

With the technological advancementlots of information/data is being generated, stored, and disseminated, which requires an efficient cryptosystemto protect them from unauthorized uses/access. Digital securitytechniques are already in use but they are being further researched considering improvement in terms of speed, robustness, and reliability. Optical technologies for security are being simultaneously developedutilizing the inherent features of optics such as high speed and parallel processing. Off late, the developed techniques have attracted increased attention of researchers. The pioneering work on optical encryption technique referred to as double random phase encoding was reported in 1995. The technique was proved vulnerable

due to involved linearity in the process. To overcome the weakness, optical asymmetric schemes have been reported, in which the encoded spectrum is amplitude- and phase-truncated. The amplitude-truncated part is stored as *decryption key* and phase-truncated part is further encoded and the process is repeated. In this process, different keys are used for encryption (*encryption keys*) and during the encryption process, '*decryption keys*' are generated. The *encryption keys* are not required for retrieval of original image/data. With the use of *decryption keys* and following the decryption process retrieves the original image/data. In order to further strengthen the technique, phase retrieval algorithm isapplied for generating phase-only functions to be used as keys. Further, an optical asymmetric encryption scheme based on generation of vector beams with non-uniform arbitrary polarization distribution has been proposed. It uses vector beam generator employing modified phase retrieval algorithm for controlling the phase of the generated vector beam. Stokes polarimetry of the generated vector beam is carried out to obtain the ciphertext and one of the keys. The encryption process can be achieved optically, while the decryption can be carried out numerically. This paper presents a review of the literature on the topic with emphasis on work carried out at IIT Patna.

References:

1. P. Kumar, A. Fatima, and N. K. Nishchal, "Arbitrary vector beam encoding using single modulation for information security for information security applications,"IEEE Photon. Technol. Lett.**33** (2021) 243-246.
2. N. K. Nishchal, *Optical Cryptosystems*, IOP Publishing Ltd., Bristol, UK (2019).
3. P. Kumar, A. Fatima, and N. K. Nishchal, "Image encryption using phase-encoded exclusive-OR operations with incoherent illumination,"J. Opt.**21**(2019) 065701.
4. P. Kumar and N. K. Nishchal, "Enhanced exclusive-OR and quick response code-based image encryption through incoherent illumination,"Appl. Opt.**58** (2019) 1408-1412.
5. A. Kumar and N. K. Nishchal, "Quick response code and interference-based optical asymmetric cryptosystem,"J. Inform. Sec. Appl.**45** (2019) 35-43.
6. A. Fatima and N. K. Nishchal, "Image authentication using vector beam with sparse phase information," J. Opt. Soc. Am. A**35** (2018) 1053-1062.

IT-20. CHARACTERIZATION AND UTILIZATION OF VISAR IN SHOCK WAVE EXPERIMENTS

Dr. Amit Rav, Applied Physics Division, BARC, Mumbai, E-mail: amitrav@barc.gov.in,

Non-contact type measurement techniques in shock wave experiments has added advantage. These techniques do not disturb the initial condition of the sample and mainly provide the complete history of the measurement. They are largly optical based techniques and measure either reflected laser light from the target surface as used in velocity interferometers or shock luminescence/emission spectrum of the target as used in radiation pyrometery. Particle/free surface velocity measurement during shock experiment is very important and it provids information about Hugoniot Eleastic Limit (HEL), Shock rise time, phase transition under compression as well as in relaxation etc. With the advent of lasers, many interferometric methods, such as VISAR[1], Febry-Perot[2], PDV[3] etc., have been developed to measure the velocity of fast moving surfaces. In prsent talk discussion will be on the laser based velocity interferometer where the measurement of time resolved Doppler shift of the laser light reflected from the free surface of the shock loaded target is used to estimate the target velocity. The Velocity Interferometer System for Any Reflector (VISAR) is one of the popular

velocity interferometer, characterization of its recording system and some measureements in shock wave experiments will be discussed.

VISAR is essentially a modified Michelson interferometer which measures the differential Doppler shift as a function of time by beating two light signals, reflected from moving free surface of the target material, at two different instants of time separated by a small time interval of order of a fraction of nanosecond to few nanoseconds. Schematic of the instrument as developed in our labortory is presented in Fig 1. As displayed in figure the defused reflected laser light from the target is divided in two different parts. One of the parts is delayed by placing optical slab/etalon while the other part is allowed to interfere without delay. The time resolved beat frequency is then utilized to deduce the free surface velocity history. The typical free surface velocities in plate impact experiments using gas guns could range from few hundred m/s to few km/s with corresponding strain rates generated in the target material ranging from ~ 10^4/s to ~ 10^8/s. The target free surface reaches such high velocities within a fraction of microseconds requiring not only the proper optimization of interferometer design parameters but also fast linear detectors and oscilloscopes. VISAR detects this transient in target free surface velocity from rest to peak by recroding shift in fringes.

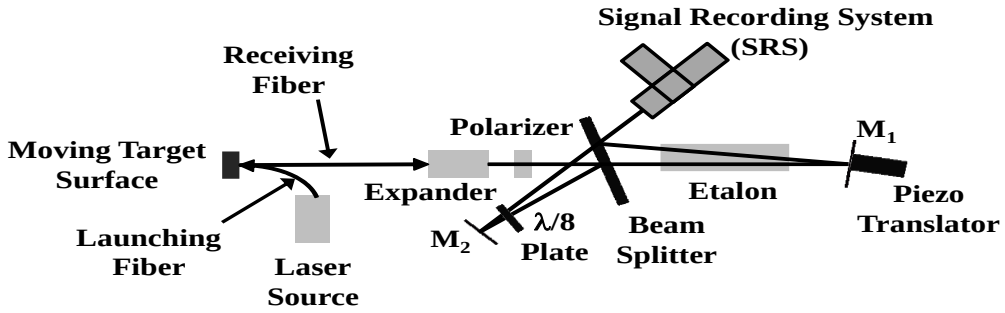

Fig. 1: Schematic of VISAR developed at our lab

These shifts in fringes are converted into measurable sinusoidal electrical signal using SRS[4] which consists of input aperture, imaging optics, photo detector (PMT in present case), load resistance (50 Ω) and high speed recording oscilloscope (DSO). Linear operation of PMT is important to determine amplitude and inturn phase information of the recorded signal accurately so as to estimate velocity of the moving surface with minimum errors.

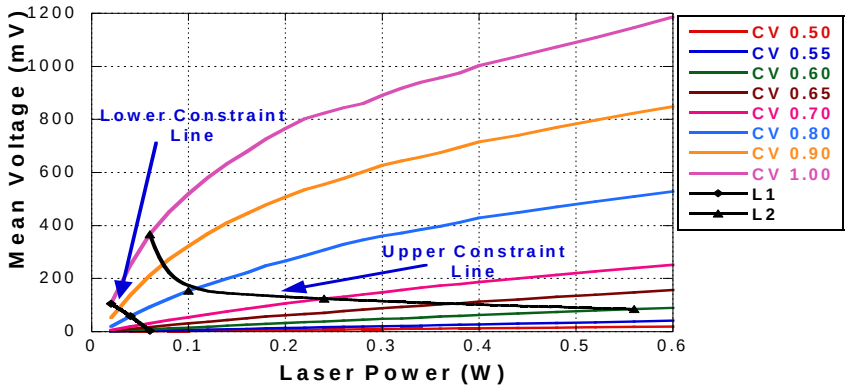

Figure 2: Measured mean output voltage with respect to input laser power at different gain setting of PMT

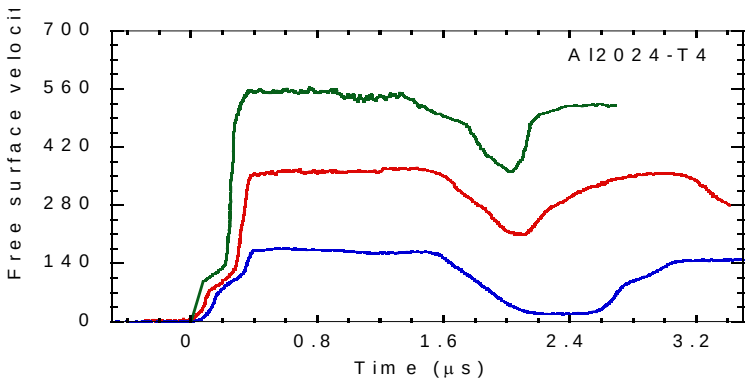

Figure 3: Free surface velocity profiles, using VISAR, of Aluminium alloy during shock wave experiments

By varying different controlling parameters for recording system like, laser power, optical aperture, PMT gain etc., a region of operation is obtained. When SRS is operated in this region it has linear operation with maximum gain and dynamic range for signal recording. Figure 2 represents this region of operation[4] with differenct PMT gain and laser power for optimized aperture opening. The optimised setup has been used in many of the experiments to obtained free surface velocity profiles and determining physical parameters like, HEL, spall fracture, strain rates etc. Fig 3, present one of such data on aluminium alloy[5] having very high strenght to weight ratio and finds application in aerospace industries.

Reference:

1. L.M. Barker *et.at., Rev. Sci. Inst.*, **36**, 1617, (1965)
2. P. M. Johnson *et.al., Rev. Sci. Instrum.*, **39**, 1100, (1968)
3. O. T. Strand *et.al., Rev. Sci. Instrum.*, **77**, 083108, (2006)
4. Amit Rav *et. al., Meas. Sci. Technol.*, **29**, 025205, (2018)
5. K. D. Joshi *et.at., AIP Conf. Proc.*, **1731**, 060013, (2016)

IT-21. NONLINEAR OPTICS: FROM INFANCY TO BLOOMING YOUTH

Dr. Pratima Sen, DAVV, Indore

The year 2022 marks 61st year of the birth of nonlinear optics soon after the demonstration of first Ruby laser in 1960. It is the intense optical frequency electric fields delivered by the laser light that gives rise to the optical nonlinearities. Optical nonlinearities are capable of amplifying the laser intensities and in turn the nonlinear optics grows with the advancement in the source intensities. The cycle confirms that the field of laser source development and nonlinear optics go hand in hand. The talk covers the introduction to nonlinear optics , progress made in it so far, its applications in everyday life as well as specialized applications along with a brief review of where things stand at present and its future aspects. The pillar on which the progress of nonlinear optics relies are the developments in the material science and the laser sources.

Due to the advancement in the material science, we now have nanostructures, waveguides, various types of optical fibers, photonic crystals, liquid crystals, conjugate polymers, chiral materials, meta materials, graphene, epsilon-near-zero materials.

The growth of research in nonlinear optics is also closely linked to the rapid technological advances in the radiation sources typically, Supercontinuum generation, Attosecond pulse generation, Zettawatt powers etc. The parametric down-conversion process is used in generating squeezed state generation. It is possible to squeeze the light below the shot noise limit.

Nonlinear optical phenomena play a key role in many applications of photonics. It is the backbone of all-optical circuitry for computing, information processing, and networking which is expected to overcome the speed limitations of electronics-based systems. The design and realization of photonic equivalents of fundamental devices that form basic building blocks in electronic circuits such as optical switches, memory elements are a step towards the practical realization of devices based on nonlinear optics.

The coherent transient effects are the optical effects that occur in times smaller than dephasing time and open up a new dimension in the study of behaviour of electrons in times hidden within it. They cover phenomena like optical nutation, free induction decay, photon echo, self-induced transparency etc. It is the progress made in this area of optics that has led to its applications in quantum computing.

After discussing the application part, a brief introduction to what is nonlinear optics, underlying mechanisms responsible for its occurrence are given. Also, one aspect of the field specifically; nonlinear refraction and nonlinear absorption is taken as a representative example of an important area of nonlinear optics in conjugate polymers, pure and doped ZnO, NiO, SnO2, and TiO2 thin films will be discussed.

The expanse of nonlinear optics is truly remarkable and is indicative of the fact that it has long way to reach its saturation limit and increasingly becoming an interdisciplinary field of research.

IT-22. DEVELOPMENT OF SINGLE MODE HIGH REPETITION RATE VISIBLE OPTICAL PARAMETRIC OSCILLATORS AND ITS SPECTROSCOPIC APPLICATIONS

Dr. C S Rao, Tunable Laser Section, ATLAF, Beam Technology Development Group, BARC, Mumbai-400094, India. Email: somu@barc.gov.in

Optical Parametric Oscillators (OPOs) are powerful sources of coherent radiation that are typically intense and tunable over a wide range of wavelengths. They invariably arise via three-wave mixing process mediated by a second-order nonlinear crystalline medium. In comparison to conventional tunable liquid dye lasers, OPOs offer the advantages of an all-solid-state medium with wide wavelength tunability, facilitating its robust use in industrial, environmental, and scientific applications. However, applications, such as trace elemental analysis by resonance ionization spectroscopy and laser isotope separation of the medical isotopes such as ^{176}Lu,^{176}Yb, ^{152}Sm etc., demandstunable laser sources delivering single longitudinal mode (SLM) output at multi-kHz repetition rates. Furthermore, the SLM tunable lasers are necessary for selective multi-step photoionization studies of the medical isotopes to investigate efficient, selective photoionization ladders and precisely determine the atomic parameters like isotope shiftsand hyperfine structures pertaining to the transitions constituting the photoionization ladder. Therefore, we have been working on developing high/low repetition rate SLM OPO devicestunable in the visible spectral region aiming to use in such applications.

Recently, we have demonstrated the high repetition rate (1–5 kHz) operation of a BBO crystal-based nanosecond OPO, pumped by the third harmonic (355 nm) output of a DPSSL tunable over visible spectral region 490–630 nm. More importantly, the single longitudinal mode operation of the BBO OPO has been demonstrated over a spectral region 500–600 nm at 1 kHz repetition rate. The developed SLM OPO system has been set up in our RIMS laser facility for the selective photoionization studies of Lu-176.

In this talk, I will discuss the factors that are impeding the development of the high repetition rate OPOs operating in the nanosecond regime and present our work on design and development of these devices, particularly the development of high repetition rate single-mode OPOs. The application of this developed SLM OPO in selective photoionization studies of Lu-176 has provided substantial enhancement in the degree of enrichment of Lu-176. The experimental results associated with the application of SLM OPO will be presented.

IT-23. MAGNETO-OPTICAL EFFECTS IN DOPED QUANTUM DOTS

Prof. Ranjani Vishwanatha, JNCASR, Bangaluru

Doping in semiconductors has given rise to some very interesting observations, specifically providing energetically accessible multiple spin state configurations. However, lack of understanding of these properties, specifically at room temperature, has not given rise to interesting spintronic applications so far. In this talk, I discuss the various magneto-optical properties using single dopant as well as the two dopants, their mutual interactions and possibility of demonstrating these properties at room temperature. Specifically, I plan to discuss the effect of optical perturbation on the two spin states producing magnetically inequivalent excitonic states and their effects on spintronic applications as well as photo-induced magnetism. We use ultrafast pump-probe spectroscopy and density functional theoretical analysis and magnetic circular dichroism to establish the presence of the Magneto-Optical Stark Effect (MOSE)[1] and the Zeeman effect.Their effects on the temperature and time will be discussed providing a stepping-stone for spin-dependent applications.

References:

M. Makkar,L. Dheer,A. Singh,L. Moretti,M. Maiuri, S. Ghosh, G.Cerullo, U.V. Waghmare, R.Viswanatha Nano Lett., 2021, **21**, 9, 3798

IT-24. ENHANCED FUNCTIONALITY OF METALLIC BIOMATERIALS USING PULSED LASER

*Dr. Sunita Kedia and J P Nilaya, L&PTD, BARC, Bhabha, Mumbai, HBNI, Anushaktinagar, Mumbai, *skedia@barc.gov.in*

With advancement in medical field, the demand for artificial body implants in orthopaedic fixation, dentistry, stents, and tissue engineering has increased over the years. However, poor osseointegration, bacterial infections, wear and corrosionof the implants arecommonchallenges faced by medical community and hence the need to improve the properties of existing biomaterials.Various materials such as, titanium alloys (Ti6Al4V), stainless steel (SS), cobalt alloys, zirconia, and calcium phosphates are accepted as biomaterials due to their biocompatibility, mechanical stability, and non-toxicity. Research shows,the functionality of metallic biomaterials can be further enhanced by altering their surface properties, either by modifying the morphology or by active coating. In this talk, I shall discuss about two approachesviz; laser surface texturing (LST) and pulsed laser deposition (PLD) which provided promising results for improvements in bio-efficiency of metallic biomaterials.

I. Laser Surface Texturing (LST)

Surface structuring depends on the rate of energy deposition onto the substrate surface that can be varied by altering the laser pulse duration. While femtosecond laser induced conical protrusions show superior osseointegration, antibacterial behaviour and cell adhesion on

Ti6Al4V surface compared to pristine sample [1-2], the larger groove widths obtainable by nanosecond treated surfaces lead to the possibility of contact guidance to cell growth that can result in quicker integration of the implant with the surroundings [3].

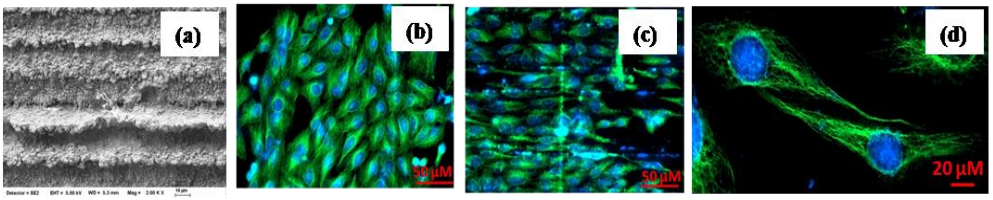

Fig. 1:*(a) FE-SEM image of laser induced micro-grooves on 316L SS, confocal microscopic images of U2OS bone cells on (b) pristine 316L SS, (c) micro-grooved samples and (d)at higher magnification*

The FE-SEM image in Fig. 1a shows micro-grooves of width about 40µm on SS biomaterial surface induced by a nanosecond laser. Adhesion, spreading and random orientation of U2OS cells was observed on pristine sample in Fig.1b. However, squeezing of cytoplasm in the vertical direction and spreading along the major axis of the grooves with extensively long dominated micro-spikes indicated contact guidance of the cells along the grooves, Fig. 1c-1d.

II. Pulsed Laser Deposition (PLD)

Modification of the surface properties of biomaterials by PLD of bio-glass [4] and zirconia (ZrO_2) thin film also result in superior growth of hydroxyapatite, antibacterial behaviour and cell adhesion as the coating improved bioactivity of the sample.

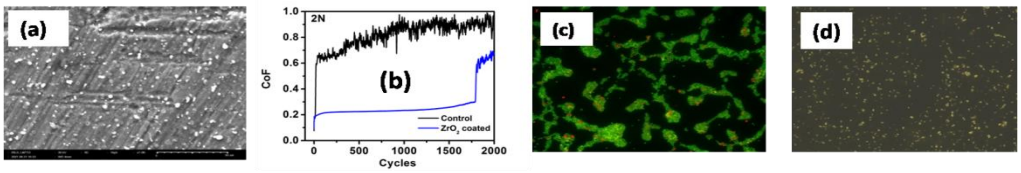

Fig. 2:*(a) SEM image ZrO_2 coated Ti6Al4V (b) Reduction in coefficient of friction after ZrO_2 coating (c) S. aureus bacterial colonies on pristine Ti6Al4V sample and (d) bacterial adhesion on ZrO_2 coated Ti6Al4V sample*

The PLD of ZrO_2thin film (Fig. 2a) showed a significant reduction in coefficient of friction (Fig. 2b), wear rate and clear inhibition of adhesion and colonization of *Staphylococcus aureus*bacteria on Ti6Al4Vbiomaterials, as shown in Fig. 2c-2d.

The work carried out in our laboratory with regard to surface modification to improve the efficiency of biomaterials will be discussed in detail during this talk.

[1]S. Shaikh, S. Kedia, A. G Majumdar, M. Subramanian, and S. Sinha,*Applied Physics A* **124** (2018) 821
[2] S. Shaikh, S. Kedia, D. Singh, M. Subramanian, and S. Sinha, *Journal of Laser Applications* **31** (2019) 022011
[3] S. Kedia, S. K. Bonagani, A. G. Majumdar, V. Kain, M. Subramanian, N. Maiti and J. P. Nilaya, *Colloids and Interface Science Communications* **42** (2021) 100419.
[4] S. Shaikh, S. Kedia, A. G Majumdar, M. Subramanian, and S. Sinha, *Material Research Express* **6** (2020) 125428

IT-25. ANTIMICROBIAL PHOTOTHERAPY: A NEW FRONTIER IN FIGHT AGAINST ANTIBIOTIC RESISTANT BACTERIA AND NEWLY EMERGING INFECTIOUS MICROORGANISMS

Dr Khageswar Sahu and Shovan Kumar Majumder, RRCAT, Indore, Email: khageswar@rrcat.gov.in ,khageswar80@gmail.com

Scientists and medical practitioners all over world are currently locked in a high-stakes race against microbial evolution, fighting against adversaries that can be spawned in a time scale before we can develop drugs to fight them. Ever since the first antibiotic penicillin was discovered, antibiotic resistance is involved in a cat-and -mouse game with antibiotic development. But, in the last decade the incidences of antibiotic resistance have increased menacingly, propelling world towards a situation of "no action today-no cure tomorrow". To tackle the problem of resistance against antibiotics, a new line of therapeutic strategies based on antimicrobial peptides, efflux pump inhibitors etc. were investigated in the last two decades of twenty first century. However, against these newly investigational therapeutic strategies, resistance in microbes can also be generated. So, altogether novel therapeutic interventions are needed urgently to circumvent antibiotic resistance. At RRCAT, we have been actively pursuing studies on antimicrobial photodynamic therapy (APDT), which is an offshoot of photodynamic therapy (PDT). APDT involves rapid binding of microorganisms with light activable drugs called photosensitizers (PS), followed by exposure to visible light of suitable wavelength,, after a suitable time gap. The ensuing photochemical reactions rapidly generate reactive oxygen species, damaging multiple biomacromolecular targets within microbial targets. The distinct advantage of APDT is that there is least chance of resistance generation. In the last half decade, our investigations have been focused on APDT mediated inactivation of antibiotic sensitive and resistant bacteria using either cationic PS or cationic peptide conjugated anionic PS (chlorophyll derivative). These investigations have suggested that a suitable APDT window can be optimized that result in ~99 % bacteria load reduction, but negligible damage to the inflammatory cells with concomitant increase in cell proliferation, angiogenesis response of wounds. In addition to antibacterial applications, we have recently forayed into APDT and Ultraviolet-C mediated inactivation of viruses such as SARS CoV-2. In the present talk, we shall give an account of our current research investigations while very briefly touching upon some of our future goals as well.

CONTRIBUTORY PAPERS

CATEGORY 01: PHYSICS AND TECHNOLOGY OF ASERS

CP-01-1.A NOVEL APPROACH TO EVALUATE DISCHARGE PLASMA IMPEDANCE OF COPPER VAPOR LASER

Dheeraj K Singh[*1, 2], *B Dikshit*[1, 2], *R Vijayan*[2], *Jaya Mukherjee*[2] *and V S Rawat*[1, 2]*[1]Homi Bhabha National Institute, Anushaktinagar, Mumbai, India [2]Beam Technology Development Group, Bhabha Atomic Research Centre, India*

A novel approach is proposed to calculate the impedance of a large bore, coaxial and longitudinally excited elemental copper vapor laser (CVL). The underdamped behavior of voltage waveform is leveraged to compute the impedance of high voltage discharge plasma of CVL. This methodology provides accurate idea of the discharge plasma resistance and inductance as it is calculated on the basis of experimental waveforms obtained in the system. The laser head inductance remains almost fixed and equivalent to 0.425 μH whereas laser resistance is 11.77 ohm during the normal laser operation and keeps varying depending on the discharge condition and its constituents. The overall impedance of the laser comes out to be 27.9 ohm.

CP-01-2.DUAL PUMPED CR:FORSTERITE LASER WITH ENHANCED LASING EFFICIENCY

Siba Prasad Sahoo[* 1, 2], *V S Rawat*[1, 2], *Jaya Mukherjee*[1], *Swarupananda Pradhan*[1, 2], [1]*Homi Bhabha National Institute, Anushaktinagar, Mumbai 400094,* [2]*Beam Technology Development Group, Bhabha Atomic Research Centre, Trombay, Mumbai 400085, Email: sibaps@barc.gov.in*

The efficiency of the Cr:forsterite solid-state laser is observed to be enhanced using dual pumping technique in which the Cr:fosterite crystal was pumped using two pump beams of distributed pulse energies instead of a single pump beam of higher pulse energy. The second pump beam is applied just before initiation of the laser pulse so that it repumps the Cr^{4+} ions depleted during the cavity buildup time of the first pump pulse and leads to enhancement in the laser output energy. This technique is studied using a polarization-based Cr:forsterite laser resonator cavity in which the output energy of the laser is doubled compared to the single pumping method using combined pulse energy. This dual pumping technique suggests, use of multiple beams of distributed energy instead of a single pump beam of higher pulse energy which will also help in avoiding damage to the crystal and other associated thermal effects in the crystal.

CP-01-3.EFFECT OF RETARDANCE ON THE FRINGE PATTERN OF A SAGNAC INTERFEROMETER

N. K. Chaitanya[1,2] *P.C. Hari Krishna*[1], *D. Dinakar*[2], *M. Sree Ramana*[1] [1]*Research Center Imarat, Hyderabad, TS, India.* [2]*National Institute of Technology, Warangal, TS, India. E-mail: praturi.chaitanya@gmail.com*

In this article, the effect of retardation offered by wave plates on the fringe pattern of a four arm Sagnac interferometer is theoretically studied and analysed. This method is useful in estimating and compensating any arbitrary retardance introduced in the path of an interferometer, which is of potential importance in case of interferometric sensors.

CP-01-4. DESIGN AND DEWVELOPMENT OF MECHANICAL SYSTEM FOR CARBON MONOXIDE (CO) LASER

*Lal Bahadur Rana, Manoj Kumar, Rajiv Kumar Yadav, R Kaul, Raja Ramanna Centre for Advanced Technology, Indore, **Email:** lbrana@rrcat.gov.in*

In this paper, we report design and development of mechanical system for carbon monoxide (CO) laser system. AutoCAD and Solid Edge software were used to design and generating manufacturing drawings. Vacuum chamber having rectangular shape which operates at pressure 1.01325×10^5 Pa leads to the compressive forces acting inside the chamber. Analytical design and buckling failure analysis of vacuum chamber were carried out. Minimum achievable leak rates were estimated for the O-ring grooves with best achieved surface finish. This estimation not only gives idea of maximum possible leakage of the vacuum system, but also gives estimates of moisture in the vacuum system whose presence beyond 200 ppm could totally kills the lasing action. The mechanical system has been manufactured and tested for its vacuum integrity. We could demonstrate operation of CO laser at sub zero temperatures..

CP-01-5. STUDY OF OUTPUT CHARACTERISTICS OF A Q SWITCHED CW CO LASER WITH MIRROR ROTATION

Utpal Nundy , BH-2-76, Kendriya Vihar, Kharghar, Sector-11, Navi Mumbai 410210 , e-mail:unundy@yahoo.co.in

Osgood used Rotating Mirror Q switching on a CW CO laser. A theoretical model developed earlier for "Q switching of lasers" is now used to study the laser developed by Osgood, at various mirror rotation frequencies from 80 to 320 Hz .Such a laser is capable of generating multi Kilowatt peak power laser pulses, with FWHM anywhere from 400 to 2000ns. The composite laser pulse contains about 200 individual vibration rotation lines spanning a wavelength range from 5.0 to 6.4 μm. An important application of such a laser is generation of additional frequencies in a nonlinear crystal. Our results show that for such an application, there is an optimu frequency of mirror rotation, which for our laser is 200 Hz.

CP-01-6. DEVELOPMENT OF MONOLITHIC 1 KW SINGLE TRANSVERSE MODE ALL-FIBER YB-DOPED CW FIBER LASER AT 1080 NM

Avdhesh Kumar, Pushkar Mishra, R K Jain, Rajpal Singh, B N Upadhyaya, K S Bindra, Raja Ramanna Centre for Advanced Technology Department of Atomic Energy, avdhesh@rrcat.gov.in

We report on the development of 1 kW of all-fiber single transverse mode (~LP_{01}) Yb-doped CW fiber laser (YDFL) using single-end pumped oscillator configuration. In this configuration, an optical-to-optical conversion efficiency of ~74% has been achieved and spatial beam profile is nearly diffraction limited with beam quality factors of $M^2_{x,y} \sim 1.3, 1.24$. Laser output has a peak at 1080.25 nm with a 3 dB FWHM linewidth of ~ 1.5 nm. Laser output was found to be stable within 1.5% for more than half an hour of continuous operation. This laser has potential applications in good quality cutting, welding and laser additive manufacturing.

CP-01-7. EFFECT DEVELOPMENT OF ENGINEERED 567 J PULSE ENERGY LONG PULSE ND:YAG LASER SYSTEM FOR WELDING APPLICATIONS

Sunil Kumar Sharma[1], V. Bhardwaj[1], M. K. Bairwa[1], Bhaskar Paul[1], Rajpal Singh[1], Ranveer Singh Meena[1], Vijay Bhawsar[2], A. A. Raju[2], R. K. Jain[1], Pawan Kumar[1], Sudheer Kushwaha[2], J. Khanwalkar[2], R. Arya[2],B N Upadhyaya[1], K S Bindra[1] [1]Laser Technology Division, Raja Ramanna Centre for Advanced Technology, Indore-452013, INDIA [2]Laser Electronics Division, Raja*

*Ramanna Centre for Advanced Technology, Indore-452013, INDIA*E-mail: sksharma@rrcat.gov.in*

We have developed an engineered high pulse energy flash lamp pumped long pulse Nd:YAG laser system generating 567 J of single pulse energy at 40 ms pulse duration using two ceramic reflector based double lamp pump chambers in a single resonator. Laser pulse duration can be varied in the range of 4-40 ms and pulse repetition rate in the range of 1-100 Hz and an electrical to laser conversion efficiency of 5.34% has been achieved. A ceramic reflector based pump chamber and laser resonator has been optimized to achieve a beam quality factor of $M^2 \sim 65$, which is good enough for beam delivery through 400 μm and 600 μm core diameter, 0.22 numerical aperture (NA) optical fibers for large depth cutting and deep penetration welding applications.

CP-01-8. COMPUTATIONALLY GENERATED DYE CELL FLOW CHANNEL FOR HIGH REPETITION RATE SLM DYE LASER IN GIG CAVITY

S K Mishra[1,2], Paramjit Rana[1], Siba Prasad Sahoo[1,2], Aditya Kumar Tiwari[1,2], Jaya Mukherjee[1], V S Rawat[1,2], [1]Advance Tunable Laser Application Facility, BTDG, Bhabha Atomic Research Center, Mumbai 400085, [2]Homi Bhabha National Institute, Mumbai 400 094, *email:smishra@barc.gov.in*

The dye cell has been designed using conversing straight diverging flow channel and utilized for generation of single longitudinal mode (SLM) pulsed dye laser in GIG cavity with solid etalon as a mode selector. The bandwidth of SLM dye laser was measured to be 450 MHz and the effect of end mirror reflectivity on bandwidth and efficiency has been studied. The long term stability of the SLM dye laser was found to be less than the bandwidth of the SLM dye laser while the short term stability is within $\pm$ 75 MHz.

CP-01-9. DEVELOPMENT OF A 5 W NARROW LINEWIDTH ALL-FIBER MULTISTAGE AMPLIFIER SETUP AT 1550 NM

Bhuvnesh[1,2], C P Singh[1], P. K. Gupta[1], P. Hedaoo[1], S. Sahu[1], P K Mukhopadhyay[1] and K S Bindra[1],[1]Laser Technology Division, Raja Ramanna Centre for Advanced Technology, Indore-452013.[2]E-mail: bhuvneshk@rrcat.gov.in13

Here, we present the development of an all-fiber laser amplifier setup at 1550 nm for the amplification of a narrow linewidth (< 1 MHz) fiber coupled laser diode at 1550 nm with~ 10 mW output power. The amplifier operates in multi-stage configuration and generates more than 5 W narrow linewidth (< 1MHz) output. Output power is stable and there is no contribution of pump or amplified spontaneous emission (ASE) in the final output. Pump to signal conversion efficiency is ~15%..

CP-01-10. DEVELOPMENT OF EDGE CLADDING OF LARGE SIZED ND: PHOSPHATE GLASS DISC FOR HIGH-ENERGY LASER AMPLIFIER

J. Sharma, [1], C. Mukherjee[1, 3], Y.P. Kumar[1], K. Rajiv[1], V.K. Dixit[2, 3], D. Daiya[1], R K Patidar[1], A. Singh[1], S. Gurram[1], M P Kamath[1], N S Benerji[1], K S Bindra[1, 3] [1]Laser Technology Division, [2] Material Science Section, RRCAT, Indore 452013, M.P., India [3]Homi Bhabha National Institute, Training School Complex, Anushakti Nagar, Mumbai, 400094 *Email: jyotis@rrcat.gov.in,*

The development and process establishment of edge cladding of large sized Nd: phosphate glass disc for high-energy laser amplifier are presented. The clad glass slabs having absorption at 1053 nm are adhesive bonded to the all the four edges of Nd: glass discs using an adhesive whose index of refraction matches both the laser glass and absorbing glass.

Studies pertinent to finding suitable epoxy based adhesives, cementing of Nd: glass disc and clad glass, stability of the bonded joint under flash lamp irradiation etc. are presented. Finally, a Nd: glass disc has been bonded with clad glass using experimentally studied suitable adhesive. The dimensions of the edge cladded Nd: glass disc is 300 mm x 170 mm x 40 mm.

CP-01-11. ENGINEERED TWO-ARM TIME SYNCHRONIZED ALL-FIBER OPTIC FRONT END SYSTEM FOR HIGH ENERGY ND: GLASS LASER

Srikanth Gurram, N.K.Varshnay, O.B.Dongre, D.Daiya, A.Singh, J.Sharma, R K Patidar, M P Kamath, N S Benerji, K S Bindra, High Energy Optics Section, Laser Technology Division, Raja Ramanna Centre for Advanced Technology, Indore-452013, ***Email****: srikanth@rrcat.gov.in.*

Develpment of an engineered two arm time synchronized all-Fiber Optic Front End System (FOFES) with central wavelength of 1053 nm has been reported here. The FOFES is a seed laser system for high energy Nd:Glass laser being developed at RRCAT. FOFES is based on all-fiber architecture for alignment-free and ruggedness. The system delivers laser pulses with a pulse width of ~3 ns and pulse energy of 40 nJ per beam with both beams synchronized in time to ~ 10 ps. It can be operated at varying repetition rates, pulse widths and pulse energies. The manuscript describes developement and preliminary results of two arm FOFES.

CP-01-12. GENERATION OF 920 W OF PEAK POWER FROM ALL-FIBER ACOUSTO-OPTIC Q-SWITCHED THULIUM-DOPED FIBER LASER AT 1940 NM

Usha Chakravarty, Antony Kuruvilla, Avdhesh Kumar, Rajpal Singh, Bacilus Ekka, R. K. Jain, B N Upadhyaya and K S Bindra , Laser Technology Division, Raja Ramanna Centre for Advanced Technology, Indore-45201,* ****E-mail****: ushac@ rrcat.gov.in*

In this paper, we report on the generation of 920 W of peak power from all-fiber acousto-optic Q-switched Thulium-doped fiber laser at 1940 nm and investigation of output pulse shapes. Study of multi-peak pulses and multiple pulses have been performed and analyzed at 30 kHz of repetition rate. Multi-peaks in the single pulse is attributed to the reflection from the ends of the fiber and was eliminated by angle cleaving of the fiber ends. For generation of smooth single pulses, optimization of window ON-time was carried out and a peak power of 920 W was achieved with FWHM pulse width of 120 ns at 30 kHz of modulation frequency. The spectrum of the Q-switched signal is centered at 1940 nm with FWHM linewidth of 1 nm.

CP-01-13. ALL-FIBER PASSIVELY Q-SWITCHED YTTERBIUM DOPED LASER USING FIBER OPTIC RING RESONATOR

Pradeep K. Gupta, C P Singh, P K Mukhopadhyay and K S Bindra; Laser Technology Division, Raja Ramanna Centre for Advanced Technology, Indore, M.P-452013; Homi Bhabha National Institute, Training School Complex, Anushakti Nagar, Mumbai-400094, India. ***E-mail:*** *pradeepg@rrcat.gov.in*

We report an Ytterbium (Yb) doped fiber laser passively Q-switched by fiber optic ring resonator (FORR) in all-fiber format. The Q-switched laser characteristics viz. pulse duration, pulse profile, repetition rate and average power are easily varied not only by pump power but also by changing the polarization state of light inside the laser resonator with the help of polarization controllers. At 330 mW pump power, the laser generates 1.07 μs duration pulses with 0.68 μJ pulse energy at 83.6 kHz repetition rate. The Q-switched laser wavelength is tunable from 1059 to 1069.7 nm by changing the polarization state inside the cavity.

CP-01-14. THEORETICAL AND EXPERIMENTAL STUDIES FOR DEVELOPMENT OF SEALED-OFF GLASS TUBE CO_2 LASER

Avantika Gautam, L B Rana, Rajiv Kumar Yadav, R Murugan, B T Rao, Manoj Kumar and R Kaul, Laser Materials Processing Division, MSG, RRCAT, Indore, ***E-mail****: avantika@rrcat.gov.in*

Sealed-off glass tube CO_2 lasers find various applications in the market and are currently imported mostly from China. In order to develop such lasers in India it is required to estimate the CO_2 dissociation rate in the discharge so that optimum catalyst could be designed and coated inside the discharge tube. Theoretical studies have been carried out where dissociation rate has been estimated for optimum gas mixture. Using the estimated dissociation rate, CO_2 dissociation with time was calculated. A good agreement between theory and experiment was observed.

CP-01-15. STUDY ON TIME DELAY ECHOES IN SEMICONDUCTOR DIODE LASER WITH OPTICAL FEEDBACK

Neethu. K and S. Sivaprakasam, Department of Physics, Pondicherry University, Pondicherry – 605014, ***Email****: neethukpgm@gmail.com, siva@pondiuni.ac.in*

Diode lasers with delayed optical feedback have been a topic of interest due to their application in secure optical communication. The security is in question when the auto-correlation data reveal information about external cavity delay time. Numerical studies of auto-correlation have been carried out for multimode lasers. This investigation provides useful results on time delay echoes of the auto-correlation and in terms of their dependence on feedback delay time and multi-modeness.

CP-01-16. REMOTE MONITORING AND CONTROL OF LASER HEAD PRESSURE OF COPPER VAPOR LASER

Rajasree Vijayan[2], Dheeraj K Singh[1, 2,], Jaya Mukherjee[2], V S Rawat[1,2], [1]Homi Bhabha National Institute, Anushaktinagar, Mumbai, India, [2]Beam Technology Development Group, Bhabha Atomic Research Centre, Mumbai 400094 India**Email****: dheeraj@barc.gov.in*

The copper vapor laser (CVL) is operated at low pressure of around 40-50 mbar with constant purging of neon gas at a flow rate of 2mbar.litre/min. The low operating pressure eases the voltage requirement and thereby assuages the complexity of power supply. The constant flow of Ne ensures removal of impurity inside the laser. It has been found that the pressure variation in CVL, varies the impedance of the laser which in turn reduces the optical output power and varies the propagation delay of the laser. The variation in propagation delay hinders the proper synchronisation of laser which in turn lowers the laser power addition from amplifier module and affects the power stability of laser in oscillator- amplifier configuration. In this paper we are presenting a methodology to control and monitor the laser head pressure in a high electromagnetic interference environment. With the control in the pressure the power stability has been achieved on oscillator amplifier configuration.

CP-01-17. LASING ACTION IN CO_2-N_2-HE GAIN MIXTURE: EVALUATION OF TRANSITION TEMPERATURE

T. Dwivedi[§+], M B Sai Prasad[§], J P Nilaya[§+], [§]Laser & Plasma Technology Division, BARC, Mumbai-400085, [+]Homi Bhabha National Institute, Anushaktinagar, Mumbai-400094, **Email:** tatsat@barc.gov.in*

We have reported in the past lasing on multiple wavelengths in the 5 μm region from a non-dispersive CW-CO_2 laser cavity when its gain length was maintained at LN_2 temperature. The

inversion obtained in the CO formed due to the dissociation of CO_2 gas in the discharge made this possible. We present here, results of experiments where the wall temperature of the discharge tube could be varied by allowing the LN2 in the surrounding jacket to gradually boil-off, and the same was measured systematically to know when the lasing action ceases on the 5 micron (CO lasing) and when it begins on 10 micron (CO_2 lasing). This assumes importance in understanding the evolution of the CO gain medium in the discharge-struck CO_2 laser gas mixture as a function of coolant temperature.

CP-01-18. DEVELOPMENT OF 5 W LINEARLY POLARIZED CW OUTPUT FROM ALL-FIBER AMPLIFIER AT 1064 NM WITH < 0.2 NM SPECTRAL WIDTH

Bhuvnesh[1,2], C P Singh[1], P K Gupta[1], P. Hedaoo[1], S. Sahu[1], P K Mukhopadhyay[1] and K S Bindra[1], [1]Laser Technology Division, Raja Ramanna Centre for Advanced Technology, Indore-452013., [2]E-mail: bhuvneshk@rrcat.gov.in,

We present the development of all-fiber amplifier setup at 1064 nm with < 0.2 nm spectral width delivering more than 5 W linearly polarized CW output. The setup is designed in MOPA (Master Oscillator Power Amplifier) configuration. The output power from the amplifier setup is stable without any contribution from pump and amplified spontaneous emission (ASE). The setup will be used as a source for reflectometric studies.

CATEGORY 02: LASERS IN NUCLEAR SCIENCE AND TECHNOLOGY

CP-02-1. SINGLE PASS LASER CUTTING OF 30 MM THICK SS316L PLATE USING REMOTELY OPERABLE 1 KW AVERAGE POWER PULSED ND:YAG LASER FOR NUCLEAR FIELD APPLICATIONS

M. K. Bairwa[1], Vijay Bhardwaj[1], R. K. Jain[1], Ranveer Singh Meena[1], Vijay Shukla[1], S K Sharma[1], Rajpal Singh[1], B. K. Saini[1], Bhaskar Paul[1], Pawan Kumar[1], B. Ekka[1], Prabhat Kumar[1], Jata Beshra[1], A. A. Raju[2], S. K. Sah[2], Vijay Bhawsar[2], J. Khanwalkar[2], R. Arya[2], B N Upadhyaya[1], K S Bindra[1], [1]Laser Technology Division, Raja Ramanna Centre for Advanced Technology, Indore-452013, India, [2]Laser Electronics Division, Raja Ramanna Centre for Advanced Technology, Indore-452013, India, [*]**E-mail:** bnand@rrcat.gov.in*

Laser cutting of thick SS pipes at fast speed is required in radioactive environment of nuclear power reactors. One such requirement is for laser cutting of 30 mm thick SS316L pipes of recirculation loop in Tarapur Atomic Power Station (TAPS-1&2) for replacement purpose. This report provides details of development of single pass laser cutting technology for 30 mm thick SS316L at high speed using remotely operable 1 kW average power fiber coupled pulsed Nd:YAG laser. A compact bending nozzle has been specially developed and laser cutting process parameters have been optimized for single pass laser cutting of large thickness of SS316L. This remotely operable laser cutting technology will be useful in laser cutting of 30 mm thick SS316L recirculation pipes at TAPS-1 & 2 reactors to minimize radiation dose consumption and time as compared to conventional mechanical methods and will also useful in laser cutting of large thickness steel sections in various industrial applications.

CP-02-2. DEVELOPMENT OF LASER CUTTING PROCESS AND MANIPULATOR FOR REMOVAL OF ERODED DANGLING PIECE FROM FEED WATER BOX OF STEAM GENERATOR AT KGS-4 REACTOR

R. K. Jain[1], Rajpal Singh[1], M. K. Bairwa[1], B. K. Saini[1], Vijay Shukla[1], Bhaskar Paul[1], Vijay Bhawsar[2], N. D. Dwivedi[3], K. O. Ulhas[3], D. N. Sanyal[4], R. Arya[2], B N Upadhyaya[1], K S Bindra[1], [1]Laser Technology Division, Raja Ramanna Centre for Advanced Technology, Indore-452013, India, [2]Laser Electronics Division, Raja Ramanna Centre for Advanced Technology, Indore-452013, India , [3]Kaiga Genearting Station, NPCIL, Kaiga , [4]Technology Development-Remote Tooling System, Nuclear Power Corporation of India Limited, Mumbai, ***E-mail:** bnand@rrcat.gov.in*

There was a specific requirement to develop laser cutting process and laser cutting manipulator for removal of eroded dangling piece from Feed Water Box of steam generator of KGS-4 reactor. Removal of eroded dangling piece was required to protect damage of steam generator (SG) tubes on the other side of fed water box. It was a difficult task due to obstructions in the path to approach the cut location of dangling portion inside the feed water box using conventional methods due to space constraints and direct visibility of location. This report provides the details of laser cutting process and development of laser cutting tool using miniature laser cutting nozzle and CCD camera based viewing system.

CP-02-3. A NOVEL TECHNIQUE FOR THERMAL LENSING MEASUREMENT IN A COPPER VAPOR LASER AMPLIFIER

Paramjit Rana[1], S K Mishra[1], V S Rawat[1, 2], Jaya Mukherjee[1,2], [1]Beam Technology Development Group, Bhabha Atomic Research Center, Mumbai-85, [2]Homi Bhabha National Institute, Anushaktinagar, Mumbai – 400094, ***E.mail:** paramjit@barc.gov.in, paramjit.rana@gmail.com*

Thermal lensing plays a significant role in efficient power extraction from amplifiers in a master oscillator power amplifier (MOPA) system. A novel technique to measure the resultant focal length of the thermal lens in an amplifier using collimated beam of the oscillator for copper vapour laser MOPA chain was demonstrated. A collimated oscillator beam of known beam diameter was passed through an amplifier and diameters of the output amplified laser beam at two known locations were measured. Subsequently, the resultant thermal focal length was estimated using ray tracing approach for a 40 W system (CVL-40). Effect of input electrical power and buffer gas pressure on effective focal length of the thermal lens was characterised using this technique. This study finds benefits for high power laser systems (MOPA) used in various industrial, research and development applications like micromachining, high speed photography, bio-medical applications and pumping dye lasers for spectroscopy.

CP-02-4. SELECTION OF TECHNIQUES FOR ASSAYING LANTHANIDE PRODUCT IN LASER ISOTOPE SEPARATION

*Anupama Prabhala[1], Dev Ranjan Das[1], R.K. Bhatia[2], Nataraju V.[2], Manisha V.[3], R. K. Singhal[3], Anitha M[4]. Sanjay Sethi[1],[1]IPDS, ATLA-F, BTDG, BARC, [2]EmA&ID, BARC, [3]ACD, BARC, MP&CED[4], BARC, **Email:** anuvivek@barc.gov.in*

Isotopic enrichment of Lanthanides for medical application by Laser isotope Separation (LIS) is being pursued by BTDG, BARC. LIS, based on selective photoioniation using high powered dye lasers, generates an ionized and isotopically enriched product. This product deposited as a thin coating on a solid substrate is recovered by acid elution. This paper is focused on the selection of the method for quantification and isotopic composition of the enriched product in the aqueous eluant solution. Among the various methods discussed, inductively coupled optical emission spectrometry (ICP-OES) for quantity determination and thermal ionization based mass spectromter (TIMS) for isotopic compositional anlysis were found suitable.

CATEGORY 03: LASER MATERIALS, OPTOELECTRONIC DEVICES AND COMPONENTS

CP-03-1. BRIGHT RED EMISSIONS FROM EU3+ DOPED ZINC ALUMINO-BORO-SILICATE GLASSES FOR SOLID STATE LASING APPLICATION

M. Monisha[1] and Sudha D Kamath[1 1*] Department of Physics, Manipal Institute of Technology, Manipal Academy of Higher Education, Manipal, Karnataka – 576104.,* ***Email :*** *sudhakamath6@gmail.com*

In this work we report the optical and luminescence studies on Eu^{3+} doped zinc alumino borosilicate glasses. The UV-Visible-NIR studies show nearly eleven transitions of Eu^{3+} ions embedded in the glass medium. Photoluminescence studies showed the transition $^5D_0 \rightarrow {}^7F_2$ has maximum emission intensity observed at 612 nm. Concentration quenching is observed beyond 2.0 mol% of Eu^{3+} ion. From, the emission spectra the radiative parameters such as radiative transition probability (A_R), branching ratio (β_R), stimulated emission cross-section (σ_{se}) and gain bandwidth were obtained. Higher emission cross section and gain band width is obtained for the Eu-2.0 mol % glass. The colour chromaticity values and CCT values show the bright red emission from the prepared glasses. Thus, the prepared glasses can act as laser gain media in solid state laser applications.

CP-03-2. PROPOSAL FOR ULTRA-COMPACT ADD DROP FILTER BASED ON HOLES IN SLAB 2D HEXAGONAL PHOTONIC CRYSTALS

Puja Sharma[a], Man Mohan Gupta[b], NilakshaGhosh[b], SarangMedhekar[a],Department of Physics, CentralUniversity of Jharkhand, Ranchi 835222, Jharkhand, India,Department of Physics, GLA University.*

In this paper, an ultra-compact add-drop filter (ADF) based on a 2D hexagonal lattice photonic crystal (PC) is proposed. The band structure of the proposed ADF is analyzed using Plane Wave Expansion technique and simulations on light propagation through it have been carried out using 2D Finite Difference Time Domain technique. Proposed ADF consists of 29*21 air holes in the slab of refractive index 3.9. Structure is having two defect waveguides Bus and Drop which are coupled to each other through a hexagonal cavity. Size of proposed ADF is only 53 μm^2 with resonance at wavelength 1554.77 nm and high quality factor of 675.98. The effect of tuning of lattice constant and refractive index on the performance of ADF is also investigated..

CP-03-3. LUMINESCENCE PROPERTY OF HYBRID IMIDAZOLIUM LEAD IODIDE

M.Jeevaraj[1], S. Sudhahar[2], M. Krishna Kumar[1], [1]International Research Centre, Department of Physics, Kalasalingam Academy of Research and Education, Krishnankoil-626 126, Tamil Nadu, [2]Department of Physics, Alagappa University, Karaikudi-630 003, Tamil Nadu,* ***Email:*** *m.krishnakumar@klu.ac.in*

The organic–inorganic Imidazolium lead Iodide (ImPI) was synthesized by simple evaporation route for light emitting devices. Preliminary investigations on the structure and vibrational analysis of ImPI confirm the incorporation of Imidazolium in the lattice. UV-Visible absorption studies evince the presence of an excitonic peak around 290 nm. The observed PL emission is red shifted from the excitonic gap by 197 nm and the radiative relaxation of the self trapped

excitons accounts for the emission band. This work reiterates the potential of Imidazolium lead iodide for optoelectronic applications.

CP-03-4. MICROSTRUCTURAL AND OPTICAL CHARACTERIZATION OF CR-DOPED ALUMINA CERAMIC

S. K. Pathak[1], S. Karmakar[1], and S. M. Gupta[1-2], [1]Laser and Functional Materials Division, Raja Ramanna Centre for Advanced Technology, Indore-452013, [2]Homi Bhabha National Institute (HBNI), Training School Complex, Anushaktinagar, Mumbai-400094, **Email:** *pathak@rrcat.gov.in*

Nano-powder of chromium doped aluminium oxide ($Cr:Al_2O_3$) is synthesized using co-precipitation route followed by vacuum sintering at 1780 °C for 2-24 hours to investigate the effect of porosity and grain size on the optical properties. Phase analysis has revealed preferred orientation in those ceramics which is dwelled for long duration (> 6hrs). Microstructural investigation has shown reduction in the porosity concentration as well as size of the pores with increase in the sintering time at 1780 °C. A transmission of ~ 28% at 800 nm for 0.2mm thickness is observed along with standard absorption peaks of Cr-ions. The attenuation coefficient is found to correlate inversely with the sintering time.

CP-03-5. MGZNO BASED MSM SOLAR BLIND UV PHOTODETECTOR GROWN BY PULSED LASER DEPOSITION

S K Chetia[,1, 2], Amit K Das[1], R S Ajimsha[1] and P Misra[1, 2], [1]Raja Ramanna Centre for Advanced Technology, Indore, [2]Homi Bhabha National Institute, Mumbai,**Email:** shantanuk@rrcat.gov.in*

We have developed solar blind UV photodetector based on mixed phase $Mg_{0.48}Zn_{0.52}O$ thin films grown on c-sapphire substrate by Pulsed Laser Deposition. The band gap of the as grown $Mg_{0.48}Zn_{0.52}O$ film was found to be ~ 4.4 eV with high transparency in the visible region. The MSM photodetector fabricated with interdigitated Pt electrodes in Pt-$Mg_{0.48}Zn_{0.52}O$-Pt geometry showed peak responsivity of ~0.9 mA/W at 267 nm at 60 V bias with single cut-off wavelength of ~ 280 nm and UV/Visible rejection ratio $R_{267\text{-}nm}/R_{400\text{-}nm}$ of ~10^3 which are promising for practical solar blind UV photodetection applications.

CP-03-6. EFFECT SMALL ANGLE NEUTRON SCATTERING STUDY OF TRANSPARENT LASER HOST ND:YAG CERAMIC

*Rachna Selvamani[1], Gurvinderjit Singh[2,3], Debasis Sen[1,3], P.U Sastry[3], [1]Solid State Physics Division, Bhabha Atomic Research Centre, Mumbai-400085, [2]Laser & Functional Materials Division, Raja Ramanna Centre for Advanced Technology, Indore-452013, [3]Homi Bhabha National Institute, Anushaktinagar, Mumbai-400094,[*]**E-mail**: srachna@barc.gov.in*

We have investigated the pore morphology of transparent Nd:YAG ceramics prepared by co-precipitation method using small angle neutron scattering technique. Results showed the pores ranging from 20nm to 800nm with mean size of 230 nm having smooth surfaces. The pores with poly-dispersity and size distribution may contribute significantly for scattering of light and the overall optical transparency of the ceramic. Detailed results are discussed.

CP-03-7. THEORETICAL ANALYSIS OF PHOTONIC SWITCHING NETWORKS USING SILICON RING ASSISTED DIRECTIONAL COUPLERS WITH FABRICATION TOLERANCE

Madhupriya Ganesh, Mubarak Ali Meerahsa, Indhumati Ravirajan and Krishnamoorthy Pandiyan, Integrated Optics Lab, Centre for Nonlinear Science and Engineering (CeNSE), School of Electrical

& Electronics Engineering, SASTRA Deemed-to-be University, Thanjavur-613401, Tamil Nadu, India., E-mail: krishpandiyan@ece.sastra.edu

In this work, we have designed a photonic switch architecture using ring assisted directional couplers(RADC) switches implemented in the SOI platform which facilitates an enhanced mode confinement. The electro optic tuning in the proposed RADC is achieved by varying the carrier concentration across the P-i-N junction. A comparitive analysis of the ring assisted Mach Zehnder intererometer (RAMZI) and the proposed RADC were done using finite difference beam propagation method. The proposed RADC has an optimized extinction ratio (ER), crosstalk performaces and has 5% tolerance in fabrication variation of the waveguide width and the height. Various qualitative factors such as free spectral range (FSR), ER, transmission characteristics, low crosstalk, insertion loss have been validated for both the proposed designs. The proposed RADC has 65% of the wafer footprint compared to the RAMZI configuration and is practically realizable in large scale switching architectures.

CP-03-8. FAST DETECTION OF REFRACTIVE INDEX INHOMOGENEITY IN UNPOLISHED NEODYMIUM-DOPED PHOSPHATE GLASS SLABS USING INDEX MATCHED LIQUID BY SCHLIEREN TECHNIQUE

Sanjiv Kumar Tiwari[1], Sarvendra Singh[1], G. Muralidharan[1], Y. Pavan Kumar[1], G. Ragoubady[1], Anil Kumar[1], S. S. Thangavel[1], Rishipal[1], A. K. Biswas[1], M P Kamath[1], N S Benerji[1] and K S Bindra[1,2], [1]Optical Design and Development Laboratory, High Energy Optics Section, Laser Technology Division, Raja Ramanna Centre for Advanced Technology, Indore 452013, [2]Homi Bhabha National Institute, Training School Complex, Anushakti Nagar, Mumbai 400094, ***E-mail**: sanjiv@rrcat.gov.in*

We describe the development of a rapid and reproducible method of detecting refractive index (RI) inhomogeneity in large size unpolished Neodymium (Nd)-doped phosphate glass slabs using index matched liquid by Schlieren technique. The system uses 300 mm diameter collimated white light beam for a single frame Schlieren imaging of large Nd-doped phosphate glass slabs and RI matched liquid to detect bulk refractive index inhomogeneity. The use of an expanded beam for detecting inhomogeneity has reduced the complexity of the scanning and stitching technique and also the index matching fluid makes the detection technique faster to a larger extent by avoiding time consuming optical polishing of the glass for bulk inhomogeneity detection. Qualitative estimate of the RI inhomogeneity of the whole glass slab can be performed by capturing a single Schlieren image. Instead of two weeks long optical polishing required for scanning and stitching Schlieren technique, only few hours optical grinding of the faces of the Nd: glass slabs (with surface roughness R_q less than 1.2 μm) is sufficient even for a RI mismatch of 0.0297 with the index of Nd: phosphate glass to detect bulk RI inhomogeneity of the order of 10^{-3}.

CP-03-9. MINIMIZING VARIATION IN SYSTEM EFFICIENCY OF A DOUBLE-PASS ACOUSTO-OPTIC MODULATOR SETUP MINIMIZING VARIATION IN SYSTEM EFFICIENCY OF A DOUBLE-PASS ACOUSTO-OPTIC MODULATOR SETUP

K. Karthick Ramanathan, Hriday Dath†, Radhika V N†and Umesh Kadhane*, *Indian Institute of Space Science and Technology, †ISRO Inertial Systems Unit,* ***E.mail*** *: karthick.ramanathan05@gmail.com*

The dependence of output intensity of a conventional double-pass in a acouto optic modulator system on the supplied RF modulation frequency presents a practical problem in laser cooling experiments that is often detrimental to the cooling process. Here, we delve into the theoretical reasons for such variation and present the results of a study conducted to identify the

experimental parameters that are crucial in affecting system efficiency. An improved setup with additional optics is proposed, which helps minimize the variation in output efficiency as the modulation frequency is varied, and also provides control in choosing the range of frequencies over which maximum efficiency is desired.

CP-03-10. EFFECT OF ANNEALING ON THE OPTICAL PROPERTIES OF TRANSPARENT ND:YAG CERAMIC

S. Karmakar[1], S. K. Pathak[1] and S. M. Gupta[1,2], [1]Laser and Functional Materials Division, Raja Ramanna Centre for Advanced Technology, Indore-452013, [2]Homi Bhabha National Institute (HBNI), Training School Complex, Anushaktinagar, Mumbai-400094, ***Email:****sanjib@rrcat.gov.in*

Effect of air annealing on the attenuation coefficient of Nd-YAG ceramic is investigated. The vacuum sintered Nd-YAG ceramic is annealed in air at different temperatures for 20 hrs. Reduction in the colour centers is observed, which is attributed to removal of oxygen vacancies related defect. Phase analysis confirms the presence of randomly oriented grains in the ceramic. Densification of the green pellet using dilatometer, revealed a sharp increase from 45 to 98% in the relative density between 1300-1450 °C, which is due to densification process and then slow increase from 98% to more than 99% relative density around 1780 °C is due to coarsening of the grain. Residual porosity present in the ceramic is visualized by scattering of He-Ne light in custom made setup and scattering loss is estimated by comparing the intensity of light before and after passing through the sample..

CP-03-11. GRAPHENE ENHANCED DUAL BAND NEAR IR ABSORBER IN A MULTILAYER GRATING STRUCTURE

C. Kar[1], S Jena[2], D V Udupa[2] and K Divakar Rao[1], [1]Photonic & Nanotechnology Section, A&MPD, BARC, Visakhapatnam 531011, [2]Optics and Analytical Spectroscopy Section, A&MPD, BARC, Mumbai 400085, **Email:** kchinmaya@barc.gov.in*

We propose a graphene enhanced high Q-factor dual mode absorber for optoelectronic applications such as photo-detectors, sensors, optical filters, and thermal emitters in the near-infrared-region (NIR). The absorber dual modes arise due to simultaneous existence of the optical Tamm state (OTS) and the Tamm plasmon polariton (TPP) in a multilayer grating structure. The OTS occurs at the interface between the silicon grating and the distributed Bragg reflector (DBR), while the TPP occurs at the interface between the silver (Ag) layer and the DBR. The TPP exhibits higher Q-factor as compared to that of the OTS. The photonic structure possesses geometrical tunability and its spectral characteristics can also be actively fine-tuned by varying the refractive index of the surrounding media.

CP-03-12. INTEGRATED OPTICAL MICHELSON INTERFEROMETER ON A CHIP

*Ashish Singh Bais, Lokendra Singh Chouhan and Joseph Thomas Andrews, Applied Photonics Laboratory, Department of Applied Physics & Optoelectronics, Shri G. S. Institute of Technology and Science, 23 Park Road, Indore 452 003 MP, India, **Email:** jtandrews@gmail.com*

Optical waveguide-based 3dB Bi-Directional Coupler is designed, simulated and fabricated using UV-photolithography. S-1813 is used as photoresist and UV laser diode at 385nm is used for writing the channel waveguide structure. The design is optimized for light propagation at 1.55□m. The optimization parameter of the interferometer design and results are discussed. The fabricated device finds potential applications and as a low-cost alternative for point-of-contact devices.

CP-03-13. GROWTH KINETICS STUDIES OF (100) FACE OF L-ARGININE PHOSPHATE (LAP) SINGLE CRYSTAL USING BIREFRINGENCE INTERFEROMETRY TECHNIQUE

S. K. Sharma[*1], *Yashpal Singh*[1] *and Indranil Bhaumik*[1,2], [1]*Laser and Functional Materials Division, Raja Ramanna Centre for Advanced Technology, Indore, (M.P.) 452013,* [2] *Homi Bhabha National Institute, Training School Complex, Anushakti Nagar, Mumbai 400094, India,* ****E-mail**: sks@rrcat.gov.in.*

In this article, the growth kinetics studies of relatively slow growing (100) face of LAP crystal with varied supersaturation is presented with an aim to find the conditions to enhance its growth rate. The growth rate of (100) face was precisely measured using the birefringence interferometry technique. The growth rate was measured by orienting a seed crystal such that the laser beam passes along the dielectric x-axis. Further the growth rate along a-axis {perpendicular to (100) faces} was evaluated by taking its vector component. The results show that the growth rate of (100) faces increases almost uniformly with the supersaturation. This indicates that high supersaturation would lead to high growth rate along (100) face. The grown crystal was also characterized for to assess its optical quality and defects density..

CP-03-14. SYNTHESIS OF CARBON-AEROGEL BASED FOAM TARGETS FOR LASER MATTER INTERACTION STUDIES

S. Bhartiya[*,a)], *D.K. Kohli*[a)], *Ashish Singh*[a)], *Rashmi Singh*[a)], *Amrendra Singh*[b)], *T. Mandal* [c),d)], *V Arora* [c),d)], *A. Moorti* [c),d)], *J A Chakera* [c),d)] *and M.K. Singh*[a)], [a)]*Laser & Functional Materials Division,* [b)]*Laser Technology Division,* [c)]*Laser Plasma Division, Raja Ramanna Center for Advanced Technology, Indore-452013,* [d)]*Homi Bhabha National Institute (HBNI), Training School Complex, Anushaktinagar, Mumbai-400094,* ****Email**: sushmitab@rrcat.gov.in*

We have formulated an approach to synthesize low density foam targets using carbon aerogel(CA) for laser matter interaction studies. Well characterized carbon aerogel having high surface area ~ 1918 m^2/g was used as the main constituent for obtaining low-density films. Suspension containing carbon aerogel with suitable binder was sprayed on metal foil substrates using fine air spray gun to achieve 10-20 µm thick targets. SEM & surface profiling of the target surface was performed which revealed uniform film formation. Initial investigations performed on Kα x-ray measuremnts showed significant improvement in signal to noise ratio (from 3.1 to ~ 7.2) with CA coated Cu target compared to bare Cu using 150 TW, 25 fs Ti:Sapphire laser.

CP-03-15. ULTRA-SENSITIVE TEMPERATURE/PHOTON SENSING USING AL/SI BIMATERIAL MICROCANTILEVER

M. Raghu Ramaiah[1,2] *and K. Prabakar*[1,2], [1]*Surface and Nanoscience Division, Materials Science Group, IGCAR, Kalpakkam-603102, India,* [2] *Homi Bhabha National Institute, IGCAR, Kalpakkam-603102, India.,* **** E-mail:** mraghuram@igcar.gov.in*

In the present work, the role of metal coating thickness on the thermomechancial sensitivity and response time of bimaterial microcantilevers (BMC) is studied through photothermal mechanism. Experiments were performed on Al/Si BMCs having varying metal layer thickness (50 – 300 nm) using an AFM head, by exposing them to 2.5 mW, UV laser source (wavelength:406 nm). Effect of metal layer thickness on the deflection sensitivity and response time are discussed in detail.

CP-03-16. QUANTIFICATION OF NUTRIENT CONTENT IN CARICA PAPAYA USING LASER INDUCED BREAKDOWN SPECTROSCOPY

K. Veerappan, V. Sathiesh Kumar, Department of Electronics Engineering, MIT Campus, Anna University, Chennai, Tamilnadu, India – 600044., Email: veerappank09@gmail.com, sathieshkumar@annauniv.edu

In this paper, the elemental composition of *Carica papaya* (papaya) sample is determined using laser induced breakdown spectroscopy (LIBS) technique. The spectrum is obtained by varying the laser irradiance in the range of 2 x 10^{11} W/cm2 to 3 x 10^{11} W/cm^2. The sample contains elements such as Calcium, Magnesium, Potassium, Chlorine, Zinc and Sodium. Assuming local thermodynamic equilibrium (LTE), the plasma parameters such as plasma temperature and electron density are estimated using the Boltzmann plot and Saha – Boltzmann equation, respectively. It is observed that the plasma temperature and electron density is in the order of 5570±600 and 1.7±0.2*10^{22}. Calibration free LIBS method is used to determine the concentration of Calcium (0.488±0.042), Magnesium (0.975±0.009) and Potassium (0.493±0.031) in *Carica papaya*.

CP-03-17. FABRICATION AND TESTING OF TSB/PMMA COMPOSITE ELEMENTS FOR X-RAY IMAGING AT INDUS-2

*Chiranjit Debnath,S Kar, Ashish K Agrawal, Sunil Verma, Shovan Kumar Majumder, Raja Ramanna Centre for Advanced Technology, Indore, **E-mal:** cdebnath1785@gmail.com*

Trans-stilbene scintillator in polymer composite form has been developed for large area x-ray detection and imaging purpose. The synthesis process and the optical quality of the polymeric scintillator has been characterized using spectrophotometer and photoluminescence measurements. Finally, TSB/PMMA polymer composite elements having different trans-stilbene concentration have been prepared and tested for x-ray imaging applications using Indus-2 facility.

CP-03-18. SYNTHESIS OF $MG_2GEO_4:MN^{4+}$ PHOSPHOR AND ITS CHARACTERIZATION FOR X-RAY BEAM POSITIONING (DETECTION) AND IMAGING APPLICATIONS USING INDUS-2 FACILITY

S. Kar [1,2,], C. Debnath [1,2], Puspen Mondal [3], Ashish K Agrawal [4], Sunil Verma [1,2], Shovan Kumar Majumder [1,2], [1] Laser Biomedical Application Division, Raja Ramanna Centre for Advanced Technology, Indore - 452013, India, [2] Homi Bhabha National Institute, BARC Training School Complex, Anushakti Nagar, Mumbai - 400095, India, [3] Synchrtrons Utilization Section, Raja Ramanna Centre for Advanced Technology, Indore - 452013, India, [4] Technical Physics Division, Bhabha Atomic Research Centre, Trombay, Mumbai - 400085, India, ***Email:** sujan@rrcat.gov.in*

Mn doped Mg_2GeO_4 phosphor material has been prepared by high temperature solid state reaction method, and optical characterization has been performed by photoluminescence and thermoluminescence techniques. Studies on optimization of the synthesis process parameters, and preliminary results obtained using Indus-2 beam-lines for x-ray beam position monitoring and x-ray imaging applications are reported.

CP-03-19. GROWTH AND INVESTIGATION OF STRONTIUM BORATE SINGLE CRYSTALS FOR NONLINEAR OPTICAL AND THERMO-LUMINESCENCE APPLICATION

*Ratna Karn[1], M. Soharab[1,2], Ashish Chadar[3], A. Saxena[1], B. K. Sajith[1], R. Bhatt[1,2], Indranil Bhaumik[1,2], [1]Laser Functional Materials Division, Raja Ramanna Centre for Advanced Technology, Indore-452 013, India, [2]Homi Bhabha National Institute, Training School Complex, Anushakti Nagar, Mumbai-400094, India, [3]Deptartment of Applied Physics, G.S. Institute of Technology & Science, Indore, India., *E.mail: ratnakarn@rrcat.gov.in

Undoped and Eu (0.1 at.%) doped Strontium tetra borate (SrB_4O_7, SBO) single crystal were grown by low gradient Czochralski method. The high viscosity and volatility associated with the borate melt poses challenge in the growth of high quality crystals, resulting in defects like, inclusions, capping, striations, opacity and cellular growth in the grown crystal. Powder XRD analysis confirmed the formation of desired phase and revealed a small variation in the lattice parameter c on Eu doping. The transmission spectra showed deep UV transmittance (more than 60% at 190nm). TL glow curve were recorded on the X-rays and UV exposed samples. Eu activated SBO samples showed higher TL intensity than undoped SBO and therefore, can be considered as a potential material for dosimetry application.

CP-03-20. SYNTHESIS & CHARACTERIZATION OF BLUE LIGHT EMITTING $NAYF_4$: YB,TM UPCONVERSION NANOPARTICLES

*Sandeep Agarwalla,[1,4] Priyanka Ruz [2], Jyotirmayee Mohanty,[3,4] G Sridhar,[1,4] and V. Sudarsan[2,4,] [1]Beam Technology Development Group,[2]Chemistry Division, [3]Radiation & Photochemistry Division, [4]Homi Bhabha National Institute, Mumbai, India, Bhabha Atomic Research Centre, Mumbai 400 085, India, E-mail: sandeepk@barc.gov.in

Tm^{3+} based upconversion process was studied in a fluoride based inorganic host namely, $NaYF_4$. Nanoparticles of $NaYF_4$ co-doped with Yb^{3+} and Tm^{3+} were prepared based on a soft chemical procedure. The photo-luminescence study shows that a 980nm laser excitation sample emits at 450 nm, 478 nm , 646 nm & 800 nm because of two photon absorption upconversion processes. From the upconversion luminescence (UCL) studies, it is informed that the ratio of 800 nm to 478 nm emission intensity decreases exponentially with increase in power of excitation laser and this has been explained based on low phonon energy of the host matrix.

CP-03-21. DEVELOPMENT OF LASER WORKSTATION ATTACHMENT (LWA) AND ITS APPLICATION FOR SURFACE PERIODIC STRUCTURE GENERATION

*S. K. Das[1,] * and P C Singh[2] , [1]School of Physics, Gangadhar Meher University, Amruta Vihar, Sambalpur, Odisha, Pin- 768004, India [2]Department of Physics, School of Applied Sciences, Kalinga Institute of Industrial Technology Deemed to be University, Bhubaneswar, Odisha, 751024.India., *Email: skdas@gmuniversity.ac.in and skdas.gmu@gmail.com

In this work a new system LWA is designed and realized. The developed LWA system was successfully tested for generation of highly uniform SPS on Si. It is compact in size, easily portable, easy to handle and cost effective. It can be interfaced to any kind of laser. Beside that the developed LWA gives a unique opportunity of using the existing lasers in the workplace for material processing like SPS. The developed LWA system can also be used for other material processing work like cutting, drilling, annealing, etching, policing, marking etc

CP-03-22. THE DESIGN AND IMAGING CHARACTERISTICS OF A RADIATION RESISTANT ACHROMATIC RELAY LENS

Sanjiva Kumar and D V Udupa, Atomic & Molecular Physics Division, Bhabha Atomic Research Centre, Mumbai – 400085,* ***E-mail** address: sanjivk@barc.gov.in

A radiation resistant 50 mm f/4 achromatic doublet lens has been designed for relaying the images from the objective to CCTV sensor of an optical periscope being developed for viewing inside a radioactive waste immobilization plant. The design utilizes a computer aided ray tracing software for a chosen pair of cerium-stabilized optical glasses for the component singlet lenses of the doublet. A specific study of imaging characteristics of the doublet in terms of its chromatic aberrations has been presented using the geometrical optics calculations.

CP-03-23. DEVELOPMENT OF METAL-DIELECTRIC NARROW BAND PASS FILTER FOR DIODE LASER INDUCED PHOTOLUMINESCENCE MEASUREMENT APPLICATIONS

R. B. Tokas S Jena, S. Thakur and D V Udupa, Atomic & Molecular Physics Division, Bhabha Atomic Research Centre, Mumbai – 400085,* ****E-mail*** *address: tokas@barc.gov.in*

In present work, a narrow band pass metal dielectric filter has been designed and developed. The filter is intended to be used in a set-up in which a diode laser (808 nm) induced photoluminescence signal from some specific nanomaterial is measured. The nanomaterials would be used for anti-counterfeiting applications. The filter has been designed to pass photoluminescence radiation (1064 nm) and extinguish excitation light of wavelength 808 nm. Ag and TiO_2 were chosen as design materials owing to their relevant optical properties in the wavelength region of interest. Peak transmission of the filter is 22.5% at 1064 nm and optical density at 808 nm is ~ 4. It is observed that measured peak transmission is less than the designed one. Process induced errors in thickness of Ag and TiO_2 layers have been attributed to the difference in peak transmission value of pass band

CP-03-24. MGZNO BASED MSM SOLAR BLIND UV PHOTODETECTOR GROWN BY PULSED LASER DEPOSITION

S K Chetia[1, 2], Amit K Das[1], R S Ajimsha[1] and P Misra[1, 2], [1]Raja Ramanna Centre for Advanced Technology, Indore, [2]Homi Bhabha National Institute, Mumbai,* ***Email:*** *shantanuk@rrcat.gov.in*

We have developed solar blind UV photodetector based on mixed phase $Mg_{0.48}Zn_{0.52}O$ thin films grown on c-sapphire substrate by Pulsed Laser Deposition. The band gap of the as grown $Mg_{0.48}Zn_{0.52}O$ film was found to be ~ 4.4 eV with high transparency in the visible region. The MSM photodetector fabricated with interdigitated Pt electrodes in Pt-$Mg_{0.48}Zn_{0.52}O$-Pt geometry showed peak responsivity of ~0.9 mA/W at 267 nm at 60 V bias with single cut-off wavelength of ~ 280 nm and UV/Visible rejection ratio $R_{267\text{-}nm}/R_{400\text{-}nm}$ of ~10^3 which are promising for practical solar blind UV photodetection applications

CATEGORY 04: NONLINEAR, QUANTUM AND ATOM OPTICS

CP-04-1. FLEXIBLE ALL-POLYMER NONLINEAR BRAGG REFLECTORS FOR IMPROVING THE OPTICAL NONLINEARITY OF 5,15-DI(PYRIDYL)-10,20-BIS(PENTAFLUOROPHENYL)PORPHYRIN

M. V Vijisha[1,2], Bharat Misra[1] and K. Chandrasekharan[1,], [1] Laser and Nonlinear Optics laboratory, Department of Physics, National Institute of Technology Calicut, Kozhikode 673601, Kerala, India, [2] International School of Photonics, Cochin University of Science and Technology, Kochi, Kerala 682022 , Email : csk@nitc.ac.in*

Nonlinear 1D photonic crystal (PC) in which alternating layers are doped with a nonlinear optical (NLO) material, is utilized to investigate the NLO characteristics of 5,15-di(pyridyl)-10,20-bis(pentafluorophenyl) porphyrin using Z-scan method. A ~3-fold enhancement in the NLO response of the porphyrin molecule is achieved with the nonlinear PC relative to the reference sample. The observed enhancement in the NLO properties with the nonlinear PC can be ascribed to the slow-light effects at the photonic band edge as well as the band-edge shifting mechanism caused by the nonlinear refraction of the porphyrin.

CP-04-2. RESIDUAL DOPPLER AVERAGING IN AN INVERTED Y TYPE SYSTEM

K. Yadav[a,] and A. Wasan[b], [a]Department of Physics, Ahir College, Rewari, 123401 India, [b]Department of Physics, Indian Institute of Technology, Roorkee, 247667 India,* ***Email:*** **kavitayiitr@gmail.com,*

Chalcogenide A theoretical model using density matrix approach has been presented to show the influence of residual Doppler averaging on Electromagnetic Induced Transparency (EIT) in inverted-Y atomic system. A four-level system is considered including one excited state as Rydberg state for ^{87}Rb showing comparison of EIT behaviour for Doppler free and Doppler broadened systems.

CP-04-3. CPT RESONANCE FREQUENCY SHIFT IN RB-NE VAPOR CELL FOR APPLICATION IN ATOMIC CLOCK

Rajaiah Kaitha[1], R. Manjula[2], Pragya Tiwari[2], Minni J. Kappen[2], Shubhajit Biswas[2], Swarupananda Pradhan[3], T. Venkatappa Rao[4], S. B. Umesh[2], P. Kalpana Arvind[2], S. Elumalai[2], K. V. Sriram[2], Prashanth C. Upadhya[2],[1]U.R. Rao Satellite Centre, ISRO, Bangalore, India, [2]Laboratory for Electro-Optics Systems, ISRO, Bangalore, India, [3]Bhabha Atomic Research Centre, Mumbai, India, [4]Department of Physics, NITW, Warangal, India, Email: krajaiah@ursc.gov.in

We have performed experiments to study CPT resonance in ^{87}Rb atoms by measuring its frequency shift as function of laser excitation and temperature of atomic vapor cell. Our results indicate that laser intensity dependent shift in the center frequency of CPT resonance is highly sensitive to temperature and its effect is minimum at an optimum temperature of ~72 ^{0}C. For temperatures above or below the optimum value, the magnitude of frequency shift increases non-linearly. In our experiment, this temperature also corresponds to the maxima of quality factor of CPT resonance. However, temperature dependent frequency shift is sensitive to laser intensity. We discuss the underlying dynamics involving interaction between laser-Rb atoms and Rb atom-buffer gas.

CP-04-4. MAGNETIC MICRO-TRAPPING OF LASER COOLED RB-ATOMS USING A GOLD Z-WIRE TRAP ON ATOM-CHIP

Vivek Singh[a,b,], V B Tiwari[a, b], A. Chaudhary[a], R. Shukla[b, c], C. Mukherjee[b, d] and S R Mishra[a, b], [a]Laser Physics Applications Section, Raja Ramanna Centre for Advanced Technology, Indore-452013, India., [b]Homi Bhabha National Institute, Training School Complex, Anushakti Nagar, Mumbai - 400094, India., [c]Synchrotons Utilization Section, Raja Ramanna Centre for Advanced Technology, Indore-452013, India., [d]Laser Technology Division, Raja Ramanna Centre for Advanced Technology, Indore-452013, India., ***E.mail:** viveksingh@rrcat.gov.in*

Here, we report the magnetic micro-trapping of cold ^{87}Rb atoms in Ioffe-Pritchard (IP) type magnetic trap created by the combination of magnetic field due to a current carrying micro-wire (200 µm x 2.5 µm cross-section) on atom-chip and bias fields. The number of atoms trapped in magnetic trap of atom-chip was ~ 1.5 x 10^6 with a life-time of ~ 65 ms. The atom-chip can be useful in developing compact cold atoms-based sensors for high precision metrology of time, magnetic field and inertial parameters (such as gravity, acceleration and rotation).

CP-04-5. ROTATION OF A LASER COOLED ^{87}RB ATOM CLOUD USING TIME AVERAGED ADIABATIC POTENTIAL (TAAP) SCHEME

Sourabh Sarkar[a, b], S P Ram[a], Kavish Bhardwaj[a], V B Tiwari[a,b], S R Mishra[a,b], [a]Laser Physics Applications Section, Raja Ramanna Centre for Advanced Technology, Indore – 452013, [b]Homi Bhabha National Institute, Training School Complex, Anushakti Nagar, Mumbai – 400094, ***E.mail**: sourabhs@rrcat.gov.in*

We have theoretically shown the possibility of rotation of an atom cloud around the circumference of a ring using time averaged adiabatic potential (TAAP) scheme. This rotation of atom cloud is useful in atom-gyro and the study of superfluidity.

CP-04-6. IMPLEMENTATION OF MAGNETO OPTICAL TRAP IN COMPACT TITANIUM UHV CHAMBER

*Hriday Dath, S. Kannan, Radhika V N, and Rekha A. R, ISRO Inertial Systems Unit (IISU), Vattiyoorkavu, Trivandrum. **E-mail**: hridaysunildath@gmail.com*

Experiments involving laser cooled atoms to study the wave property of matter has garnered a lot of attention in the past decades. It shows real promise in inertial sensing, metrology, time keeping, studies on fundamental constants, and quantum computing. There are multiple groups around the world working on cold atom interferometry aiming to develop high sensitive inertial sensors for very high accuracy autonomous navigation. The attempts towards the miniaturization of the laboratory setup are crucial for such experiments to be used in field applications. In this paper we discuss the design and implementation of Magneto Optical Trap of Rb 87 atoms in the miniaturized vacuum chamber, and the generation and characterization of the cold atom cloud.

CP-04-7. EFFECT OF OFF-RESONANT LIGHT ON THE TRAP LOSSES IN A QUADRUPOLE MAGNETIC TRAP

Kavish Bhardwaj[a], S P Ram[a], S. Sarkar[a,b], V B Tiwari[a,b] and S R Mishra[a,b], [a]Laser Physics Applications Section, Raja Ramanna Centre for Advanced Technology, Indore-452013, India. [b]Homi Bhabha National Institute, Training School Complex, Anushakti Nagar, Mumbai -400094, India, *E.mail: kavish@rrcat.gov.in*

We have performed magnetic trapping of laser cooled atoms in an ultra high vacuum (UHV) chamber. The lifetime of atoms in magnetic trap was estimated to be ~ 5.5 s. The trap loss in the magnetic trap due to inelastic collisions has been studied. In presence of an off-resonant laser beam, the two body trap loss coefficient was found to increase significantly as compared to background collision loss coefficient.

CP-04-8. EFFICIENT SECOND HARMONIC AND TERAHERTZ GENERATIONS FROM BIBO CRYSTAL USING ULTRASHORT LASER PULSES

Chandan Ghorui[1], A.M. Rudra[2], Udit Chatterjee[3], A.K. Chaudhary[1], and D. Ganesh[1] Advanced Centre for Research in High Energy Materials , University of Hyderabad, Telangana,500046, India, [2]Physics Department, Raj College, Burdwan, W.B, 713104,[3]Laser Laboratory, Department of Physics, Burdwan University,Burdwan,W.B,713104,* ***Email:*** akcphys@gmail.com

The paper reports the second harmonic in UV region and terahertz (THz) generations between 0.1-3 THz range from a Type I, $\theta=28.9^0$ cut, 1.29 mm thick BIBO crystal using ultrashort pulse-based femtosecond laser. We have employed 800 nm wavelength pulses of 50 and 140 fs at wavelength 800 nm that is obtained from a Ti: Sapphire laser amplifier and oscillators at 1 kHz and 80 MHz repetition rates laser . The conversion efficiency of SHG was ~ 50 % while that for THz generations was of the order of 1.85×10^{-5} %. R.I and absorption coefficient also ascertained.

CP-04-9. MANIFESTATION OF JANUS-FACED NATURE OF QUANTUM STATES IN ENERGY DENSITY

S. Kannan, Hriday Dath, and Radhika V N, ISRO Inertial Systems Unit, Thiruvananthapuram, 695 013, India. HBNI, Jatni 752050, ***E-mail:*** *kns.phys@gmail.com*

The manifestation of squeezing in the energy density was discussed in a recent work . In this work, we see how the `Janus-faced' properties of the partner states are mirrored in the energy density plot. As already established, the presence of squeezing is easily obtained from the negativity in the energy density. As an example, we consider two important pair of quantum states: (i) Even cat state and the squeezed vacuum state , and (ii) Odd cat state,[2] and the squeezed excited state. We see the interesting signatures of these 'Janus-faced' partner states in the energy density plot.

CP-04-10. NONLINEAR OPTICAL CHARACTERISTICS OF AQUEOUS CHLOROPHYLLIN SODIUM COPPER SALT USING Z-SCAN TECHNIQUE UNDER UV EXCITATION

*C. Pradeep *, V. Pradeep Kumar, Pramod Gopinath, International School of Photonics, Cochin University of Science and Technology, Cochin 682022, Kerala, India* ***Email:*** *chandran@cusat.ac.in*

Chlorophyllin sodium copper salt was investigated as an excellent organic nonlinear optical materials. Using single-beam transmissive open aperture Z-scan technique with a nanosecond, frequency tripled Nd:YAG laser, the aqueous chlorophyllin sodium copper salt solution showed good nonlinear absorption properties. The reverse saturable absorption was analysed and confirmed to be a two-photon absorption model. The nonlinear absorption parameters such as nonlinear absorption coefficient and nonlinear absorption cross-section was estimated. The two-photon absorption cross-section of this salt at 355 nm was found to be of the order of 10^8 GM.

CP-04-11. SPECTRAL CHARACTERISTICS OF THE 355 NM PUMPED NANOSECOND SLM OPO FOR SELECTIVE PHOTOIONIZATION STUDIEG

C S Rao, D Biswal, Asawari D Rath, S Kundu, Tunable Laser Section, Advanced Tunable Laser Applications Facility, Beam Technology Development Group, Bhabha Atomic Research Centre,* ***Email:*****somu@barc.gov.in*

We have developed a 355 nm pumped (20 Hz PRF) single longitudinal mode (SLM) Optical Parametric Oscillator (OPO) which is continuously tunable over a spectral range of 500 – 600 nm. The developed SLM OPO was configured as a first step excitation source in the three-step selective photoionization scheme developed for the selective photoionization studies on Lu-176. The performance of the SLM OPO has been evaluated. The spectral measurement shows that the time averaged spectral linewidth of the OPO is less than 200 MHz with a long term spectral stability of $\pm$ 10 fm.

CATEGORY 05: LASER PLASMA INTERACTION

CP-05-1. EXPERIMENTAL STUDY ON SELF-COMPRESSION OF INTENSE ULTRASHORT LASER PULSE PROPAGATING IN OXYGEN GAS SHEATH

*A. Ansari[a], M. Kumar[a], H. Singhal[a,b] and J A Chakera,[b], *[a]Raja Ramanna Centre for Advanced Technology, Indore [b]Homi Bhabha National Institute, Anushaktinagar, Mumbai,* ***Email:*** *ajmal@rrcat.gov.in*

We have experimentally investigated the temporal self compression of intense femtosecond laser pulse at laser intensity close to the ionizing threshold by focusing it in oxygen gas sheath flowing from a needle. The self-compression is accomplished by broadening of spectral bandwidth due to self-phase modulation and required negative chirp through strong spatio-temporal reshaping of the laser pulse. We have temporally and spectrally characterized the output laser pulse. The laser pulse is observed to compress temporally with increase in gas pressure from ~55fs (no gas condition) to ~35fs (at ~1bar).

CP-05-2. DEMONSTRATION OF SUPER-PONDEROMOTIVE ACCELERATION OF FAST ELECTRONS IN ULTRASHORT HIGH-INTENSITY LASER FOIL INTERACTION

T. Mandal[1,2], V Arora[1], A. Moorti[1,2], R.A. Khan[1] and J A Chakera[1,2]. [1]RRCAT, Indore 452 013. [2]HBNI, Training School Complex, Anushaktinagar, Mumbai 400 094. ***E.mail:** tirtham@rrcat.gov.in*

We present the experimental demonstration of super-ponderomotive acceleration of fast electrons through varying preplasma scale length in the interaction of ultrashort (~25 fs) high intensity (~3-4x10^{19} W/cm^2) laser with thin foil (Cu 7µm) target. Generally, fast electron temperature in intense laser solid interaction is limited by ponderomotive scaling (T_f^{pond} ~1.46 MeV at *I*~3x10^{19} W/cm^2) due to relatively small density scale length. However, it has been shown that temperature beyond the ponderomotive limit could also be achieved by increasing preplasma scalelength using a separate pre pulse (~600ps, *I~1x10^{13} W/cm^2*). The results are understood considering applicable additional absorption mechanisms in case of larger pre plasma scale length.

CP-05-3. EFFECT OF THIN GOLD (AU) COATING ON PROTON ACCELERATION FROM A TRANSPARENT MYLAR FOIL TARGET

M. Tayyab[1], S. Bagchi[1], A. Upadhyay[2], A. Moorti[1,3] and J A Chakera[1,3] ; [1]Laser Plasma Division, RRCAT, Indore – 452 013, [2]Laser Technology Division, RRCAT, Indore – 452 013, [3]Homi Bhabha National Institute, Anushakti Nagar, Mumbai – 400 094 ***Email****: tayyab@rrcat.gov.in*

In the present work the effect of thin metallic Gold (Au) coating on proton acceleration from transparent Mylar foils have been studied. A quite different result of thin Au coating was observed for the two cases of coating i.e. at the front surface (laser facing side) or at the foil back surface. In the former case, enhancement in accelerated proton energy as well as flux was observed, whereas, in the later case it was found to be highly detrimental for proton/ion acceleration. The observations are explained by considering the target transparency for 800 nm laser pulse and subsequent pre-plasma formation. The experimental observations are also supported by the PIC simulations.

CP-05-4. EFFECTS OF CARRIER HEATING ON AMPLIFICATION CHARACTERISTICS OF BRILLOUIN SCATTERED STOKES MODE IN III-V AND II-VI SEMICONDUCTOR MAGNETO-PLASMAS

Pinki Kumari[1,], B.S. Sharma[1], Manjeet Singh[2], [1]Department of Physics, Lords University, Chikani, Alwar – 301028, (Rajasthan) India, [2]Department of Physics, Government College, Matanhail, Jhajjar – 124106 (Haryana) India, *Email: pinki.lordsuniv@gmail.com*

We develop a theoretical formulation followed by numerical analysis to study the effects of carrier heating on Brillouin amplification characteristics of Brillouin scattered Stokes mode in III-V and III-VI semiconductor magneto-plasmas. Numerical analysis is made for three different Brillouin cells and illuminated by a pulsed CO_2 laser. The nature of dependence of parameters characterizing Brillouin amplification on applied magnetic field is explored with excluding and including effects of carrier heating.

CP-05-5. INVERSE COMPTON SCATTERING GAMMA RAY SOURCE: PIC SIMULATION

A. Upadhyay, K. Madhubabu, Y.B.S.R. Prasad and K S Bindra, Laser Technology Division, Raja Ramanna Centre for Advanced Technology, Indore – 452 013. *Homi Bhabha National Institute, Training School Complex, Anushakti Nagar, Mumbai, 400094, **E.mail :** ajitup@rrcat.gov.in.*

In the present work the particle-in-cell (PIC) simulation of Gamma radiation emitted due to inverse Compton scattering of a laser pulse with laser-wakefield accelerated electrons is reported. In the simulation, an intense ultra-short laser pulse (25 fsec with laser intensity of 2.6 x 10^{19} W/cm^2)was focused to a spot of 18 μm diameter inside a gas jet of plasma density 7x10^{18}cm^{-3} yielding quasi-monoenergetic electrons of energy 250 MeV ± 35 MeV. When a second laser pulse of intensity 1.0x10^{18} W/cm^2 collided with these accelerated electrons, Gamma ray photons (>10^7 photons) up to energy 1.75 MeV were observed within an emission cone of ±2 degrees from the direction of propagation of electron bunch..

CP-05-6. ENHANCEMENT OF REAL AND IMAGINARY PARTS OF RAMAN SUSCEPTIBILITY OF SEMICONDUCTOR MAGNETO-PLASMAS UNDER OFF-RESONANT LASER IRRADIATION

Gopal[1,], B.S. Sharma[1], Manjeet Singh[2], [1]Department of Physics, Lords University, Chikani, Alwar – 301028, (Rajasthan) India, [2]Department of Physics, Government College, Matanhail, Jhajjar – 124106 (Haryana) India, *Email: gopal.lordsuniv@gmail.com*

Using the coupled-mode approach, we obtain expressions for real and imaginary parts of Raman susceptibility of semiconductor magneto-plasmas. Numerical estimates are made for n-InSb/CO_2 laser system. Efforts are made towards optimizing the doping level, applied magnetic field and pump intensity to achieve enhanced value of Raman susceptibilities and change of their sign. The potential of semiconductor magneto-plasmas for the fabrication of efficient optoelectronic devices is established.

CP-05-7. ENHANCED SYNCHROTRON X-RAY RADIATION FROM COLLECTIVE OSCILLATIONS OF ELECTRON BUNCH IN LASER-PLASMA ACCELERATOR AND WIGGLER

*Shikha Mishra[1], B. S. Rao[1,2], A. Moorti[1,2] and J A Chakera[1,2], [1]Raja Ramanna Centre for Advanced Technology, Indore, [2]Homi Bhabha National Institute, Mumbai, **Email:** shikham@rrcat.gov.in*

We report an experimental study on the enhanced synchrotron X-ray emission due to collective betatron oscillations of energetic-electrons in laser-plasma accelerator and wiggler driven by a positively chirped 45fs, Ti:Sapphire laser-pulse interaction with 4mm long helium gas-jet at intensity ~2.8×10^{19}W/cm^2. We observed electron beams with broad-spectrum extending to 300MeV and displaying collective oscillations. The oscillations grew stronger at higher plasma density and efficient x-ray emission with peak brightness of $\geq1\times10^{21}$ph/s/sr/0.1%BW at critical energy of 35±5keV was observed at plasma density $\geq1\times10^{19}$cm^{-3}. The study will be useful towards the efforts to improve the performance of the X-ray source for its applications.

CP-05-8. LASER-DRIVEN SHOCK STUDY IN ALUMINIUM FOILS COATED WITH PMMA POLYMER

A. Kumar[*,1], *S. Barnwal*[1], *A. Singh*[1], *Suparna Pal*[1], *A.P. Kulkarni*[1], *S. Jain*[1], *R K Patidar*[1], *C. Mukherjee*[1, 2], *Y.B.S.R. Prasad*[1], *N S Benerji*[1], *K S Bindra*[1,2] , [1]*Laser Technology Division, RRCAT, Indore 452013, M.P., India,* [2]*Homi Bhabha National Institute, Training School Complex, Anushakti Nagar, Mumbai, 400094,* [*]***Email:** *katul@rrcat.gov.in*

Results from laser shock wave experiments by irradiating foil targets of (a) polymer (PMMA: Poly Methyl Methacrylate) coated Aluminum (Al) and (b) bare Aluminium with an intense nanosecond laser pulse are compared. The laser produced shock propagation in these thin pre-coated and uncoated foil targets are recorded using two frame shadowgraphy technique. The low density pre-coating can enhance the particle velocities (i.e. shock pressures) due to the impedance mismatch (low density to high density). An increase of ~20% in particle velocities with PMMA coated Al- foil targets as compared to bare Al-foils is measured. The scaling of particle velocities with laser intensity is obtained in both cases as (0.38-0.48). Filtered x-ray diodes were also used for measurement of soft and hard x-ray emission. It is seen that hard X-ray emission from PMMA coating is much lower compared to Aluminium, thus minimizing the preheating of the target.

CP-05-9. ROLE OF BACKGROUND GAS PRESSURE IN SPATIAL CONFINEMENT OF LASER ABLATIVE PLASMA

D. P. S. L. Kameswari[1], *G. Nagaraju*[1], *S. Sai Shiva*[1], *V. R. Ikkurthi*[2,3], *P. Prem Kiran*[*1,4], [1]*ACRHEM, University of Hyderabad, Gachibowli, Hyderabad,* [2]*Computational Analysis Division (CAD), Bhabha Atomic Research Centre (BARC), Visakhapatnam, India,* [3]*Homi Bhabha National Institute, Anushaktinagar, Mumbai, India,* [4]*School of Physics, University of Hyderabad, Gachibowli, Hyderabad,* ***E.mail** : **premkiranuoh@gmail.com***

A numerical study of spatial confinement of laser ablative plasma from a 20 μm thick aluminum foil by changing the background pressure (varied between 0.1 – 1 atm) is performed using FLASH 2D radiation hydrodynamic code. The underlying mechanism behind the varying background gas pressure is discussed in detail and its effect on the plasma plume and the subsequent shock pressures generated were determined..

CP-05-10. THREE-DIMENSIONAL (3D) HYDRODYNAMIC SIMULATIONS OF LASER INDUCED MATERIAL BLOW-OFF FROM THIN METAL FOILS: MODELING CHALLENGES

S. Sai Shiva[1], *V. R. Ikkurthi*[3, 4], *and P. Prem Kiran*[1, 2*] [1]*Advanced Centre of Research in High Energy Materials (ACRHEM), University of Hyderabad, Gachibowli, Hyderabad-500046, India.* [2]*School of Physics, University University of Hyderabad, Gachibowli, Hyderabad-500046, India.* [3]*Computational Analysis Division (CAD), Bhabha Atomic Research Centre (BARC), Visakhapatnam-530012, India.* [4]*Homi Bhabha National Institute, Anushaktinagar, Mumbai, Maharashtra 400094, India.* ***Email:** *prem@uohyd.ac.in.*

We present modeling challenges involved in performing a three-dimensional (3D) hydrodynamics simulation of laser induced material blow-off from the rear side of thin metal foils confined with a glass substrate. The challenges such as, implementing laser focusing at the glass-foil interface, implementing eauation-of-state (EOS) of the materials, laser absorption models and restriction of physical movement of the target foil arising due to density and pressure gradients between the target and ambient conditions and validation of the results will be addressed. The modeling was setup in the FLASH radiation hydrodynamics (RHD). The hydrodynamic behavior of material blow-off from the rear side of 20 μm thick metal film is discussed.

CP-05-11. SPATIO-TEMPORAL MAPPING OF THE ULTRAFAST EVOLUTION OF HOT-DENSE PLASMA GENERATED BY INTENSE FEMTOSECOND LASER PULSES

Amit D. Lad,[1] Kamalesh Jana,[1] Yash M. Ved,[1] David West,[2] Will Trickey,[2] Chris Underwood,[2] A. P. L. Robinson,[3] J. Pasley,[2] and G. Ravindra Kumar[1], [1]Tata Institute of Fundamental Research, 1 Homi Bhabha Road, Colaba, Mumbai 400 005, INDIA, [2]York Plasma Institute, University of York, Heslington, York YO10 5DQ, United Kingdom, [3]Central Laser Facility, Rutherford-Appleton Laboratory, Chilton, Didcot OX11 0QX, United Kingdom, ***E.mail :*** *amitlad@tifr.res.in*

A detailed understanding of the critical surface motion of high intensity laser produced plasma is very crucial parameter for understanding the interaction. Here, we present a novel technique based on pump-probe Doppler spectrometry to map spatially and temporally the ultrafast dynamics of hot-dense plasma generated by femtosecond, intense laser pulses[1]. Our technique offers hundreds of femtoseconds time resolution simultaneously with a few micrometer spatial resolution across the transverse length of the plasma. The experiment was carried out using TIFR 150 TW laser system with peak intensity of 5×10^{18} W/cm^2. The up-converted harmonic probe (400 nm) allows us interrogate the dynamics in plasma which is over-dense with respect to pump laser. A normally incident time-delayed probe pulse reflected from its critical layer experiences a change in its wavelength due to the motion of the critical layer. Measuring the time dependent Doppler shifts at different locations across the probe beam we obtain two-dimensional velocity maps of the probe-critical plasma layer at ultrafast timescales (Fig. 1). Harmonics of the pump can be used to penetrate more deeper and capture the ultrafast motion of the solid density plasma[2,3]. Early time measurements using this technique provide very important information about shock wave generation and propagation in dense medium[2].

CP-05-12. DEVELOPMENT OF MULTI-CHANNEL, SINGLE-SHOT, HIGH RESOLUTION DOPPLER SPECTROSCOPY FOR 2D VELOCITY MAPPING OF INTENSE LASER PRODUCED PLASMAS

Yash M. Ved,[1] Amit D. Lad,[1] Kamalesh Jana,[1] and G Ravindra Kumar[1], [1]Tata Institute of Fundamental Research, 1 Homi Bhabha Road, Colaba, Mumbai 400 005, INDIA, ***E.mail*** *: yash.ved_002@tifr.res.in*

We have conceptualised, designed, assembled, and developed two-dimensional high resolution Doppler spectrometry to spatial and temporal map the velocity of hot dense laser produced plasma [Fig. 1]. The measurements are carried out with TIFR 150 TW, ultrashort, high-contrast laser system. Our instrument is capable of providing an optical resolution of 0.03 nm (inset of Fig. 1) and hence extremly small Doppler shifts can be measured[1]. The pump-probe technique offer high temporal resolution to study plasma dynamics. The device is designed with 16 high-spectrual resolution spectrometers which can be triggered in single shot mode. These spectometers are coupled to individual fibers across the reflected probe from the plasma. The spectrum at several spatial location of the reflected probe beam can be measured with a single laser shot and hence the corresponding Doppler shift. This technique

has very high temporal resolution of the order of probe pulse-width (tens of femtosecond). As a result, it is possible to capture ultrafast dynamics of plasma at very early times which is not easily accessible by most of the other diagnostics. Spatial resolution offered by our technique depends on the total number of points across the probe beam (16, presently) (inset of Fig. 1) and it can be improved by increasing the number of spectrometers. The time dependent velocity map can be inferred from the Doppler shifts due to large sptial locations offered by a technique[1].

CP-05-13. PROTON RADIOGRAPHY OF MICROSTRUCTURE AND LASER PRODUCED PLASMA PLUME

S. Bagchi[1], M. Tayyab[1], A. Moorti[1,2] and J A Chakera[1,2] [1] Advanced Plasma Acceleration Section, Laser Plasma Division, Raja Ramanna Centre for Advanced Technology (RRCAT), Indore – 452 013 [2] Homi Bhabha National Institute, Anushakti Nagar, Mumbai – 400 094 ***e-mail****: sbagchi@rrcat.gov.in*

We report proton radiography of static microstructure and evolving laser-produced plasma plume in real time. The proton beam was produced by interaction of 25 fs, 800 nm Ti: Sapphire laser pulse with 5 μm thick Nickel foil target. The plasma plume was created by extracting stretched pulse (duration of ~560 ps) from the laser system. Initial measurements showed plume expansion velocity of 2.6×10^6 m/s. The nature of the radiograph images points toward the role of radially outward electric field responsible for the proton beam deflection.

CP-05-14. REDUCTION OF DOPPLER WIDTH IN COLLIMATED ATOMIC BEAM: SIMULATION STUDY AND EXPERIMENT

T. Garg, B Jana, S. Baruah, G. K. Sahu B Dikshit, Advanced Tunable Laser Applications Facility, BTDG, BARC, Trombay – 400085, ***Email****: tarang@barc.gov.in*

In Laser Isotope Separation (LIS) process of ^{176}Yb, the targeted ^{176}Yb isotope is selectively excited and ionized through three step resonant photoionization method. The good selectivity of the process is obtained when the Doppler width of atomic vapors is less than the isotope shift from the neighbouring isotopes. Thus a collimated atomic beam with reduced Doppler width less than 300 MHz is required in LIS process of ^{176}Yb. One of the strategies of reducing Doppler width has been shown earlier[1]. In this paper, we will describe new collimator geometry to achieve the desired Doppler width, DSMC simulation study with new geometry, measurement of Doppler width using three step photo-ionisation process and its comparison with computed Doppler width from simulation.

CP-05-15. PHOTON EMISSION ENHANCEMENT STUDIES FROM THE INTERACTION OF\R\NULTRA-INTENSE LASER PULSE WITH SHAPED TARGET

S. Chintalwad, S. Krishnamurthy, and B. Ramakrishna, Indian Institute of Technology Hyderabad, C. P. Ridgers, Department of Physics, University of York, Heslington, York ***Email****: chintalwadsachin@gmail.com*

We study the photon emission by Bremsstrahlung and Non-linear Compton Scattering(NCS) from interaction of ultra-intense laser pulses with cone target and flat foil using particle-in-cell (PIC) simulations. The simulations are performed for laser pulse interacting with Al and Au targets. The strength of the two mechanisms of photon emission from Bremsstrahlung and nonlinear Compton scattering are compared. When an ultra-intense (I > 10 22 W cm −2) laser interacts with a cone and a foil target, photon emission by Bremsstrahlung is found to be comparable to that from nonlinear Compton scattering. The obtained electron energy as well

as the energy and number of photons emitted were found to be higher in case of cone shaped target compared to that of a foil target. The enhanced photon emission from cone shaped target is attributed to the guiding or collimation of hot electrons towards the cone tip from the self-generated magnetic field and electrostatic field along the cone surface which pushes the hot electrons towards the tip

CATEGORY 06: ULTRAFAST LASERS AND ITS APPLICATIONS

CP-06-1. ENHANCED OPTICAL NONLINEARITIES IN METAL-DIELECTRIC 1D PHOTONIC STRUCTURES

Jitendra Nath Acharyya[a], D Narayana Rao[b], R B Gangineni[c], and G. Vijaya Prakash[, a], [a]Nanophotonics Lab, Department of Physics, Indian Institute of Technology Delhi, New Delhi-110016, India; [b]School of Physics, University of Hyderabad, Hyderabad-500046, India., [c]Department of Physics, Pondicherry University, Puducherry-605014, India.,* ***Email:*** *prakash@physics.iitd.ac.in*

The present study reports enhanced nonlinear optical responses in one-dimensional (1D) $(Ag/SiO_2)_4$ metal-dielectric (MD) photonic structures using intense femtosecond laser pulses. Alternate layers of Ag and half-wave ($\lambda/2$) thickness SiO_2 form a series of coupled Fabry–Pérot (FP) resonators (Ag-SiO_2-Ag) which induces huge optical field enhancement inside the SiO_2 layer. The giant optical confinement leads to a many-fold enhancement of $\chi^{(3)}$ of Ag, which results in a strong two- and multi-photon absorption and strong optical limiting behavior. The composite transparent metals with a very high laser damage threshold (~50 GW/cm^2) are potentially beneficial for novel femtosecond optical limiters, optical Bragg coatings, spatial optical filters for extremely high-power ultrafast laser operations.

CP-06-2. QUASI-PERIODIC SILVER NANOSTRUCTURES ACHIEVED WITH ULTRAFAST BESSEL BEAM ABLATION FOR REAL-TIME SENSING OF EXPLOSIVES

Banerjee[1], R. Beeram[1], S.V. Rao[,#] [1]Advanced Centre of Research in High Energy Materials (ACRHEM), [2]School of Physics, University of Hyderabad, Hyderabad 500046, Telangana, India. [#]***e-mail:*** *soma_venu@uohyd.ac.in,*

In this study we demonstrate the fabrication of silver nanostructures (NSs) produced by Bessel beam engaging picosecond (30 ps, 10 Hz) laser pulses with different input enegies. The topographical features of these structures were thoroghly characterised using FESEM imaging at the sub ~50 nm scale, wherein, the formation of finger-like quasi periodic structures were observed resulting from the picoseocnd laser-matter interaction. Quantitatively, the absence of any oxidation effect was confirmed from the EDX spectra. Subsequently, these Ag nanostructures were implemented in applications such as sensing realtime explosives and other molecules using the surface enhanced Raman scattering (SERS) technique. Significantly, the lowest possible trace detection numbers turned out to be 500 nM for Picric Acid- an explosive molecule and 500 pM, 50 nM for MG, Thiram. The RSD values of each of these molecules were observed to be <10%, confirming the homogenety of the enhacned Raman signal from the fabricated quasi-periodic NSs.

CP-06-3. FEMTOSECOND LASER INDUCED HEAT PROPAGATION AND DAMAGE THRESHOLD ANALYSIS OF AU/CR TWO-LAYER FILM

Aeaby C. D. and Aditi Ray, Theoretical Physics Section, Bhabha Atomic Research Centre, Mumbai, India, ***Email****: aeabycd@barc.gov.in, aray@barc.gov.in*

We report development of two temperature model based Python code **TTM-FS** for analysis of non-equilibrium energy transport and electron-lattice coupling mechanism as encountered in femtosecond (fs) laser interaction with matter. The code has been rigorously validated with

available results for fs laser absorption and successive heat propagation in Au/Cr two-layer target. We have extended the study towards damage threshold (DT) analysis of two different thickness Au/Cr target. Our simulation reveals that with opimum thickness of Au layer, DT of 100 nm and 200 nm Au/Cr target, irradiated by 100 *fs* laser in visible range, can be enhanced up to 6% and 9% respectively from same thickness single layer Au film. Further, it is shown that detailed modelling of thermophysical parameters, namely, electron thermal conductivity and electron-lattice coupling strength greatly influences the temperature evolution and hence damage threshold

CP-06-4. PRODUCING LIQUID MICROJETS USING PICOSECOND LASER PULSE EXCITATION

B. Rana [a] and K C Jena [a,b], [a] Department of Physics, Indian Institute of Technology Ropar, Rupnagar, Punjab-140001, India, Manipal University, [b] Department of Biomedical Engineering, Indian Institute of Technology Ropar, Rupnagar, Punjab-140001, India ***Email:*** *bhawnaraizada@gmail.com*

Liquid microjets have shown immense potential in painless needle-free drug injections, liquid scalpels, and gene delivery devices, imperative in the medical industry. In recent years, lasers have revolutionized the field as they are helpful in the generation of fast and focused liquid jets. We have developed an in-house experimental set up, where a picosecond (ps) laser system is utilized for the generation of liquid mirojets. We have achieved the jet formation when a focused ps-laser beam is made to impinge on the air/liquid interface of a liquid filled microcapillary. A qualitative and quantitative demonstration of the production of liquid microjets using ps-laser pulses is presented.

CP-06-5. NOISE-LIKE PULSE FROM ALL-NORMAL DISPERSION YTTERBIUM DOPED ALL-FIBER OSCILLATOR WITH SEMICONDUCTOR SATURABLE ABSORBER

Nitish Paul[1,2], C P Singh[1,2], Bhuvnesh[1], P K Gupta[1,2], P K Mukhopadhyay[1,2] and K S Bindra[1,2], [1]Laser Technology Division, Raja Ramanna Centre for Advanced Technology, Indore, [2]Homi Bhabha National Institute, Training School Complex, Anushakti Nagar, Mumbai, ***E-mail:*** *cpsingh@rrcat.gov.in*

We present generation of noise-like pulse (NLP) from all-normal dispersion ytterbium doped all-fiber unidirectional ring cavity consisting of semiconductor saturable absorber without any bandpass filter. NLP characterized by its autocorrelation trace exhibits ~500 fs spike riding on a broad pedestal of ~200 ps in a 45 m long cavity. Numerical simulations are also performed to show generation of NLP for a range of cavity parameters and results are in accordance with the experimental findings.

CP-06-6. WEB-LIKE SI STRUCTURES FABRICATED VIA FEMTOSECOND LASER ABLATION AND THEIR APPLICATION FOR SURFACE ENHANCED RAMAN SPECTROSCOPY

Reshma Beeram[1], Dipanjan Banerjee[1], A. Mangababu [2], Soma Venugopal Rao[1,#], [1]Advanced Centre of Research in High Energy Materials (ACRHEM), [2] School of Physics, University of Hyderabad, Hyderabad 500046, Telangana, India., ***e-mail:*** *soma_venu@uohyd.ac.in OR soma_venu@yahoo.ac.in*

Femtosecond laser ablation is novel and green technique for precise surface processing of different metals and semiconductors. The simplicity of the experimental setup and diversity of the material processing have expanded new horizons across diverse fields. Here we present

web-like structures on Silicon using a femtosecond laser oscillator with 80MHz repetition rate. These structures exhibited interesting morphology with Si nanoparticles aggregating into nan chains which further self-assembled into web like structures. The mechanism of formation of these web like structures is understood and effects of different experimental conditions on these structures were studied. These web-like structures were further coated with gold to use it for SERS. The structures offered clear advantage in SERS studies with Methylene Blue as the probe molecule relative to plain Silicon.

CP-06-7. GENERATION OF VECTOR DARK-BRIGHT PULSES FROM FIBER LASER MODE LOCKED BY NONLINEAR MULTIMODE INTERFERENCE

Pradeep K. Gupta, C P Singh, P K Mukhopadhyay and K S Bindra; Laser Technology Division, Raja Ramanna Centre for Advanced Technology, Indore, M.P-452013; Homi Bhabha National Institute, Training School Complex, Anushakti Nagar, Mumbai-400094, India. ***E-mail:*** *pradeepg@rrcat.gov.in.*

We report, dark-bright pulse pair generation from Ytterbium doped fiber laser mode locked by cascaded nonlinear multimode interference (MMI) effect under all-normal dispersion configuration. The MMI is implemented in step index single mode-multimode-single mode fiber structure. Two MMI structures, combination of which act like a saturable absorber, have been used for stable mode locking operation in the resonator. By adjusting the polarization controller attached to one of MMI structure, stable dark-bright pulses are observed. Dark-bright pulses in the pair are resolved by placing a polarizing component confirming their vector nature.

CP-06-8. LASER INDUCED OPTICAL AND THERMAL EFFECTS DUE TO HIGH REPETITION RATE PULSED LASERS

Sugandh Sirohi, Soumyodeep Dey and Prem Ballabh Bisht, Department of Physics, Indian Institute of Technology Madras ***Email:*** *ph20d038@smail.iitm.ac.in*

When high power laser beam interacts with a highly absorbing material, along with the nonlinear optical effects, thermal effects are also induced inside the material. These thermal effects change the refractive index of the material leading to spatial self-phase modulation (SSPM). The temperature changes in the sample depend on the pulse energy, repetition rate and pulse duration of the ultrafast laser. The finite difference method (FDM) simulations have been used to numerically estimate the observed effects. The SSPM creates diffraction pattern of the laser beam at the far field of the sample, which is experimentally investigated as a function of laser intensity.

CP-06-9. FEMTOSECOND-LASER ASSISTED FABRICATION OF FLUORESCENT PHOTONIC CRYSTAL

Sweta Rani, Arun Jaiswal, Gaurav Pratap Singh, Sumit Saxena, Shobha Shukla, IITB-Monash Research Academy, ***Email:****sweta.rani@monash.edu*

Fluorescent photonic crystals (PCs) have attracted significant attention owing to their unique properties such as photonic bandgap and fluorescence. However, conventionally used fluorescent materials such as organic dyes, metal-ligand complexes and lanthanide chelates suffer from inherent drawbacks such as the reduced quantum yields, poor photostability and small two-photon absorption cross-section area. Here, we report a novel material system and a facile strategy for fabrication of fluorescent PCs using femtosecond-laser assisted two-photon lithography. A two-photon patternable polymeric material system, doped with carbon quantum dots (CQDs), is employed for fabrication of PCs. CQDs offer many advantages such as braod

absorption spectra, very narrow emission spectra, long fluorescence lifetime, high photostability, low production cost, tunable fluorescence, easy synthesis, and high-quantum yield. The fabricated PC exhibits strong fluorescence as well as structural coloration owing to the photonic bandgap and presence of CQDs, respectively. The PC has been characterized by scanning electron microscopy, fluorescence imaging and numerical techniques.

CP-06-10. CARBON DOTS: A NEW PHOTOINITIATOR FOR EFFICIENT TWO-PHOTON POLYMERIZATION

Arun Jaiswal[1], Sweta Rani[2], Gaurav Pratap Singh[1], Mahbub Hassan[3], Aklima Nasrin[3], Vincent G. Gomes[3,4], Sumit Saxena[1,2] and Shobha Shukla[1,2], [1]Nanostructures Engineering and Modeling Laboratory, Department of Metallurgical Engineering and Materials Science, Indian Institute of Technology Bombay, Mumbai 400076, MH, India, [2]Nanostructures Engineering and Modeling Laboratory, Department of Metallurgical Engineering and Materials Science, Indian Institute of Technology Bombay-Monash Research Academy, Mumbai 400076, MH, India, [3]School of Chemical and Biomolecular Engineering, The University of Sydney, NSW 2006, Australia, [4]Nano Institute, The University of Sydney, NSW 2006, Australia,* ***Email:*** **sshukla@iitb.ac.in*

Three-dimensional additive manufacturing is extensively used for realization of micro/nanostructures with predefined structural and functional attributes; aimed towards development of constructs targeting specific applications. In recent past, two-photon polymerization-based fabrication has become a popular choice, due to its capability of generating true three-dimensional geometries with sub-wavelength resolved features in a single exposure step. Although this technology has attracted wide attention, but the limited availability of two-photon processable resins is still hindering the further growth of this technology. Most of the efficient, two-photon active molecules are either specific to few resins or proprietary. Furthermore, their design and synthesis involve complex and time-consuming processes, so there is a need to develop a material system with good non-linear activity, along with efficient two-photon polymerization sensitivity. To address these challenges, we have formulated acrylate and carbon quantum dots composite based two-photon processable resin. We have demonstrated two-photon fabrication of emissive microstructures and evaluated the structural and emissive traits of the fabricated structures. The formulated resin eliminates the dependency on conventional two-photon sensitizers, and hence the implementation of hydrothermally synthesized carbon dots as two-photon initiator has paved pathway for further progress of this technology and is anticipated to introduce a paradigm shift in various areas such as metamaterials, energy storage, drug delivery, optoelectronics to name a few.

CATEGORY 07: LASERS IN MATERIAL SCIENCE, CHEMISTRY, BIOLOGY AND MEDICINE

CP-07-1. ANALYTE ENRICHMENT USING NANOSECOND LASER TEXTURED SUPERHYDROPHOBIC SURFACES

S. Ahlawat[a], P K Mukhopadhyay[a], A. Singh[a], R. Singh[b], K S Bindra[a], [a]Laser Technology Division, Raja Ramanna Centre Advanced Technology, Indore, M.P. 452013, India, [b]Laser and Functional Materials Division, Raja Ramanna Centre Advanced Technology, Indore, M.P. 452013, India, *Email: rsunita@rrcat.gov.in*

We show that nanosecond laser texturing can produce superhydrophobic stainless steel surfaces over which a water droplet (5 µl) keeps on continuously reducing its footprint while evaporating and eventually deposits its entire content in a spot of ~100 µm diameter. Such reduction in dried spot area allowed fluorescence detection of Rhodamine 6G at a very low concentration of 10^{-18} M originally contained in a 5 µl water droplet. When compared with the results obtained on unprocessed stainless steel substrate, the superhydrophobic steel surfaces provided four orders of magnitude enhancement in the lowest detectable concentration of Rhodamine 6G.

CP-07-2. HEMATOLOGY ANALYSIS USING SELF-REFERENCING DIGITAL HOLOGRAPHIC MICROSCOPE

*Chetna M. Patel[1], Shilpa G. Das[2], Bahram Javidi[3], Arun Anand[1], [1]Applied Physics Department, Faculty of Technology and Engineering, The Maharaja Sayajirao University of Baroda, Vadodara, India, [2] Applied Physics Department, Sardar Vallabhbhai National Institute of Technology, Surat-395007, [3]Department of Electrical Engineering, University of Connecticut, Storrs, CT, 06269-4157, USA, **E-mail:** aanand-apphy@msubaroda.ac.in*

Hemoglobinopathies have always been a case of concern in developing countries. Though Bright field microscopy is the benchmark for such disease identification, there is still a requirement for cost-effective and field-portable devices. We present a common path Lateral Shearing Digital Holographic Interferometer that can be developed into one such device. It is used to capture holographic videos of blood samples, especially red blood cells (RBCs). The recoded holographic videos are then reconstructed to extract biophysical and biomechanical cell features. These features can be used to identify and classify the test sample.

CP-07-3. FLEXIBLE FABRICATION OF MICRO-OPTICAL ELEMENTS BY USING MASK PROJECTION BASED EXCIMER LASER ABLATION

*Jai Khare[1], S. K Rai[2,3], [1]Photonics Nanomaterial Lab, Laser Materials Processing Division,[2]Synchrotrons Utilization Section., Raja Ramanna Centre for Advanced Technology, Indore 452 013, [3]Homi Bhabha National Institute, Training School Complex, Anushaktinagar, Mumbai 400094, *E.mail: jkkhare@rrcat.gov.in*

Yttrium stabilized zirconium oxide (YSZ) with high ionic conductivity, electron blocking layer and thermal barrier properties are used extensively in technological applications such as in fuel cell, photovoltaic cell, thermal barrier coating materials etc. Thin films of YSZ on ITO were grown by ablating pellet of YSZ powder using pulsed laser deposition technique at various laser fluence (3-8 J/cm^2). The X-ray diffraction diffraction analysis of films revealed that film grown at lower fluence, up to 5 J/cm^2, were amorphous while film grown at higher fluence of 8 J/cm^2 was in crystalline cubic phase. In inverted geometry of solar cell amorphous phase of

YSZ could be better choice as electron blocking layer because of high transmission in visible range.

CP-07-4. COMPARISON OF STRUCTURAL AND OPTICAL PROPERTIES OF THERMAL AND LASER ANNEALED THIN FILMS OF METHYL AMMONIUM LEAD IODIDE ($CH_3NH_3PBI_3$)

*Kireet Semwal[1], T. S. Dhami[1], Jai Khare[1], S. K Rai,[2,3] M P Joshi[1,3], [1]Photonics Nanomaterial Lab, Laser Materials Processing Division,[2]Synchrotrons Utilization Section, Raja Ramanna Centre for Advanced Technology, Indore 452 013,[3]Homi Bhabha National Institute, Training School Complex, Anushaktinagar, Mumbai 400094, ***Email:** tsdhami@rrcat.gov.in*

The paper presents a comparative study of thermal and laser annealing effects on the structural and optical properties of photovoltaic perovskite material methyl ammonium lead iodide ($CH_3NH_3PbI_3$). Enhancement in optical absorption as well as improvement in crystalline quality was observed when annealed at optimum laser fluence using 532 nm nanosecond duration laser pulses. This study indicates laser annealed thin films showed better structural and optical properties in comparison to films annealed thermally. The present study suggests potential use of laser annealing in the fabrication of patterned and improved crystalline quality perovskite thin films.

CP-07-5. PHOTOSENSITIZERS IMMOBILIZED ON ALUMINIUM HYDROXIDE MICROPARTICLES FOR PHOTODYNAMIC INACTIVATION OF BACTERIA AND WATER DISINFECTION

*A. Dube, A. Chowdhury and Shovan. Kumar. Majumder, Laser Biomedical Applications Division, RRCAT, Indore, **Email:** okdube@rrcat.gov.in*

An anionic chlorophyll derivative (ChD) and cationic toluidine blue (TBO) immobilized on Aluminum hydroxide microparticles (AlOH-PS) has been investigated for photodynamic inactivation of bacteria and disinfection of tap water. The combination of anionic/cationic PSs improved their adsorption on AlOH microparticles through electrostatic interaction. Photodynamic treatment of *P. aeruginosa and E. coli* with AlOH-PS and red light ~640 nm) showed ~ 4 logs reduction in bacterial counts. Tap water containing water born microorganisms could be disinfected completely. Results demonstrate that ChD+TBO immobilized on AlOH is useful for antimicrobial photodynamic applications.

CP-07-6. ANTICANCER PHOTODYNAMIC TREATMENT EFFICACY OF CYCLOIMIDE PURPURIN-18, A NEAR-INFRA RED ABSORBING PHOTOSENSITIZER, IN HUMAN BREAST CARCINOMA CELLS

*S. Chatterjee[1,2] , A. Dube[1,2] , Shovan Kumar Majumder[1, 2] [1]Homi Bhabha National Institute, Training School Complex, Anushaktinagar, Mumbai 400094, India;[2]Laser Biomedical Applications Division, Raja Ramanna Centre for Advanced Technology, Indore 452013, India. **Email ID**: sucharita@rrcat.gov.in*

Photodynamic efficacy of Cycloimide Purpurin-18 (CIPp-18), a near Infra-red absorbing photosensitizer (NIRPS) (λ_{max} ~700 nm) was investigated in-*vitro* in Human Breast Carcinoma cells by assessing its cellular uptake, intracellular localization and phototoxicity. Results show that CIPp-18 interacts with serum protein which prevents its aggregation and facilitates uptake in cells. CIPp-18 localizes in cell membrane and ER, and induce ~ 90% phototoxicty in cells after irradiation with NIR light at 1.4J/cm^2 dose. Studies show that CIPp-18 is a promising photosensitizer for PDT of cancer.

CP-07-7. A PORPHYRIN BASED TETRACATIONIC FLUOROPHORE FOR THE DETECTION OF HEPARIN IN 100 % HUMAN SERUM

S. P. Pandey,[a,] P. Jha[a] and P. K. Singh[b,c], [a]Amity Institute of Biotechnology, Amity University, Mumbai-Pune Expressway, Panvel, Mumbai, 410206, INDIA, [b]Radiation& Photochemistry Division, Bhabha Atomic Research Centre, Mumbai 400 085, INDIA, [c]Homi Bhabha National Institute, Anushaktinagar, Mumbai-400085, INDIA, [*]**Email:** shrish1411@gmail.com*

Designing efficient fluorescent probes, especially for sensing biologically important analytes, is an intensive area of investigation. Heparin is a well-known blood anticoagulant, and is routinely used as a very important medication in clinical setups. Further, sensing Heparin in 100% serum matrix is a challenging task and is rarely reported in literature. Herein, we present a tetra-cationic porphyrin based probe, that senses Heparin selectively in 100% serum matrix with a clinically relevant LOD (2.1 $\pm$ 0.2μM). The porphyrin-based probe undergoes aggregation in presence of Heparin recording significant changes in the photophysical features. The probe also registers high selectivity towards Heparin, compared to its two most common structurally related analogues, i.e., Chondroitin sulfate and Hyaluronic acid. Most importantly, the probe could work in 100% serum, which is rarely reported in literature. Overall, we have identified a multi-cationic probe which senses Heparin in a selective and sensitive way through dual optical output of the signal, i. e., via both colorimetry as well as fluorimetry. The easy commercial availability of the probe coupled with its other desirable attributes is expected to significantly impart its prospect in Heparin sensor applications and Heparin related bio-chemical research.

CP-07-8. COMPARISON OF TIME EVOLUTION OF LASER PRODUCED PLASMA PRESSURE AND LASER SHOCK PRESSURE IMPULSE (LSPI) FOR 10NS AND 30PS LASER PULSES OF DIFFERENT SHAPES UNDER WATER CONFINEMENT REGIME

G.S. Sasank[1], Dr.P. Prem Kiran[1,] and Dr. Ashok Vudayagiri[1,*], [1]School of Physics, University of Hyderabad, **Email:** prem@uohyd.ac.in*

Laser Shock Peening (LSP) has become most sought-after technique, where a laser-produced shockwave is used to induce compressive residual stresses into a material, which improves its strength and fatigue properties. In order to determine the shockwave pressure on the surface of a material, the study of pressure evolution of plasma is essential. In this paper, analytical model by Fabbro et al[1], was used to simulate the plasma pressure profile and laser shock pressure impulse (LSPI) on the target surface due to 10ns and 30ps laser pulses of different temporal profiles. A correlation between peak intensity of laser and peak shockwave pressure was established. Also, the effect of temporal width and fluence of laser on LSPI delivered to the target was studied

CP-07-9. NONDESTRUCTIVE, NONINVASIVE, EXTRACTION FREE ASSESSMENT OF THE BIOCHEMICAL CHANGES ASSOCIATED WITH THE RIPENING OF UNDERUTILIZED KADAM FRUIT BY CONFOCAL MICRO RAMAN SPECTROSCOPY

*Chhavi Baran[1], Aradhana Tripathi[2,] Sweta Sharma[2,3], and K. N. Uttam[2], [1]Centre for Environmental Science, IIDS, University of Allahabad, Prayagraj, [2]Saha's Spectroscopy Laboratory, Department of Physics, University of Allahabad, Prayagraj, [3]Department of Applied Science and Humanities, Faculty of Engineering, and Technology, Khwaja Moinuddin Chishti Language University, Lucknow **Email:**.charvi16@gmail.com*

The present study demonstrates the potential of confocal micro Raman spectroscopy for the assessment of the biochemical changes occurring at the different stages of growth and ripening of the underutilized and commercially viable fruits of kadam. For this, Raman spectra of the different stages of fruits of kadam have been acquired in the spectral region 0-2000 cm^{-1}. The analysis of the acquired Raman spectral data depicts spectral signatures of the carbohydrates, cellulose, and carotenoids with varying intensity. The principal component (PCA) analysis reveals that PC 1 is able to capture 93.57% while PC 2 is able to explain 1.83% of the total variation

CP-07-10. USE OF COMBINED OFF-CONFOCAL RAMAN SPECTROSCOPY (OCRS) AND SWEPT SOURCE OPTICAL COHERENCE TOMOGRAPHY (SSOCT) SYSTEM FOR MONITORING DERMAL WOUND HEALING PROGRESS IN MOUSE MODEL

Alka[1], Khageswar Sahu[1], Khan Mohd. Khan[1], Hemant Krishna [1], Sunil Verma[1] and Shovan Kumar Majumder[1,2] [1]Laser Biomedical Applications Division, Raja Ramanna Centre for Advanced Technology, Indore-452013,[2]Homi Bhabha National Institute (HBNI), Training School Complex, Anushakti Nagar, Mumbai-400094 ***Email:*** *shkm@rrcat.gov.in*

We report results of dermal wound healing progress in mouse model monitored using a home-built dual modal system developed by combining a Raman spectroscopy (RS) system and an optical coherence tomography (OCT) system in a single optical platform. A particularly noteworthy feature of the developed OCRS-SSOCT (off-confocal RS- swept source OCT) system is that it allows sub-surface interrogation of layered turbid samples without requiring any adjustment in the sample arm, while SSOCT provided faster image acquisition rate. The day wise monitoring of both Raman spectra and OCT images shows wound crust formation, leading to new epidermis and normal healing of wound. The depth sensitive OCRS spectra measurement on day 2 and day 3, in addition provided quick assessment of healing stage, which will be helpful for appropriate therapy management.

CP-07-11. OPTICAL STUDY OF GRAPHENE OXIDE IN POLY-VINYL ALCOHOL

Athira.A, Alok Sharan*α ,*Department of Physics, Pondicherry University, R V Nagar, Kalapet, Puducherry, India,* ***Email:*** *athira7rythm@gmail.com*

Graphene Oxide (GO) is the primary tool for chemically altering graphene, which is made by extensive graphite oxidation and has a set of functional groups containing oxygen. These functional groups play an important role in increasing GO dispersion in polymers via covalent or non-covalent connections. The presence of hydroxyl groups in PVA polymer, aids in the creation of polymer complexes. GO polyvinyl alcohol nanocomposites are projected to be employed for a variety of electronic and optoelectronic applications due to the dispersion of GO in PVA, which results in a substantial improvement in various aspects such as mechanical, thermal stability, and electrical properties. The development of stable dispersions with high graphene concentrations has attracted a lot of interest in recent years and finds applications in photonics, and optoelectronics. In this study, we measure refractive index and extinction coefficient as a function of the weight percent of graphene oxide in polyvinyl alcohol using He-Ne laser having wavelength 632.8 nm.

CP-07-12. PICOSECOND LASER INDUCED GROOVE STRUCTURES ON TI6AL4V BIO-ALLOY TO IMPROVE APATITE GROWTH AND CELL ADHESION

S. Kedia[1,2], P. S. Gaikward[3], R. Checker[2,4], S. K. Sandur[2,4] and J P Nilaya[1,2]. , [1]L&PTD, BARC, Mumbai, [2]HBNI, TSC, Anushaktinagar, Mumbai, [3] Ex. Student, KBP College, University of Mumbai, Navi Mumbai, [4]RB&HS Division, BARC, Mumbai. ***Email:*** *skedia@barc.gov.in*

In this report, we present the results of our studies on the effect of picosecond laser induced groove structures on osseointegration and cytocompatibility of Ti6Al4V bio-alloy. By tailoring the experimental parameters, unique groove structures of varying surface roughness were created on the biomaterial. The *in vitro* osseointegration was performed by immersing samples in simulated body fluid for 10 days. To rule out the possibility of laser induced toxicity, cytocompatibility test in terms of fetal bovine serum protein adhesion and growth of L292 normal cells was performed. The altered surface properties due to laser treatment revealed superior osseointegration and biocompatibility in comparison to untreated Ti6Al4V sample.

CP-07-13. MODULATION OF FLUORESCENCE PROPERTIES OF 5-AMINOQUINOLINE BY AG^+ IN AQUEOUS MEDIA

Sanjay Pant[1], Nupur Pandey[1], Mohan Singh Mehata[2] , [1]Photophysics Laboratory, Department of Physics (CAS), DSB Campus, Kumaun University, Nainital, Uttarakhand, India. [2]Laser Spectroscopy Laboratory, Department of Applied Physics, Delhi Technological University, Delhi, India, ***E.mail*** *: sanjayphotophys@gmail.com*

The effect of silver ions (Ag^+) on the photophysical behavior of 5-aminoquinoline (5AQ) has been studied in an aqueous environment using steady-state and time-resolved spectroscopic techniques. The successive addition of Ag^+ ions to the aqueous solution of 5AQ amplify the fluorescence intensity of the large Stokes shifted band upto 21 folds accompanied by a red-shift as a result of the acceleration of charge transfer process and restriction of hydrogen bonding in the excited state. 5AQ exhibits good selectivity for Ag^+ ion over other metal ions (Li^+, K^+, Pb^{2+}, Zn^{2+}, Fe^{2+}, Mn^{2+}, Mg^{2+}, Cu^{2+}, Cd^{2+}, Co^{2+}, Cr^{3+}, Ni^{2+}). The Benesi-Hildebrand and Hills equations together with DFT calculations demonstrated the formation of 1:1 complex between 5AQ and Ag^+. Furthermore, 5AQ can perform as an INHIBIT logic gate triggered by Ag^+ and H^+ ions. Hence, the proposed study appears to be interesting in the detection of Ag^+ ions in aqueous media to a certain extent, indicating that 5AQ would have potential applications in the environmental and biological monitoring of Ag^+ ions.

CP-07-14. MEASUREMENT OF SHOCK VELOCITY IN LASER COMPRESSED C_6H_6:C_6F_6 ADDUCT USING TIME RESOLVED RAMAN SPECTROSCOPY

Ashutosh Mohan[1], K. C. Gupta[1], S. Chaurasia[1], John Pasley[2], T. Sakuntala[1], [1]High Pressure & Radiation Physics Division, Bhabha Atomic Research Centre, Mumbai - 400085, India, [2]York Plasma Institute, Department of Physics, University of York, York, YO10 5DQ, UK,* ***E.mail:*** *[*]shibu@barc.gov.in*

Understanding the behaviour of materials under extreme conditions is critical to quite a few research fields including ICF (inertial confinement fusion), condensed matter physics, astrophysics and geological sciences. Amongst the various means of dynamic compression such as gas guns, chemical explosives, impact loading and laser shock compression, laser based compression is usually the preferred choice of dynamic compression due to low cost, compact size, reliability and high repeatibility. And, measurement of shock velocity is critical to

understanding the behaviour of materials under dynamic compression. In this paper, we present measurement of shock velocity in C_6H_6:C_6F_6 adduct using nanosecond TRRS at 300 mJ and 500 mJ laser energy. 1D radiation hydrodyanmics simulations are also performed to verify the experimental findings. At 300 mJ, experimental shock velocity comes out to be 2.984 ± 0.177 km/s while simulated velocity is 3.348 km/s while at 500 mJ, shock velocity comes out to be 4.020 ± 0.100 km/s and 4.212 km/s from experiments and simulations respectively. Experimentally calculated velocities are in good agreement with the simulations considering the fact that experimental mixture has a molar ratio of 1.67:1 (C_6H_6:C_6F_6) while simulations are performed for equimolar mixture (due to unavailability of bulk modulus of the specific experimental mixture).

CP-07-15. EFFICIENT GENERATION OF LASER RADIATION IN THE RANGE 605-620 NM USING 532 NM PUMPED RHODAMINE DYES IN AQUEOUS MEDIUM

Ayentika Sen[1], A. Wahid[1], T B Pal[1], A K Singh[1], Asawari D Rath[1,2], S. Kundu[1], [1]TLS, ATLA Facility, BTDG, BARC, Mumbai-400085, [2]Homi Bhabha National Institute, Mumbai-400094,* ***Email:*** *skundu@barc.gov.in*

Choice of both the dye and solvent plays a key role in determining the efficiency and sustainability of high average power and high repetition rate dye lasers. Aqueous dye laser systems offer significant advantages over conventional organic solvents in terms of safety considerations and superior thermo-optic properties. Further, a suitable pump source also determines the dye to be used for generation of a certain wavelength range with sufficient efficiency. In this paper, we have explored the possibility of generating laser emission beyond 600 nm in aqueous medium using second harmonic (532 nm) of Nd-YAG based DPSSGL (Diode Pumped Solid State Green Laser) as the pump source

CP-07-16. THIN PHOTONIC CRYSTAL TEMPLATES WITH PLASMONIC NANOPARTICLES FOR TRACE MOLECULE DETECTION USING SURFACE ENHANCED RAMAN SPECTROSCOPY

*Saranya Narayanan[1], Pratyasha Sahani,[1] Jagannath Rathod,[2] B.V.R. Tata,[1,3] Soma Venugopal Rao[2], [1]School of Physics, [2]Advanced Centre of Research in High Energy Materials (ACRHEM), University of Hyderabad, Gachibowli, Hyderabad-500019, Telangana, India, [1]Presenting author: saranyam894@gmail.com; [3]****Email:****: bvrtata@uohyd.ac.in*

Gold nanoparticles drop-casted on the surface of thin (monolayer and bilayers) photonic crystals (PhCs) of polystyrene colloidal particles have been employed as templates for the molecules (methylene blue is taken as analyte for the case study) at low concentrations using surface enhanced Raman scattering (SERS) technique. Our detailed SERS investigations clearly reveal that PhC templates significantly enhance the Raman signal, hence lowering the detection limits to sub micromolar levels. Our results also reveal that number of PhC layers in the template play an important role in enhancing the Raman signal. The resluts are qualitatively understood by performing Electromagnetic clalcuations using COMSOL Multiphysics software for different array sizes

CP-07-17. AUGMENTATION OF THE EXPERIMENTAL SET-UP FOR LASER ASSISTED NOZZLE SEPARATION EXPERIMENTS

A. Ghosh[§,+], T. Dwivedi[§,+], R C Das[§,+], M B Sai Prasad[§,+], B. R. Gonde[†], A. M. Kasbekar[†], V. Nataraju[†], J P Nilaya[§,+,], Martin Mascarenhas[§], [§]Laser & Plasma Technology Division, BARC, Mumbai-85; [+]Homi Bhabha National Institute, Anushaktinagar, Mumbai-94; [†]Electromagnetic Application & Instrumentation Division, BARC, Mumbai-85; *****Email:*** *jpnilaya@barc.gov.in*

The experimental set-up for carrying out Laser assisted nozzle separation process at rotary vacuum conditions has been improved for repeatability and ease of analysis. The modifications include, devising ingenuous methods for nozzle-skimmer alignment as well as that of the focused laser beam at the nozzle exit; utilisation of premixed gas-mixture and an efficient core gas collection system; utilising a residual gas analyser for analysis of skimmed gas and realizing the desired pressure differential between the expansion and the skimmer chambers. Initial experiments with an external QMS has resulted an enrichment factor of 1.155 for ^{34}S isotope in the skimmed gas.

CP-07-18. ULTRA-ELONGATED PHOTONIC NANOJETS GENERATED BY PARTICLES WITH ELLIPSOIDAL GEOMETRY

B. Sugathan[1,2], J P Nilaya[2], V.P.M. Pillai[1], D.J. Biswas[2] [1]Laser and Plasma Technology Division, BARC, Mumbai-400085 [2]Department of Optoelectronics, University of Kerala, Thiruvananthapuram, Kerala-695581 ***Email:****bijoysugathan@gmail.com*

Simulation results of photonic nanojets generated by using partilcles with ellipsoidal geometry are presented. It was observed that as the minor to major axis of the particle (i.e., thickness to diameter of the particle) decreases the length of the photonic nanojet was increasing making it suitable for ultra elongated photonic nanojet generation.

CP-07-19. EFFECT OF LASER RE-MELTING ON THE MICROSTRUCTURE OF HIGH ENTROPY ALLOYS

P. Chakraborty, N.K. Sarkar, S. Saini, R.P. Kushwaha, S. Kumar, R. Tewari, Materials Science Division, BARC, Mumbai – 400094, ***Email:*** *poulamic@barc.gov.in*

A low density equiatomic High Entropy Alloy of composition Nb-Zr-V-Ti-Al was synthesized for nuclear reactor applications. The alloy in as-cast condition showed a coarse dendritic structure with a major BCC/B2 type dendritic phase while seggregation of Zr and Al in the form of intermetallics was noted in the inter-dendrtitic region. Remelting a part of the alloy surface with the help of 400 W Nd-YAG LASER resulted in formation of very fine grains (~500 nm) with a significant reduction in compositional seggegations with respect to Zr and Al. The microhardness of the LASER melted region was found to be similar to the BCC phase in as – cast microstrucure. This indicated that LASER melting may prove to be an effective method in reducing compositional and microstructural inhomogenities and push the multiphase structure towards single phase. It is expected that the fine grained structure in combination with a low density of 5.76 gm/cc in the present alloy may result in high specific strength which an important parameter for light weight applications

CP-07-20. AN ANIONIC TETRAPHENYL ETHYLENE BASED SIMPLE AND RAPID FLUORESCENT FLUORESCENCE "TURN-ON" PROBE FOR DETECTION OF ALKALINE PHOSPHATASE

J. Kaur [a] and P.K. Singh [b], [a] *Radiation & Photochemistry Division, Bhabha Atomic Research Centre, Mumbai 400 085, India,* [b] *Homi Bhabha National Institute, Training School Complex, Anushaktinagar, Mumbai 400 094, India,* **E-mail**: kaurjasvir8787@gmail.com

Alkaline phophatase (ALP) is indispensable for physiological functioning of living systems. The abnormal concentration of ALP in serum is an indicator of many diseases. Thus, ALP detection is very crucial to evaluate cellular physiological and pathological conditions. In this report, we have exploited the unique phenomenon of aggregation induced emission (AIE) to design a rapid, easy, sensitive and highly selective fluorescence "Turn-On" probing system for monitoring ALP activity. The sensing units are made up of an AIE active dye, di-anionic

1,2-Bis[4-(3-sulfonatopropoxyl)phenyl]-1,2-diphenylethene salt (BSPOTPE) and polycationic protamine sulphate (PrS) that interact electrostatically to make a highly fluorescent BSPOTPE-PrS supra-molecular complex. Subsequently, the fluorescence of BSPOTPE-PrS complex is efficiently quenched by hexa-anionic sodium hexametaphospahte. Finally, a rapid recovery in the fluorescence is obtained by adding ALP in the basic buffer conditions. The method is efficient in detecting as low as 28.7 µU/ml of ALP in 10 minutes.

CP-07-21. METHOD FOR QUANTIFYING ACTINIDE COLLOIDS BY LASER INDUCED BREAKDOWN DETECTION

Rama Mohana Rao Dumpala[a], Neetika Rawat[a], Bhupendra Singh Tomar[b], Radiochemistry Division, Bhabha Atomic Research Centre, Mumbai – 400085, India , Homi Bhabha National Institute, Training School Complex, Anushaktinagar, Mumbai – 400094, India., ***E.mail*** *: rammohan@barc.gov.in; ramamohandumpala@gmail.com*

Actinide colloids play a key role in the sorption and migration of actinides from the nuclear waste storage facilities. The characterization, quantification of actinide colloids over a long period of time gives crucial inputs for the geochemical modelling of safety and decommissioning strategies of nuclear contaminated sites. Laser Induced Breakdown Detection (LIBD) system (MAGELLAN model) used in the present studies was developed by Cordouan Technologies (France) in collaboration with the Karlsruhe Institute of Technology (KIT), Germany. The LIBD comprises of a stable pulsed nanosecond laser, typically a frequency doubled Nd:YAG laser emitting at 532 nm. The energy of the pulses is adjusted automatically with the help of a variable attenuator and recorded by an energy detector.

CATEGORY 08: LASER IN INDUSTRY AND DEFENSE

CP-08-1. LASER-ASSISTED REMOVAL OF WELD HEAT TINTS FROM STAINLESS STEEL SURFACS

Aniruddha Kumar[$], Saradhi Gumma[^] , Supratik Roychowdhury[^], R. B. Bhatt[$], J P Nilaya[+], [$]Fuel Fabrication, Bhabha Atomic Research Centre,Tarapur, Maharashtra,401504, [^]Materials Processing & Corrosion Engineering Division, BARC,Mumbai,400085,[+]Laser & Plasma Technology division, BARC,Mumbai,400085. ***Email****: nontee65@yahoo.com*

The heat generated during the welding of stainless steel results in the oxidation of the surface that, apart from aesthetics, adversely affects its corrosion property too. This communication reports the successful removal of heat tint generated by gas tungsten arc welding process off a stainless steel surface in addition to improvement in its pitting corrosion resistance by exposure to the emission of a nano- second pulsed fiber laser. The laser cleaning experiments, conducted with six different laser pulses having different temporal shapes and duration that varied from 20 ns to 1020 ns, revealed that removal of the weld heat tint was possible in all conditions provided the effective laser fluence exceeded a definite threshold value. This threshold value, in turn, was found to increase with increase in pulse duration. The laser cleaned specimens were subsequently analyzed for pitting corrosion resistance. The pitting corrosion resistance of the laser treated specimens was compared with the as-welded specimens and welded specimens with heat tint removed using conventional methods like wire brush cleaning and chemical pickling. The superior quality of tint removal, improved pitting corrosion resistance and the ease of non-contact operation indicates the significant potential of fiber laser based weld tint removal method to substitute the conventional mechanical or chemical cleaning methods currently in use in the manufacturing industry.

CP-08-2. DESIGN & DEVELOPMENT OF AN AUTOMATED CONTROL SYSTEM FOR CO_2 LASER ASSISTED TRITIUM FILLED GLASS TUBE CUTTING & SEALING FOR BRIT, MUMBAI

Rajiv Kumar Yadav[1], Manoj Kumar[1], L B Rana[1] M Murugan[2],N Jayachandran[3] and R Kaul. Laser [1]Materials Processing Division, RRCAT, Indore, [2]Laser Components Design & Fabrication Section, TDSG, RRCAT, Indore, [3]Board of Radiation & Isotope Technology (BRIT), Mumbai ***Email:*** *rajivyadav@rrcat.gov.in*

Internally phosphor coated and tritium filled glass vials having self-illumination life of up to 15 years without needing any external excitation source; are proven to be a very reliable source of light. Presently these vials are imported and cost of each is very high. A CO2 laser assisted indigenous technology has been developed for cutting and sealing of Tritium filled tubes of various diameters into vials of different length at LMPD, RRCAT. This system will save huge outflowing Indian currency against import of such costly vials, which can be produced inexpensively within country to meet strategic demand of vials. They are required in Lakhs of quantities. Tested leak integrity of cut and sealed vials is better than 1 x 10-10 mbar.l/sec.

CP-08-3. INTERMETALLIC-FREE JOINING OF STAINLESS STEEL AND PURE ALUMINUM FOILS USING INNOVATIVE LASER MICRO-WELDING TECHNIQUE

Aniruddha Kumar[*], R. B. Bhatt[*], Suman Neogy[#], [*]Fuel Fabrication, Integrated Nuclear Recycle Plant, Operations),Bhabha Atomic Research Centre, Tarapur, Maharashtra, India, 401502,[#] Materials Science Division, Bhabha Atomic Research Centre, Mumbai, India, 400085. ***Email****: nontee65@yahoo.com*

We present the result of laser micro-welding of stainless steel (AISI 304) and pure aluminum foils of 50µm and 70µm thick respectively. A repetitive single-mode nano-second fiber laser was made use to carry out the weld in lap joint configuration. During welding stainless steel remained in solid state, while aluminum underwent localized melting over a narrow zone at the interface. Electron microscopy studies along with EDS composition analysis revealed the weld interface to be free of any intermetallic compound. Use of short duration laser pulses with lower heat input restricted the bulk diffusion of elements across the interface during welding and thereby generation of intermetallic compounds. Tensile shear testing established the weld joint to withstand ~ 140N load before fracture.

CP-08-4. EFFECT OF SCAN STRATEGY ON PART DEFORMATION IN SINGLE LAYER LASER–BASED DEPOSITION

Ankit Shrivastava[a,d], Shitanshu Shekhar Chakraborty[a,d], Samik Dutta[b,d], Surjya Kanta Pal[c], [a]Materials Processing and Microsystems Laboratory, CSIR-Central Mechanical Engineering Research Institute, Durgapur-713209 , [b]Surface Engineering and Tribology, CSIR-Central Mechanical Engineering Research Institute, Durgapur-713209, [c]Mechanical Engineering Department, Indian Institute of Technology, Kharagpur, 721302, [d]Academy of Scientific and Innovative Research (AcSIR), Ghaziabad, PIN-201002, Uttar Pradesh, India , ***E.mail** : situspeaks@gmail.com; ss.chakraborty@cmeri.res.in.*

Part deformation is a major concern in additive manufacturing and remanufacturing applications for achieving close dimensional tolerance. Thermal history is of paramount imporantace in laser based deposition process. This not only dictates the microstructural properties but also affects the deformation. Different scan strategies results in different maximum temperature and cooling rate achieved by the system. In this article deformation of inconel-625 has been compared for deposition with three different scan strategies (i.e. 0°, 90° and 67°) using thermo-mechanical finite element analysis. The depostion using 67° scan strategy resulted in lowest deformation as compared to the other two.

CP-08-5. EFFECT OF SCAN STRATEGY ON PART DEFORMATION IN SINGLE LAYER LASER–BASED DEPOSITION

Vijay Shukla[1], Pawan Kumar[1], A. K. Rai[1], Himanshu Singhal[2], Ranveer Singh Meena[1], Rajpal Singh[1], M. K. Bairwa[1], Bhaskar Paul[1], R. K. Jain[1], B. K. Saini[1], B. Ekka[1], B N Upadhyaya[1] and K S Bindra[1], [1]Laser Technology Division, Raja Ramanna Centre for Advanced Technology, Indore-452013, INDIA, [2]Laser Plasma Division, Raja Ramanna Centre for Advanced Technology, Indore-452013, INDIA, ***E-mail**: shuklavs@rrcat.gov.in*

In this paper, we report on profile cutting of 0.6 mm thick silicon wafer of 100 mm diameter using fiber coupled millisecond pulse Nd:YAG laser. Laser process parameters such as pulse energy, pulse duration, pulse frequency and cutting speed were optimized and characterization of cut edges were performed using optical microscope and scanning electron microscope. These profiles cut silicon samples will be used for fabrication of gold coated mirrors and will be utilized for laser plasma experiments.

CP-08-6. PRELIMINARY TEST RESULTS OF THE GAAS BASED PCSS SWITCH USING A FIBRE COUPLED ND:YAG LASER

*Amitava Roy[2], Ankur Patel[2], Ritu A[2], R. I. Bhaktsingh[2], Archana Sharma[2], P. D. Mehta[1], V. B. Chandratre[1] A.P. Shah[3], Arnab Bhattacharya[3], [2]Accelerator & Pulse Power Division, Bhabha Atomic Research Centre, Mumbai, [1]Electronics Division, Bhabha Atomic Research Centre, [3]Tata Institiute of Fundamental Research, Mumbai, **Email:** vbc@barc.gov.in, aroy@barc.gov.in, arnab@tifr.res.in*

Accelerator and Pulse Power Division, BARC have been working on the design and development of single shot and repetitive pulse power systems. Several high voltage pulse power systems having voltage ranges from 200 kV to 1 MV, current ranges from 5 kA to 30 kA, pulse width from 5 ns to 300 ns and repetition rate from 1 Hz to 100 Hz have been developed. All these pulsed power systems are based on spark-gap and magnetic switches. However, spark-gap switches have the limitation of pulse repetition rate due to high recombination time of plasma. Magnetic switches can be used at kHz repetition rate but has the limitation of reliable high voltage operation and complex reset circuitry. Hence, it was proposed to develop a compact solid state semiconductor switch and to explore it as an alternative to spark-gap switches in pulse power systems. Photoconductive Semiconductor Switch (PCSS) is device exhibiting sub-nano-second temporal resolution together with High voltage and high current operation ability. Electronics Division, BARC designed GaAs based PCSS devices, and fabricated at Tata Institute of Fundamental Research (TIFR). The preliminary wafer level tests were performed to ascertain the electrical characteristics (Current-Voltage) in the static case. The dynamic switching characterization using a nano-second Laser (λ = 532 nm, t_w = 7 ns) yielded a holding voltage of 20 kV for a current of 300 A & rise-time of 0.7-10 ns.

CP-08-7. SYNCHRONIZED TRIGGERING OF MULTIPLE SPARK GAPS USING OPTICAL PULSED LASER BEAM

Ritu Agarwal, Amitava Roy, Ankur Patel, Archana Sharma, Accelerator & Pulse Power Division, Bhabha Atomic Research Centre, Mumbai, ***Email:*** *ritu@barc.gov.in, aroy@barc.gov.in,*

Synchronised triggering of multiple spark gaps is one of the important requirements for the development of the pulse power systems. Multiple spark gaps switching, triggered using optical Laser Pulse beam is presented. A Nd:YAG laser of 7 ns pulse duration with 19 fiber optic beam delivery system each having less than 1mJ of energy at wavelength of 532 nm is used for the triggering. The Laser beam is focused on the electrodes of spark gaps. The power density of laser beam when it hits the electrode is 0.40 GW/cm^2. The multiple spark gaps were Laser triggered at 35kV and delay of 50ns to 2.5µs was observed. This spark gap is highly reliable for repetitive switching and it is capable of delivering high voltage and current operated in the triggering mode using Laser. Effect of variation of applied voltage and synchronization of multiple spark gaps was done. The switch performance has been also studied in nitrogen gas up to 1.2kg/cm^2 pressure and voltage up to 52kV.

CP-08-8. COMPARATIVE STUDY OF SERIES AND PARALLEL FLOW LASER PUMP CHAMBERS FOR HIGH POWER ND:YAG LASER APPLICATIONS

V. Bhardwaj, M. K. Bairwa, Rajpal Singh, Bhaskar Paul, B. Ekka, S. K. Sharma, B N Upadhyaya, K S Bindra, Laser Technology Division, Raja Ramanna Centre for Advanced Technology, Indore-452013,* ***E-mail:*** *vbhardwaj@rrcat.gov.in.*

Laser pump chambers are the backbone of high power lamp pumped Nd:YAG laser systems. It is required to achieve high efficiency and efficient heat removal from Nd:YAG laser pump chambers to attain good beam quality. We have performed a comparative study of series flow and parallel flow type pump chambers for high power Nd:YAG laser applications. It has been found that series flow pump chamber provides a better performance and has a lower risk of rod damage as compared to parallel water flow pump chamber in case of degradation in water pump.

CP-08-9. COMPARATIVE STUDY OF LASER WELDING AND TIG WELDING OF METAL THERMOCOUPLE FINE WIRES

Abhishek K. Yadaw, Amit Kulshreshtha, Aniruddha Kumar, Fuel Fabrication Facility, Bhabha Atomic Research Centre, Tarapur, Maharastra, 401504, India, ***Email:*** *abhisheky@barc.gov.in*

Thermocouples are widely used in heating furnaces to measure temperatures with high accuracy and repeatability. In this work, Nd-YAG solid state laser welding and TIG (Tungsten inert gas) welding is used to produce thermocouples of wire diameter 0.5 mm. We have studied the effect to laser welding of wavelength 1064 nm, and TIG welding on the performance of Type D (97%W/3%Re–75%W/25%Re) thermocouple. An evaluation of bead geometry is carried out for both laser welded and TIG welded thermocouples. Performance of thermocouple is predicted by accuracy of temperature measurement. Welding parameters were optimized for heat input, and to achieve weld bead diameter nearly equal to wire diameter. This paper discuss the challenges involved in the laser welding and TIG welding of Tungsten/rhenium-alloy thermocouple wire to obtain defect free weld.

CP-08-10. LASER BEAM WELDING (LBW) OF HERMETICALLY SEALED DRIFT TUBES FOR DRIFT TUBE LINAC

Prashant Kumar, Vikas Teotia, Elina Mishra, Rajesh Chimurkar, Sanjay Malhotra, ***E-mail:*** *pkarn@barc.gov.in*

Drift Tubes which houses permanent magnet quadrupoles are hermetically sealed as the RF heat generated on the surfaces are required to be removed by water flowing in channels built in the Drift Tube assembly. Presence of permanent magnet precludes the usage of E-beam welding and brazing. Laser welding is an attractive alternatives which is explored, tried and established for sealing more than 50 Drift tubes during various stages of the project. This paper gives details of laser welding performed on drift tubes of drift tubes of LEHIPA

CATEGORY 9: LASERS SPECTROSCOPY AND ITS APPLICATIONS

CP-09-1. MICRO-PHOTOLUMINESCENCE STUDIES ON MOS_2 TWO-DIMENSIONAL MONOLAYER USING CW AND FEMTOSECOND LASER

Saleem Khan[1], Durga Prasad Khatua[1,2], Salahuddin Khan[1,] and T K Sharma[1,2], [1]Materials Science Section, Raja Ramanna Centre for Advanced Technology, Indore – 452013, [2]Homi Bhabha National Institute, Training School Complex, Anushakti Nagar, Mumbai – 400094, *E.mail : skhan@rrcat.gov.in*

The Transition metal dichalcogenides are promising materials for application in optoelectronic, spintronics and quantum technology. MoS_2 is one such materials which is of direct band gap nature in its monolayer form and possesses an indirect band gap at higher number of layers. Using micro photoluminescence (PL) measurements, we have shown that at photon fluence of nearly $10^{14}/cm^2$, the PL peak is red shifted with respect to the PL measured using a cw laser. This is explained by bringing the sample heating and/or the band gap renormalization leading to a 2 nm red shift of the PL peak. Further details will be presented during the symposium.

CP-09-2. LASER BASED REMOTE MONITORING OF HYDROGEN FLUORIDE

*Anita Gupta, Kishor Thapa, and D V Udupa, A&MPD, Bhabha Atomic Research Centre, Mumbai, India, **Email:** anitag@barc.gov.in*

Laser absorption spectroscopy plays a vital role in detection of pollutants and toxic gases present in the environment. It is possible to design compact gas detectors using available tunable diode lasers in near infrared range. In this paper we present feasibility study on design of laser based remote monitor for hydrogen fluoride (HF). The HF monitor utilizes HF absorption line at 7788 cm^{-1}. The absorption in the laser beam path from source to retro-reflector and back to detector is used to estimate the HF concentration. A comparison has been made between direct absorption and wavelength modulation spectroscopy (WMS) techniques.

CP-09-3. ATOMIC FOUNTAIN OF RUBIDIUM ATOMS WITH MOVING MOLASSES

S Singh[1], B. Jain[1], V B Tiwari[1,2] and S R Mishra[1,2], er Physics Applications Section, Raja Ramanna Centre for Advanced Technology, Indore - 452013, India. , [2]Homi Bhabha National Institute, Training School Complex, Anushakti Nagar, Mumbai - 400094, **Email:** surendra@rrcat.gov.in*

The laser cooled ^{87}Rb atoms in a magneto-optical trap (MOT) have been launched in vertical geometry using moving optical molasses technique to make an atomic fountain. The launch velocity for atoms was measured as function of relative detuning between downward and upward propagating MOT beams arranged in [1,1,1] configuration. The fountain will be used for precision measurement of earth's gravitational acceleration (g).

CP-09-4. OPTICAL PUMPING IN UNCOATED AND ANTI-RELAXATION COATED ATOMIC CELL

*Saptarshi Roy Chowdhury[1] and Swarupananda Pradhan [1,2,3], [1]Beam Technology Development Group, Bhabha Atomic Research Centre, Mumbai-400085, [2]Homi Bhabha National Institute, Anushaktinagar, Mumbai-400094, [3]**Email**: spradhan@barc.gov.in*

We study the optical pumping in Rubidium atoms in an uncoated and an anti-relaxation coated (ARC) atomic cell. The optical pumping laser is tuned to the Rb D2 transition and the ground state population is measured by a probe beam tuned to the Rb D1 transition. The Lamb dip and optically pumped sub-Doppler resonances are seen in the uncoated atomic cell. These sharper resonances get washed-out by the velocity changing collisions (for longer duration) as the spatial separation between pump and probe beams are increased. For the ARC cell, these sharp resonances are not observed even with overlapping pump and probe beam. It indicates the presence of residual gas in the ARC cell that rapidly equilibrates the velocity distribution in the atomic sample. The relative probability of elastic and inelastic processes for both the cells are discussed in accord with the experimental observations

CP-09-5. RAY TRACING MODEL FOR OPTICAL RE-INJECTION IN OFF-AXIS INTEGRATED CAVITY-OUTPUT SPECTROSCOPY

A. K. Pal[a,b] and N. Kumar[a], [a]Infrared Laser Spectroscopy Section, Bhabha Atomic Research Centre, Mumbai-400085, [b]Homi Bhabha National Institute, Anushaktinagar, Mumbai – 400094, E mail: ayaniitb@gmail.com

Off-axis integrated cavity-output spectroscopy (OA-ICOS) is a highly sensitive absorption spectroscopic technique based on long optical path length. The longer path length in OA-ICOS technique is achieved with application of high reflectively mirrors. However, the cavity throughput in off-axis method is significantly lowered as the mirror reflectivity increases, which limits sensitivity of OA-ICOS. This limitation can be overcome by optical reinjection method with application of placing additional astigmatic mirror (re-injection mirror) in front of the first cavity mirror to re-inject the back-reflected light from the first cavity mirror into the cavity. Therefore, in this paper, numerical simulation of optical reinjection phenomena in OA-ICOS cavity using paraxial ray tracing model has been carried out and described to see the impact on number of reinjection. In the simulation, maximum number of re-injection of 1335 for re-injection cavity length 70 cm and minimum number of re-injection of 6 for re-injection cavity length 50 cm are observed.

CP-09-6. GAS PHASE KINETICS OF A CYCLIC ETHER WITH THE OH RADICAL STUDIED USING LASER PHOTOLYSIS-LASER INDUCED FLUORESCENCE

Anmol Virmani, Mohini P. Walavalkar, Asmita Sharma, Sumana Sengupta, Ankur Saha, and Awadhesh Kumar Radiation & Photochemistry Division, Bhabha Atomic Research Centre, Trombay, Mumbai- 400085, India ***Email:*** *avirmani@barc.gov.in*

In this work, we have used a pump-probe technique employing nanosecond lasers to study the kinetics of the reaction of 1,2-propylene oxide with the OH radical. Reaction with OH radical happens to be the major degradation channel for most of the Volatile Organic Compounds (VOCs) released in the atmosphere. Kinetic studies of the gas phase reaction of a VOC with the OH radical is therefore required to obtain the tropospheric lifetime of the VOC. In this context, we have determined the absolute bimolecular rate coefficient of the reaction of 1,2-propylene oxide with the OH radical using Laser Photolysis-Laser induced Fluorescence (LP-LIF) technique over the temperature range of 261-335 K. We have found the rate coefficient of the reaction of 1,2-propylene oxide with the OH radical to be $(4.64 \pm 0.24) \times 10^{-13}$ cm^3 $molecule^{-1}$ s^{-1} at 298 K, and the corresponding tropospheric lifetime to be 12 days. Rate coefficients of this reaction are found to vary arbitrarily within a narrow range of $(4.65 \pm 0.24) \times 10^{-13}$ cm^3 $molecule^{-1}$ s^{-1} to $(4.80 \pm 0.24) \times 10^{-13}$ cm^3 $molecule^{-1}$ s^{-1} over the temperature range of 261 - 335 K, suggesting invariance of reactivity with altitude and a barrier-less mechanism.

CP-09-7. SYNTHESIS OF BODIPY ANALOGUES FOR THEIR USE AS EFFICIENT DYE LASER

Goutam Chakraborty[a], Pooja L. Bhargude[b], J P Nilaya[a,d], Sunita Kedia[a], Soumyaditya Mula[c,d]*, [a]Laser and Plasma Technology Division, Bhabha Atomic Research Centre, Mumbai-400085, [b] Former student of Jai Hind College, Mumbai- 400020, [c]Bio-Organic Division, Bhabha Atomic Research Centre, Mumbai-400085, [d]Homi Bhabha National Institute, Anushaktinagar, Mumbai-400094.**Email**: gchak@barc.gov.in*

In this present contribution, we report synthesis, characterization and photophysical studies of two BODIPY analogues BDY-An and BDP-Sty for their use as active dye laser medium. From the solvatochromism studies it is evident that both the dye shows red shift in absorption and emission spectra with increasing polarity of the solvent, clearly indicating polar character of the synthesized dyes. Moreover, while BDY-An dye was found to show low fluorescence quantum yield due to its intramolecular charge transfer (ICT) character, the dye BDP-Sty is highly emissive in nature with quantum yield of >0.7 in almost all the solvents used in the study. More importantly, optical stability studies reveal that both the synthesized dyes, BDY-An and BDP-Sty are found to be more stable than the commercially available pyrromethene-597 (PM-597), which is being used as efficient laser dye till date. Thus, the present study provides a basic idea about the type of BODIPY dyes, which can be potential candidates to be used as laser dyes.

CP-09-8. POTENTIAL OF THE CONFOCAL MICRO RAMAN SPECTROSCOPY FOR THE DETERMINATION OF IMPACT OF TREATMENT OF SILICON DIOXIDE NANOPARTICLES ON MAIZE SEEDLINGS

*Aradhana Tripathi[1], Chhavi Baran[2], Sweta Sharma[1, 3] and K. N. Uttam[1], [1]Saha's Spectroscopy Laboratory, Department of Physics, University of Allahabad, Prayagraj, [2]Centre for Environmental Science, IIDS, University of Allahabad, Prayagraj, [3]Department of Applied Science and Humanities, Faculty of Engineering and Technology, Khwaja Moinuddin Chishti Language University, Lucknow, **Email**:aradhnagate@gmail.com*

This study examines the potential of confocal micro Raman spectroscopy coupled with principal component analysis for the determination of the alterations of the biochemicals present in the leaf of the maize plants at an early stage upon the treatment of different concentrations of silicon dioxide nanoparticles (SiO_2NPs). For this, the maize seedlings were developed in the laboratory under the control conditions such as light flux, temperature and moisture. The treatment of the SiO_2 nanoparticles was given to the seedlings through the root with the Hoagland solution. The Raman spectra of the adaxial surface of the secondary leaf of control and silicon dioxide nanoparticles treated maize seedlings were acquired in the spectral region <2000 cm^{-1}. The analyses of the spectral data show that the treatment of the different concentration of the SiO_2 NPs (0.2, 0.6, 1.0, 1.4 and 1.8 mM) enhanced the level of biochemicals like cellulose, hemicellulose, carotenoid, anthocyanin, lignin, alkaloid structures. The principal component analysis of the acquired Raman spectral data shows that the principal component 1 explains 92.88 % while the principal component 2 are able to explain 3.26 % of total variation in data sets.

CP-09-9. DEMONSTRATION OF A STAND-OFF LASER INDUCED BREAKDOWN SPECTROSCOPY SETUP

S. Ahlawat, P K Mukhopadhyay, K S Bindra, Laser Technology Division, Raja Ramanna Centre Advanced Technology, Indore, M.P. 452013, India, ***Email**: rsunita@rrcat.gov.in*

We have developed a stand-off laser induced breakdown spectroscopy set up where samples placed at a distance of 6 m from the detector could be analyzed. A 1064 nm nanosecond laser with 180 mJ energy was used to produce plasma from the samples surfaces and the light emitted by the plasma was collected by a telescope coupled with a multi-channel Czerny Turner spectrometer. The setup was tested using different grades of stainless steel samples and different rock samples, and found to be able to successfully differentiate between different metallic or rock samples.

CP-09-10. RAPID DETECTION OF CR(III) AND MO(VI) IONS IN THE AQUEOUS MEDIUM BY SURFACE ENHANCED RAMAN SCATTERING USING VANILLIC ACID FUNCTIONALIZED SILVER NANOPARTICLES

Sweta Sharma[a,c], Aarti Jaiswal[b], Aparna Tiwari[a] and K. N. Uttam[a], [a]Saha's Spectroscopy Laboratory, Department of Physics, University of Allahabad, Allahabad, India; [b]Centre for Material Science, IIDS, University of Allahabad, Allahabad, India, [c]Department of Applied Science and Humanities, Faculty of Engineering and Technology, Khwaja Moinuddin Chishti Language University, Lucknow ***Email:*** *swetasharma3989@gmail.com*

The present study exploits the utility of vanillic acid functionalized silver nanoparticles (V-AgNPs) synthesized by chemical reduction method for the colorimetric and surface enhanced Raman scattering detection of the heavy metal in aqueous solution. The addition of synthesized V-AgNPs colloidal solution to control and metal ion laced water samples turns the colour of solution greyish black except for Cr(III) ions. It has been observed that addition of V-AgNPs colloidal solution to the water samples containing Cr(III) ions turns the colour of the solution transparent. Furthermore, the addition of V-AgNPs to water samples containing Cr(III) ions and Mo(VI) creates unique Raman spectral signatures with considerably large intensity that can be used for the identification of these metal ions in aqueous solution. The obtained colour pattern and Raman spectral signatures show the potential of V-AgNPs for low cost, timeless, affordable, convenient, sensitive, selective and rapid detection of heavy metal ions.

CP-09-11. DEVELOPMENT OF HIGH -Q HELMHOLTZ PA CELL FOR SPECTROSCOPY OF ACETONE BETWEEN UV- MID-IR AND TERAHERTZ REGION AND HIGHER HARMONICS

*Arjun V.S. Kidavu and A. K. Chaudhary*Advanced Centre for Research in High Energy Materials, University of Hyderabad, Hyderabad-500046, India,* ****Email****: akcphys@gmail.com, akcsp@uohyd.ernet.in,*

We report the use of high-Q Helmholtz photoacoustic cell for the spectroscopy of Acetone, a biomarker between UV- Mid –IR and Terahertz region. UV pulsed laser of wavelength 266nm tuneable repetition rate, Quantum Cascade pulsed Laser (QCL) tuneable between 5.2- 11μm (Mid-IR) range and electronic Terahertz (THz) source at 0.11 THz were used separately to record the spectra of the acetone vapour The designed Helmholtz cell resonance frequency is tuneable between 1.6-3.2 kHz ranges. The designed cell has High Q value of ~500. We also generated the higher acoustic harmonics of PA signal using Lock-in-amplifier coupled detection system.

CP-09-12. ENHANCEMENT OF DEFECT PEAKS IN WSE_2 UNDER TWISTED LIGHT EXCITATION

A. K. Pattanayak, A. Dhara, P. Das, D. Chakrabarty, S. Paul, M. M. Brundavanam, S. Dhara, Department of Physics, Indian Institute of Technology Kharagpur, Kharagpur-721302, West Bengal, India ,* ****Email:*** *tapu10@iitkgp.ac.in*

Defects play important role in optical and electronic properties in TMDs monolayer. In W-based TMDs the peaks appearing below dark excitons are mostly considered as defects peak or localized excitons. In our study, we have shown enhancement of these defects peak emission with the increase in topological charge of twisted light in the WSe_2 monolayer.

CP-09-13. AN INVESTIGATION OF THE SURFACE ACTIVITY FOR AQUEOUS BINARY MISCIBLE POLYMER BLENDS BY NON-LINEAR LASER VIBRATIONAL SPECTROSCOPY

S. Kaur[1] and K C Jena[1,2,], [1]Department of Physics, Indian Institute of Technology Ropar, Rupnagar, Punjab-140001, India, [2]Department of Biomedical Engineering, Indian Institute of Technology Ropar, Rupnagar, Punjab-140001, India, [*]**E.mail:** kcjena@iitrpr.ac.in*

In our present study, we employed sum frequency generation vibrational spectroscopy to study the molecular structure of the aqueous solution of binary miscible polymer blend composed of methoxyethoxyethoxy phosphazene (MEEP) and polyethylene oxide (PEO) at the air/aqueous interface. PEO and MEEP are polymer gel electrolytes with tremendous promise for polymer gel electrolyte device applications require surface insight to understand blending interactions and interfacial significance. Our experimental observation reveals the presence of the dilute MEEP at the interface has a significant impact on the hydrogen bonding network of the interfacial water structure in comparison of PEO polymer chains. This study allows understanding PEO-MEEP intermolecular interactions and looks into the dimensionality stability of MEEP in aqueous phase under variable PEO fractions. At the conference, we will give a detailed analysis of our surface studies on the aqueous solution of binary blend polymer and its impact on the interfacial water structure.

CP-09-14. PROMPT AND NON-DESTRUCTIVE ASSESSMENT OF THE PIGMENTS OF THE WATER CALTROPS BY LASER INDUCED FLUORESCENCE SPECTROSCOPY

*Aparna Tiwari[1], Aishwary Awasthi[1], Renu Singh[2] and K. N. Uttam[1], [1]Saha's Spectroscopy Lab, Department of Physics, University of Allahabad, Prayagraj, [2]School of Basic and Applied Sciences, G D Goenka University, Gurugram, Haryana, **Email:** aparnatiwari945@gmail.com*

The pigments present in the parts of the fruits are found to play an important role in determining the quality attributes of the fruits and human health. The water caltrops are used to treat sore throat, anaemia, fractures, urinary disorders and bronchitis. These properties of the water caltrops are attributed due to the presence of various biochemicals in it. Therefore biochemical investigation especially presence and amount of pigments estimation is highly desired to keep safe, usable and fresh water caltrops. For this, the laser induced fluorescence spectrum of the exocarp and mesocarp region of the dark green and red water caltrops have been recorded in the spectral region 400-800 nm. The analysis of the fluorescence spectrum shows the presence of spectral signatures of the chlorophyll and anthocynin. The evaluated areal intensity by curve fitted spectra has been used for the comparison of the level of detected pigments in the different region of the variety of the water caltrops. The study demonstrate that laser induced fluorescence spectroscopy is a non-destructive, non-invasive, prompt, label free, extraction free, robust and fast evaluation technique for the estimation of pigments present in the fruits.

CP-09-15. NON-DESTRUCTIVE ASSESSMENT OF NUTRIENT PROFILE OF MANGO AND JAMUN SEEDS USING CONFOCAL MICRO RAMAN SPECTROSCOPY

Sweta Sharma[1, 2], Abhi Sarika Bharti[1], Shrishti Sharma[1], and K. N. Uttam[1], [1]Saha's Spectroscopy Laboratory, Department of Physics, University of Allahabad, Prayagraj, India, [2]Department of Applied Science and Humanities, Faculty of Engineering and Technology, Khwaja Moinuddin Chishti Language University, Lucknow, India, ***Email:*** *swetasharma3989@gmail.com*

Adequate nutrition is pivotal for public health and it is very challenging to fulfil the nutritional requirements of overpopulated world. Therefore it is the need of the day to identify the potential of underutilized food alternatives that are highly nutritious, have health-promoting properties and widely available. Seeds of fruits like jamun and mango are reported to have immense health promoting constituents and medicinal properties but still they are largely discarded as waste due to lack of knowledge about their nutrient profile. Therefore, the present study aims at demonstrating the potential of confocal micro Raman spectroscopy for the non-destructive, rapid and label free assessment of the phytochemical and elemental profile of the jamun and mango seeds. The analysis of the Raman scattering spectral profile shows that seeds of jamun and mango are rich source of carbohydrates like glucose and starch, fatty acids and antioxidant compounds like carotenoids and phenolic compounds. The information obtained in the form of spectral features is highly beneficial for the administrators and nutrition scientists in assessment of quality of the diet, tackling malnutrition in effective manner and exploring the use of these seeds in various industries and breeding programs.

CP-09-16. IMPACT OF DIFFERENT MODIFIER FLUORIDES ON OPTICAL PROPERTIES OF SM^{3+} DOPED $BIPO_4$ NANO CRYSTALS IN BISMUTH PHOSPHATE GLASS (LI) AND GLASS CERAMICS(NA, MG, K, CA AND SR)

M. Kumar and Y.C. Ratnakaram*, Sri Venkateswara University, Tirupati, India,517502., ****E.mail:*** *maddilakumar7@gmail.com*

Transparent glass ceramics containing $BiPO_4$ nanocrystals in bismuth phosphate glass ceramics doped with Sm^{3+} ions were synthesized by melt quenching method. Powder XRD analysis was used to confirm the $BiPO_4$ crystalline phase. Confirmations of structural units were done by FTIR. Optical parameters from absorption spectra and emission spectra have been investigated. Effect of mixed alkali and alkaline metal on radiative properties of various levels of Sm^{3+} ions studied. Out of studied networks, potassium glass ceramic exhibit productive properties and could be potential in the development visible laser applications

CP-09-17. ADOPTION OF LIBS TECHNIQUE FOR QUALITY CONTROL OF NANOPARTICLES PRODUCED BY AUTOMATED WIRE EXPLOSION PROCESS

Chillu Naresh[1], Gandluri Parameswarreddy[1], Rengaswamy Jayaganthan[2], Ramanujam Sarathi[1], Archana Sharma[3], [1]Department of Electrical Engineering, Indian Institute of Technology Madras, Chennai, India., [2]Department of Engineering Design, Indian Institute of Technology Madras, Chennai, India., [3]Head, Pulsed Power & Electro-Magnetics Division, Bhabha Atomic Research Centre, Visakhapatnam, India, ***E.mail*** *: rsarathi@iitm.ac.in*

Recent research indicates that the plasma temperature recorded during laser ablation of the material surface provides a qualitative description of material's hardness. The solid aluminium, along with the metal Al nanoparticles produced by automated electrical wire explosion technique, are pelletized into a circular disc to evaluate the plasma temperature upon

subjecting the specimens to laser ablation using Laser Induced Breakdown Spectroscopy (LIBS). The results indicated that the pelletized nano powder have characteristics of plasma formed is very close to that of a solid aluminium wire.

CP-09-18. ADOPTING LASER INDUCED BREAKDOWN SPECTROSCOPY TO MONITOR AS AN AGEING MARKER FOR PRESSBOARD MATERIAL

*S. K. Amizhtan[1], A. J. Amalanathan[1], R. Sarathi[1], Hans Edin[2] and Nathaniel Taylor[2], [1]Department of Electrical Engineering, Indian Institute of Technology Madras, Chennai 600036, India., [2]School of Electrical Engineering and Computer Science, KTH-Royal , Institute of Technology, SE-10044, , **Email:** ee19d207@smail.iitm.ac.in*

Sulphur diffusion into pressboard material is one of the major causes for catastrophic failure of transformer during operation. Identification of Sulphur content in pressboard material is a major challenge. A methodical experimental study were carried out through accelerated thermal ageing and the presence of sulphur content in pressboard material is diagnosed adopting Laser induced breakdown spectroscopy (LIBS). The quantitative parameter identified from LIBS provides an indication on the end of life of pressboard insulation in transformers. Further, these LIBS spectral database are coupled with Principal Component Analysis (PCA) for its effective classification of aged pressboard material to demonstrate its use for the condition monitoring of transformer insulation.

CP-09-19. INVESTIGATION ON POLLUTION PERFORMANCE OF SILICONE RUBBER MICRO NANOCOMPOSITES BY ADOPTING LIBS ANALYSIS

*Pabbati Vinod[1], Myneni Sukesh Babu[1], Ramanujam Sarathi[1] and Stefan Kornhuber[2], [1]Department of Electrical Engineering Indian Institute of Technology Madras, Chennai 600036, India., [2]Department of High Voltage Engineering, University of Applied Sciences, Zittau/Görlitz, Zittau, Germany., **E.mail:** rsarathi@iitm.ac.in*

Laser induced breakdown spectroscopy (LIBS) is adopted to understand the pollution performance of silicone rubber micro nanocomposites. The elemental composition of the pollutant present on the sample is effectively determined from LIBS spectral data. The temporal characteristics of the LIBS spectral data have been studied to understand the lifetime variation with respect to pollution severity. A comparative study on different artificial neural network (ANN) training algorithms have been performed, for the classification of contaminated silicone rubber micro nanocomposite samples based on severity of the pollutant.

CP-09-20. THREE-STEP THREE-COLOUR SELECTIVE PHOTOIONIZATION OF NATURAL YTTERBIUM FOR ENRICHMENT OF ^{168}YB

D Biswal[1,3], A. U. Seema[1], R C Das[2,3], D. R. Rathod[1], A K Singh[1], A. Khattar[1], J. S. B. Singh[1], A. Wahid[1], P. R. Mohite[1], S. K. Maurya[1], J. S. Dhumal[1], J. Thomas[1], Asawari D Rath[1,3], S Kundu[1*],[1] Tunable Laser Section, Advanced Tunable Laser Applications Facility, BTDG, BARC,[2] Laser & Plasma Technology Division, BTDG, BARC, Mumbai-400085.[3]Homi Bhabha National Institute, Mumbai-400094, Email: dbiswal@barc.gov.in*

Recently there have been continual efforts focused on the developement of technologies towards enrichment of precuesor isotopes to radioisotopes having radiopharmaceutical applications to facilitate high purity production of later using nuclear reactions. Among them, laser based enrichment is most versiatile, highly selective and efficient process which uses

multistep resonant selective photo ionisation to selectively excite and subsequently ionise the target isotope. Laser parameters like wavelengths, linewidths, intesities etc., are key factors in determining the isotopic selectivity of a photo ionisation ladder. This paper presents details of precise determinaton of the transition wavelengths pertaining to three-step three-colour selective photoionisation of ^{168}Yb in a time of flight mass spectrometer using resonant ionization mass spectroscopy. Further, the laser-matter interaction process was qualified in terms of laser intensities to achieve spectroscpoic selectivity of ~99% for ^{168}Yb. Incorporation of optimized laser parameters in enrichment experiments yielded > 15 % enriched ^{168}Yb (nat. abundance 0.13%).

CP-09-21. HIGH-SPEED, LOW COST SOLUTION TO ESTIMATE K AND ZN CONCENTRATION IN SOIL USING MULTI-WAVELENGTH REFLECTION MEASUREMENT SYSTEM

M.Thangaraja[1], V.Sathiesh kumar[1] , Department of Electronics Engineering, Madras Institute of Technology, Anna University, Chennai-600044, ***E.mail*** *: rajaeee83@yahoo.co.in, sathiieesh@gmail.com*

In this paper, a high speed, low cost potassium and zinc estimator in soil is proposed and demonstrated. It makes use of the reflection principle at different incident laser wavelengths by the soil surface. The device incorporating this principle is coined as Multi-wavelength Reflection Measurement System (MRMS). This system is used to determine the elemental concentration (K and Zn) in soil. It is observed that the element identification is highly dependent on the wavelength of the incident laser. In case of soil with varying zinc concentration, the reflection intensity at 444 nm is on higher scale when compared to 636 nm. The opposite trend is observed while estimating potassium concentration in soil. The potassium and zinc concentration in soil is estimated by utilizing a linear calibration equation with a correlation coefficient R^2 of 0.950 and 0.970, respectively. To perform multi-elemental identification in soil sample, the laser-induced breakdown spectroscopy (LIBS) technique is utilized. The macronutrients (N, K, Ca, S, and Mg) and micronutrients (Fe, Cl and Mo) are identified. In summary the LIBS method can be used as multi-elemental detector and MRMS method can be used to determine the concentration of particular element.

CP-09-22. THEORETICAL ESTIMATION OF ISOTOPIC COMPOSITION OF TARGETED LU-176 IN THREE STEP PHOTOIONIZATION METHOD

Biswajit Jana and Biswaranjan Dikshit, ATLA Facility, BTD Group, Bhabha Atomic Research Centre, Mumbai-85, India., ***Email:*** *biswajit@barc.gov.in*

Enriched Lutetium 176 (Lu^{176}) isotope is required to generate Lutetium 177 (Lu^{177}) radiopharmaceutical isotope having potential applications in cancer treatments. From its natural abundance of ~ 2.6 %, the required isotopic enrichment (more than 75%) of Lu^{176} is achieved by Atomic Vapor Laser Isotope Separation (AVLIS) Process. Three-step resonant photoionization method is used to selectively excite and ionize the targeted Lu^{176} isotope. In this paper, the ionization yield and the isotopic composition of targeted Lu-176 isotope are estimated by taking into account all possible transitions between hyperfine components in first step and second step of the scheme.

CP-09-23. DISCRIMINATION OF HUMAN TEETH OF DIFFERENT AGE GROUPS USING LASER INDUCED BREAKDOWN SPECTROSCOPY

A. K. Tarai[1], R. Junjuri[1,2], A. Dhobley[3], M. K. Gundawar[1], [1]Advanced Centre of Research in High Energy Materials, University of Hyderabad, Prof C R Rao Road, Central University Campus PO, Gachibowli, Hyderabad, Telangana, 500046, India, [2]LUT School of Engineering Science,*

Lappeenranta University of Technology, 53851 Lappeenranta, Finland 3Department of Oral & Maxillofacial Pathology, Maitri College of Dental Sciences and Research Institute ***Email:*** *akashktarai@gmail.com*

Classifying human teeth from one another is very difficult since they contain the same chemical composition. In this context, we report classification of human teeth of different age groups using Laser-induced breakdown spectroscopy (LIBS). The LIBS experiment included nine teeth from three age groups: child, young adults, and middle-aged adults. Principal component analysis (PCA) was performed to classify between them. Even though all teeth have the same chemical composition, PCA and LIBS provide superior age-group differentiation. Our findings show that LIBS paired with PCA can be a powerful tool in archaeology and forensic odontology.

CP-09-24. NON-DESTRUCTIVE MONITORING OF BIOCHEMICAL RESPONSE OF MUNG (VIGNA RADIATE) SEEDLINGS TREATED WITH COPPER OXIDE NANOPARTICLES USING LASER INDUCED FLUORESCENCE SPECTROSCOPYE

Aishwary Awasthi, Chhavi Baran, Aradhana Tripathi, Sweta Sharma and K. N. Uttam. Saha's Spectroscopy Lab, Department of Physics, University of Allahabad, Prayagraj, ***Email****: aish91298@gmail.com,*

The study aims to investigate the effect of copper oxide nanoparticles on the biochemical profile of the mung leaves using label free, non-destructive, rapid, sensitive spectroscopic probe like laser induced fluorescence spectroscopy. The laser excited steady state fluorescence spectra of the control and copper oxide nanoparticles treated mung leaves have been recorded in the spectral region 400-800 nm. The treatment of the copper oxide nanoparticles increases the chlorophyll content and interfere biosynthesis and structure of cell walls of the mung leaves. The changes in the integrated area ratios of chlorophyll bands at 685 nm and 732 nm demonstrate disorder in membrane integrity. This study establishes the efficiency of non-invasive, label free, rapid protocols based on laser induced fluorescence to monitor the interaction of nanoparticles with plants at an early stage of plant growth before the visual signs of toxicity appearance.

CP-09-25. THREE-COLOUR ISOTOPE SELECTIVE PHOTOIONISATION OF YTTERBIUM FOR ^{174}YB ENRICHMENT

A. U. Seema[1], D Biswal[1], R C Das[2,3], D. R. Rathod[1], A K Singh[1], A. Khattar[1], J. S. B. Singh[1], A. Wahid[1], P. R.Mohite[1], S. K. Maurya[1], J. S. Dhumal[1], J. Thomas[1], Asawari D Rath[1,3*], S Kundu[1], [1] Tunable Laser Section, Advanced Tunable Laser Applications Facility, BTDG, BARC, Mumbai-400085, [2] Laser & Plasma Technology Division, BTDG, BARC, Mumbai-400085, [3]Homi Bhabha National Institute, Mumbai-400094.* ***Email****[*]: auseema@barc.gov.in, asawarim@barc.gov.in*

Resonance ionization mass spectroscopy is performed in a time of fligth mass spectrometer (TOFMS) to precisely determine the laser wavelengths for three step isotope selective photoionization of ^{174}Yb. Photoionisation is performed by using the well known reported scheme $4f^{14}6s^2\ ^1S_0$(0 cm^{-1}) $4f^{14}6s6p\ ^3P_1$ (17992 cm^{-1}) $4f^{13}6s^26p$ (35197 cm^{-1}) followed by ionisation via autoionisation state $4f^{13}6p^26s$ (52353cm^{-1}). We have precisely determined the laser wavelengths with an accuracy of ±30 MHz and optimised the laser intensities to achieve a spectroscopic selectivity better than 99% for ^{174}Yb in TOFMS. These optimised laser parameters were utilised in the enrichment experiments to collect the final product (^{174}Yb) enriched to 98% from its natural abundance of 31.38% with a production rate of 3.5mg/h.

CP-09-26. MEASUREMENT OF ISOTOPE SHIFTS OF SAMARIUM BY TWO-COLOR THREE-STEP PHOTOIONIZATION TECHNIQUE

A. C. Sahoo[1,2], P. K. Mandal[1], Jaya Mukherjee[1], M. L. Shah[1], [1]BeamTechnology Development Group, Bhabha Atomic Research Centre, Trombay, Mumbai-400085,[2]Homi Bhabha National Institute, Training School Complex, Anushakti Nagar, Mumbai-400094, ***Email:*** *asahoo@barc.gov.in*

Two-color three-step photoionization spectroscopy has been performed to investigate isotope shifts between even mass number isotopes (^{154}Sm and ^{150}Sm) of samarium. The experiments have been carried out in an atomic beam coupled to a time-of-flight mass spectrometer. Isotope shifts between ^{154}Sm and ^{150}Sm for two first-step transitions have been measured and the values are in good agreement with the values reported in literature. Isotope shifts between ^{154}Sm and ^{150}Sm for five second-step transition have been measured for the first time

CP-09-27. MEASUREMENT OF PHOTOIONIZATION CROSS SECTION OF ATOMIC SAMARIUM USING SPATIALLY APERTURED AND FOCUSED LASER BEAM

P. K. Mandal[1], A. C. Sahoo[1,2], Vas Dev[2], Jaya Mukherjee[1], M. L. Shah[1], [1]Beam Technology Development Group, Bhabha Atomic Research Centre, Trombay, Mumbai-400085, [2]Homi Bhabha National Institute, Training School Complex, Anushakti Nagar, Mumbai-400094, ***Email:*** *pkmandal@barc.gov.in*

Three-step three-color photoionization spectroscopy has been employed to measure photoionization cross section of an autoionizing transition 34,929.9 cm^{-1}→51,032.2 cm^{-1} of atomic samarium. The photoionization cross section of the above transition has been determined by saturation method for both unfocused spatially apertured and focused laser beam. In case of focused laser beam, measured cross section value was significantly lower compared to the apertured beam. To understand the saturation curve with focused laser beam, a numerical code based on population rate equations for three-step photoionization pathways incorporating laser spatial profile has been developed to generate saturation curve. A very good agreement between the experimental and numerically generated saturation curves were observed for photoionization cross section value measured by apertured laser beam. Thus, for focused laser beam detailed numerical studies are required to extract cross section values from the experimental data points.

CP-09-28. DOPPLER WIDTH REDUCTION BY GEOMETRICAL COLLIMATION FOR LASER ISOTOPE SEPARATION OF YB-176

S. Baruah, T. Garg, B Jana, B Dikshit, G.K. Sahu, S. Kundu, Beam Technology Development Group, Bhabha Atomic Research Centre, Trombay, Mumbai-400085, ***E mail****: sudarshan.baruah@gmail.com*

Doppler width of the atomic beam plays a crucial role in limiting selectivity in the laser isotope separation process. In this paper, reduction of Doppler width by employing a collimating structure has been reported. Mass flux measurements have been carried out to find the vapor distribution profile for Yb evaporation using the deposition method. Results from the Direct Simulation Monte Carlo (DSMC) based simulations are found to be in good agreement with the experimental data. The velocity distribution profile extracted from the simulation data is used to estimate the Doppler width of the atomic beam. It is found that the Doppler width reduces from ~ 655 MHz to ~ 327 MHz with the implementation of the collimating structure corresponding to the first transition of the 3-step photo-ionization process for YB-176

CP-09-29. LASER-INDUCED DISPERSED FLUORESCENCE SPECTROSCOPY OF VANADIUM MONOFLUORIDE

Sheo Mukund[1,], Soumen Bhattacharyya[1,2], and S.G. Nakhate[1,2], [1]Infrared Laser Spectroscopy Section, Physics Group, Bhabha Atomic Research Centre, Mumbai-400085, India, [2]Homi Bhabha National Institute, Bhabha Atomic Research Centre, Mumbai-400085, India,* ***Email:****sheo@barc.gov.in*

The vanadium monofluoride (VF) molecules were produced in a pulsed supersonic molecular beam setup by reaction of laser ablated vanadium metal plasma with 3% SF_6 gas seeded in helium. Laser-induced fluorescence (LIF) and dispersed fluorescence (LIDF) spectroscopy were employed to investigate excited electronic states and ground state vibrations. The equilibrium vibrational constants of ω_e = 669(3) cm^{-1} and $\omega_e x_e$ = 4.3(7) cm^{-1} were obtained for the ground state. Two of the five spin-orbit components, separated by ~70 cm^{-1}, of the ambiguous ground state $X^5\Pi$ (or $X^5\Delta$) were detected. Few electronic states were detected in the ~14,400-15,000 cm^{-1} region, where rotationally resolved excitation spectra were recorded from the ground state.

CATEGORY 10: LASER IN LASER ABD FIBER BASED INSTRUMENTATION

CP-10-1. A REFLECTION TYPE MAGNETIC FIELD MEASUREMENT PROBE USING FARADAY EFFECT

*Kanchi Sunil[1,2], Rohit Shukla[1,2] Premananda Dey[2], A K Dubey[2], K. Sagar[2] and Archana Sharma[1,2], [1]Homi Bhabha National Institute, Mumbai-400094, [2]Pulsed Power & Electro-Magnetics Division, Bhabha Atomic Research Centre Facility, Visakhapatnam-531011., **E.mail** : sunilkanchi8125@gmail.com*

Based on Faraday effect, reflection type magnetic field measurement probe is designed and its experimental results are reported in this paper. The Faraday effect produces the non-reciprocal circular birefringence i.e., when the light source traverses the magnetized medium through the sensor element twice, the Faraday rotations doubles. In the designed probe, Terbium Doped Borosilicate Glass (TDBG) is used as a sensor element. The light is reflected after traveling the TDBG glass length from the mirror and again traverses through the glass making the double transit through the sensor element. For measuring the Faraday rotations, fast photodetector assembly is used. The complexity in alignment of laser source, sensor element and detector is eliminated because all the components are part of the probe structure and the source and detector can be placed on same side. The designed probe is easily portable and can be used in various applications like Z/θ pinch devices, fusion reactors such as tokamaks, ITER, etc. for magnetic field measurements.

CP-10-2. STUDY OF GAMMA RADIATION EFFECTS ON FBGS INSCRIBED IN DIFFERENT PHOTOSENSITIVE FIBERS

*S.Chaubey, J. Kumar, R. Mahakud, R. Biswal, O. Prakash, S K Dixit; Fibre Grating Lab, FSOSS, Raja Ramanna Centre for Advanced Technology, Indore-452013; **Email:** smita@rrcat.gov.in*

This paper presents the study of gamma radiation effects on Fiber Bragg Gratings (FBGs) inscribed in different photosensitive fibers. These FBGs were inscribed indigenously using high repetition rate (5.5 kHz) 255 nm radiation, in hydrogen loaded high germanium doped fiber, high germanium doped fiber and boron germanium codoped fiber. All observations in this study were made in real time. All of these FBGs showed a red Bragg wavelength shift (BWS) initially. After attaining a certain maximum BWS, these FBGs showed a blue BWS up to 500 kGy. Highest BWS of 40 pm was observed for the FBG inscribed in hydrogen loaded high germanium doped fiber at 200 kGy gamma radiation dose.

CP-10-3. LASER BASED OPTICAL FIBER TECHNIQUE FOR VELOCITY MEASUREMENT

*Pankaj Deb, Premananda Dey, Avneesh Dubey, Karuna Sagar, A Appa Rao, Rohit Shukla, Archana Sharma, PPEMD Division BARC, Visakhapatanam, **Email**:pankajdeb24@gmail.com,*

The paper illustrates the measuement system to determine the projectile velocity in plasma environment. The measurement system is employed in electromagnetic railgun experiement to determine the muzzle velocity of projectile. The design of the system consists of Laser source, Optical Fiber and Photodetector It is based on the projectile time of flight in cutting of optical fiber and distance between the optical fibe.

CP-10-4. SINGLE PASS LASER CUTTING OF 30 MM THICK SS316L PLATE USING REMOTELY OPERABLE 1 KW AVERAGE POWER PULSED ND:YAG LASER FOR NUCLEAR FIELD APPLICATION

M. K. Bairwa[1], Vijay Bhardwaj[1], R. K. Jain[1], Ranveer Singh Meena[1], Vijay Shukla[1], S. K. Sharma[1], Rajpal Singh[1], B. K. Saini[1], Bhaskar Paul[1], Pawan Kumar[1], B. Ekka[1], Prabhat Kumar[1], Jata Beshra[1], A. A. Raju[2], S. K. Sah[2], Vijay Bhawsar[2], J. Khanwalkar[2], R. Arya[2], B N Upadhyaya[1], K S Bindra[1] [1]Laser Technology Division, Raja Ramanna Centre for Advanced Technology, Indore-452013, India, [2]Laser Electronics Division, Raja Ramanna Centre for Advanced Technology, Indore-452013, India, [*]**E-mail**: bnand@rrcat.gov.in,*

Laser cutting of thick SS pipes at fast speed is required in radioactive environment of nuclear power reactors. One such requirement is for laser cutting of 30 mm thick SS316L pipes of recirculation loop in Tarapur Atomic Power Station (TAPS-1&2) for replacement purpose. This report provides details of development of single pass laser cutting technology for 30 mm thick SS316L at high speed using remotely operable 1 kW average power fiber coupled pulsed Nd:YAG laser. A compact bending nozzle has been specially developed and laser cutting process parameters have been optimized for single pass laser cutting of large thickness of SS316L. This remotely operable laser cutting technology will be useful in laser cutting of 30 mm thick SS316L recirculation pipes at TAPS-1 & 2 reactors to minimize radiation dose consumption and time as compared to conventional mechanical methods and will also useful in laser cutting of large thickness steel sections in various industrial applications.

CP-10-5. TEMPERATURE SENSITIVITY OF DUAL RESONANCE PEAK OF LONG PERIOD FIBER GRATING OPERATING NEAR TURN AROUND POINT

V.K. Srivastava, R. Mahakud, J. Kumar, S. Kumar, O. Prakash, S K Dixit, Fibre Grating Lab, FSOSS, Raja Ramanna Centre for Advanced Technology, Indore-452013, ***Email:*** *vkshrivastava@rrcat.gov.in*

This paper presents study on temperature sensitivity of dual resonance peak of a long period grating (LPG) operating near phase matching turning point. The long period gratings were written in Ge-B codoped fiber by point-by-point method, using 255 nm pulsed UV beam. The evolution of separation between centre wavelengths of dual resonance of the LPG operating near PMTP investigated in temperature range 75 - 150 °C. The temperature sensitivity of about 7 nm/ °C near dispersion turning point (at 75 -80 °C) is very high. The temperature sensitivity of dual resonant peak decreased from 7 nm/ °C to 3.12 nm/ °C as the temperature interval increased from 5 °C to 70 °C from reference. The temperature sensitivity nonlinearly decreased with increase in temperature.

CP-10-6. ANALYSIS AND EXPERIMENT ON THE EFFECT OF CLAD ETCHING ON REFRACTIVE INDEX SENSITIVITY OF A LONG PERIOD FIBER GRATING

S. Kumar[1], R. Mahakud[1, 2], J. Kumar[1, 2], O. Prakash[1, 2], S K Dixit[1, 2], [1]Fiber Grating Lab, Fiber Sensors and Optical Spectroscopy Section, RRCAT, Indore,[2]Homi Bhabha National Institute, Anushaktinagar, Mumbai,* ***Email:*** *sudhir@rrcat.gov.in*

This paper presents analysis and experiment on refractive index sensitivity enhancement of long period grating (LPG) by clad etching. The variation of effective RI of a typical cladding mode with change in surrounding RI calculated for two different cladding diameters of 125 μm and 110 μm using dispersion relation for two-Layer geometry. The RI sensitivity of a typical mode simulated for typical parameters increased with decrease in clad diameter.

Experimentally, an LPG of period 300 μm fabricated in-house. The evolution of resonant wavelength with change in SRI recorded for ambient RI ranging from 1.33 to 1.40. It was observed that the average RI sensitivity of a typical cladding mode (7th) increased from 42.85 nm/RIU to 240 nm/RIU as the cladding diameter reduced from 125 μm to approximate value of 110 μm. The analytical results qualitatively agree with experiment.

CP-10-7. PROTOTYPE DEVELOPMENT OF LASER BASED TILT MEASUREMENT SYSTEM FOR FUELING MACHINE ALIGNMENT

Pooja Chakraborty, Nitin O Kawade, Bhabha Atomic Research Centre, Mumbai ***Email:*** *poojac@barc.gov.in*

In this paper, we described the development of a prototype Fueling Machine Tilt measurement system for alignment of the Fueling Machine Head with the End fitting of the Coolant system. To cater to the need of operation in harsh environmental condition such as high temperature and high radiation, an all-fiber solution based design has been proposed where the sensor head is kept in the field and the optical signal is carried by collinear optical fiber array to the remotely placed CMOS camera. The target displacement is measured by computing the shift in the centre of the laser spot using a Fourier transform based algorithm. In the present system each sensor head is designed to work for a standoff distance of 70 mm, measurement range of +/- 10 mm and resolution of 1 mm.

CP-10-8. INSCRIPTION OF FIBER BRAGG GRATING BASED FABRY-PERROT INTERFEROMETER IN SINGLE MODE PHOTOSENSITIVE FIBER BY 255 NM UV BEAM

R. Mahakud, V. K. Srivastava, J. Kumar,S. Kumar, O. Prakash, S K Dixit, FSOSS, Raja Ramanna Centre for Advanced Technology, Indore, ***E-mail:*** *rkmahakud@rrcat.gov.in*

This paper presents the fabrication of a fiber Bragg grating based Fabry–Perot interferometer (FBG-FPI) in the core of a photosensitive fiber by frequency doubled copper vapour laser (255 nm UV beam). The transmission function of FBG-FPI is caused by interference between the multiple reflections of light between the two Bragg reflectors. The free spectral range decreased with increase in cavity length between two FBGs. The feasibility of such an FBG-FP structure as strain sensor is tested by detecting and measuring axial strain.

CP-10-9. DEVELOPMENT OF PHOTON DOPPLER VELOCIMETRY (PDV) FOR HIGH SPEED LASER DRIVEN FLYER VELOCITY MEASUREMENT

Ashutosh Mohan[1], A. K. Poswal[2], K. C. Gupta[1], S. Chaurasia[1], [1]High Pressure and Synchrotron Radiation Physics Division, Bhabha Atomic Research Centre, Mumbai - 400085, India, [2]Atomic and Molecular Physics Division, Bhabha Atomic Research Centre, Mumbai - 400085, India,* ***E.mail:*** *[*]shibu@barc.gov.in*

Measurement of particle velocity is critical for equation of state (EOS) determination of materials using laser-driven shock. Here, we report the development of a simple, robust and low cost high speed velocimetry diagnostic for measuring the velocity of laser-driven mini flyers. The main components of the system are: 2W CW erbium doped fibre laser (1550 nm),

a fibre-optic probe, 3 port circulator, a high bandwidth digitizer (8 GHz) and a fast photodiode (< 35 ps rise time and bandwidth > 10 GHz). Maximum measurable flyer velocity of our diagnostic is about 5 km/s (limited by the bandwidth of the oscilloscope). We measured flyer velocity at five different pump laser energies. PDV signal was analyzed using in house developed software (based on short-time Fourier transform and Hilbert transform). 1-D radiation hydrodynamics simulations using HYADES codes were also performed to compare the experimental results.

CATEGORY 11: ELECTRONICS & INSTRUMENTATION FOR LASERS

CP-11-1. HIGH VOLTAGE PICOSECOND PULSE GENERATION BY AN AVALANCHE TRANSISTOR STACK ON MICROSTRIP PCB

M. L. Sharma, S. Nigam, K. Aneesh, Y.B.S.R. Prasad and K S Bindra#,Laser Technology Division,#Homi Bhabha National Institute, Training School Complex, Anushakti Nagar, Mumbai, 400094, Raja Ramanna Centre for Advanced Technology, Indore 452013, M.P., India,* ***Email****: mlsharma@rrcat.gov.in*

A sub-ns pulsed voltage driver was developed using a transistor stack fabricated on a printed circuit board (PCB) in micro-strip configuration and operated in avalanche mode. The stack consisted of 9 stages of 2N5551 transistors, and was biased with a 3 kV dc supply. The switched output was observed with a 50 ohm load, transmitted through a 0.5 meter cable after using a high voltage attenuator of 20 dB and a low voltage co-axial attenuator of 24 dB. The rise time of the leading edge of the voltage pulse was of 225 pico second (ps), amplitude of -1.2 kV with a full width at half maximum (FWHM) of 500 ps. This will be used for gating a micro-channel plate for time resolved studies of x-ray emission from capillary discharge plasmas as well as laser produced plasmas.

CP-11-2. OPTICAL PHASE LOCK LOOP WITH DIRECT DIGITAL SYNTHESIZER CONTROL FOR COLD ATOM INTERFEROMETRY EXPERIMENTS

Safeer S. S., Sasikumar K. K., S. Kannan, Hriday Dath, Radhika V N., Rekha A. R., and Venkata Ramana B., ISRO Inertial Systems Unit (IISU), Vattiyoorkavu, Trivandrum., **Email:**sasikumarkk2000@yahoo.com,

A simple, versatile and inexpensive optical phase locked loop is introduced for applications in atomic physics experiments, especially Cold Atom Interferometry. Phase locked Raman laser beams are required for Cold Atom Gravimeter. Optical phase Locked Loop technique is used to phase lock the Raman beams withrespect to master laser which is already locked to Rubidium (Rb) atomic spectrum. Digital Phase frequency Discriminator (PFD) chip is utilized to extract the phase difference information between the master and slave laser beams. RF signal required for the working of PFD chip is generated using a Direct Digital Synthesizer (DDS). Microcontroller based decoder is used to drive the DDS and the generated RF signal is amplified usinga RF power amplifier module.

CP-11-3. WAVELENGTH TUNING AND LOCKING SYSTEM FOR TUNABLE SLM DYE LASER

Anchal Gupta[1], Pooja Chakraborty[1], Anil S Nayak[1], Paramjit Rana[1], Siba Prasad Sahoo [1,2], S K Mishra[1,2], Nitin O Kawade[1,2], Jaya Mukherjee[1], V S Rawat[1,2], [1]Beam Technology Development Group, Bhabha Atomic Research Centre, Trombay, Mumbai 400085, [2]Homi Bhabha National Institute, Anushaktinagar, Mumbai 400094, ***Email****:anchalg@barc.gov.in*

The control system for precise wavelength control of single longitudinal mode (SLM) pulsed dye laser is presented for long-term stability in the range of ± 0.002 cm^{-1}. The wavelength control architecture has been implemented for SLM pulsed dye laser pumped by high repetition rate copper vapour laser (CVL). The absolute wavelength is measured using laser wavelength meter to address the long term drifts in the SLM dye laser wavelength. The functionality such as remote tuning of the wavelength followed by wavelength stabilization has been implemented

in the control loop. The SLM Dye laser wavelength was actively stabilized for hours of operation.

CP-11-4. MODELING OF MODE DIVISION MULTIPLEXING FOR HIGH-CAPACITY RO-FSO TRANSMISSION

Harlan. L, Shyamal Mondal , Dept. of Electronics and Communication Engineering, SRM Institute of Science and Technology, Kattankulathur, Chennai, Tamil Nadu, 603203, India, ***E.mail*** *: harlanfdo@gmail.com, shyamal.kgec@gmail.com*

The demand for ubiquitous connectivity, high data capacity, faster data speed, low latency, and reliable services increases day by day with the persistent growth of mobile users and new technologies. The stringent requirements for 5G heavily rely upon the interconnected backbone network. Thus, in order to achieve the requirements of 5G, fiber-wireless integration is inevitable. Radio-over-Free-Space-Optics (Ro-FSO) is a promising technology for future wireless networks. The capacity of the channel is increased by using Mode Division Multiplexing (MDM) which entails launching several propagation modes, each carrying different information into FSO channel and demultiplexing them at the other end to obtain a separate data stream from each. In this work, a hybrid Orthogonal Frequency Division Multiplexing (OFDM) Ro-FSO system for transmission of independent channels by Mode Division Multiplexing (MDM) was designed and analyzed.

CP-11-5. DEVELOPMENT OF PXIE BASED CONTROL SYSTEM FOR PHYSICS PROTOTYPE LASER

Yogesh Sahu, Bhupinder Singh, M. S. Ansari, LPSD, RRCAT, Indore, ***Email:*** *ysahu@rrcat.gov.in,*

RRCAT, Indore has taken up development of MOPA based Nd: glass 2 - beam high energy laser. In this regard, a single beam physics prototype has been developed to carry out preliminary studies. The paper describes the control system implemented for the laser which is based on PXIe scheme. The control system generates specific control signals for operation of each stage in the laser by its PXIe modules. LabVIEW based application software with GUI, in addition to providing operation & control, enables user to provide configuration data and selection of required operation modes. The prototype laser is routinely operated and up to 40 J laser pulse has been generated as final output.

CP-11-6. OPTICAL MULTIPASS SYSTEM USING TWO PLANE MIRRORS FOR ENHANCED LASER ATOM INTERACTION

Aditya Kumar Tiwari[*1,2] , Anchal Gupta[1], Jaya Mukherjee[1,2], V S Rawat[1,2], [1]Advanced Tunable Laser Facility, BTDG , BARC, Mumbai, [2]Homi Bhabha National Institute, Mumbai,* ***Email:*** *adityakt@barc.gov.in*

It is proposed to use an optical mutlpass system using two plane mirrors for enhancing the photon utilization in the processes involving laser atom interactions. A simple analytical model is used to show the effectiveness of the multipass system by maneuvering the angles between the two mirrors using stepper motor. This model predicts the requirement of the critical angle needed for retracing the laser beam inside the multipass system. By careful alignment of multipass mirrors the effectiveness of the process can be increased significantly.

CP-11-7. DEVELOPMENT OF PROTOTYPE OF ALBUMIN ANALYZER FOR THE MEASUREMENT OF ALBUMIN CONCENTRATION USING FLUORIMETRY

Rushal Shah, Goutam Chakraborty, Mandar Joshi, Nitin O Kawade, Laser & Plasma Technology Division, Bhabha Atomic Research Centre; ***Email:*** *:rushal@barc.gov.in*

Serum albumin produced by the liver, is essential for maintaining the oncotic pressure needed for proper distribution of body fluids between blood vessels and body tissues. In order to maintain physiological activity uninterrupted, periodical quantification of serum albumin is extremely necessary. The prototype instrument for the measurement of the Serum Albumin Concentration using fluorimetry technique was developed. The instrument comprises of Green LED source, the photodiode, Photo Multiplier Tube (PMT), pre-amplifier and signal conditioning circuit, and LCD display. During the experiment and calibration, the bovine serum albumin (BSA) was used. The instrument was calibrated using the test samples of different concentration of BSA in the aqueous buffered solution of LDS 798, and the fluorescence intensity was measured. The instrument is able to measure the concentration in the range of 0 to 30 uM with 5 % accuracy.

CP-11-8. DEVELOPMENT OF LOW COST IMAGING UNIT BASED ON FREQUENCY UPCONVERSION NANOPARTICLE USING NIR DIODE LASER

Mandar Joshi[1], Rushal Shah[1], Sandeep Agarwalla[2], G Sridhar[2] and Aseem Singh Rawat[1], [1]Laser and Plasma Technology Division, BARC, [2]Advanced Tuneable Laser Application Facility, BARC,* ***Email:*** *mandarj@barc.gov.in,*

A florescence detection instrument based on filter based scheme has been developed for florescence spectroscopy. For the material chosen, the excitation wavelength is 980nm whereas the florescence emitted is in the visible range. The system constitutes a Raspberry Pi board, CCD camera with optics, 980nm diode laser, in house developed laser driver board and a touch screen panel for user interface. A compact instrument cabinet has also been fabricated. In-house developed diode laser power supply board is interfaced with the Raspberry Pi board using I/O line. The laser is switched ON only when during image capture process. Python[3] based software ensures a focused colour image of the florescence emitted is captured. The captures image is then processed to determine the presence of material under test within the printed matter. The software generates a pass / fail result for the user to indicate presence / absence of the material.

CP-11-9. DEVELOPMENT OF CONSTANT CURRENT LASER DIODE DRIVER FOR NANO PARTICLE UP-CONVERSION APPLICATION

Anil S Nayak[1], Rushal Shah, Mandar Joshi, Aseem Singh Rawat, Jaya Mukherjee, Beam Technology Development Group, Bhabha Atomic Research Centre, India, ***Email:*** *anilsn@barc.gov.in*

This paper is intended to report the development of constant current laser diode driver for nano-particle up-conversion application. A florescence detection instrument based on filter based scheme has been developed for florescence spectroscopy of indigenously developed material in BARC. The Infrared laser diode is used for the excitation of the material and fluorescence emitted is in the visible domain. The instrument includes low cost and indigenously developed laser driver board. The technique includes voltage-controlled current source circuit that drives a constant current into the pump laser diode. It utilizes MOSFET as the driving element which is being driven by Operational Amplifier. Laser diode current is sensed by

differentially measuring the voltage drop across a resistor in series with the laser diode. The circuit has been tested up to constant current of 2 A reliably for long duration.

CP-11-10. SURFACE TEMPERATURE MEASUREMENT USING INFRARED RADIATION

Aseem Singh Rawat, Ram Gangurde, Rushal Shah,Laser & Plasma Technology Division, BARC, Mumbai 400085, ***Email****: aseem@barc.gov.in*

An infrared radiation based surface temperature measuring instrument has been developed which is calibrated for human skin temperature measurement. A thermopile sensor converts the incident infrared radiation to voltage which is proportional to the target temperature. A microcontroller calculates the temperature from the generated voltage and displays it on LED display. The microcontroller also drives an optical proximity switch which makes its measurement operator less. It is used for thermal screening of employees entering premises to comply with COVID-19 guidelines. The operator less instrument ensure social distancing with the security personnel during thermal screening and it is a low cost solution unlike IR camera based solution. It can measure skin temperature in the range of 90°F to 110°F with an accuracy of ±1°F.

CP-11-11. ONLINE ESTIMATION OF PHOTO-ION COLLECTION RATE IN LASER ISOTOPE SEPARATION PROCESS

Dev Ranjan Das, S. P Dey, Biswajit Jana, Anupama Prabhala., Sanjay Sethi, ATLA-F, BTDG, BARC, Mumbai, ***Email:*** *drdas@barc.gov.in*

A new methodology is developed to estimate and log the real time ion collection rates during laser isotope separation experiment. The ion collection rate depends on various parameters like neutral atom density (temperature of vapour source), ionization yield (laser power, stability of laser wave length) and ion extraction efficiency (voltages applied on ion-extraction plates). So the availability of real-time trend of the ion collection rate during the experiment helps to monitor the process output, check for any deviation of various system parameters and to understand their effect on the output of laser isotope separation process. The technique gives an estimate of both the instantaneous ion collection rate as well as the cumulative ion collection on the product collector over the duration of experiment.

THESIS

TH-1. PHASE EXTRACTION OF OPTICAL INTETERFEROMETRIC SIGNALS BASED ON IMPROVED TIME-FREQUENCY METHOD WITH APPLICATION TO HIGH STRAIN RATE MEASUREMENT

Amit Sur, Bhabha Atomic Reaserch Center, Mumbai, ***E.mail :*** *amitsur@barc.gov.in*

Abstract: Laser based instrumentation technique such as optical interferometry plays a key role in determination of free surface velocity of target material under high strain rate experiments. Michelson interferometer in velocity as well as displacement mode configuration is widely used. As the information of velocity is hidden in phase or instantaneous frequency (IF), it is important to extract the phase or IF of the fringe signal. In time domain approach, multiple fringes are required to extract phase and numerical differentiation which is noise sensitive required to get the IF. Although computationally less expensive, the accuracy of this method may get affected significantly by various measurement imperfections like, nonlinearity, amplitude and phase angle error. On the other hand, in frequency domain approach single fringe may be sufficient to extract IF and numerical differentiation could be avoided. In this thesis, phase extraction based on quadrature phase shifting method, reassigned Continuous Wavelet Transform (CWT) method and Smoothed Pseudo Wigner-Ville Distribution (SPWVD) method have been described and developed. Finally, some of these developed phase extraction algorithms are applied to free surface velocity measurement under high strain rate experiments and different dynamic mechanical properties of AL2024T4 target material are derived from extracted velocity profile.

Introduction:

In the advancement of highly coherent, extremely narrow linewidth and high power lasers, many tiny measurements are now achievable with non contact type interferometric method. In most of the interferometric measurement the required information is encoded in the phase or instantaneous frequency (IF) of the recorded fringe signals. The accurate phase and IF extraction of optical fringe signals is an extremly important task for measurement of various physical parameters such as displacement, strain, velocity, surface profile etc. employing non-contact based interferometery [1]. Necessity of such measurements arises during non-destructive testing, precesion engineering, profilometry, plasma physics, astronomy, shock physics etc. For example, in shock physics velocity history of target material under high strain rate loading carries useful information on material behavior [2-4]. In these techniques the information of these physical quantities are stored in phase or instantaneous frequency (IF) of the recorded interference fringe signal. Therefore the extraction of phase or IF of the fringe signal using various signal processing algorithms becomes an important problem.

Phase extraction algorithms are available in literature in the context of fringe analysis with application to metrology by using digital holographic interferometry, fringe projection interferometry and digital speckle pattern interferometry etc. [1] broadly categorized as-(1) time (2) frequency domain approaches [1]. In time domain approach multiple fringe signals are required to extract the phase. But in frequency domain approach single fringe is capable of producing phase of the signal. Moreover, in this technique phase and frequency can be simultaneously obtained which is often requirement. For use in high strain rate impact experiments, Michelson and Fabry-Perrot based interferometers are used. However, Michelson interferometers in displacement and velocity mode configuration according to their implementation are quite popular [2-4]. A typical setup of displacement type Michelson-interferometer is depicted in Fig 1(a). In this configuration, surface of the target plate is polished to form one of the legs of the interferometer. Other leg of the interferometer is a stationary mirror *Mirror1*. A highly collimated and coherent laser beam is split in to two parts

using a beam-splitter and these two beams incident on the polished target surface and the mirror *Mirror1*. The laser beam reflected from the target surface and the mirror *Mirror1* are superimposed and a stationary interference fringe pattern is generated. Interaction with the shock wave causes the free surface of the target to move.

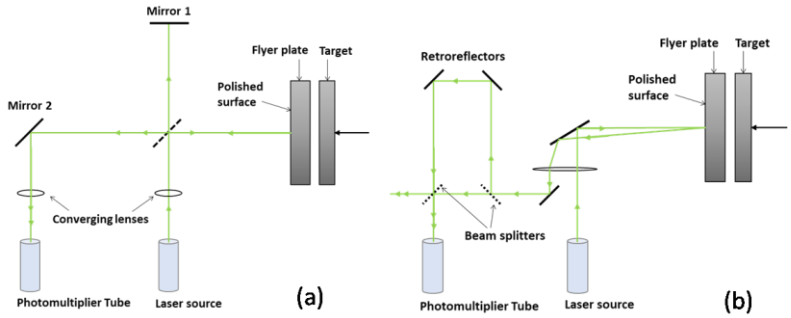

Fig. 1 (a) Displacement and (b) Velocity mode Michelson interferometer

This movement of free surface of target results in time dependent changes in the path difference between the beams from the two legs thereby generating shift in fringes. This shift in fringes is then used to infer the velocity of free surface as a function of time by applying following expression:

$$v(t) = \frac{\lambda}{2} f_i(t) \qquad (1)$$

where, $v(t)$ is velocity of the free surface in time t, $f_i(t)$ is instantaneous frequency of fringe in time t, and λ is wavelength of the original laser beam. The fringe shift of optical signal is converted to an electrical signal using photomultiplier tube and recorded in oscilloscopes. The instrument is very sensitive and has excellent distance resolution. This interferometer can generate one complete fringe shift for a small free surface displacement of $\lambda/2$ only. Though, the extreme sensitivity has advantage of very fine resolution, it imposes a limitation on the maximum velocity that can be measured using this instrument. This problem arises due to frequency response limitation of the electronic equipment such as photomultiplier tube, amplifier, oscilloscopes used in the system. In contrast, the velocity interferometer employ measurement of differential Doppler shift of the light reflected off the moving target surface. In this configuration, interference pattern is generated by interaction of two laser beams reflected from the free surface at two different instants of time. The delay in between reflection of the two beams is created either by increasing the path length known as Specular Velocity Interferometer (SVI) or, by placing a solid etalon bar known as Velocity Interferometer System for Any Reflector (VISAR) in one of the legs of the interferometer [2-4]. This allows inferring velocity history of the free surface with very few numbers of fringes and also overcomes the fringe frequency limitations of displacement type interferometer. The velocity history of the target free surface is encoded in the phase of the fringe signals.

The objective of the present research activities is to develop novel analysis technique of phase and frequency extraction of interferometric fringe signals using both time and frequency domain approaches by addressing the existing shortcomings of the different techniques with application to velocity measurement in high strain rate experiments. The thesis is outlined in total seven chapters. Chapter 2 presents detailed literature survey of existing phase extraction techniques of both temporal and frequency domain approaches. Chapter 3 introduces phase shifting method of phase extraction algorithm and highlights the shortcomings of existing technique and presents possible solution. Chapter 4 presents frequency domain approach of phase extraction by using Continuous Wavelet Transform (CWT). Chapter 5 proposes Reassigned Smoothed Pseudo Wigner Ville Distribution method for cubic phase signal. Chapter 6 highlights the application of some of the proposed methods in free surface velocity measurement in high strain rate experiments. Chapter 7 summarizes the contribution of work

and presents scope of possible future work. Literature survey is briefly described in the context of each chapter.

Chapter 3: Quadrature Phase Shifting Method

In time domain approach multiple fringe signals are required to extract the phase known as phase shifting method [5]. Different algorithms are proposed in this technique- N-bucket algorithm, least square approach, Carre's algorithm etc. N-bucket algorithm with four frames based technique is quite popular. Accuracy of phase measurement depends upon the correctness of the phase shifting technique, which is often affected by various nonlinearities, hysteresis and other imperfections. To address this issue, various error compensating techniques have been proposed in literature [5]. Further, in many cases amplitude and phase angle error between two quadrature fringe signals is unavoidable. However, this can be corrected by ellipse fitting technique as quadratre fringe signals represent family of ellipse in Lissajous pattern. In certain applications, measured fringe signals do not complete the angular 2π rotation in Lissajous pattern and ellipse becomes incomplete or fractional. Search for proper fitting algorithm for analyzing fractional fringe signal is still an important research problem.

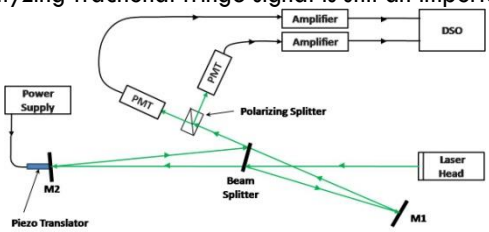

Fig. 2 Michelson interferometer in displacement mode configuration

Optical fringe signal is generated by using basic displacement Michelson interferometer by periodic movement of one of the mirrors while keeping other mirror stationary. The PZT transducer is used to generate periodic displacement. Two fringe shift based configuration is shown in Fig.2. Measured quadrature fringe signals along with applied PZT voltage are shown in Fig.3(a). This optical fringe signal is converted to electrical signal by using PMT and stored in digital storage oscilloscope (DSO). The recorded two quadrature finge signals can be expressed as

$$I_1(t) = a_1(t) + b_1(t)\cos(\phi(t)) \tag{2}$$

$$I_2(t) = a_2(t) + b_2(t)\sin(\phi(t) - \varepsilon) \tag{3}$$

By using equation (2) and (3) phase can be expressed as-

$$\phi(t) = \arctan\left(\frac{I_2(t) - a_2(t)b_1(t)}{I_1(t) - a_1(t)b_2(t)}\sec\varepsilon + \tan\varepsilon\right) \tag{4}$$

Equation (2) and (3) form an ellipse equation whose centre is at (a_1,a_2) and major axis, minor axis and angle of rotation are b_1, b_2 and ε respectively. These five unknown parameters are obtained proper ellipse fitting method. Figure 3.(d) shows the fitted ellipse corresponding fringe signals of Fig. 3(a) The required phase can be obtained using equation (4). However, this phase is wrapped and phase unwrapping algorithm is applied to get the unwrapped phase. After calculating the unwrapped phase, number of fringe shifts is determined using equation (5) and finally displacement is calculated using equation (6) and shown in Fig.3(b).

$$s(t) = \frac{\lambda}{2}\frac{\phi(t) - \phi(t_i)}{2\pi} \tag{6}$$

Here, $s(t)$ is the displacement of the mirror, Laser wavelength λ=532 nm, $\phi(t_i)$ is the initial phase. Measured peak displacement is 2.06 μm. Figure 3(c) also depicts the power spectral density of one of the fringe sginals.

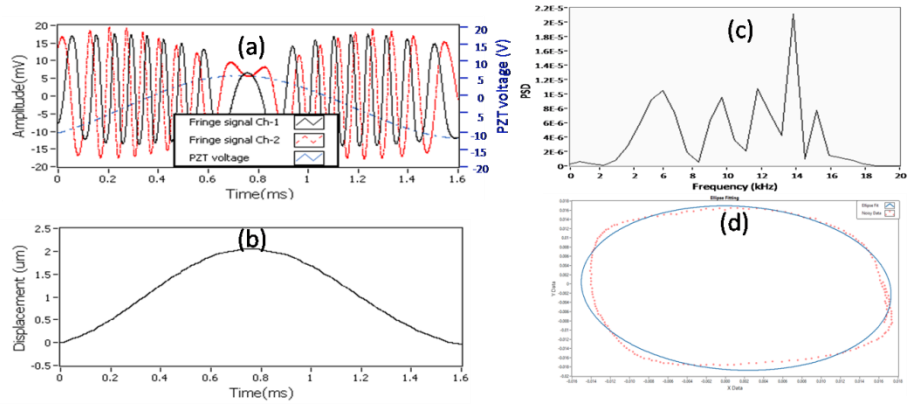

Fig. 3 (a) Measured fringe signals (b) Extracted displacement profile (c) PSD of fringe signal(d) Fitted ellipse

Chapter 4: Reassigned Continuous Wavelet Transform Method

In frequency domain approach, single fringe is capable of producing phase of the signal. Moreover in this technique, phase and frequency which are often required, can be simultaneously obtained. Fourier transform based technique is most popular choice of frequency domain approach of phase extraction [6-7]. But when the fringe signals become non stationary, windowed Fourier transform and wavelet transforms based techniques are applied [8-10]. Continuous Wavelet Transform (CWT) is more suitable as it makes use of adaptive time window that overcomes the fixed resolution problem in windowed Fourier transform. Morlet wavelet as mother wavelet is widely applied as it utilises modulated sinusoidal signal in Gaussian window which is qualitatively similar to fringe signal . Comparative studies with other mother wavelet like Mexican hat, Paul, Morse, DOG etc. are also available in literature but Morlet wavelet is quite popular [9]. Modification of Morlet wavelet parameters was explored by Abid et al [11] who suggested that time variance of 0.5 is optimum for fringe analysis. However, modifying only Morlet wavelet parameters do not always provide the best possible result, increasing time-frequency energy density may be required for preserving good localisation properties.

A wavelet is an oscillatory function $\psi(t) \in L_2(R)$ with limited number of oscillation, zero mean and centred at $t=0$.The function $\psi(t)$ is called "mother wavelet". A wavelet $\psi_{a,b}(t)$ at any time and scale obtained by dilating and translating the mother wavelet with a, b respectively can be expressed as:

$$\psi_{a,b}(t) = \frac{1}{\sqrt{a}}\psi\left(\frac{t-b}{a}\right),\ a \in R^+,\ b \in R \qquad (7)$$

The Continuous Wavelet Transform (CWT) of a function $f(t) \in L^2(R)$ is the inner product of $f(t)$ and $\psi_{a,b}(t)$

$$W_f(a,b;\psi) = \left\langle f, \psi_{a,b} \right\rangle = \int_{-\infty}^{\infty} f(t)\psi^*\left(\frac{t-b}{a}\right)dt \qquad (8)$$

$\left|W_f(a,b;\psi)\right|$ forms a local time-scale energy density of the signal called scalogram. Further scalogram can be converted to time-frequency spectrogram as scale is invesely proportional to frequency. Ideally ridge can be extracted from the time-frequency (T-F) energy density using the maximum modulus of complex array. Once the instantaneous frequency is extracted by ridge dtection [12] method, velocity is calculated using equation (1) and further displacement is derived by numerical integration of velocity profile. Morlet as mother wavelet is used and central frequency and bandwidth parameters of Morlet wavelet are optimized and simulataneous reassignment technique is applied for improving measurement accuracy of simple ridge detection method. Figure 5(a,b,c,d) describes measured fringe signal, Morlet spectrogram, extracted displacement and velocity profile respectively.

The peak displacement using reassigned and modified CWT is estimated as 2.23 μm. This may be compared with 2.06 μm obtained by phase stepping technique and also 2.20 μm obtained by well established peak-picking technique.

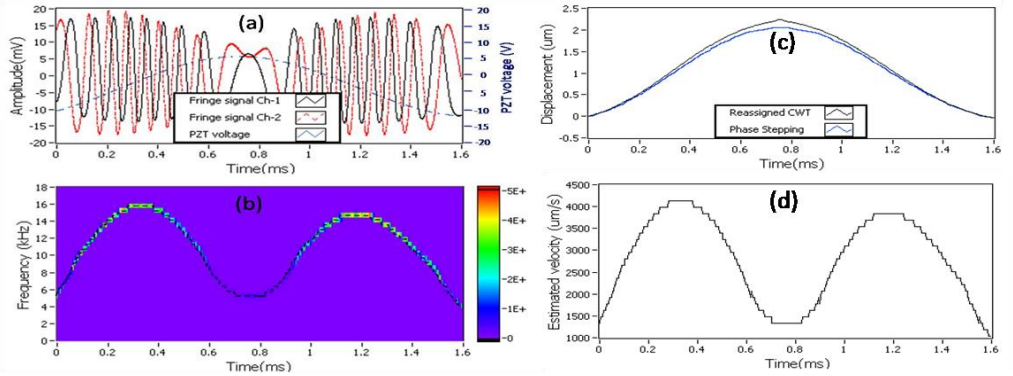

Fig. 5. (a) Measured fringe signal (b) Morlet spectrogram (c) extracted displacement (d) velocity

Chapter 5: Pseudo Wigner Ville Distribution Method

Wigner Ville Distribution (WVD) method is recently introduced for direct phase as well as frequency estimation of fringe signal [13]. In this method complex phase unwrapping can be avoided. Though WVD has many good properties and provides best possible resolution among all of the time-frequency (TF) techniques, undesirable cross-term interference effect is its main drawbacks [14]. Windowing operation is performed in suppression of cross-term effect to some extent for multi-component signal. When the window function is separable, an independent and progressive control can be applied to the WVD in both time and frequency directions known as Smoothed Pseudo Wigner-Ville Distribution (SPWVD) [14]. WVD has an optimum *t-f* representation for linear FM or quadratic phase signal. For nonlinear FM signal this optimality is lost and smeared spectral representation obtained. To address this problem polynomial Wigner-Ville distribution has been introduced [15]. However, when signal comes with polynomial phase along with nearly discontinuous IF, no investigation is yet carried out. Reassigned SPWVD with Gaussian separable kernel may be explored.

WVD of signal $f(t)$ is defined as the Fourier transform of time-dependent instantaneous auto-correlation function and represented as

$$WVD(t,\omega) = \frac{1}{2\pi}\int_{-\infty}^{+\infty} f(t+\frac{\tau}{2}) f^*(t-\frac{\tau}{2}) e^{-j\omega\tau} d\tau \qquad (9)$$

where t, ω and τ represent the time, angular frequency and lag variable respectively and $(*)$ denotes the complex conjugate. Though WVD has many good properties like marginality, preserving total energy, real valued distribution and possibly best resolution among all of the time-frequency (TF) techniques, undesirable cross-term or interference effect due to presence of signal product terms, is its main drawback. Smoothed Pseudo Wigner-Ville Distribution (SPWVD) [14] is used to reduce the cross term effect with Gaussian separable window function. SPWVD can be expressed as -

$$SPWVD(t,\omega;g,h) = \int_{-\infty}^{+\infty} h(\tau) \int_{-\infty}^{+\infty} g(u-t) f(u+\frac{\tau}{2}) f^*(u-\frac{\tau}{2}) e^{-j\omega\tau} du d\tau \qquad (10)$$

Figure (6) describes the highly nonlinear firnge signal and correseponding velocity and displacement profile extracted using proposed SPWVD technique. The measured peak velocity and displacement are 1.86±0.06 mm/s and 2.54±0.04 μm respectively.

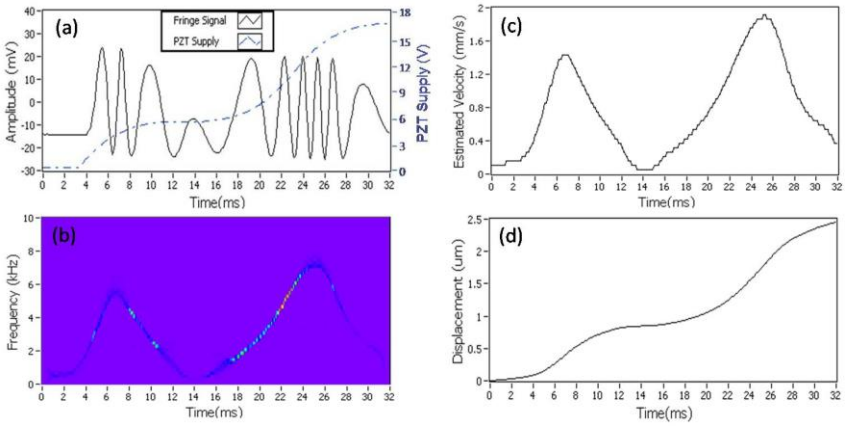

Fig. 6 (a) Experimentally observed fringe signal with PZT supply voltage (b) Reassigned SPWVD with modified kernel of experimental signal (c) Velocity (d) Displacement profile of experimental signal

Chapter 6: Application to Free Surface Velocity Measurement in High Strain Rate Experiments

Free surface velocity measurement of the target material subjected to transient compressions in shock wave experiments is an important problem. Many interesting material properties like Hugonoit Elastic Limit (HEL), dynamic yield strength, spall strength etc can be inferred from the free surface velocity history of target material [2-4]. These material properties find immense applications in the area of defense, geophysics, aerospace, automobile etc. Michelson interferometer in two different configuration-(1) Velocity mode and (2) Displacement mode are widely used for free surface velocity measurement of target material under shock compression. In velocity mode VISAR is used in shock compression experiments. Quadrature coded interference fringes are utilized for differentiating between the acceleration and deceleration of target free surface.

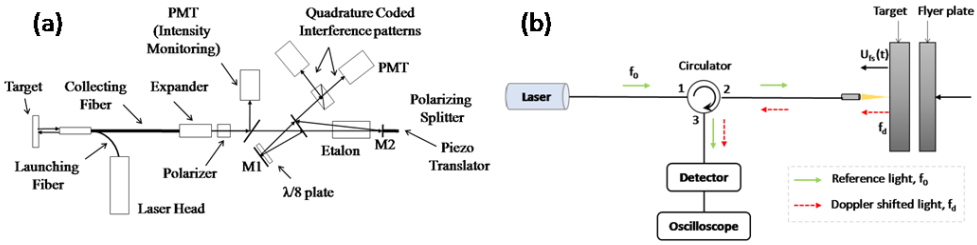

Fig.7 Schematic of (a) VISAR system (b) Heterodyne laser interferometry system

The VISAR signals are analysed using propsed quadrature phase shifting method. A detailed investigation of various elleipse fitting technique [16-17] is carried out and Gauss Newton method of geometric technique with initail condition from Bookstein algorithm is proposed. Plate impact experiments on Al2024-T4 target material are conducted in single stage gas gun. The VISAR instrument is used to record the time resolved fringe shift arising due to motion of free surface of the target. Different dynamic mechanical properties such as spall strength (σ_S=1.1±0.013 GPa), Hugoniot elastic limit (σ_{HEL}=0.73±0.008 GPa) and dynamic yield strength (Y=0.37±0.005 GPa) of Al2024-T4 target material derived from free surface velocity profiles are also calculated. In displacement mode heterodyne method is widely used in shock compression experiments [18-19]. This technique is commonly used in telecommunication for generating new frequency by mixing two frequencies based on trigonometric identity. Similar technique is implemented in heterodyne laser interferometry by mixing (using a circulator) a reference laser frequency (f_0) and its Doppler shifted frequency (f_d) from a moving target, generating heterodyne beat signals. Figure 9 briefly describes the schematic of the

system, where laser light (wavelength 1550 nm) enters to the circulator through port 1 and comes out of port 2 and focuses to the target plate. When flyer with velocity v(t) hits the target plate, free surface of the target plate starts moving causing Doppler effect.

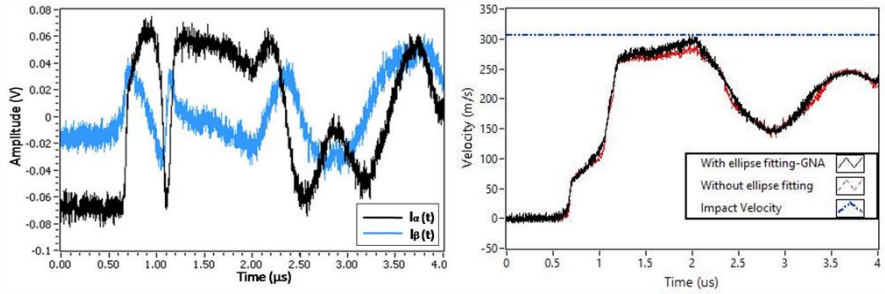

Fig.8 Measured VISAR fringe and corresponding velocity profile

Then Doppler shifted light with frequency (f_d) enters to the circulator through port 2 and heterodyne beat signal comes out through port 3, converted to electrical signal by photodiode and stored to high speed oscilloscope. Figure 10(b) describes the simulated heterodyne fringe signals corresponding VISAR velocity profile Fig. 10(a). Fringe signal is analyzed using proposed CWT technique and more accurate results are obtained. Figure 10(b, d) describe Morlet spectrogram with f_0t=1 and reassigned and modified Morlet spectrogram with f_0t=0.6.

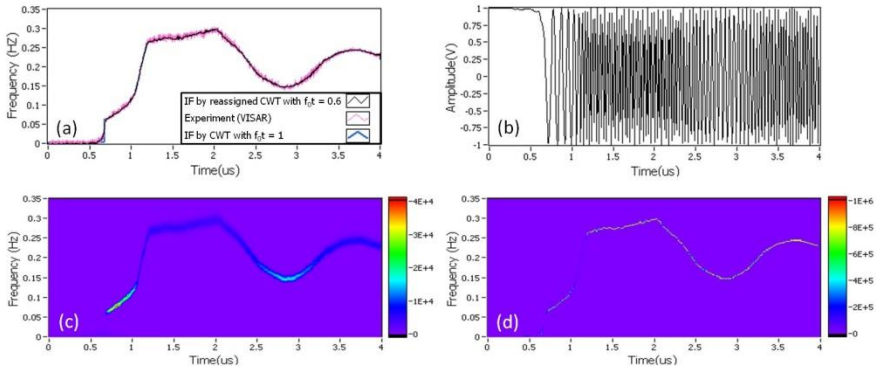

Fig.10 (a) Instantaneous frequencies obtained from VISAR velocity profile and two CWT techniques (b) Deduced heterodyne type fringe signal (c) Morlet spectrogram with f_0t=1 (d) Reassigned and modified Morlet spectrogram with f_0t=0.6.

Chapter 3: Conclusions and Future Directions

The current research explored some novel techniques for optical phase extraction algorithm with aim to velocity measurement in high strain rate experiments by laser interferometric technique. Phases as well as frequency of the fringe signals are explored from single fringe as well as multi fringe signals. In phase shifting method phase unwrapping technique is developed and demonstrated and ellipse fitting technique is introduced for correcting various measurement imperfections. In CWT method two different techniques namely phase estimation method and frequency estimation are explored. Importance of ridge extraction is highlighted and modification of mother wavelet (complex Morlet) in conjunction with reassignment technique is proposed to extract the phase. Reassigned smoothed pseudo Wigner Ville distribution (RSPWVD) based technique provides an elegant approach of phase extraction from single fringe based cubic phase signal. Finally an elaborate study of some of the proposed phase extraction algorithms with the application to free surface velocity measurement in high strain rate experiments is carried out. Novel ellipse fitting technique is introduced to correct the measurement imperfections like phase angle and amplitude and Gauss Newton algorithm with initial condition from Bookstein method is proposed. The thesis also discusses the possible application of IF extraction of fringe signals for measuring free surface velocity profile using

heterodyne laser interferomerty. Reassigned CWT based technique is proposed for accurate extraction of velocity profile.

For future work, ridge detection technique with less computational burden could be investigated for proper representation of instantaneous frequency of the signal which has enormous applications in practical. Generalization of CWT in time frequency analysis is also an interesting problem. Polynomial Wigner Ville Distribution could be studied for multi-component polynomial phase signal. Complex time distribution (CTD) could be explored for polynomial fringe signal.

References:

1. G. Rajshekar, P rastogi, "Fringe analysis: Premise and perspectives," *Opt. and lasers in Engg*. **50**, iii (2012).
2. L. M. Barker, and R.E. Hollenbach, "Laser interferometer for measuring high velocities of any reflecting surface"*J. Appl. Phys*. **43**, 4669 (1972).
3. W. Hemsing, "Velocity sensing interferometer (VISAR) modification" *Rev. Sci. Instrum*. **50**, 73 (1979).
4. K. D. Joshi, A. S. Rav, S. C. Gupta , *BARC Report* , BARC/2011/E/002.
5. Hariharan P, Oreb BF, Eiju T, "Digital phase shifting interferometry: a simple error compensating phase calculation algorithm", *Appl Opt*. **26**(13), 2504 (1987).
6. M. Takeda, H. Ina, S. Kobayashi, "Fourier transform method of fringe pattern analysis for computer-based topography and interferometry", *J. Opt. Soc. Am*.**72**, 156 (1982).
7. Q. Kemao, "Windowed Fourier transform for fringe pattern analysis", *Appl. Opt*.**43**(13), 2695 (2004).
8. L.R. Watkins, "Review of fringe pattern phase recovery using 1-D and 2-D continuous wavelet transform," *Opt. Lasers Eng*. **50**(8), 1015 (2012).
9. M A Gdeisat, A Abid, D R Burton, M J Lalor, F Lilley, C Moore and M Qudeisat, "Spatial and temporal carrier fringe pattern demodulation using one-dimensional wavelet transform: Recent progress,chllanges, and suggested developments, *Opt. Lasers Eng*. **47**, 1348 (2009).
10. C. J. Tay, C. Quan, W. Sun, X. Y. He, "Demodulation of a single interferogram based on continuous wavelet transform and phase derivative," *Opt. Commun*. **280**, 327 (2007).
11. A Z Abid, M A Gdeisat, D R Burton and M J Lalor, " Fringe pattern analysis using a one-dimensional modified Morlet continuous wavelet transform" *SPIE*. **7000**, 1 (2008).
12. R.A. Carmona, W.L. Hwang and B. Torresani, "Multiridge Detection and Time-Frequency Reconstruction" *IEEE Trans. Sig. Proc*. **47**, No. 2, (1999).
13. G Rajshekhar, SS Gorthi, P Rastogi, "Strain, curvature and twist measurements in digital holographic interferometry using pseudo-Wigner-Ville distribution based method", *Rev Sci Instrum*. **80**(9), 093107 (2009).
14. Francois Auger, Patrick Flandrin, Paulo Goncalves and Olivier Lemoine, "Tutorial on Time-Frequency Toolbox in MATLAB" *CNRS-France and Rice University-USA*, (1996).
15. G Rajshekhar, SS Gorthi, P Rastogi, "Polynomial Wigner-Ville distribution based method for direct phase derivative estimation from optical fringes", *J. Opt. A: Pure Appl. Opt*. **11**(12), 125402 (2009).
16. W. Gander, G.H. Golub, and R. Strebel, "Least-squares fitting of circles and ellipses", *BIT*, **34**, 558 (1994).
17. P. D. Sampson, "Fitting conic sections to 'very scattered' data: An iterative refinement of the bookstein Algorithm", *Computer Graphics and Image Processing*, **18**, 97 (1982).
18. S. Liu, D. Wang, T. Li, G. Chen, Z. Li and Q. Peng, "Analysis of photonic Doppler velocimetry data based on the continous wavelet transform" *Rev. Sci. Instrum*. **82**, 023103 (2011).
19. H. Song, X. Wu, C. Huang, Y. Wei and X. Wang, "Measurement of fast-changing low velocities by photonic Doppler velocimetry" *Rev. Sci. Instrum*. **83**, 073301 (2012).

TH-2. DYNAMICS OF CONFINED LASER INDUCED/ABLATIVE PLASMAS AND SHOCK WAVES

Nagaraju Guthikonda *ACRHEM* University of Hyderabad Telangana, India-500046.**Email**: naga.gk@uohyd.ac.in

The This thesis discusses the dynamics of the confined laser induced/ablative plasmas and shock waves visualized through shadowgraphy technique to understand and develop a nano-second laser based milli-meter (mm) sized shock tube. The downscaling of the shock wave effects such as pressure, velocity attenuation during propagation, laminar and turbulence flow from macroscopic to mm or micro range, requires a proper extensive study to balance the interplay between the down scaling of the shock waves to mm size and maintaining the shock wave properties. This can be achieved by studying the enhancement of the plasma and shock wave properties in different confined geometries. Based on the experimental geometry used for plasma confinement, the confinement methods can be divided into two categories, (a) axial confinement (b) lateral or spatial confinement w.r.t. laser axis. In axial confinement, the plasma source is confined by a fluid (liquid/plasma/gas) or solid (glass) confining layer along laser propagation axis. The collision dynamics of the two counter propagating laser induced plasmas (S1 and S2) and shock waves in ambient air revealed the effect of the separation distance (d) between the confining plasma and confining medium (another plasma as fluid confinement). Here, the plasma source S2 is used as the temporally expanding fluid confining medium, which confines the plasma source S1 generated with 25 mJ laser energy. This study also helps to understand the effect of the relative impedance of the confining plasma and fluid confining medium with different impedances ($Z=\rho U_{sw}$) along with the effect of separation distance between two plasma sources (S1 and S2). The results showed that, when the two laser pulses are focused with $d < 2$ mm separation distance, both the plasma sources were merged into a single colliding plasma source which lead to the increment in plasma and shock wave properties as shown in figure 1. For separation distance $d \geq 2$ mm, we have observed the plasma jetlet formation in the source S1 due to the impedance mismatch between S1 and S2 plasma sources, along with a stagnation layer at the interaction zone as shown in figure 2.

The evolution dynamics of the laser induced blow off shock waves (LIBO SWs) in ambient air from metal films (Al, Cu, Ti) and polymer films (PVA, Au doped PVA) confined with glass (BK-7) substrate, revealed that the efficient blow off the shock waves can be achieved for optimal laser input energy by varying focusing conditions. This has resulted in the efficient coupling of the laser energy to the target material.

In this study, we have shown that the efficient laser energy coupling to the target material can be achieved by precisely shifting the laser focal plane around the interface as shown in figure 3. This study also useful in understanding the effect of the relative impedance between target and confining metal layer on the blow off shock wave properties. The results showed that the PVA and AuPVA polymers gave higher LIBO SWs than Al (20 μm), Cu (20 μm) foils by shifting the focal plane to F2 (2 mm) focusing condition with an optimal 50 mJ laser input energy.

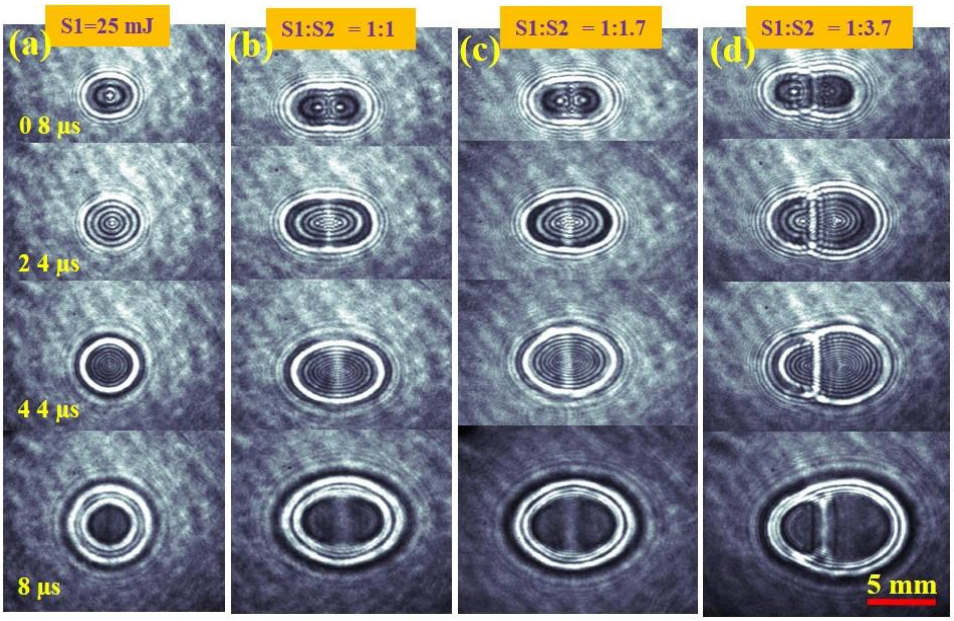

Figure 2. Shadowgrams of the temporal evolution of the (a) single plasma S1 evolution; colliding plasma sources of (b) equal and (c-d) unequal energy ratios with d=1 mm.

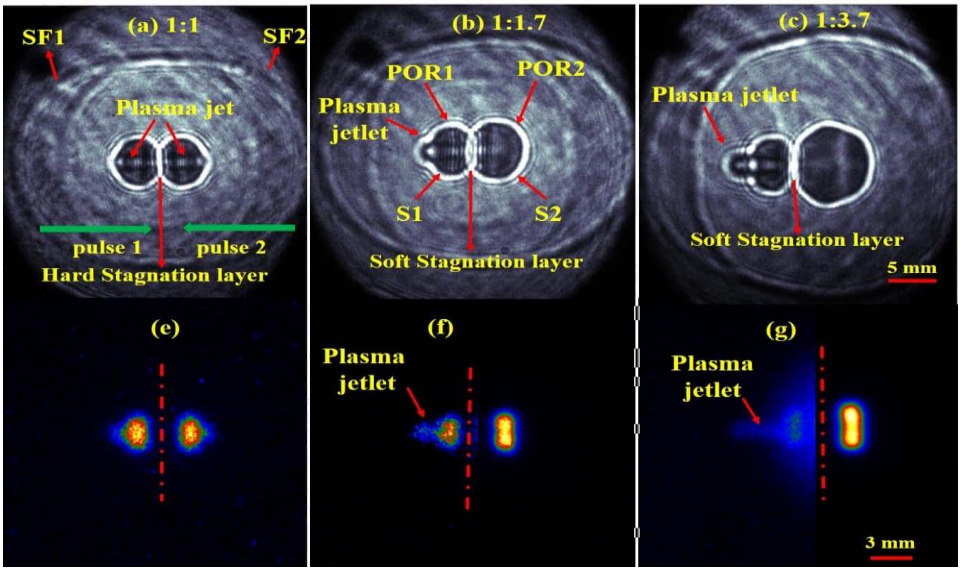

Figure 3. Shadowgrams of two counter propagating laser induced plasma shockwaves for d=4mm, at t=30 µs with different energy/impedance ratios of (a) 1:1, (b) 1:1.7, and (c) 1:3.7. The vertical lines in Figure 2(e-g) represent d=0.

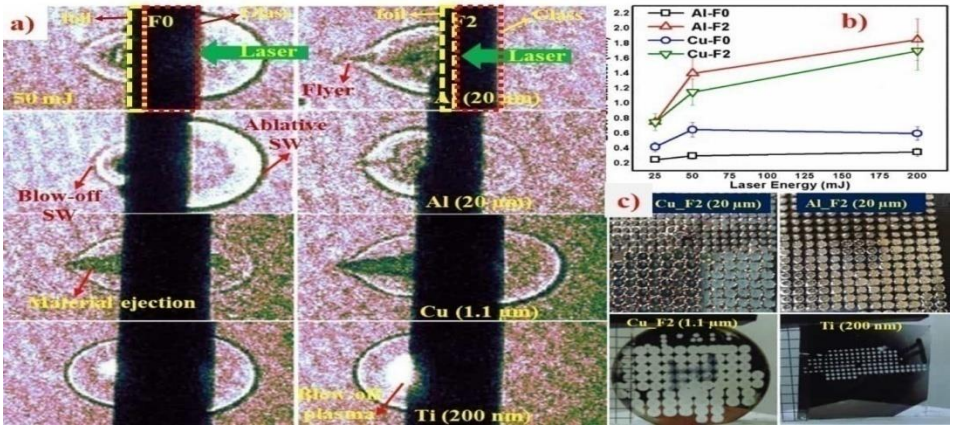

Figure 4. LIBO studies of different samples (a) shadowgrams at 3.05 μs (b) energy dependence behavior of blow off diameter of Al (20 μm) and Cu (20 μm) foils (c) samples after experiment.

The study of the spatial confinement of the air plasma inside mm size tubes (with 4.7 to 13 mm tube diameters) revealed the inter-dependency and interaction of the plasma and shock waves, which highly depend on the input laser energy and tube aspect ratio (L/D). In spatial confinement of air plasma, the reflected radial/transverse shock waves compression increased the plasma properties such as plasma length, plasma life time, plasma number density and plasma temperature. The squeezing of the air plasma forced out the plasma mass density which increased the axial shock wave position i.e., its velocity as shown in figure 4. This study also helped us to understand the air plasma generated shock wave propagation inside mm sized tubes and the effect of spatial confinement on axial shock wave propagation.

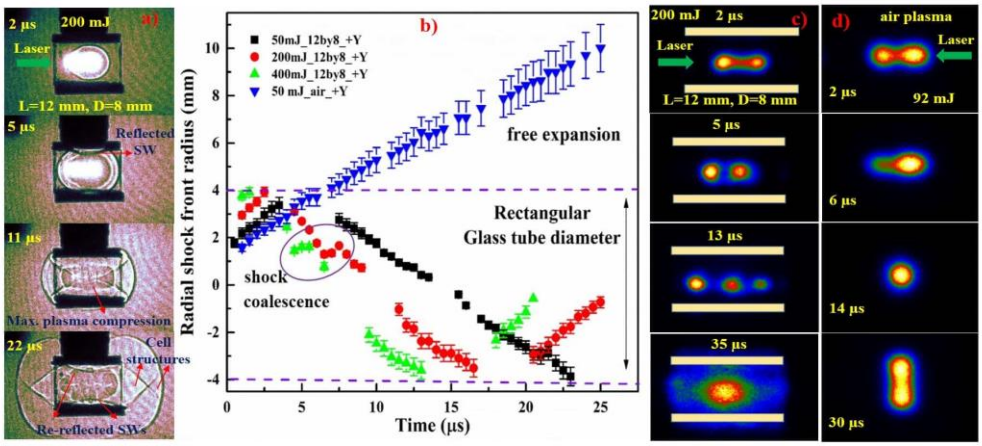

Figure 5. Temporal evolution of (a) shadowgrams of plasma and shock waves (b) radial shock waves along +Y direction, plasma self-emission images of (c) spatially confined 200 mJ air plasma inside glass tube with L/D=1.5 (d) ambient air plasma with 92 mJ energy.

Finally, this work also investigated the shock wave propagation inside transparent solid material, which will be helpful to understand the Laser Shock Peening (LSP) process. The dynamics of the temporal evolution of the laser induced/ablative shock waves inside a transparent dielectric material, BK-7 glass slab is used to understand the effects of both the

axial confinement and spatial confinement on the shock wave propagating inside a transparent solid material. The axial confinement of shock waves is achieved using an overlay of 20 µm Al/Cu foils, while the dimensions of BK-7 glass have provided the spatial confinement to shock waves launched and propagated inside BK-7 glass slab as shown in figure 5.

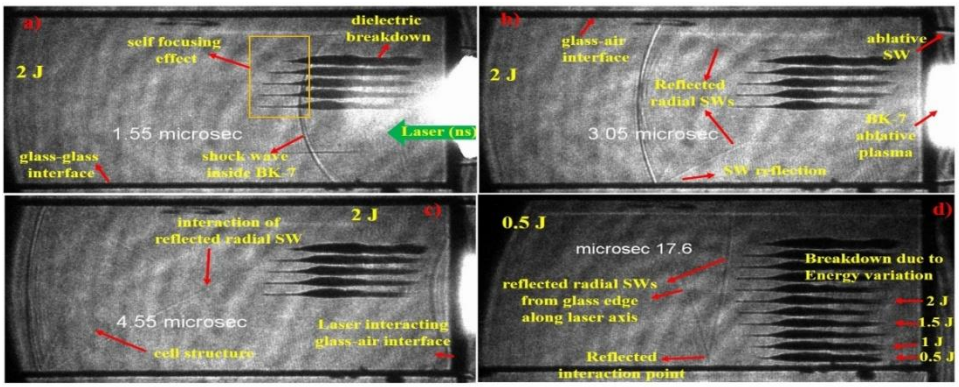

Figure 6. Dielectric breakdown of BK-7 glass slab for laser energies (a-c) 2 J (d) 0.5 J in direct ablation geometry

The results showed that, the shifting of the laser beam focal plane from F0 to F2 (6 mm) focusing condition enhanced (around 0.6 - 2.2 km/s) the shock wave velocities inside the BK-7 glass due to the 20 µm Al foil confinement of the BK-7 glass, but it has not affected for the 20 µm Cu foil confinement of the BK-7 glass. The energy dependence study on the shock wave propagation inside BK-7 glass revealed that, the enhancement of the shock wave inside BK-7 glass greatly depends on the relative acoustic impedance of the confining layer (20 µm Al and Cu thin foils) and BK-7 glass as well as on the laser energy density in the focal volume at the interface. Future roadmap for the development of nano-second laser based micro shock tubes with optimal input laser energies, better laser focusing conditions, selection of confining layer material and aspect ratio (L/D) of the tube based on the thesis is proposed. The experimental set up used for the initial data from mm sized shock tube is shown in figure 6.

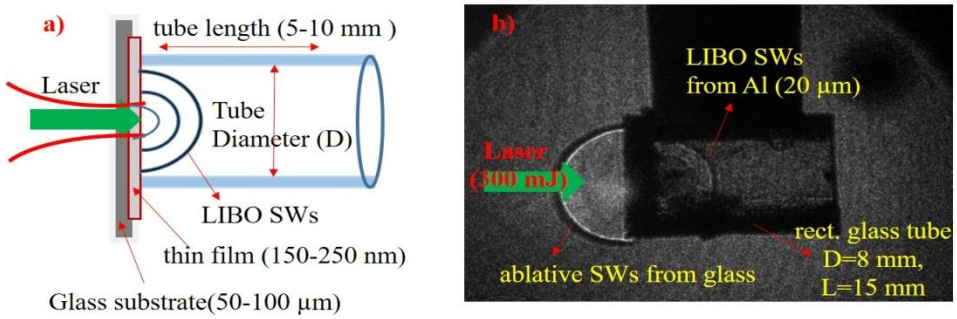

Figure 7. (a) Schematic used for the LIBO SWs propagation inside the mm sized tubes (b) experimental visualization of ns laser shock tube using rectangular tube geometry

TH-3. ULTRAFAST MOLECULAR DYNAMICS AND THIRD-ORDER NONLINEAR OPTICAL STUDIES OF NOVEL ORGANIC, INORGANIC AND ENERGETIC MATERIALSS

Katturi Naga Krishnakanth *ACRHEM* University of Hyderabad Telangana, India-500046
email: k.n.krishnkanth@uohyd.ac.in

This thesis is organized into eight (8) chapters. The content of each of these chapters are summarized and organized as follows:

Chapter 1: This chapter provides a broad introduction to the investigated molecules and basic nonlinear optics. Mainly the following aspects are explained in detail: (a) the significance of these molecules over the state of the art materials existing so far with a brief literature survey(b) the advantage of nano sized materials such as perovskite nanocrystals (NCs) and metal nanoparticles for NLO/photonic applications (c) organic molecules and their nonlinear properties (d) ultrafast electronic and vibrational relaxation processes of energetic molecules for a better understanding of the performance of different EMs (e) the advantages and complete details of experimental techniques used in the thesis (Z-scan, degenerate four-wave mixing, transient absorption spectroscopy and coherent anti-Stokes Raman spectroscopy)

Chapter 2: This chapter provides a complete description of the femtosecond lasers and experimental techniques used. Further, (a) techniques of ultrafast pulse generation (nanosecond to femtosecond) and different components used to generate these pulses in the cavity (b) chirped pulse amplification process (c) regenerative amplification (d) ultrashort pulse propagation and dispersion effects in different media (e) pulse characterization using intensity and single-shot autocorrelation techniques (f) preparation of samples and steady state measurements such as absorption and emission experimental details are summarized. The experimental techniques of (a) Z-scan (b) Degenerate Four-Wave Mixing (c) Transient absorption with global and target analysis and (d) Time-resolved Coherent Anti-Stokes Raman spectroscopies are described in detail.

Chapter 3: This chapter encompasses the NLO studies of perovskite nanocrystals, mainly results obtained from the single beam Z-scan and degenerate four-wave mixing experiments. The complete details of the NLO studies and their properties (multi-photon absorption and nonlinear refractive index) and the response of perovskite nanocrystals ($CsPbBr_3$ NCs and Cs_4PbBr_6 zero-dimensional NCs) are described. We have obtained strong two-photon absorption coefficients order of 10^4 GM from $CsPbBr_3$ NCs and multi-photon absorption studies on Cs_4PbBr_6 zero-dimensional NCs showed strong cross-section values (two-photon absorption cross-section, $\sim 10^6$ GM in the 500–800 nm region, three-photon absorption cross- section, $\sigma^{(3)} \sim 10^{-73}$ cm^6 s^2 in the 900–1200 nm region and four-photon absorption cross- section, $\sigma^{(4)} \sim 10^{-100}$ cm^8 s^3 in the 1300–1500 nm spectral region). The DFWM measurements confirmed strong third-order nonlinear susceptibility with ultrafast response time.

Chapter 4: This chapter discusses the intra and interband relaxation dynamics of pure Au and $Au_{50}Ag_{50}$ laser-ablated bimetallic nanoparticles at 400 nm and 800 nm photoexcitation. The electron-electron relaxation times (<0.5 ps) were obtained for Au and $Ag_{50}Au_{50}$ alloy NPs and have a fast response at both inter and intraband excitation. Both the NPs have similar electron- phonon relaxation times (<4 ps), which shows the homogeneity of the composite material. The obtained electron dynamics from these NPs are exhibiting fast response compared to other studies on Au and $Ag_{50}Au_{50}$ nanocomposite materials. The NLO properties were measured using Z-scan technique at 800 nm wavelength are presented. The alloy nanoparticles have shown strong NLO properties and their significance is discussed

Chapter 5: This chapter discuss the ultrafast photophysical processes and third-order nonlinear optical properties of D-π-D based porphyrin molecules. From the transient absorption spectroscopy, we have obtained different decay rate and time constants, corresponding to internal conversion from (S_n-S_1), of <1 picosecond, vibrational relaxation within S_1 states in <10 ps, radiative relaxation of S_1-S_0 in nanosecond time scale, intersystem crossing from S_1- T_0 in picosecond and nanosecond time scales and triplet relaxation from T_0-S_0 in

microsecond time scale (1-100 μs). The third-order nonlinear (NLO) coefficients recorded with ~50 fs, 1 kHz repetition rate pulses at a wavelength of 800 nm. The magnitude of the TPA coefficients and cross-sections (~10^3 GM) of these molecules was compared with some of the recently reported porphyrin moieties and were found to be superior. The time-resolved degenerate four- wave mixing (DFWM) measurements confirmed a large magnitude and an ultrafast response of the $\chi^{(3)}$ in these molecules.

Chapter 6: This chapter presents the results from the studies aiming to understand and evaluate the ultrafast photophysical processes and third-order nonlinear optical properties of newly synthesized donor-acceptor based free-base [(C6F5)3] and phosphorus [P-(OH)2(C6F5)3] corroles. The femtosecond transient absorption data reveals several photophysical processes such as (a) internal conversion ($\square_{IC}$) in the 260-280 fs range (b) vibrational relaxation ($\square_{VR}$) in the 2.5-5ps range and (c) nonradiative relaxation times ($\square_{nr}$) in the 4.15-7.6 ns range and finally (d) triplet lifetimes in the range of 25-50 μs. The nonlinear optical measurements were performed using the femtosecond, kHz pulse Z-Scan technique at 600 nm, and 800 nm and. The TPA cross-section values were in the range of ~10^2 GM. Degenerate four-wave mixing measurements illustrated a large third-order nonlinear optical susceptibility $\chi^{(3)}$ with a magnitude of 6.9×10^{-14} esu and instantaneous (sub-picosecond) response, suggesting a pure electronic contribution to the nonlinearity of these corroles

Chapter 7: This chapter discusses the molecular dynamics of the complex and nitrogen-rich amino, and nitro substituted tetrazole derivatives [2,6-dinitro-4-(1H-tetrazole-1-yl)aniline ($C_7H_5N_7O_4$) and 1-(3,4,5-trinitrophenol)-1H-tetrazole($C_7H_3N_7O_6$) are labelled as 6 and 8] with the results obtained from femtosecond time-resolved coherent anti-Stokes Raman spectroscopy and transient absorption studies. The present study is beneficial in enhancing the applications of energetic materials since the tetrazole derivative 8 demonstrated energetic properties those comparable with the secondary explosives such as RDX and TNT. Fourier transforms of the recorded CARS transients revealed the possible IVR mechanisms in tetrazole-N-(hetero)aryl derivatives. Further, dephasing times estimated from the CARS transients were ~137-200 fs. We have found that the low energy modes those corresponding to the C-H vibrations exhibiting faster dephasing times compared to higher energy vibrational modes, Consequently, the C-H vibrational modes could be excited first upon photoexcitation and causing an initial chemical reaction. The transient absorption spectroscopy at 400 nm photoexcitation with the help of target analysis different decay rate and time constants are discussed. The vibrational relaxation within S1 states occurred within 0.3-0.8 ps time scale and a possible intermediate state (S1-S^*- T0) is discussed at the intersystem crossing with a lifetime of 9.7 and 120 ps. The S1 state decays to S^* with a lifetime of 2.2 to 4.7 ps and the triplet lifetime was found to be in a microsecond time scale

Chapter 8: This chapter summarizes the obtained results in this thesis and presents the future scope of the work including (i) implementation/extension of transient absorption experiments in the NIR regime to study the structural dynamics (ii) development of femtosecond standoff CARS setup for explosives detection and (iii) multi-photon absorption studies such as five-photon and above at NIR wavelengths for biological applications
sensing.

TH-4. INFLUENCE OF BIOFOULING ON SHIP RESISTANCE AND LASER SPECTROSCOPIC ANALYSIS

Della Thomas Indian Institute of Technology, Madras ***E.mail*** *: della.thomas.mec@gmail.com*

Biofouling has been a severe problem affecting marine hulls since time immemorial. Marine biofouling refers to the undesirable growth and adhesion of marine organisms, such as barnacles, algae, microbial slimes, etc., on immersed structures leading to the formation of

biofilms. On static marine structures, biofouling can accelerate corrosion and hence result in mechanical failure. A typical example of fouling is the clogging of seawater intake pipelines. Biofouling in ships can reduce speed and create difficulty in maneuverability, leading to increased fuel consumption and maintenance costs. In a moving vessel, biofouling growth creates additional drag and increases fuel consumption while maintaining a constant speed. Hence, marine biofouling is an issue of grave concern for marine structural designers. Some of the locations of ship hull which require attention are appendages like rudder and structs, sea-chests, propellers, etc.

Biofouling formation mechanism:

Structures submerged in the marine environment are colonized by microorganisms that promote biofouling resulting in bio corrosion. There are four main stages in the formation of biofouling attachment, proliferation, detachment and Predation. The light slime starts to begin within 24 - 48 hours of water submergence. Light slime acts as a food source and mechanism of attachment for microbial cells. During the attachment stage of microorganisms on a rigid substrate, proliferation takes place, forming biofilms. Once bacteria attach to the surface, they produce extracellular polymers and result in heavy slime. A complex community develops called calcareous fouling and consists of multicellular species, macro-algae, debris, sediments, etc. Later larger marine invertebrates like barnacles, mussels, macroalgae, etc., attach, resulting in heavy calcareous fouling. A few bacteria detach from biofilm, searching for a less crowded surface for colonization during the detachment phase. Predation also takes place.

Conventional methods to measure biofouling:

Different factors, such as environment, pollution, turbidity, organic and inorganic materials, influence the type and growth of marine biofouling. Conventional methods of measuring biofouling are biological methods and metallurgical methods to measure corrosion etc., via sampling. Alternatively, the identification of corrosion by-products related to Microbiologically Induced Corrosion (MIC) can be measured by biological methods and **metallurgical methods.** Biological methods identify the presence of microorganisms related to MIC by Onboard sampling and Laboratory testing. Onboard sampling can be done by a hand-held peristaltic pump with an extendable rod. Sampling the bilge water and limited access testing are also methods for onboard analysis. Metallurgical processes consist of observation of MIC-related corrosion morphology. The corrosion was examined through SEM images of marine grade hull steel immersed in bilge water containing Sulphate Reducing Bacteria (SRB), bilge water, and clean water without SRB.

Preventive measures to avoid biofouling

There are a lot of methods for fouling control. Some of the methods commonly employed are as follows. Material selection (e.g., copper alloys) is an essential factor. The coatings which are widely used are Active biocides and hard inert non-stick fouling release. Mechanical removal techniques are the application of Brush, water jet, and air bubbles. Chemical treatments are halogenation, ozonation, copper anodes/organic biocides, and pH. Electrical methods are high voltage/current, corrosion, cathodic chalk formation. Radiation methods are ultra-violet, magnetic, sound, and radioactive. Thermal processes are heating and freezing. Biological methods are predation, infection, etc.

LIBS technique to study biofouling

Laser-Induced Breakdown Spectroscopy (LIBS). It is an elemental analysis technique that gives fast measurement results with minimum sample destruction. This method involves the removal of a small amount of sample mass and its conversion into plasma. Hence this technique is usually classified as a minimally destructive or a non-destructive process. It can be used as a real-time monitoring technique for quality control checking across various domains. The main advantage of the LIBS technique is its rapid analysis capability and minimal sample preparation. Remote monitoring is also an added advantage that can be employed for **continuous monitoring applications**.

Laser-induced breakdown spectroscopy (LIBS) technique can also be considered for analyzing and monitoring biofouling. LIBS technique involves pulsed laser irradiation of the material of interest and elemental analysis using the emission spectra from the plasma generated during the laser ablation [1]. Analysis of the spectral emission from laser induced plasma can provide an insight into the chemical composition of the biofilm bacteria. The database can later help formulate suitable antifouling coatings with additives to inhibit biofouling formation. The possibility of employing laser irradiation for biofouling reduction would also be investigated. Hence, the study would help in proposing a novel method for the in-situ biofouling monitoring on ships or any submerged marine structures using the LIBS technique.

Biofouling research trends

The major biofouling research trends are outlined below. One approach has been the detection or monitoring of biofilm. A plethora of literature is available regarding the analysis of biofilms via biochemical techniques and imaging methods. Biochemical techniques and imaging methods have been used to analyze biofouling, and there is an increasing interest in developing techniques for detecting and monitoring biofilm. The samples are specified in biochemical process in terms of macromolecules, viz. carbohydrates, proteins, lipid, and nucleic acids. An organism's growth can be tracked with the variation of the relative amount of various macromolecules, mainly constituted by lipids. Similarly, multiple reports are available about the imaging techniques dealing with the studies of the biofilm layer structure.

The biofilm bacteria can be characterized in terms of its constituent elements, by using the novel technique of LIBS. In contrast with the other methods, LIBS possesses many advantages. A few benefits of LIBS, such as the remote analysis capability, minimum sample preparation required, and quantitative measurement of minor elements, make it an attractive method for analysis. LIBS can provide an insight into the chemical composition of the biofilm. Elemental analysis is possible with LIBS irrespective of the physical state. Biofilm analysis can be done either in suspension or as biofilms coated on substrates. Depth profiling of structures is possible with LIBS. Information about the composition of the biofilm along the depth using LIBS combined with Principal Component Analysis (PCA) can be used to classify marine biofouling and its constituents.

Literature survey

Biofouling composition is determined by collecting samples from marine structures and vessels and analyzing them in the laboratories. Alternatively, an approach of online sensing based on Laser-Induced Breakdown Spectroscopy (LIBS), which consists of the analysis of the spectral emission from laser-induced plasma, can be considered for the elemental **composition of biofouling.**

Current LIBS research includes the study of various biological samples, viz. algae, bacteria, etc., with the help of this technique. Porizka et al. [2] have analyzed algal biomass for industrial biotechnology using double-pulse LIBS. Both wet and dry procedure has been demonstrated in this work. The investigation was carried out in terms of elemental compositions of Mg, Ca, K, Na, Cu, etc.

Better discrimination of similar bacteria samples was also possible with sequential testing in two ambient gas environments [3]. Identification of bacterial constituents has also been possible in mixed cultures [4]. Baudelet et al.[1] have done a study comparing the femtosecond and nanosecond LIBS spectra for the bacteria have been done in this work.

Biochemical techniques and imaging methods have been used to analyze biofouling, and there is an increasing interest in developing techniques for detecting and monitoring biofilm. Chandy et al. [5] have employed optical fiber sensors to develop an online fouling sensor for closed-loop process systems.

Objective of the work

Based on the literature survey, it is essential to understand the influence of fouling on ship resistance. The study of the growth of biofouling on different materials is also useful to understand the mechanism of formation of the biofouling film. No such combination of studies

has been reported elsewhere by other research groups in the area. Hence, the objectives of the present study were as follows.

1. To simulate the influence of fouling on the resistance of ship hulls and determine the effect experimentally.
2. To extend the simulation to voyage simulation for specific routes considering weather conditions.
3. To demonstrate an application of LIBS to study the elemental composition of biofilms in laboratory-controlled conditions. To extend the study the biofilm growth on different materials.

Scope of the thesis

Based on the objectives of the study, the scope of the work is as follows.

1. To perform studies concerning ship resistance due to biofouling. To perform voyage analysis to determine speed reduction and additional fuel consumption to maintain the speed in a harsh environment.
2. To determine the effect of fouling on ship hull in a towing tank.
3. To study elemental analysis of marine fouling bacteria and algae species grown in controlled conditions.
4. To characterize biofilms grown on materials, namely, stainless steel and fiber-reinforced plastic composites. To study mapping of the substrate.

REFERENCES

1. Baudelet, M. *Laser Spectroscopy for Sensing. Fundamentals, Techniques and Applications*. (Woodhead Publishing Series in Electronic and Optical Materials, 2014).
2. Pořízka, P. *et al*. Application of laser-induced breakdown spectroscopy to the analysis of algal biomass for industrial biotechnology. *Spectrochim. Acta - Part B At. Spectrosc.* **74–75**, 169–176 (2012).
3. Rehse, S. J. & Mohaidat, Q. I. The effect of sequential dual-gas testing on laser-induced breakdown spectroscopy-based discrimination: Application to brass samples and bacterial strains. *Spectrochim. Acta - Part B At. Spectrosc.* **64**, 1020–1027 (2009).
4. Rehse, S. J., Mohaidat, Q. I. & Palchaudhuri, S. Towards the clinical application of laser-induced breakdown spectroscopy for rapid pathogen diagnosis: The effect of mixed cultures and sample dilution on bacterial identification. *Appl. Opt.* **49**, 27–35 (2010).
5. Philip-Chandy, R. *et al*. Optical fiber sensor for biofilm measurement using intensity modulation and image analysis. *IEEE J. Sel. Top. Quantum Electron.* **6**, 764–772 (2000).

TH-5. LASER-INDUCED UNDERWATER ACOUSTIC SIGNALS AND THEIR APPLICATIONS

Janapati Yellaiah, ACRHEM University of Hyderabad Telangana, India-500046.**Email:** *janapatiyellaiah@gmail.com*

Despite years of research on underwater acoustics, the complex mechanisms that allow dolphins to learn so much about their surroundings via echolocation are still intriguing for scientists. In light of this, we want to explore the generation of broadband acoustic spectra using high-power pulsed lasers as a source for remote detection and identification of underwater objects via echolocation, where the objects are not visible or characterizable using conventional optical techniques. In this thesis, I have demonstrated that laser-induced breakdown can be used as a high-frequency broadband point source for underwater acoustic measurements. It has access to a broader acoustic spectrum and provides for remote variable location of the source by changing the input laser properties. In search of the non-contact laser-induced underwater acoustic source (LIUAS) evolution, propagation and their interaction across the water-air and water-solid interfaces have been investigated in this thesis. The LIUAS propagation and their interaction across the water-air and water-solid interfaces have intriguing research for non-

contact detection and precise location of the underwater targets. The laser-based technique can find application over varied ranges to detect entities like mines, divers, and small submersibles, to large moving objects such as unmanned underwater vehicles and submarines via acoustic mapping by using LIUAS.

High-energy nanosecond (ns) and picosecond (ps) laser pulses focused underwater will cause the breakdown of water due to catastrophic cascade ionization or Multiphoton ionization around the focal plane leading to laser-induced plasma (LIP) formation [1–4]. The basic mechanism of laser-induced plasma formation and expansion, shockwave propagation, cavitation bubble oscillation, breakdown threshold, and conversion efficiency [1–4] have been extensively studied by several authors over the decades. The plasma formation occurs over the elongated region with multiple LIP sources, which in turn depends on the input pulse energy. Each of these plasma sources expands supersonically launches a shockwave compressing the surrounding water medium [4]. These shockwave with pressures higher than that of the ambient water pressure decay rapidly while propagating through water and, over the time, reaches the acoustic speed [4–6]. The laser-induced plasma channel itself is a source of cavitation bubble generation, acoustic shockwave emission, stimulated Raman scattering (SRS), meter long filament generation [4] etc. The input peak power of laser pulses is much higher than the liquid medium's threshold power, leading to multiple LIP sources elongated the focal region [4]. When the plasma cools down, due to an imbalance between inside and outside pressure of cavitation bubbles, violent contraction and collapse of the cavitation bubbles generate secondary acoustic shock waves [1–5]. The shock waves rapidly detach from the LIP owing to its velocity much higher than the particle velocity behind it. So, shockwave's hypersonic velocity loses energy, generates pressure impulse, and propagates at the sound speed [1–6].

Overview of the thesis: This thesis is organized into six (6) chapters. The content of each of these chapters are summarized and organized as follows:

Chapter 1: This chapter outlines a review of the various mechanisms such as catastrophic cascade ionization or Multiphoton ionization that involved in the LIUAS formation. There are several methods to understand the LIUAS source and associated acoustic signals. The LIUAS has the potential to expand and improve both naval and commercial underwater acoustic applications, including undersea surveillance operations, acoustic imaging, port monitoring, object recognition, and oceanographic survey etc. The scope of LIUAS for simulating the blast wave from underwater explosion in the laboratory, where the information on their propagation, reflection, and transmission across the water-air interface is vital in mitigating the possible damage. And also, the LIUAS as a proof-of-concept where the pressure impulses produced by airborne lasers can be utilized for undersea communications and explorations with much simplified hardware fitted in aircraft. In view of the potential unexplored applications of LIUAS, this chapter describes the organization of the thesis starting from the experimental schematics to the observed results and their analysis culminating in the proof-of-concept of laser-induced SONAR.

Chapter 2: This chapter provides a complete description of the nanosecond and picosecond lasers delivering 10ns and 30ps pulses respectively, sensors and their deployment for different experimental techniques used in the thesis. The details of the underwater sensors such as hydrophones (M/s, Teledyne RESON and Precision Acoustics) and microphone (1/8" 40DP GRAS) are presented. The basic mechanism and working principles of hydrophone and microphone sensors for the non-contact detection of acoustic pressure impulses have been discussed. The effect of sampling rate, window function and overlapping on UAS measurements are presented. The construction of acrylic water chamber with BK-7 glass windows to carry out the experiments is discussed.

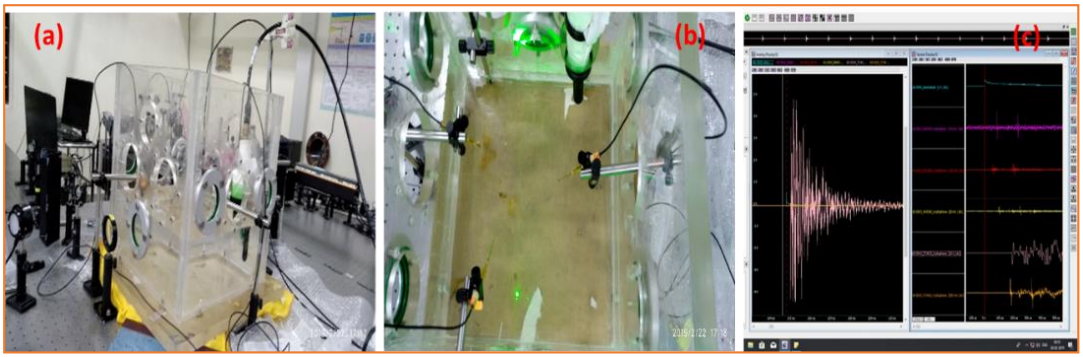

Figure 8: (a) side view (b) top view of water chamber with hydrophones placed at various positions (c) typical response of the hydrophones signals

Apart from the time domain information, the time-frequency information is also essential for the evolution of LIUAS source detection and precise location. In the time-frequency domain, the spectrogram obtained via STFT provides spectral information and arrival time of both direct and reflected signals simultaneously. The experimental schematic used for the generation of UAS from ns- and ps-LIB (chapter 3) and their interaction across the water-air interface and various solid targets (chapter 4) as well as the spatial acoustic scan of a laser plasma due to ns laser-induced underwater meter scale filaments (chapter 5) are presented. Measurements of UAS done in time and time-frequency domains as well as the reproducibility of UAS at various laser energies, pulse duration and focal geometry under similar conditions is presented.

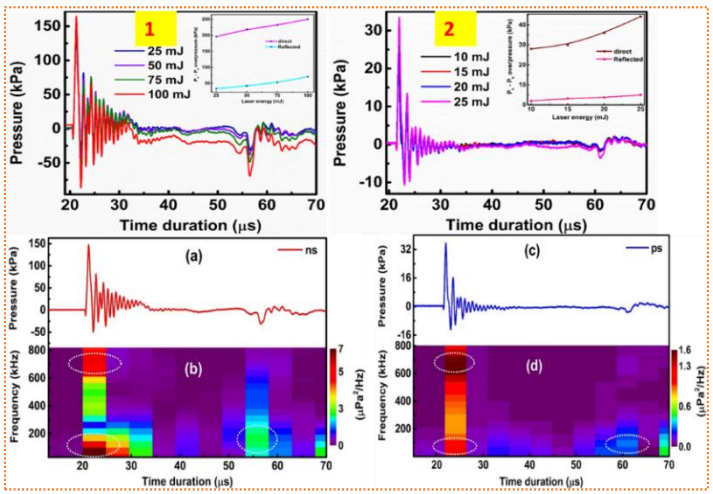

Figure 9: Time domain signals of UAS as a function of laser energy for (1) ns (2) ps laser, (a) and (c) time domain signals of UAS for 25mJ laser energy. The spectrogram for (b) ns and (d) ps laser pulses.

Chapter 3: This chapter presents the characteristics of underwater acoustic signal from ns- and ps-laser-induced breakdown experiments. The generation and their propagation, interaction of acoustic signal across the water-air interface studied for both ns- and ps-LIB of water. The UAS is well-known to undergo a complete reflection at the water-air interface due to the enormous acoustic impedance (Z) mismatch between the two media ($Z_1 = 1.485 \times 10^6$ for water and $Z_2 = 410$ Pa. s/m for air at 20^0 C) [7, 8]. The water-air interface is often considered as a perfectly reflecting for the UAS and as an example of an application of Snell's law and Fresnel reflection and transmission coefficients. Recently it was found that the interface becomes anomalously transparent to acoustic signals due to evanescent waves. With water-air interfaces occupying about two-thirds of the Earth's surface, the phenomenon of anomalous transparency is likely to have important geophysical and biological implications [9]. LIUAS interaction across

the water-air interface is ideal for simulating the blast wave from the underwater explosion in the laboratory, where the information on their propagation, reflection, and transmission across the water-air interface is vital. However, very few studies were performed to study the shock wave characteristics across water-air interface. Hosseini et. al. (2014) have studied the propagation characteristics of underwater blast waves generated by laser initiated Silver Azide pellet via shadowgraphic imaging which demonstrated the significant transmission of pressure across the water-air interface [7, 8]. With the advent of high energy table top laser sources, blast of an explosive can be easily mimicked by a focused ns pulse. Hence in this chapter we used the acoustic emissions emanated from the shockwaves due to a focused ns pulse, which mimics micro-explosion in the laboratory, to study the reflection and transmission of the acoustic signal across the water-air interface.

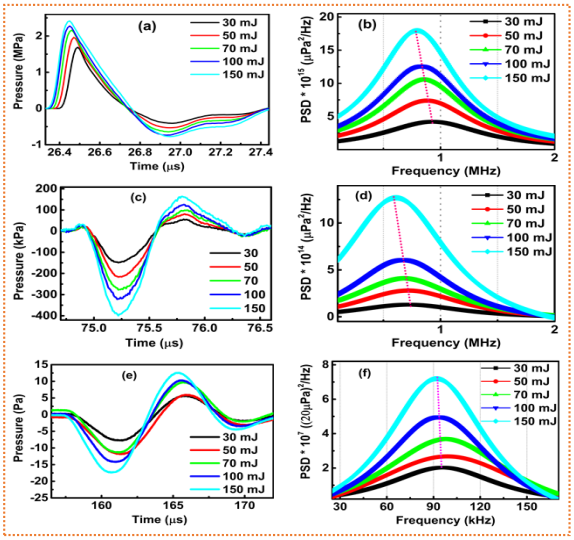

Figure 10: (a) direct signals of UAS (b) spectra of direct signal (c) reflected signals (d) spectra of reflected signals and (e) Microphone signals (f) spectra of microphone signals as a function of laser energy. The frequency response of the direct and reflected signals has broad-spectra spanning from 0.5–2 MHz and for transmitted in air 20 Hz–140 kHz. The dotted lines of pink color represent the peak frequency shifting.

The significant variation of acoustic parameters such as arrival time, peak-to-peak (P_k-P_k) overpressure, acoustic pulse width, pressure impulse, signal energy and conversion efficiency etc., have been presented. The effect of various important parameters such as laser energy, pulse duration, focal geometry and lens tilt, radial and angular distributions etc., on UAS and their interaction across the water-air interface were presented. The UAS comprises the direct and reflected signals. The laser–induced underwater acoustic emissions have observed to be high for ns-LIB than the ps-LIB, indicating higher conversion efficiency of optical energy into mechanical energy in water [5]. The dependence of acoustic emissions on incident laser energy revealed that the reflection and transmission of UAS could occur at the water-air interface due to the acoustic impedance and frequency mismatching [5, 7]. The spectrogram revealed that the transient UAS has broad acoustic spectra spanning from 10–800 kHz, perpendicular to the laser propagation direction. The initial laser impulse resulted in two major instantaneous frequencies centred around 105 kHz and 690 kHz with a standard error of 30 kHz. Upon reflection from the water-air interface, only the instantaneous peak frequency corresponding to ~105 kHz was reflected while the longer frequency is observed to get dissipated. Our results demonstrate the ns-LIB is more suitable for applications compared to the ps-LIB owing to stronger acoustic impulse of both direct and reflected signals.

Chapter 4: This chapter summarizes the interaction of LIUAS across the various materials with different shapes and presents the time and time-frequency domain results. In the time domain, the acoustic energy content of the reflected signal classifies the materials [5–6].

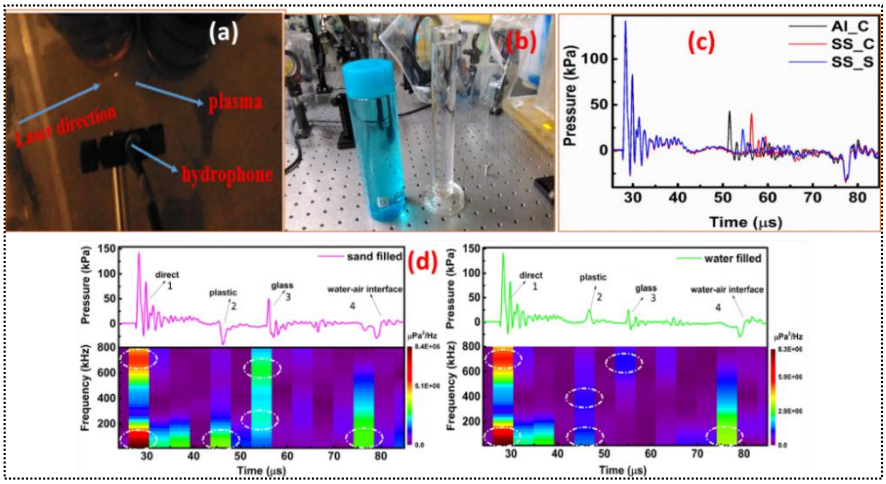

Figure 11: (a) experimental schematic (b) plastic bottle and glass targets (c) cylindrical (c) and spherical (c) shape of Al and SS targets (d) the spectrogram is visualized the plastic and glass targets filled with sand and water

The effect of laser energy on reflected signals from various materials in time and time-frequency domain presented. The experimental schematic used for the interaction of UAS across the water-air interface and various materials of different shapes in various positions across the water medium is described. We have used the materials with planar geometry (Metals-Al, Cu, Brass, SS, Ceramics-glass, BK-7, Plastic and other materials-Teflon, PVC, Nylon, Foam and Acrylic or PMMA, etc.), cylindrical geometry (Al, SS) and spherical geometry (SS) for classification via non-contact detection technique. We also used sand and water filled plastic and glass targets as shown in Figure 4 for the feasibility study of laser-induced SONAR. The effect of target shape and size on acoustic signal both in time and time-frequency domains were presented.

Chapter 5: This chapter presents the characteristics of underwater acoustic emissions emanated from nanosecond (ns) laser-induced filamentation (LIF) in the time, and time-frequency domains. In the time domain, significant variation of acoustic parameters such as arrival time, P_k-P_k overpressure, were presented. With increasing input laser energy, the P_k-P_k overpressures are increasing, and the arrival time remains constant for a given filament to hydrophone distance. We observed that the P_k-P_k overpressures are higher in linear polarization (LP) than circular polarization (CP) pulses. Acoustic measurements due to ns-LIF of water showed a linear increase in the filament length with input laser energy despite the interference due to the multiple plasma sources along the laser propagation direction. The time-frequency plane or the STFT has shown that the underwater acoustic pressure impulses have broad-spectra spanning from 10–800 kHz, perpendicular to the laser propagation direction for both LP and CP pulses. The instantaneous frequencies obtained from spectrogram are observed to be ~80 kHz range. We also collected the forward SRS (FSRS) using a CCD spectrometer (Maya, M/s. Ocean Optics). The effect of input laser energy, polarization and lens tilt on UAS measurements and FSRS signals were presented.

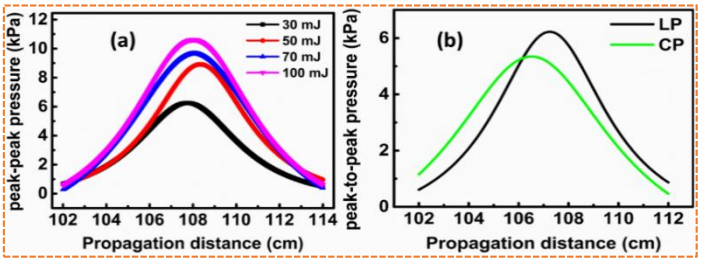

Figure 12: The peak-to-peak overpressure as a function of propagation distance for (a) incident laser energy (b) linear (LP) and circular polarization (CP)

Applications: During the past several years, the investigations of LIUAS have attracted particular interest for immense potential applications including clinical surgery, photoacoustic applications, drug delivery, microsurgery, LIBS for spectro-chemical analysis, microfluidic operations, remote generation of acoustic sources, electrical discharge guiding for high voltage switching, laser shock processing, and laser lithotripsy, laser-induced meter-scale filaments, nanoparticle synthesis, precise location and identification of underwater objects, remote detection of uneven surface of ice layers, simulating a blast wave from an underwater explosion in the laboratory for studying the associated propagation effects and sea bed sensing etc. Laser-based method can find application over varied ranges to detect entities like mines, and divers, to large moving objects such as, unmanned underwater vehicles, and submarines via acoustic mapping by using LIUAS [5–6, 10–11].

References:

1. Vogel, Alfred, S. Busch, and U. Parlitz. Journal of the Acoustical Society of America, 100, 148-165 (1996).
2. Vogel, A., and W. Lauterborn. Journal of the Acoustical Society of America 84, no. 2, 719-731 (1988).
3. Vogel, Alfred, J. Noack, Rockwell, and R. Birngruber. *Appl. Physics B: Lasers & Optics* 68, no. 2 (1999).
4. Lei Fu, Siqi Wang, Jing Xin, Shijia Wang, and Jing Wang, Opt. Express 26, 28560-28575 (2018).
5. J. Yellaiah and P. Prem Kiran, Appl. Opt. 60, 4582-4590 (2021).
6. Janapati, Yellaiah, and Prem Kiran Paturi. In *POMA UACE*, vol. 44, no. 1, p. 070003. ASA 2021.
7. Hosseini, H., S. Moosavi-Nejad, H. Akiyama, and V. Menezes. Applied Physics Letters 104, no. 10 (2014).
8. Yellaiah, J., and P. Prem Kiran. In *Frontiers in Optics*, pp. JTu1B-50. Optical Society of America, 2020.
9. Godin, Oleg A. Physical review letters 97, no. 16, (2006).
10. Jones, Theodore G., Tsih C. Tang, Edward R. Franchi, and Kwang B. Yoo. U.S. Patent 8,228,760, (2012).

TH-6. ELECTRONIC AND NONLINEAR OPTICAL PROPERTIES OF UNDOPED AND DOPED CR_2O_3 AND NIO THIN FILMS

P.Baraskar, DAV, Indore, Email: *priyanka.physics2015@gmail.com*

The understanding of the electronic and nonlinear optical properties of the materials is necessary in designing optoelectronic devices which play key role is in the present age of information technology. The materials used in existing optoelectronic devices include II-VI and III-V semiconductors. However, transition metal oxides have added advantage of magnetic properties arising due to partially filled d-orbitals. It is expected that the optoelectronic devices made from the transition metal oxides can be controlled by applied electric as well as magnetic field making them more suitable for technological applications. In view of this, NiO and Cr_2O_3 appear to be promising candidates for various devices applications. They have

proven utility in resistive switching, display devices, lasing materials, solar energy applications etc. The properties of these materials can be monitored by controlling their growth condition and suitable doping. In the present thesis, we have reported the study of the electronic and nonlinear optical properties of undoped and Al doped NiO as well as Ti, Mg doped Cr_2O_3 thin films.

Organization of the thesis

The study of structural, electronic, magnetic, nonlinear optical and magneto optical properties of undoped and doped NiO and Cr_2O_3 thin films are reported in the present thesis. Chapter-I discusses the importance and the basic understanding of the topics covered in the forthcoming chapters while in chapter-II the details of the deposition technique and characterizations are given. Chapters III-VI are devoted for the nonlinear optical, magnetic and band offset studies in undoped and Ti, Mg doped Cr_2O_3 thin films. Chapters VII-IX are focused on the study of pure, doped and bilayer NiO thin films. In the chapter- VII, we studied the electronic and optical properties of pulse laser deposited ZnO/NiO bilayer film. Chapter-VIII deals with the dispersive optical nonlinearities of undoped and Al doped NiO thin films and optical path length compensation in undoped NiO/Al doped NiO bilayer films for optoelectronic device applications. Chapter-IX explores the magneto-optic Kerr effect of Al doped NiO thin films. The conclusions and future scope are discussed in Chapter-X. A brief description of research work carried out in the relevant fields are discussed in each chapter is given below:

Chapter I: Introduction

The motivation for the selection of the materials and their respective properties as evident from the work already carried out by other researchers in this area is given in this chapter. Also, the fundamental properties viz; structural, optical (both linear and nonlinear), electronic and magnetic properties of the bulk as well as thin films of Cr_2O_3 and NiO are described. The chapter ends with a brief plan of the organization of the thesis.

Chapter II: Synthesis and characterization techniques

In this chapter the description of the experimental techniques employed by us in the thin film deposition and their characterization is given. All the films were deposited using pulsed laser deposition (PLD) technique. The details of solid-state reaction route method and PLD technique for the synthesis of bulk target material and thin film formation, respectively are described here. This chapter gives information about the basic principle and instrumentation of the various characterization techniques which include X-ray diffraction (XRD), Ultraviolet-Visible spectroscopy (UV-Vis), X-ray photoelectron spectroscopy (XPS), Ultraviolet photoelectron (Valence band) spectroscopy (UPS/VBS), Superconducting quantum interference device (SQUID), Magneto-optic Kerr effect (MOKE) and Z-scan optical measurement technique.

Chapter III: Linear and nonlinear optical properties of Ti doped Cr_2O_3 thin film: Effect of magnetic field

We report the magnetic field effect on the linear and nonlinear optical properties of the PLD ablated Ti-incorporated Cr_2O_3 nanostructured thin film in this chapter. Optical properties have been experimentally analysed under Voigt geometry by performing ultraviolet-visible spectroscopy and closed aperture Z-scan technique using a continuous wave He–Ne laser source. Nonlinear optical response reveals a single peak-valley feature in the far field diffraction pattern in absence of magnetic field (B =0) confirming self-defocussing effect. This feature switches to a valley-peak configuration for B =5000 G, suggesting self-focusing effect. For B $\leq$750 G, oscillations were observed revealing the occurrence of higher order nonlinearity. Origin of nonlinearity is attributed to the near resonant d-d transitions observed from the broad peak occurring around 2eV. These transitions are of magnetic origin and get modified under the application of external magnetic field. Our results suggest that magnetic field can be used as an effective tool to monitor the sign of optical nonlinearity in Ti-incorporated Cr_2O_3 nanostructured thin film.

*This work is published in **Physics Letters A**, 860-864, 382, (2018).*

Chapter IV: Weak ferromagnetism at room temperature in Ti doped Cr_2O_3 thin film

In order to analyse the magnetic properties of Ti doped Cr_2O_3 thin film, we performed magnetic measurements for undoped and Ti incorporated Cr_2O_3 films. This chapter express a striking feature of enhanced weak ferromagnetism at room temperature that observed in the Ti incorporated Cr_2O_3 film, apart from structural and morphological modifications due to Ti doping. The X-ray photoelectron spectroscopic of the films revealed increased number of oxygen vacancies in the Ti incorporated Cr_2O_3 films. Our study suggests that, the origin of weak ferromagnetism in the Ti incorporated Cr_2O_3 thin film is assigned to the presence of the oxygen vacancies.

This work is reported in ***Physica B: Physics of Condensed Matter*** *,36-40,571, (2019).*

Chapter V: Band offset studies in $Cr_2O_3/Ti_{0.02}Cr_{1.98}O_3$ bilayer film using photoelectron spectroscopy

Realization of oxide/oxide semiconductor heterostructures based high performance electronic/optoelectronic/ magneto-optical devices warrants in-depth understanding of energy band alignment at the respective interface. The important parameters needed in the design of semiconductor heterostructure are its band offset and band alignment. Knowledge of band offset gives information about the type of carriers which can be confined in the heterostructure. Here, we report energy band alignment in pulsed laser ablated $Cr_2O_3/Ti_{0.02}Cr_{1.98}O_3$ bilayer film from the information of core level energies and valence band maxima positions in the corresponding Cr_2O_3 and $Ti_{0.02}Cr_{1.98}O_3$ single layer films and their respective shifts in $Cr_2O_3/Ti_{0.02}Cr_{1.98}O_3$ bilayer film. A type II (staggered) band alignment was identified with the valence band offset and conduction band offset which equals to 1.40 eV and 1.13 eV, respectively. Thus, this investigation provides further insights into the fundamental properties of $Cr_2O_3/Ti_{0.02}Cr_{1.98}O_3$ heterojunction, which can be effectively utilized for the design, modelling and analyses of optoelectronic/magneto-optical devices.

The details of this work are published ***Physica B: Physics of Condensed Matter****, 412590 (1-6) 599, (2020).*

Chapter VI: Dispersive and absorptive optical nonlinearities in undoped and Mg doped Cr_2O_3 thin film

The need of development of modern optical technology is to monitor the intensity of light using appropriate materials that have good nonlinear optical properties. In this regard the knowledge of dispersive and absorptive optical nonlinearities of the films is important in making optical switches, thermo-optic compensator, Bragg wave detector, optical limiters, optical detectors, etc. In this chapter, our objectives were to measure nonlinear refraction and absorption coefficient using Z-scan technique in undoped and Mg doped Cr_2O_3 thin films. The present chapter also aims at overcoming the restriction of aperture size to determine optical nonlinearities in thin film sample by Z-scan transmittance. At high excitation intensity, the induced nonlinear phase shift is of complex nature and its real and imaginary part contribute to nonlinear refraction and absorption, respectively. An integral theoretical approach supported by experimental observations is developed to obtain complex nonlinear phase shift and corresponding nonlinear refractive index and absorption coefficient of undoped and Mg doped Cr_2O_3thin films by a single experimental arrangement, wherein, the aperture size can be selected as a fitting parameter. We have also analysed the effect of fifth-order optical nonlinearities and the crucial role of aperture size on the asymmetrical behaviour of the transmittance.

These results are communicated for publication.

Chapter VII: Electronic and optical studies of pulse laser deposited ZnO/NiO bilayer film

This chapter describes the structural, optical and electronic properties of polycrystalline ZnO and NiO thin films and amorphous ZnO/NiO bilayer film, prepared by pulsed laser deposition technique. Despite of the presence of both Zn and Ni in +2 state in the bilayer film, the grown bilayer shows no reflections (in XRD) corresponding to ZnO or NiO. The difference in crystal structure of ZnO and NiO leads to the strain in the grown bilayer film. An increase in the band gap has been observed in bilayer film which can be attributed to the amorphous nature of the structure.

This work is published ***Journal of Physics: Conference Series,*** *012036(1-4),755, (2016).*

Chapter VIII: Dispersive optical nonlinearities and optical path length compensation in NiO and Al doped NiO single layer and bilayer thin film

Dispersive optical nonlinearities in pulsed laser deposited undoped and 5% Al doped NiO thin films reveal negative and positive optical nonlinearities, respectively. The cause of optical nonlinearity is assigned to the presence (absence) of oxygen vacancies in undoped NiO (5% Al doped NiO) thin film which leads to photo-densification (photo-expansion) and gives rise to thermo-optic effect. Quite interestingly, the observation of opposite kinds of nonlinearities in a NiO/Al doped NiO bilayer film, leads to the neutralization of the dispersive optical nonlinearity and one expects a resultant optical path length compensation.

This work has been published in ***Optical Materials****, 109278(1-6), 96, (2019).*

Chapter IX: Magnetic and magneto-optical properties of Al doped NiO thin films

NiO is an antiferromagnetic transition metal oxide and also having the partially filled outer most d-orbitals. While doping, formation of nanoparticles and uncompensated surface spin can induce finite magnetic moment in NiO. The interaction of light with these materials is expected to cause magneto-optic Kerr effect. For this study, 5% Al doped NiO thin films were grown by PLD technique using a single phased composite target prepared by standard solid-state reaction technique. Depositions were carried out under two conditions viz; (i) in the presence of 200mTorr oxygen partial pressure (OPP) and (ii) in absence of oxygen flow. Under the growth condition of oxygen environment, Al doped NiO film exhibits mixed antiferromagnetic and ferromagnetic phase while, vacuum-deposited film shows room temperature ferromagnetism along with surface plasmon enhanced magneto-optic Kerr effect. The origin of magnetism is attributed to the oxygen vacancies in the films. Our observations of strong coupling of optical and magnetic properties and hence the improved magneto-optic Kerr effect, suggest that the vacuum-deposited film can be useful for sensitive read-out measurements.

These results are communicated for publication.

Chapter X: Conclusion and future scope

Now days, transition metal oxides have an important role in optoelectronic devices based upon the control of light by light. The knowledge of nonlinear optical parameters is a pre-requirement for making such optoelectronic devices like optical limiting and optical switching devices. Therefore, in the present thesis, we have focused our attention on the electronic and nonlinear optical properties of undoped and doped Cr_2O_3 and NiO thin films. However, transition metal oxides have an added advantage of magnetic properties arising due to partially filled d-orbitals. It is expected that the optoelectronic devices made from the transition metal oxides can be controlled by applied electric as well as magnetic field making them more suitable for advanced technological applications. The magnetic properties of Cr_2O_3 and NiO thin films are also very important and interesting, these properties can be modified by doping. Accordingly, nonlinear optical properties in the presence of applied magnetic field in these materials can open a new dimension of magneto-optic device applications.

To implement any material for device application there is a huge lacuna of their conductivity. The conductivity of the materials can be monitored with appropriate doping as well as their growth condition. In view of these, we will propose to further our research on the improvement of their conductivity along with desired optical properties.

TH-7. ELECTRONIC TRANSPORT STUDIES ON GAN EPITAXIAL LAYERS FOR THE FABRICATION OF RADIATION HARD ULTRAVIOLET PHOTODETECTORS

Abhishek Chatterjee, Raja Ramanna Center for Advance Technology*l, Indore Email: cabhishek@rrcat.gov.in*

Recent advances in nitride semiconductors have led to a significant progress in the development of GaN based numerous optoelectronic devices including light-emitting diodes, lasers and detectors [1- 4]. GaN based ultraviolet (UV) photodetectors (PDs) for light detection in the spectral range of 280 to 360 nm have found many applications including visible blind UV detection, usage in strategic sectors, UV astronomy, and medical science and also in the industry as flame detectors and solar UV monitors [4]. Due to their visible blind nature, radiation-resistance and thermal stability, these devices offer several advantages over conventional photomultiplier tubes and Si-based UV detectors [5]. A large band gap of GaN enables the operation of GaN devices under high electric field often exceeding 1 kV [6]. Further, GaN devices can withstand high temperature up to 600°C [7]. Compared to Si and GaAs-based devices, nitride devices are more radiation tolerant because of a high displacement energy. It makes GaN a suitable candidate for potential applications in the harsh environments of nuclear reactors, accelerators and spacecraft [8].

Although great achievements have been made in GaN based optoelectronic devices, there are several challenges in growing good quality GaN films. The lack of a suitable substrate for GaN is the first and foremost difficulty in growing high crystalline quality material. Among all the foreign substrates like sapphire, SiC and Silicon, Sapphire is the primary choice for growing GaN due to its availability, low cost, surface morphology and high temperature stability compared to other substrates, irrespective of having a large lattice mismatch of ~14% with GaN [9]. However, such a large lattice mismatch leads to high density of threading dislocations in epilayers usually in the range of $\sim 10^{9}$–10^{11} cm^{-2} [10]. A major consequence of this appears in terms of a large n-type conductivity of GaN epilayers due to the unintentional doping by residual impurities such as silicon and oxygen. The large dislocation density has major role on efficiency droop of near-ultraviolet micro-LEDs fabricated on GaN substrates [11]. Significant efforts have been made by many researchers for reducing the density of threading dislocations by incorporating low temperature grown buffer layers [12], SiN_x interlayer [13], substrate patterning, and innovative surface treatments of the substrate. Moreover, several kinds of point defects such as N and/or Ga vacancies, interstitial and substitutional defects are also present in GaN [14]. Although considerable progress has already been made, the realization of good rectifying contacts on GaN with reproducible junction properties is still a major technical hurdle [15]. Insertion of an insulating layer between metal and semiconductor is found to be an effective method. In this regard, significant efforts have been made by many researchers by incorporating several insulating layers, such as SiO_2, ZrO_2, GaO_x, and Al_2O_3 [16] in the architecture of a photodetector. Although, considerable amount of work is already carried out on GaN-based metal–insulator–semiconductor (MIS) PDs, a consensus among researchers is yet to arrive on the choice of material and thickness of the insulating layer. Also device fabrication with small geometry in a reproducible manner demands a good control on the procedures such as etching. Precise pattern transfer during the fabrication of optoelectronic devices therefore involves dry etching methods which require bombardment with high energy ions for breaking relatively strong Ga-N bonds [17]. Although there exist a few reports on the impact of dry etching on the optoelectronic properties of GaN, a systematic study related to the response of GaN UV photodetectors is missing [18]. This thesis deals with the fabrication of high performance GaN based UV detectors for potential application in high radiation environment. A good control on the dislocation formation during epitaxial growth and a knowledge of dislocation behavior are the two pre-requisite for optimizing the performance of a nitride device. The two issues are addressed in this thesis where 1) results from epitaxial growth of GaN are presented by highlighting the issues related to dislocation density, and 2) role of dislocations in the performance of GaN based radiation hard UV detectors is explored. In particular, results from the metal-semiconductor-metal (MSM) and metal-oxide-semiconductor (MOS) configurations of GaN photodetectors are presented, where a state-of-the-art performance of GaN based MOS devices is demonstrated. A few samples are also tested under a high dose of ^{60}Co gamma rays which proves the radiation resistant nature of indigenously developed GaN devices along with a fast self-recovery, which signifies their usefulness for possible applications in harsh radiation environment.

In the beginning, Electronic transport properties of 5 µm thick GaN/Sapphire epilayers grown by hydride vapour phase epitaxy (HVPE) and metal organic vapour phase epitaxy (MOVPE) are investigated. It is found that though the two samples possess a carrier density of ~2×10^{18} cm^{-3}, their electrical characteristics are very different. It is observed that the carrier concentration measured by Hall for HVPE grown samples is two orders larger than the value provided by C-V technique. Such a large difference in carrier concentration is associated with the formation of a degenerate layer at the layer-substrate interface, which is consisted of a large density of threading screw and edge dislocations. A two layer model is used to extract the appropriate values of carrier concentration of HVPE grown samples from Hall data [19]. It is learnt that there exists a critical thickness of HVPE GaN epilayers below which the electronic transport properties of layers grown on top of them are severely limited by the interfacial charged dislocations. On the contrary MOVPE grown samples are found to be free from such limitations, which makes them attractive for device fabrication. The understanding developed is expected to be useful in the development of GaN PDs, especially for the cases, when charge transport is severely affected by the presence of a degenerate layer at GaN/Sapphire interface and dislocations lines pierce through the Schottky junction to enable the tunneling of carriers.

With the knowledge of the electronic transport properties of GaN epilayers, the next step is to fabricate GaN MSM UV photodetectors. MSM photodetectors are made on MOVPE and HVPE GaN epilayers for comparison purpose [20]. Contrary to the general understanding, it is surprising to note that the photo response of HVPE based PDs is found to be ~3 times higher than that of the MOVPE based devices [21]. It is explained by considering the difference in the depletion width which is primarily determined by the different procedures adopted for the doping of HVPE and MOVPE GaN templates. This indicates that controlling the density of threading dislocations is not the sole criteria for improving the performance of GaN Schottky PDs, rather one also need to be careful about the density of point defects which can also marginalize the key figure-of-merits. The impact of threading dislocations and point defects on the performance of MSM UV photodetectors is carefully estimated by performing systematic electronic transport measurements. Further, to improve the device performance by including an oxide layer in the device architecture, GaN based MOS photodetectors are fabricated. A thin layer of ZrO_2 (SiO_2) is inserted between the metal and the semiconductor to obtain Au/Ni/ZrO_2 (SiO_2)/GaN MOS PD structure. It is observed that the leakage current reduces drastically by 28 (8) times due to insertion of ZrO_2 (SiO_2) leading to a considerable improvement in the photo responsivity. The oxide passivated samples show a relatively flat response in shorter wavelength side due to a suppressed surface recombination of photo generated carriers. Moreover, at an optimum ZrO_2 thickness of 3 nm, a high photo responsivity of 27 A/W is achieved along with the fast response of the device with a rise (fall) time of 28 ms (178 ms), respectively. It is also found that the thickness of ZrO_2 layer plays a critical role in controlling the photo-response and transient response of the devices. However, beyond an optimum thickness of oxide interlayer, the device response slows down along with a reduction in responsivity which is mainly governed by the impediment of hole tunneling across the oxide layer. It is worth to note that the detectivity of PDs with optimized thickness of ZrO_2 interlayer is found to be similar or better than the recently reported state-of-the-art values for visible blind UV GaN PDs with similar dark current [22].

Fabrication of an optoelectronic device with smaller geometry requires precise pattern transfer which can be achieved by photolithography and selective spatial etching of the material. In case of GaN, reactive ion etching (RIE) is a preferred method since wet chemical etchants are not available. However, during this process, several kinds of plasma-induced damages can lead to the creation of lattice defects and dislocations, ion implantation or formation of dangling bonds on the surface [23]. Impact of RIE induced damage on the optoelectronic properties of GaN epilayers and also on the photoresponse of Schottky PDs is investigated further. The observation of surface morphology of GaN epilayers post RIE confirms a large degradation with increasing energy of the reactive ion beam. More than 70% reduction in the intensity of near band edge photoluminescence peak is observed after 250W RF BCl_3 plasma etching which along with the etch insensitive yellow luminescence band suggests that etch induced non-radiative centres are located rather close to the surface. The peak spectral response of PDs also shows up to 90% reduction post plasma etching. A

method for the recovery of plasma etch induced damage by O_2 plasma treatment is also demonstrated. A substantial recovery of the spectral and transient response along with an improved deep UV response of the PDs is achieved through O_2 plasma treatment.

After applying various methods for improving the performance of GaN UV PDs, the next objective is to test the performance of devices under high radiation environment. Here, the effect of ^{60}Co gamma irradiation on the electronic transport properties of highly doped n-type GaN epilayers and Schottky PDs is studied [24]. A steady rise of carrier concentration with increasing irradiation dose is observed. The bulk carrier concentration is fitted by using the charge balance equation which indicates that no new electrically active defects are generated by gamma radiation even at 500 kGy dose. The irradiation induced rise of carrier concentration is attributed to the activation of native Si impurities that are already present in an electrically inert form in the pristine sample. This observation is found to be unique, especially for highly conducting samples. It is also seen that the irradiation induced nitrogen vacancies stimulate the diffusion of oxygen impurities, leading to the observed increase of the interfacial carrier concentration.

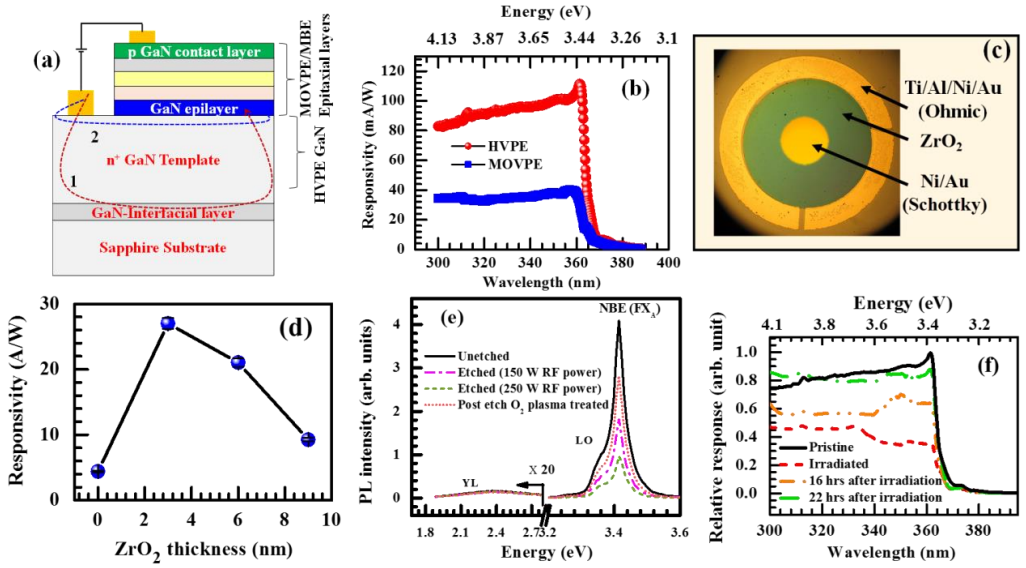

Figure 1 (a) Schematic layer structure of a nitride device grown on top of HVPE GaN templates where the conduction paths 1 and 2 describe the dislocation limited and usual current transport, respectively, (b) Room temperature spectral response of GaN MSM PDs (c) Optical microscopic image of the device with oxide inter-layer, (d) Spectral response of GaN PDs without and with different thickness of ZrO_2 layer (e) Room temperature photoluminescence spectra of GaN epilayers before and after etching with different RF power (f) Photo response of GaN Schottky photo detector after irradiation with ^{60}Co γ source.

Further, the leakage current of GaN PDs is compared with that of GaAs which clearly demonstrates a high radiation resistance of GaN. A fast self-recovery of the device response within a day after irradiation is also demonstrated, which signifies the compatibility of devices for operation in high radiation zones.

In conclusion, in-depth electronic transport measurements are performed on commercially available MOVPE and HVPE grown GaN samples. Presence of a highly conducting interfacial layer is observed in HVPE GaN epilayers. On the other hand, MOVPE GaN epilayers are found to be free from this limitation which makes them attractive for the device development. MSM PDs are thereafter made on both the samples where the performance of devices made on HVPE GaN turns out to be better, which is rather surprising. It is explained by citing the difference in the doping method of GaN layers in the two samples. A method to enhance the detector performance is demonstrated by the insertion of a thin layer of ZrO_2 forming GaN MOS PDs. The role of ZrO_2 layer thickness is found to be rather critical where specific

detectivity of the devices is found to be similar or better than the state-of-the-art values reported in literature. Further, the role of RIE in the fabrication of smaller devices is discussed where a method to recover the RIE induce damage is demonstrated by using post etch O_2 plasma treatment. Finally, the detectors are tested under a high dose of gamma irradiation where a fast self-recovery of the spectral response signifies their usefulness for possible applications in radiation environment.

In future, the understanding developed in this thesis is useful for the development of GaN based radiation hard ultraviolet photodetectors. A comparisons of the spectral and transient response of PDs fabricated on GaN templates will help the device manufacturers in making a judicious choice for specific applications. Also the effect of dislocation density on efficiency droop on GaN based micro-LEDs need to be investigated.

1. S. Nakamura, S. Masayuki, M. Takashi, Jap. J. Appl. Phys. 32 (1993) L8.
2. S. Li, A. Waag, J. Appl. Phys. 111 (2012) 071101.
3. S.P. DenBaars, D. Feezell, K. Kelchner, S. Pimputkar, C.-C. Pan, C.-C. Yen, S. Tanaka, Y. Zhao, N. Pfaff, R. Farrell, M. Iza, S. Keller, U. Mishra, J.S. Speck, S. Nakamura, Acta Materialia, 61 (2013) 945-951.
4. S. J. Pearton, J. C. Zolper, R. J. Shul, F. Ren, J. Appl. Phys. **86** 1 (1999)
5. M. Brendel, M. Helbling, A. Knigge, F. Brunner, and M. Weyers, J. Appl. Phys. **118** 244504 (2015)
6. B. J. Baliga, Semiconductor Science and Technology **28** 074011 (2013)
7. A. Suria , A. Yalamrthy, T. Heuser, A. Bruech, H. So and D. Senesky Appl. Phys. Lett. **110**, 253505 (2017)
8. J. Grant, W. Cunngham, A. Blue, V. Shea, J. Vaitkus, M. Rahman Nucl. Instr. and Meth. A 546 213 (2005)
9. S. Nakamura and M. R. Krames, Proc. IEEE **101**, 2211 (2013)
10. Abhishek Chatterjee, V. K. Agnihotri, R. Kumar, S. Porwal, A. Khakha, Jayaprakash G., Tapas Ganguli and T. K. Sharma, Sadhana, 45, 249 (2020).
11. C. C. Li, J. L. Zhan, Z. Z. Chen, F. Jiao, Y. F. Chen, Y. Y. Chen, J. X. Nie, X. N. Kang, S. F. Li, Q. Wang, G. Y. Zhang, B. Shen, Optics Express 27, A1146 (2019)
12. H. Amano, N. Sawaki, I. Akasaki, and Y. Toyoda, Appl. Phys. Lett. **48**, 353 (1986)
13. Z. Huang, Y. Zhang, G. Deng, B. Li, S. Cui, H. Liang, Y. Chang, J. Song, B. Zhang, G. Du J Mater Sci: Mater Electron **27** 10003 (2016)
14. M. A. Reshchikov and H. J. Morkoc, Appl. Phys. **97** 061301 (2005)
15. R. T. Tung, Mater. Sci. Eng., R **35**, 1 (2001)
16. X. Sun, D. Li, H. Jiang, Z. Li, H. Song, Y. Chen, G. Miao Appl. Phys. Lett. **98**, 121117 (2011)
17. J. I. Pankove, J. Electrochem. Soc. **119**, 1118 (1972)
18. G. Lukens, H. Yacoub, H. Kalisch, and A. Vescan, J. Appl. Phys. 119, 205705 (2016)
19. Abhishek Chatterjee, S. K. Khamari, R. Kumar, V. K. Dixit, S. M. Oak, and T. K. Sharma, Appl. Phys. Lett., 106, 023509 (2015).
20. Abhishek Chatterjee, S. K. Khamari, V. K. Dixit, S. M. Oak, and T. K. Sharma, J. Appl. Phys., 118, 175703 (2015).
21. Abhishek Chatterjee, S. K. Khamari, R. Kumar, S. Porwal, A. Bose and T. K. Sharma, Superlattices and Microstructures, 148, 106733 (2020).
22. Abhishek Chatterjee, S. K. Khamari, S. Porwal, and T. K. Sharma, Physica Status Solidi: Rapid Research Letters, 3, 1900265 (2019).
23. Abhishek Chatterjee, V. K. Agnihotri, S. K. Khamari, S. Porwal, A. Bose, S.C. Joshi and T. K. Sharma, J. Appl. Phys., 124, 104504 (2018).
24. Abhishek Chatterjee, S. K. Khamari, S. Porwal, S. Kher, and T. K. Sharma, J. Appl. Phys. 123, 161585 (2018).

TH-8. TOWARDS DEVELOPMENT OF NEW GENERATION SPIN-ORBIT PHOTONIC TECHNIQUES IN OBSERVATIONAL ASTRONOMY

Athira B S CESSI, IISER Kolkata, Email: abs16rs013@iiserkol.ac.in

Objects in the universe emit electromagnetic radiation at different wavelength depending upon the composition, density, temperature and environments. Radiation with wavelengths between roughly 400 nm and 700 nm is called visible light because these are the waves that humans can perceive with one of the five senses, vision. The amount of radiation from the sky as a function of time, wavelength, direction and polarization is the fundamental measurement, an astronomer makes. Bartholin Erasmus and Étienne Malus are credited for the early days of polarimetry. But, the first polarimeter was built by Jean-François Dominique Arago in 1811 and was used for measuring the polarization of the Sun light reflected from the Moon. It is to note that his polarimeter already used the basic principle of all good polarimeters in astronomy today. Along with the requirement of developing new polarimetry techniques and analysis schemes for probing the dynamics in the astrophysical domain where high cadence and high precision measurement of spatial polarizations are desirable, there is a need to amplify the polarization signal to overcome the detection limit, especially when the incoming photon count is less. Weak measurement is one tool which can amplify tiny effects up to several orders of magnitude under some special cases. The weak measurement process involves preparation of the system state in a definite initial (pre-) state, which due to weak coupling to the observable results in a superposition of "slightly" shifted eigenstates and subsequent post- selection in a final (post-) state which is nearly orthogonal to the initial state. The outcome of a pre- and post- selected weak measurement is weak value and the scheme is called weak value amplification.

It is well known that light (photon) carries angular momentum, spin angular momentum (SAM) is associated with polarization and orbital angular momentum (OAM) is associated with phase of wavefront. A circularly polarized beam, with rotating electric and magnetic fields, carries SAM. Light, being an electromagnetic wave, consists of orthogonal electric and magnetic fields that oscillate, coupled to each other. The azimuthal phase dependence is physically manifested as helical phase fronts. For a light beam carrying OAM *l* (topological charge), the beam will have *l* intertwined helical phase fronts. Similar to circularly polarized light, the sign of OAM indicates the handedness of its helicity with respect to the beam direction. A characteristic of helical beams is the phase singularity on the beam axis, which makes the intensity on the axis zero, often referred to as an optical vortex. Light, on propagation, acquires a phase due to its optical path length. This is termed as the dynamical phase, which is the cause of most of the observable interference effects. On the other hand, the geometric phase is independent of the optical path length. It is solely determined by the topology of evolution of the light beam. This phase is directly related to the change in the polarization state of an electromagnetic wave when it evolves in an inhomogeneous isotropic or anisotropic medium. Geometric phase is of two types: (i) Spin-redirection Berry Phase: This is the phase that originates from parallel transport of the electric field when the direction of wave propagation varies continuously. (ii) Pancharatnam-Berry (PB) Phase: This originates for a wave which propagates in a fixed direction (constant *k* vector), but subject to a continuous change in the polarization state. The spin and the orbital degrees of freedom of light can get coupled under certain circumstances leading to interesting consequences like spin orbit interaction (SOI). Thus, knowledge on SOI is crucial for both fundamental understanding of the interactions and for optimizing experimental parameters for practical applications in diverse systems such as biological systems, complex materials apart from astronomy. Observations suggest the existence of inhomogeneities in the interstellar medium. Martin Harwit in 2003 has described several astrophysical processes that generate OAM, light scattering in the interstellar medium, rotating black holes etc. In astrophysical domain, solar coronal magnetic field measurement is one such example wherein the time scale of various dynamic processes such as eruptions are of the order of several seconds. Also, the

circular polarization signal which determines the strength of coronal magnetic field is weak (10^{-4}) to estimate. Therefore, it is main objective of the present thesis to explore SOI and to develop novel spin orbit photonic techniques in observational solar astronomy unlike traditional differential photometric measurements. The techniques included in the thesis are not only limited to its application to solar astronomy but also to other fields such as biomedical imaging, nanophotonics, etc.

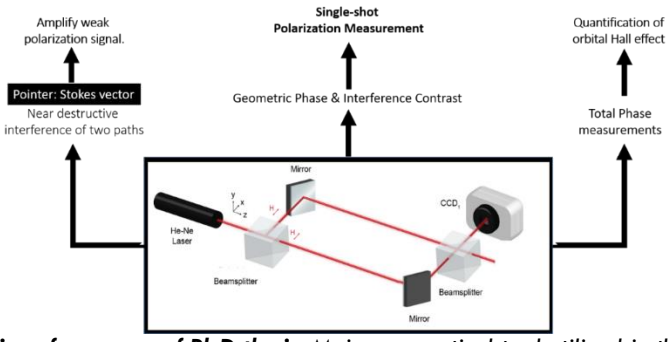

Figure 1: Pictorial representation of summary of Ph.D thesis. *Main core optical tool utilized in the thesis is Mach-Zehnder interferometer.*

The broad objectives of the thesis work are as follows:

1. Single-shot measurement of space varying polarization state of light.
2. Amplification of small polarization signals which cannot be detected by the traditional polarization measuring instruments by employing weak measurement protocol.
3. Understanding the orbit-orbit interaction of light leading to the first experimental observation of orbital Hall effect of light for randomly and radially polarized light.
4. Prediction of global polarization map of solar corona with the knowledge of three-dimensional magnetic field of solar corona.

1. Single-shot measurement of polarization.

Light beam carrying spatially varying state of polarization generates one variant of the geometric phase, space varying PB geometric phase, while propagating through homogeneous anisotropic medium. We show that determination of such space varying geometric phase provides a unique way to quantify the space varying polarization state of light using a single-shot interferometric measurement. We demonstrate this concept in a Mach-Zehnder interferometric arrangement using a linearly polarized reference light beam, where full information on the spatially varying polarization state is successfully recovered by quantifying the space varying geometric phase and the contrast of interference. Figure 2 summarizes the results obtained with the technique.

Weak value amplification (WVA) can also be interpreted as near destructive interference between the eigenstates of the measuring observable as a consequence of nearly mutually orthogonal pre and post selections of the system states. Experimentally we demonstrate this concept that uses near destructive interference of two paths of an interferometer having slightly rotated linear polarization states of light (playing the role of weak interaction). Real and imaginary WVAs of extremely small polarization rotation effect is obtained using small amplitude and phase offsets of the waves in near destructive interference, respectively. The corresponding WVAs are manifested in the polarization state pointer profile, leading to large rotation of the polarization vector orientation angle and large changes in the circular (elliptical) polarization descriptor Stokes vector element of light respectively. Figure 3 summarizes the results obtained with the technique

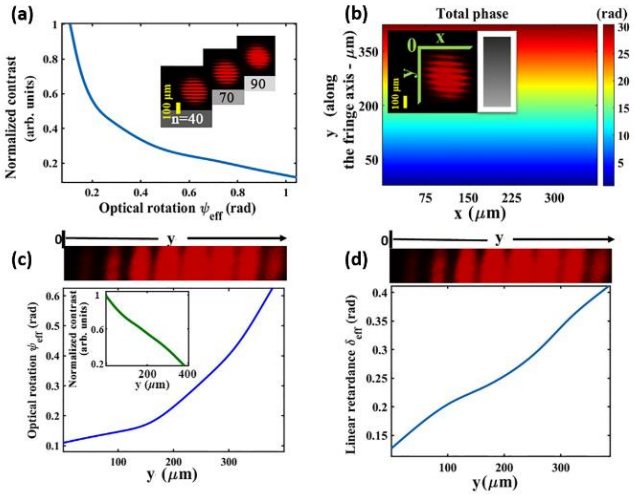

Figure 2. *(a) The calibration curve which shows the dependence of the contrast of interference on varying optical rotation parameter of the SLM obtained for different sets of homogeneously polarized beam. The inset shows the corresponding interference patterns. (b) The total phase (dynamical + PB geometric) extracted from the interference fringe (shown in the inset). (c) The spatial variation of optical rotation derived from the spatially varying contrast (corresponding to the fringe shown in the top panel) when spatially varying polarized beam is used. The inset shows the corresponding spatial dependence of the contrast. (d) The derived spatial variation of the linear retardance parameter of the SLM for the spatially varying polarized beam.*

2. Interferometric weak value amplification of weak polarization signal.

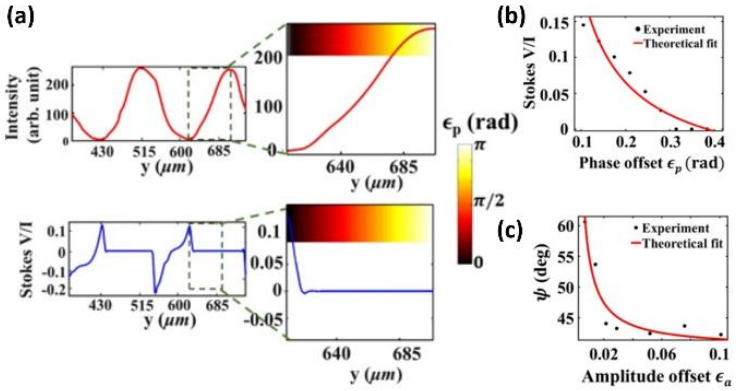

Figure 3. *(a) The spatial variation of the intensity of obtained interference fringe and the corresponding Stokes vector element. The magnified views of the variations around the position of the intensity minima (destructive interference with phase difference π) are shown along with the phase offset from π, ϵ_p (shown by the color bar). (b) The corresponding variation of V/I with ϵ_p and theoretical fit (red line). (c) The results of real weak value amplification and theoretical fit (red line). The variation of the polarization vector orientation angle as a function of the amplitude offset parameter ϵ_a recorded at the spatial position of intensity minima corresponding to the destructive interference.*

.

3. Experimental observation of orbital Hall Effect of light.

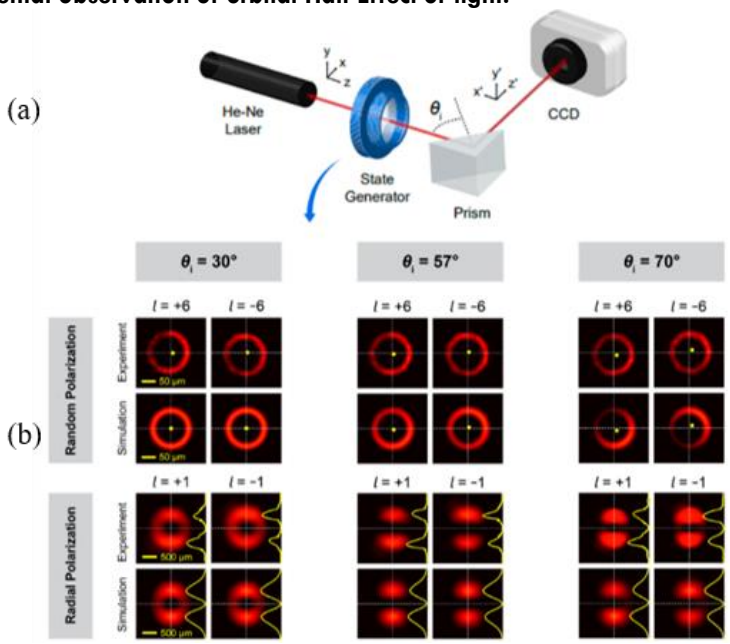

Figure 4: *(a) Experimental setup to observe polarization-independent vortex-induced beam shifts. (b) Experimentally observed shifts for a randomly and radially polarized LG beam and the corresponding numerically simulated profiles. The yellow dot indicates the center of gravity of the intensity distributions and yellow solid lines indicate the line profiles along the vertical axes of the lobes.*

An important manifestation of spin-orbit interaction of light is photonic spin Hall effect, elucidated as spin to extrinsic OAM conversion which arises due to symmetry breaking. This is interpreted using the balance and conservation of the total angular momentum, the sum of SAM and the extrinsic OAM. In an analogous manner, the coupling between the intrinsic OAM and the extrinsic OAM of light beam gives rise to the orbit-orbit interaction which results in the orbital Hall effect of light. In this scenario, intrinsic OAM carrying vortex beams exhibit opposite shifts of the beam trajectory depending upon the opposite (positive or negative) topological charge of the optical beam. We demonstrate this extraordinary effect in partial reflection of randomly and radially polarized vortex beams carrying intrinsic OAM but with no net SAM of light beam, and the effect is manifested as spectacular shifts of the beam trajectory depending upon the input OAM state of the light beam. Figure 4 summarizes the experimental observations.

4. Prediction of solar coronal polarization.

Magnetic field structure in the solar corona is primarily governed by the photospheric magnetic field distributed at the bottom boundary of the corona. We predicted the large-scale coronal magnetic field structures during 2019 July 2 solar eclipse by applying the potential field source surface, extrapolation technique on the predicted surface magnetic field distribution generated from the newly developed data-driven surface flux transport model. We also forward model the polarization characteristics of the coronal emission. To generate he synthetic Stokes data we utilize the FORWARD tool set using a spherically symmetric hydrostatic temperature and density profile weighted differently to open and closed field lines for the background corona which is incorporated using the TOPOLOGY module. FORWARD uses the Coronal Line Emission polarimetry code developed by Judge & Casini (2001) to synthesize Stokes line profiles. Our prediction of two large-scale streamer structures and their locations on the east and west limbs

of the Sun match eclipse observations reasonably well. Figure 5 shows the prediction and observation of the eclipse

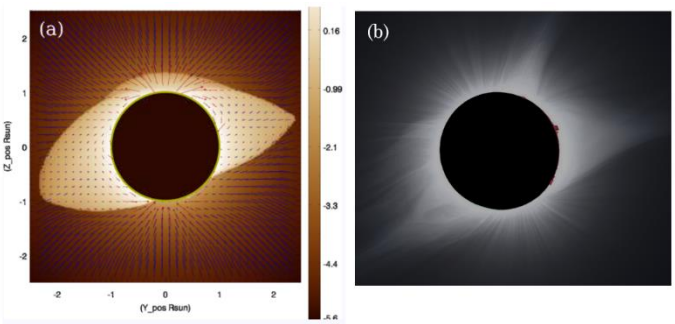

Figure 5: *(a) Predicted plane of sky magnetic field vectors (red arrows) and linear polarization vectors (blue lines) with polarization brightness in the background (b) Observed polarization brightness during full solar eclipse.*

The thesis concludes with an outlook on the prospects of spin orbit interaction techniques and optical weak measurements towards practical applications. With the developed laboratory module of interferometry technique to recover unknown space varying polarization and amplifying the small ellipticity and rotation, the next phase is to install it to a telescope which observes the solar corona and tests the performance of the novel instrument. Since the approach is based on geometric phase, an effort has been put towards the studies on metasurface which will generate OAM carrying beams upon circular polarized light incident on it. The new direction is towards the development of tunable OAM generating metasurface by tuning the input polarization. The system may be explored to develop a PB phase controlled high contrast imaging system in the telescopes. The techniques included in the thesis are not only limited to its application to astronomy but also to other fields such as biomedical imaging, nano photonics, etc.

References

1. B S. Athira, M. Pal, S. Mukherjee, J. Mishra, D. Nandy and N. Ghosh, *Phys. Rev. A*, **101** (1), 2020.
2. S. Guchhait, B S. Athira, N. Modak, J K. Nayak, A. Panda, M. Pal and N. Ghosh, *Sci. Rep*, **10 (1)**, 2020.
3. S. Dash, P. Bhowmik, B S. Athira, N. Ghosh and D Nandy, *Astrophys. J*, **890** (37), 2020.
4. B S. Athira, S. Mukherjee, A. Laha, K. Bar, D. Nandy and N. Ghosh, *JOSA B*, **38** (7), 2021.
5. N. Modak, A K. Singh, S. Guchhait, B S. Athira, M. Pal and N. Ghosh, *Current Nanomaterials*, **5** (1), 2020.
6. N. Modak, B S. Athira, A K. Singh and N. Ghosh, *Phys. Rev. A*, **103** (5), 2021.
7. M. Pal, S. Saha, B S. Athira, S D. Gupta and N. Ghosh, *Phys. Rev. A*, **99** (3), 2019.

TH-9. HIGH-HARMONIC SPECTROSCOPY OF TWO-DIMENSIONAL MATERIAL

Mrudul M S, *Indian Institute of Technology, Mumbai, Email:* mrudul@iitb.ac.in

Ultrafast science is a branch of physics that deals with the characterisation and applications of laser pulses shorter than picoseconds (1 ps = 10^{-12} s). Following the inverse relation of peak power and pulse duration of laser pulses, ultrafast pulses can trigger and probe ultrafast electron in matter. The induced dynamics can be perturbative or non-perturbative in nature. Needless to say, there are interesting processes to explore in the non-perturbative regime of light-matter interaction. For example, intense femtosecond pulses are used to probe molecular dynamics on femtosecond timescale (1 fs = 10^{-15} s). Moreover, attosecond pulses are required

to probe ultrafast electron dynamics on its characteristic timescale, attosecond (1 as = 10^{-18} s). High-harmonic generation (HHG) is one of the practical ways to generate attosecond pulses. HHG is a highly nonlinear up-conversion process in which higher-order harmonics of the incident photon energy are generated during intense laser-matter interaction. Figure 1 presents a typical HHG spectrum. Presence of the plateau regime in Fig. 1 is a signature of the non-perturbative interaction of laser with matter. Inert gases were used to observe HHG in 1988. Paul Corkum proposed a semiclassical three-step model to explain the mechanism of HHG. According to the three-step model, a bound electron can tunnel ionise through the barrier, lowered under the influence of an intense laser field during the first step. The tunnel-ionised freed electron can accelerate in the presence of laser field and recollides with the parent ion when the direction of the laser field changes as the third step. As a result of recollision, a photon is emitted with an energy equal to the total energy of the recombining electron.

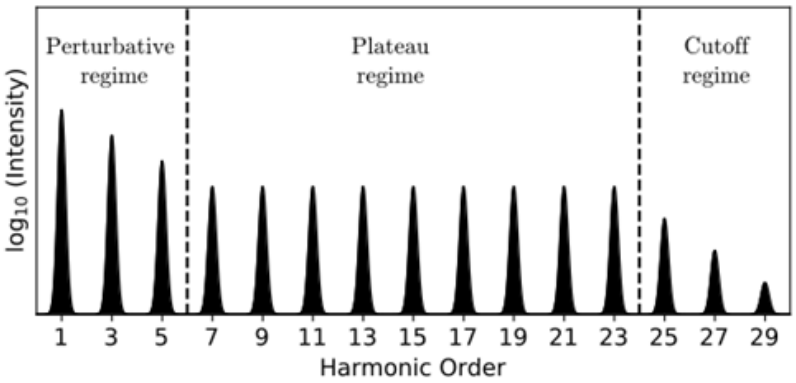

Fig. 1: A typical HHG-spectrum

Recent developments in mid-infrared and terahertz laser sources have enabled scientists to observe HHG from semiconductors, dielectrics and semimetals. The characteristic spectrum of high harmonics from solids is drastically different from the one shown in Fig. 1 for the gaseous atom. The HHG spectrum of solids consists of multiple plateaus, and the cutoff energy depends linearly on the laser amplitude. These observations signify a different underlying mechanism of HHG from solids. In recent years, HHG from solids has been employed to probe quantum phase transitions, dynamical Bloch oscillations, band-structure tomography, and the realisation of petahertz currents in solids. Undoubtedly, HHG is an emerging method to explore static and dynamical properties of solids.

To describe the electron dynamics in the presence of a strong laser-field, time-dependent Schrödinger equation (TDSE) is solved. For this purpose, the usual perturbative treatment of light-matter interaction is not appropriate. Thus, we rely on methods to real-time propagate TDSE and obtain time-dependent wave function. The relevant physical quantity to simulate the HHG spectrum is the acceleration of electrons in the presence of the laser field. For solids, this quantity can be obtained as the time-derivative of the total current. The Fourier transform of the electron acceleration provides the high-harmonic spectrum.

Unlike atoms, the HHG spectrum has a direct correlation with the energy band structure in solids, which is evident even for a one-dimensional periodic model potential. The harmonic spectrum has multiple plateaus and well-defined cutoff energy. The cutoff energy has a direct correlation with the bandgap energies between different pairs of energy bands. This indicates that an important contribution to HHG is stemming from the time-varying interband polarisation. Moreover, electrons in the conduction bands and holes in the valence band accelerate within their respective bands in the presence of laser, leading to the intraband current. Therefore, the total current is generated by the strong interplay of interband and intraband contributions.

In addition to the recollision picture in reciprocal space, we have found numerical evidence of the recollision in the real-space as presented in our work in Ref. [4]. The signature of the structural minima for a bichromatic potential is observed, which resembles to the Cohen-Fano interference observed in diatomic molecules. With these reciprocal and real space perspectives, let us analyse how these methods can be extended to realistic solids.
In this thesis, we employ two different numerical methods. Firstly, we solve Semiconductor Bloch Equations (SBE), in which TDSE for a single-active electron is solved within the Houston basis. This approach also enables us to separate interband and intraband contributions. The matrix elements for any real materials can be obtained either from ab-initio or tight-binding methods. We have also performed a full quantum mechanical calculation in the framework of time-dependent density functional theory (TDDFT), as implemented in the Octopus package. This approach is computationally expensive yet helps us understand the role of electron-electron interaction in ultrafast electron dynamics.

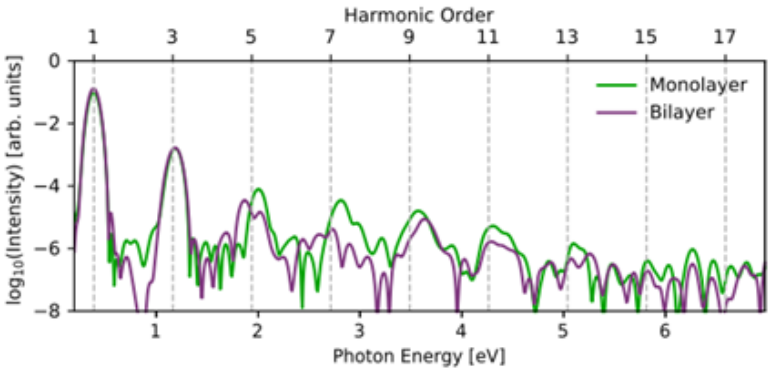

ig. 2: HHG-spectrum of monolayer and AB-stacked bilayer graphene

Graphene is the first realised 2D material, which has revolutionised science and technology over the years. The band structure of graphene is fascinating with zero bandgap and linear dispersion, arising from its inversion and time-reversal symmetries. Moreover, electrons near the K-points follow the Dirac equation and are known as massless Dirac fermions. Due to all of these exceptional properties, electron dynamics in graphene is distinct in comparison to its bulk counterpart. Carbon atoms are arranged in a honeycomb lattice in graphene. Few-layer graphene, obtained by stacking monolayer graphene, also has exceptional transport and optical properties.
In this thesis, we study how the electron dynamics in semimetals like monolayer and bilayer graphene are different. We consider both AA and AB stacked bilayer graphene. The ground state of graphene is obtained from tight-binding calculations, and time-dependent properties are obtained by solving SBE.
Due to similar band-structure and interband coupling, the spectrum of AA-stacked bilayer graphene and monolayer graphene are comparable. However, the harmonic spectrum for monolayer and AB-stacked bilayer graphene are considerably different. As a result of inversion symmetry, only odd harmonics are present in both materials. Also, due to the vanishing bandgap, interband and intraband contributions are comparable for monolayer and bilayer graphene. The difference in the harmonic spectrum in Fig. 3 is due to the interlayer coupling. Furthermore, different harmonics are affected differently by the interlayer coupling, and the dependence is highly nonlinear.
The polarisation-direction dependence in monolayer graphene shows that the real-space symmetry is imprinted in the harmonic spectrum. Moreover, both monolayer and bilayer graphene shows anomalous driver-ellipticity dependence. The harmonic yield is maximum for

a finite value of ellipticity. This further asserts the correlation of this effect with the semimetallic nature. We also show this effect is emerging from the interband contribution.

Another interesting class of 2D materials is gapped graphene. A finite bandgap in monolayer graphene can be introduced by growing it on SiO_2 substrate. Materials such as transition metal dichalcogenides, hexagonal boron nitride, etc., can be treated as gapped graphene. Theoretically, gapped graphene can be modelled, within the tight-binding framework, by imposing different onsite energies at A and B sublattices in graphene. Consequently, gapped graphene lack inversion symmetry.

As a result of broken inversion symmetry, even harmonics are present in gapped graphene, and the direction of even harmonics depends on the direction of laser polarisation. The observed selection rules for even harmonics can be explained using group theory. The presence of even harmonics, polarised perpendicular to the laser polarisation, is the signature of non-vanishing Berry curvature in gapped graphene. The driver-ellipticity dependence of gapped graphene follows atomic-like behaviour, unlike the anomalous dependence observed in gapless graphene. This shows how the electron dynamics in semimetal and semiconductor are distinct.

Electrons in hexagonal 2D materials have an additional degree of freedom, the valley-pseudospin, associated with populating two inequivalent conduction band minima in the reciprocal space. In gapped graphene materials, valley-selective excitations can be performed using a circularly polarised light resonant with the material's bandgap. The helicity of the exciting light determines the valley to be excited. This valley-control of electron-excitations, known as valleytronics, and has potential applications in quantum information technology.

In contrast to other 2D materials, the conventional technique of valleytronics is not applicable to graphene due to its vanishing bandgap and Berry curvature. In this thesis, we propose a complete recipe for light-induced valleytronics in graphene. This comprises methods for writing and reading valley-selective excitation in graphene. We use a superposition of two counter-rotating circularly polarised pulses of frequencies ω and 2ω . The resultant field has a trefoil profile. The relative orientation of the trefoil can be controlled by the relative phase, φ.

How the presence of a bicircular field breaks the inversion symmetry of graphene in real space. In the complementary reciprocal-space picture, electron momentum follows $\mathbf{k}(t) = \mathbf{k}_i + \mathbf{A}(t)$, where $\mathbf{A}(t)$ is the vector potential of the laser field.

Most of the electron's excitation takes place near the **K**-points. The energy landscape around two **K**-points are isotropic close to these points. As we move away from **K**-points, the energy landscape of nearby **K**-points are related by mirror symmetry. For a particular value of φ, vector potential matches one of the valleys, not the other -- this results in completely different dynamics in two valleys and thus different electron excitations.

Valley-asymmetry close to 40% can be achieved using an intense pulse of wavelength 6 μm. It is also exciting to see that the valley-polarisation is modulated as a function of φ. Furthermore, a significant valley-polarisation is achieved only when an electron traverses the anisotropic part of the reciprocal space; thus, valley-polarisation is absent below a certain threshold of the laser field.

The harmonic spectrum generated by the bicircular field contains $(3n \pm 1)\,\omega$ circular harmonics with opposite helicity, consistent with its selection rules. Interestingly, not only the conduction band population but the generated harmonics are also valley-polarised. This is the result of different electron dynamics in two valleys under the bicircular field.

Finally, a method is proposed for measuring valley-polarisation using a probe pulse of frequency 3ω. The frequency of the probe pulse is chosen for a background-free measurement, as $3n\omega$ harmonics are absent in the harmonic spectrum. As a result of the inversion symmetry breaking, we get even harmonics from the probe pulse. Here, valley polarisation is imprinted in the phase of these even harmonics. This phase can be measured by interfering the signal with the reference second harmonic of 3ω generated, e.g., from a beta barium borate crystal.

Defects are unavoidable in materials due to the growth process. The macroscopic modifications due to defects have significant implications in materials' macroscopic properties. Defects in materials can be classified as vacancies, impurities, interstitials, dislocations, etc. Here, we explore how spin-polarised vacancy defects play a vital role in strong-field driven electron dynamics. We consider monolayer hexagonal boron nitride (h-BN) for this study. This material falls within the class of gapped graphene, whereas nearby atoms are replaced with boron and nitrogen. Here, we use TDDFT to analyse both effects of defects and electron-electron interaction. h-BN is a wide bandgap semiconductor with a theoretical bandgap of 4.7 eV.
HHG from pristine and boron-vacant h-BN (V_B) is different in two regions, below the bandgap and near the energy cutoff. In the below bandgap regime, the intensity of the harmonics is enhanced for the defected material. This effect is found to be spin-dependent and most of the contribution is originating from the spin-down channel.
On close inspection of the effective band structure of V_B, we note that the in-gap defect states are the source for spin-polarised contributions. There is one defect state from spin-up and two from spin-down defect channels present within the bandgap. These defect states allow enhanced interband transitions in the below bandgap regime, resulting in strengthening the harmonics. Due to the spin-polarised nature of the band-structure in this energy regime, the contributions from spin up and spin down channels are different.
On the other hand, the harmonics near cutoff is found to be suppressed and spin-independent. A careful investigation reveals that electron-electron interaction is responsible for the suppression near cutoff. For pristine material, electron-electron interaction does not play any significant role for a laser with in-plane polarisation. In contrast, when there is a defect state, electrons are excited to the localised defect wavefunctions. These induced charges act as a local oscillating dipole in the presence of the external field. The corresponding induced local electric field screens the external field. This effect is called the local field effects, responsible for the role of electron-electron interaction in a defected material.

TH-10. FEMTOSECOND PULSE PROPAGATION IN AIR TOWARDS FILAMENTATION NONLINEAR OPTICS

Samuel Anurag Nalam, ACRHEM *University of Hyderabad Telangana, India-500046, Email: samuel.anurag@uohyd.ac.in*

Long range propagation of fs pulses in atmosphere leading to filamentation first demonstrated by Braun et. al. in 1995, has found applications in groundbreaking directions paving the way for accessing novel regions which were inaccessible earlier. Filamentation termed as “collapsing light”, “light bullets” has opened up surrealistic advances such as Filament induced Atmospheric monitoring, Filament assisted population inversion and lasing in air, Filament assisted precipitation, lightning discharge control and attosecond pulse generation to name a few. Plasma build up and intensity dependant refractive index which come about only at high intensities lead to a dynamic interplay of focusing and defocusing effects enabling the long range propagation which is home to many other higher order phenomena like Supercntinuum Generation (SCG), Higher Harmonic generation and mechanical waves. Although the highly dynamic and intense nature of filamentation is the primary reason for finding broad application and interest, it also makes characterization a challenge. We have explored multiple invasive and non-invasive chracterization techniques and further applied them to optimize and control filament dynamics. The generation, characterization and applications of femtosecond filamentation studied from different approaches is discussed. These characteristics were used to control and enhance the understanding into filament-matter interaction.
Filament Characteristics and emissions need to be understood under the influence of the multiple effects and distortions that a femtosecond pulse undergoes. Keeping this in mind we have studied the filament characteristics and emissions under four different configurations to correlate input laser pulse modifications to filament behaviour. The various configurations vary

a single input pulse characteristic while keeping the other properties constant. In the first configuration we have seen the effect of input pulse energy and focal length and identified loose and tight focused regimes of filamentation. In the second configuration we have identified different aberrations that are induced by focusing elements on the input laser pulse and observed the corresponding filament structure, emissions, intensity and electron density. The study showed drastic changes in filament structure under the same focusing geometry, but varying aberrations. This study helped us choose the right optics according to the desired application and study using femtosecond pulses. In the third configuration, the temporal profile of the pulse was modified by inducing a known amount of chirp to the frequency distribution in the pulse. Filament behaviour under varying pulse duration and chirp was also done under tight and loose focusing geometry. The filament onset, length and intensity can be tuned using this chirp tuning. In the fourth configuration, the effect of lens tilt on filamentation was explored and the modifications in the wavefront due to tilting of lens was found to create elongation of the filament leading to filament splitting. Tilting of the lens under tight focusing geometries causes interaction of two filaments generated from the same lens in a particular range of angles, which causes a sudden plasma build up with increase in filament spatial extent. By using optimal lend tilt, Supercontinuum can be largely suppressed when fluorescence studies are to be done.

Figure 13. : Images of the filaments imaged using the DSLR Nikon t4i camera. Exposure and gain was adjusted to capture complete spatial extent of the filaments generated using the lens with focal length=50mm, 150mm, 300mm, 500mm, 1000mm and 2000mm.

Among the third orer processes that come about during filamentation kerr self focusing was studied, but we also observe self-phase modulation and third hamonic generation (THG) in the form of supercontinuum generation and UV respectively. We have systematically correlated the THG and SCG emission from filaments generated under different focusing conditions while varying power, Chirp and polarization. The results not only show large correlation but also provide insight into the various competing mechanisms during filamentation and provide knowledge of the filament structure. Change in the SCG and THG with input pulse properties like pulse energy, focusing geometry, polarization, chirp and lens tilt reveal energy exchange between the underlying processes that facilitate these emissions like Third harmonic generation and self-phase modulation. This work not only shows the large susceptibility of filaments to the input pulse characteristics but also provides a strong tool for remote sensing and detection using Filament generated UV and Continuum for LIDAR applications. Moreover filamentation induced THG shows its sensitivity towards the phase matching conditions which exist in the highly dynamic filamentation process which are repeated from pulse to pulse and consequently influence SCG which although does not require phase matching is also found to be susceptible to input laser conditions. Figure 2 shows variation of THG spectrum with quarter wave plate angle showing dependance of THG on polarization.

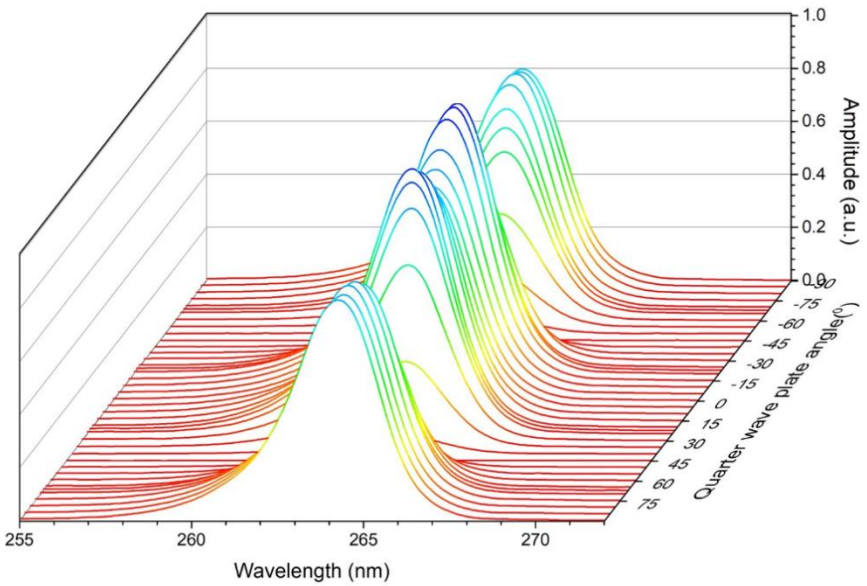

Figure 2: Shows the typical THG spectrum with change in quarter wave plate angle from a filament generated from 150mm lens and 2mJ pulse energy.

Femtosecond filamentation causes the generation of acoustic waves from the filament due to plasma that expands into ambient atmosphere which launch acoustic waves propagating with varying parameters such as peak-peak overpressures, burst length, arrival time, frequency distribution. In this chapter the non-optical characterization of fs filaments in atmosphere is presented. Filament characteristics such as the intensity and electron density were correlated to the acoustic emission profile along the filament. We find that the plasma density is proportional to peak to peak overpressures associated to the observed acoustic signals. Acoustic profiling of filaments can therefore probe the plasma dynamics existing inside a filament. The Fourier transform of the acoustic signals was done to provide the frequency distribution of the acoustic pulse as well. We have found that acoustic profiling of plasma density in the filament is more sensitive than optical techniques, especially when we observe weak filaments whose optical emissions cannot be collected and also because it has a dynamic range of three orders. The temporal pulse length along with the spectral decomposition of the pulse shows the development and termination of multiple filamentation in the filament. The longitudinal acoustic emission profile was also able to distinguish single and multiple filamentation, such that we can also identify the exact region of multiple filament coalescence into a single filament. Figure 3 shows the difference in acoustic signals at regions of single and multiple filamentation. To further explore the extent of acoustic characterization of filaments, filaments with varying aberrations were compared. The acoustic characterization of filament from an achromat doublet lens with varying chirp was done and it can be seen that plasma and intensity trends observed using spectroscopic trends are reproduced in the acoustic signals observed. The studies were extended towards sensing of molecular aerosols by using acoustic data from filament aerosol interaction.

We have observed RF from filaments generated from femtosecond pulses where the highly transient nature of femtosecond pulses ionizes the medium by multiphoton ionization alone and bulk charge oscillations are not significant. The role of input focusing conditions on the RF generated was shown and we can see from the RF pulse profile that loosely focused filaments have lesser amplitude but have a uniform pulse profile for linearly polarized pulses, whereas tightly focused filaments have larger amplitude but the pulse profile has many irregularities.

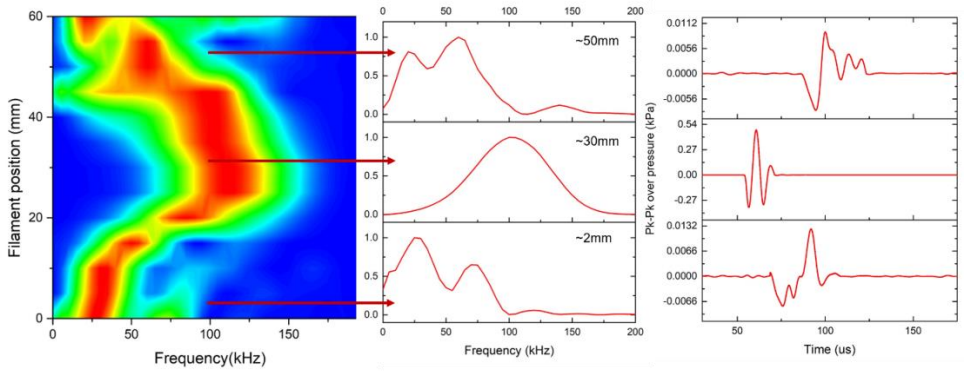

Figure 3: Spectrum and time domain signal from filament generated using a 500mm lens shows clear distinction between multiple filaments and single filaments.

These irregularities get more prominent when a Fourier transform is taken, we observe multiple maxima in the frequency domain for the RF generated from tightly focused filaments which can be due to the presence of multiple filaments. The study was extended to find the influence of input polarization on the RF emission, which showed drastic changes in the RF observed. We firstly find enhancement with filaments from both loose and tight focusing conditions when polarization changes from linear to circular. Closer observation shows that RF signal from loosely focused filament are enhanced much more than tightly focused filaments at circular polarization. Multiple maximums observed in the frequency domain from the filament generated from the 150mm lens disappear at circular polarization and we observe a single maximum with a broad distribution. Knowing that tilting lens introduces different plasma dynamics in the filament because of the asymmetry that gets induced in the pulse wavefront, we have studied RF from filaments generated under lens tilt. Significant enhancement was observed from at certain angle of lens tilt, where we have seen that not only signal gets amplified but we also see a disappearance of the irregularities in the pulse profile observed for filament under zero tilt, which can be seen in the smooth frequency distribution observed in the frequency domain. The effect of change in polarization shows drastic enhancement. The combination of lens tilt and circularly polarized light gave enhanced RF signal with a uniform pulse profile. The frequency at maximum amplitude was also seen to shift to higher frequencies with change in input polarization from linear to circular. The large dynamic variation of RF emission from filament with change in input pulse conditions shows that we can control the RF generated from a filament that is generated remotely, providing a highly promising tool for remote detection and probing. Figure 4 summarized the results from RF charaterization of femtosecond filaments.

Femtosecond filament application towards remote sensing was explored to apply the findings from this study. Aerosols of multiple solvents and organic matter were interacted with filaments and the correspoding spectra showed distinction between the various samples used. Filament interaction with solid materials was also done using FIBS of different solid materials and one can easily extract the elemental composition of the different samples. Aluminum was used as the primary characterization element to test the material damage induced by filamentation.

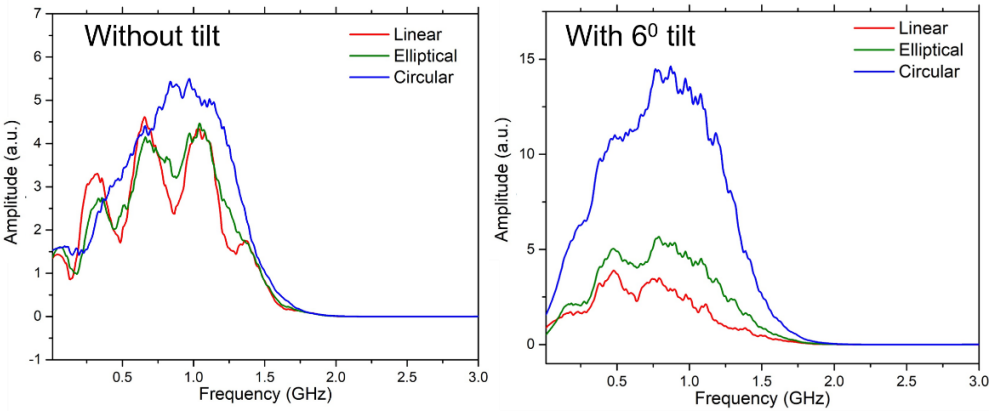

Figure 4: Shows RF spectrum with change in input polarization and lens tilt from a filament generated using a 150mm lens.

The solid material characterization that was done was extended to study damage done to a composite material with surface irregularities. Reflectance of damaged spot can be distinguished between various filaments and filament positions, showing the characteristic reproducibility of filament induced damage that can be modulated. In summary, this thesis aims to create a holistic understanding of filament behaviour and the corresponding emissions to establish the foundation to apply and control femtosecond filamentation.

TH-11. POROUS GROWTH AND CHARACTERIZATION OF N_2 NANOSECOND PULSED LASER INDUCED BLACK SILICON (LIBSI) FOR OPTOELECTRONICS APPLICATIONS

P. Chandrakanta Singh, *KIIT,* Bhubaneswar, Odisha, Email: p.chandrakantsingh@gmail.com, skdas@gmuniversity.ac.in

Introduction and motivation of the work

Microstructures on Si surface are found to be very promising for optoelectronics applications, such as solar cell, photodiode, photodetectors, CCD camera, surface enhanced Raman spectroscopy chip, etc.[1-10] These devices are based on absorption or scattering of incident radiation by the electrons. Generally, the polished Si wafers have the high surface reflectance. This causes low absorption or scattering of incident radiation resulting lowering in efficiencies. To overcome this demerit, several techniques have been established to reduce the reflection of the incident radiation. Amongst them, the surface micro/nanotexturing of Si surface is one of the most competent, highly promising and extensively used technique. When the Si surface containing fine micro/nanostructures and comprising of other structures i.e., columns, needles, spikes and holes like structures in place of smooth, then the surface of Si reduces the reflectance drastically and the capability of absorption of light is enhanced significantly, such Si is called as Black Si[11–15]. Apart from this low reflectance, it has many other unique properties, as high luminescence efficiency, a large surface area and chemically active, when the feature size of the surface is in nanometers. Several practical black Si texturing techniques have been established such as, metal-assisted chemical etching[16–19], reactive ion etching[20–22], wet chemical etching[23], electrochemical method[24] and laser irradiation technique[25-28], etc. Significant evolution has been made in analyzing and studying on laser surface texturing process which has advantageous over the other texturing process as (i) well controllable (ii) highly reproducible (iii) direct single-step processing (iv) dry process and eco-friendly. Many works have been carried out using this method for growth of LibSi to reduce the reflectance of monocrystalline, polycrystalline and bulky amorphous and thin film of Si. Nevertheless, these types of works have mostly been done by solid-state fs, ps or ns lasers[29-38]. The costs of these lasers are extremely high. And hence the optoelectronics devices fabricated from the produced LibSi will be very high cost. So, the first motivation of our work to overcome this limitation by the use of low-cost pulsed Nitrogen (N_2) nanosecond

(ns) gas laser. Also, it is to note that, most of the aforementioned works have been carried out in the vacuum medium and in presence of corrosive gas. Second motivation of this work is to overcome this demerit. Further in this work, the reflectance behavior study has been done on the generated LibSi to do its optical characterization.

2. Objectives of the work

(i) Objective 1: Development of a compact Laser Workstation Attachment (LWA) system for growth of LibSi.

(ii) Objective 2: Effect of laser material processing parameters on morphology of laser induced microtextured Si using N_2 ns laser.

(iii) Objective 3: Growth of LibSi and sub-wavelength LIPSS using N_2 ns laser.

(iv) Objective 4: Reflectance behavioral study of grown LibSi.

3. Organization of thesis

Chapter 1: Introduction

This chapter contains firstly, the introduction and motivation of the work. Secondly, the objectives of the work as well as the organization of the thesis.

Chapter 2: Literature review

Chapter 2 contains the literature review on texturing, laser surface texturing and the effects of laser material processing parameters. Also analysed briefly, the work done on LIPSS on Si, LibSi, microgroove based LibSi and their optoelectronics applications.

Chapter 3: Development of a compact Laser Workstation Attachment (LWA) system for growth of LibSi

Laser workstations are oftentimes used for material processing like surface texturing, cutting, drilling, annealing, etching, polishing, marking and advance functional material growth etc. Presently the existed conventional commercial laser workstations are integrated with laser source, optomechanical mounts, beam delivery optics, motion control hardware and software etc. The major drawback of these workstations is that there is no option for interfacing of different kind of laser sources for multitasking. To overcome this drawback of the existing conventional commercial laser workstation, we have introduced the concept of Laser Workstation Attachment (LWA) system. An LWA system can easily be interfaced to any kind of laser sources, so it provides more degrees of freedom in the required workplace. The schematic diagram of this LWA system is given in Fig. 1.

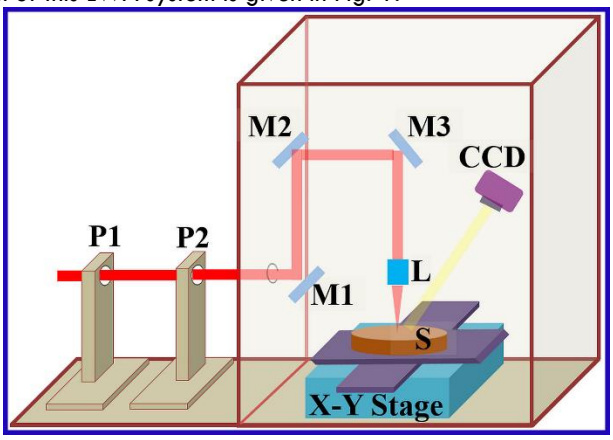

Fig 1: *Schematic diagram of LWA (P1 and P2 = Pin holes, M1, M2 and M3 = Mirrors, CCD = Charge Coupled Device, L = Lens, S = Sample)*

It is basically a metallic chamber consisting of three mirrors (M1, M2, M3), a spherical lens (L), a motorized X-Y stage (X-XY-LSM025A-KX13A-SQ3, Zaber technologies Inc) and a Charged Coupled Device (CCD) camera, and Sample (S). The system is fully automated through the LabVIEW program. Outside this chamber two pin holes (P1, P2) are placed. Any laser can be interfaced/configured to this LWA after its beam passed though the two pin holes. For

processing, the sample is placed on the motorized x-y stage (at the focal length of the focusing lens). The CCD camera is used to get the real time view of the work. This LWA system was used for growth of LibSi by interfacing a N_2 laser ns laser. Details of this work is discussed in this chapter.

Chapter 4: Morphological study of laser induced micro/nanotextured Si surface using low cost UDME camera

In this chapter, it is reported an investigation on the use of compact and inexpensive USB digital microscope endoscope (UDME) camera for morphological characterization to optimize the processing parameters and overlapping condition for growth of large area LibSi. The details of experimental set up and testing of UDME camera is discussed briefly in this chapter.

Chapter 5: Effect of laser material processing parameters on morphology of laser induced microtextured Si using N_2 ns laser

This chapter reports the laser material processing parameters effect on morphology of laser induced textured Si surface. The brief details are given on the change of morphological behaviour by varying the repetition rate of laser pulses and sample scanning velocity. From these investigations it is decided to generate the large area LibSi with proper optimization of laser material processing parameters. The detail of this work is given in this chapter.

Chapter 6: Growth of LibSi and sub-wavelength LIPSS on large area Si using low cost N_2 ns laser and its reflectance behavioral study.

In this chapter the reflectance behavior of LibSi containing sub-wavelength LIPSS is reported. The FESEM images of such sub-wavelength LIPSS are shown in Figure 2. As it can be seen from this figure, the smallest period of LIPSS (37nm) is found to be close to λ /9 times of the irradiated laser wavelength (337 nm).

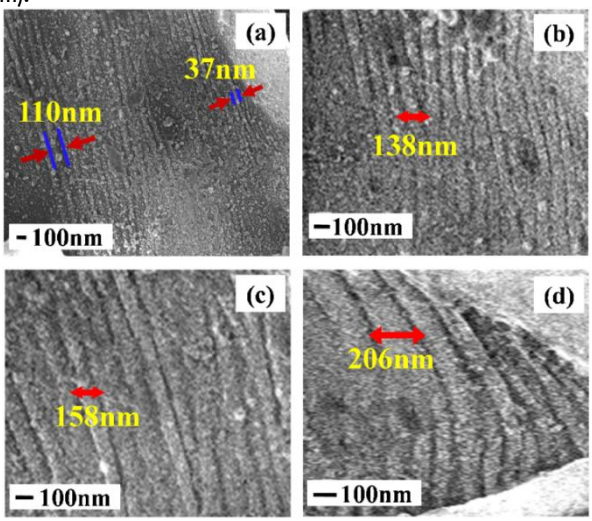

Fig 2. *The FESEM images of sub-wavelength LIPSS generated on Si using N_2 ns laser*

For doing reflectance study large area LibSi is required. The FESEM image of such large are LibSi is shown in Fig 3. Here Figure 3(a) and Fig 3(b) shows the FESEM images of microstructures generated on Si surface in large area in raster scanning mode at velocities of 0.5mm/s, and 0.05mm/s respectively. The total reflectance behavior of these large area LibSi is shown in Fig. 4. The total reflectance means sum total of diffuse reflectance and specular reflectance. This behavior of LibSi was studied by using a UV visible spectrophotometer attached with an integrating sphere. The Curve (a) of Fig. 4, represents the total reflectance of unstructured Si. It indicates that for untextured Si, the reflectance value is 53-45% within the wavelength range of 330 - 850 nm. Curve (b) and curve (c) show the total reflectance behavior of Si surface microtextured at the velocity of 0.5 mm/s and 0.05 mm/s respectively. For the case of 0.5mm/s the reflectance value is 35-25% within the wavelength range of 330 - 850 nm whereas for 0.05mm/s it is found to be 17-10% in the same wavelength range. This difference can be explained by taking the processed region into account.

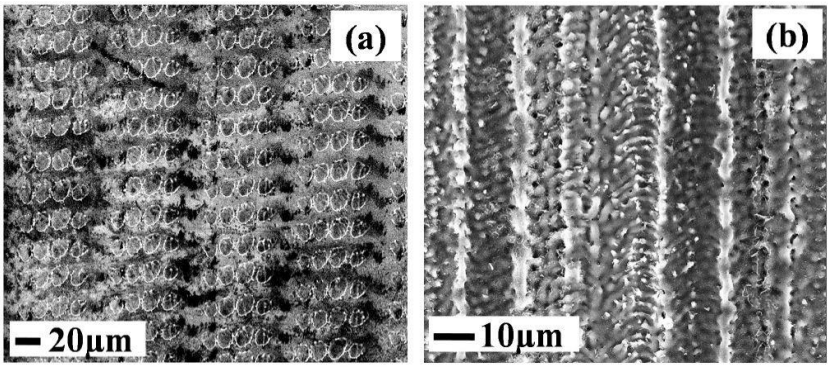

Fig 3. *FESEM images of N_2 ns laser treated large area Si textured in air medium with sample scanning velocity (a) 0.5 mm/s, (b) 0.05 mm/s.*

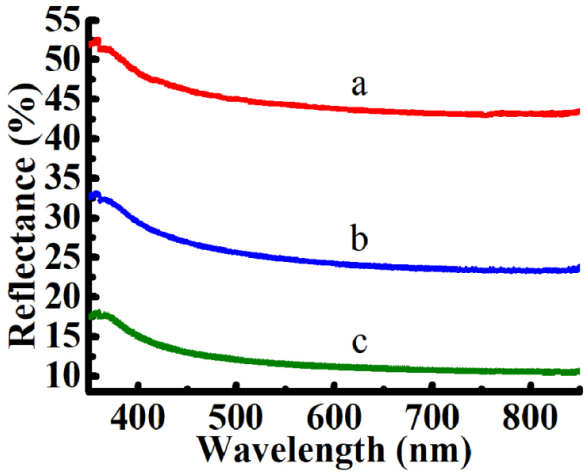

Fig 4. *Total reflectance behavior of untextured Si (curve a), large area Si surface microtextured at the velocity of 0.5 mm/s (curve b) and 0.05 mm/s (curve c).*

For the case of the 0.05mm/s, 100% processing of the sample surface was there due to complete overlapping of the damage spot (please ref. Fig. 3b), whereas for 0.5mm it was about 60% due to non-overlapping of the laser damage spot. Therefore, the reflectance in the case of 0.05mm/s scanning velocity is reduced too much smaller value than the case of 0.5 mm/s.

Chapter 7: Summary and future scope of the work

This chapter contains the summary of all the work done. It also contains future scope of this work.

4. References:

1. V. V. Iyengar, B. K. Nayak and M. C. Gupta, Sol Energ Mat and Sol C, **94**, 2251 (2010).
2. R. A. Myers, R. Farrell, A. M. Karger, J. E. Carey, and E. Mazur, Appl. Opt. **45**(35), 8825 (2006).
3. J. E. Carey, C. H. Crouch, M. Shen, and E. Mazur, Opt. Lett. **30**, 1773 (2005).
4. K. Xu, C. Zhang, R. Zhou, R. Ji, & M. Hong, Opt. Express, **24**(10), 10352 (2016).
5. I. Gnilitskyi, L. Orazi, T. White and V. Gruzdev, Conference on Lasers and Electro-Optics (CLEO), San Jose, CA, USA, 13-18 May, AM1M.6 (2018).
6. S. Kontermann, T. Gimpel, A. L. Baumann, K. M. Guenther, W. Schade, Energy Procedia 27, Silicon PV, Leuven, Belgium, April 03-05, 390 – 395 (2012).
7. Z. Huang, J. E. Carey, M. Liu, X. Guo, E. Mazur, and J. C. Campbell, Appl. Phys. Lett. **89**, 033506 (2006).

8. T. Chen, J. Si, X. Hou, S. Kanehira, K. Miura and K. Hirao, J Appl Phys. **110**, 073106 (2011).
9. J. Yang, J. Li, Z. Du, Q. Gong, J. Teng & M. Hong, Sci. Rep. **4**(1),1 (2014).
10. J. Lv, T. Zhang, P. Zhang, Y. Zhao & S. Li, Nanoscale Res. Lett. **13**(1), 1 (2018).
11. Z. Fan, D. Cui, Z. Zhang, Z. Zhao, H. Chen, Y. Fan, P. Li, Z. Zhang, C. Xue, S. Yan, Nanomaterials, **11**(1), 41 (2020).
12. Q. Tan, F. Lu, C. Xue, W. Zhang, L. Lin, J. Xiong, Sensors Actuators A Phys. **295**, 560 (2019).
13. M. Otto, M. Algasinger, H. Branz, B. Gesemann, T. Gimpel, K. Fuchsel, T. Kasebier, S. Kontermann, S. Koynov, X. Li, Adv. Opt. Mater. **3**, 147 (2015).
14. E. Juzeliunas, D.J. Fray, Chem. Rev. **120**, 1690 (2020).
15. X. Liu, P. R. Coxon, M. Peters, B. Hoex, J.M. Cole, D.J. Fray, Energy Environ. Sci. **7**, 3223 (2014).
16. R. Younkin, J. E. Carey, E. Mazur, J. A. Levinson, C. M. Friend, J. Appl. Phys. **93**, 2626 (2003).
17. T. H. Her, R. J. Finlay, C. Wu, S. Deliwala, E. Mazur, Appl. Phys. Lett. **73**, 1673 (1998).
18. A. Y. Vorobyev, C. Guo, Appl. Surf. Sci. **257**, 7291 (2011).
19. J. H. Zhao, Z. H. Lv, C. H. Li, X. Y. Yu, X. B. Li, IEEE Sens. J. **17**, 1 (2016).
20. S. Cheng, B. Cai, Y. Zhu, In Proceedings of the 2015 Opto-Electronics and Communications Conference (OECC), Shanghai, China, 28 June–2 July, 1–3 (2015).
21. S. Jurecka, T. Matsumoto, K. Imamura, H. Kobayashi, Appl. Surf. Sci. **395**, 150 (2017).
22. P. Zhang, H. Sun, K. Tao, R. Jia, G. Su, X. Dai, Z. Jin, X. Liu, J. Mater. Sci. Mater. Electron. **30**, 8667 (2019).
23. T. L. Phan, W. J. Yu, Sci. Rep. **10**, 1(2020).
24. X. G. Zhang, J. Electrochem. Soc. **151**, C69 (2004).
25. Y. Qiu, H. C. Hao, J. Zhou, M. Lu, Opt. Express, **20**, 22087 (2012).
26. M. Hildebrandt, J. Zhou, M. Lu, J. Appl. Phys, **109**, 053513 (2011).
27. M. Steglich, T. Kasebier, F. Schrempel, E. B. Kley, Infrared Phys. Technol. **69**, 218 (2015).
28. Q. Tan, L. Tang, H. Mao, Y. Chen, Y. Ren, C. Lei, F. Yuan, W. Ou, J. Xiong, Mater. Lett. **164**, 613 (2016).
29. V. V. Iyengar, B. K. Nayak, and M. C. Gupta, Sol Energ Mat Sol C, **95**, 2745 (2011).
30. Y. E. B. Vidhya, N. J. Vasa, J. Photonics Energy, **6**(1), 014001 (2016).
31. O. García, J. García-Ballesteros, D. Munoz-Martin, S. Núnez-Sánchez, M. Morales, J. Carabe, I. Torres, J. Gandía, C. Molpeceres, Appl. Surf. Sci. **278**, 214 (2013).
32. C. Wu, C. Crouch, L. Zhao, J. Carey, R. Younkin, J. Levinson, E. Mazur, R. Farrell, P. Gothoskar and A. Karger, Appl. Phys. Lett, **78**(13), 1850 (2001)
33. C. H. Crouch, J. E. Carey, J. M. Warrender, M. J. Aziz, E. Mazur and F. Y. Genin, Appl. Phys. Lett. **84**(11), 1850 (2004).
34. M. Halbwax, T. Sarnet, P. Delaporte, M. Sentis, H. Etienne, F. Torregrosa, V. Vervisch, I. Perichaud and S. Martinuzzi, Thin Solid Films, **516**(20), 6791 (2008).
35. X. C. Wang, H. Y. Zheng, C. W. Tan, F. Wang, H. Y. Yu and K. L. Pey, Opt. Express, **18**(18), 19379(2010).
36. X. Zhu, H. Zhu, D. Liu, Y. Huang, X. Wang, H. Yu, S. Wang, X. Lin, P. Han, Adv. Mater. Res. **418**, 217 (2012).
37. D. A. Zuev, O. A. Novodvorsky, E. V. Khaydukov, O. D. Khramova, A. A. Lotin, L. S. Parshina, V. V. Rocheva, V. Y. Panchenko, V. V. Dvorkin, A. Y. Poroykov, G. G. Untila, A. B. Chebotareva, T. N. Kost, M. A. Timofeyev, Appl. Phys B. **105**(3), 545 (2011).
38. D. Differt, B. Soleymanzadeh, F. Lükermann, C. Strüber, W. Pfeiffer, H. Stiebig, Sol Energ Mat Sol C. **135**, 72 (2015).

TH-12. ULTRAFAST QUASIPARTICLE DYNAMICS IN LAYERED TRANSITION METAL DICHALCOGENIDES AND OTHER METAL MONOCHALCOGENIDES

Manobina Karmakar, IIT Kharagpur, ***Email:*** *barnatuli@gmail.com,*

After graphene, transition metal dichalcogenides (TMDC) have appeared as the front-runnersof layered semiconductors offering a plethora of intriguing optoelectronic properties. Weak van derWaal bonding between layers enables peeling off single to multiple layers through various top-downapproaches (mechanical exfoliation and liquid phase exfoliation). Unlike graphene, TMDCs possessbandgaps in optical to near-infrared wavelength regions, allowing their incorporation in versatile optical and electronic applications like- photodetectors, light-emitting diodes, transistors, optical switches, etc. Due to reduced dielectric screening and strong Coulomb potential, optoelectronic properties inthis class of semiconductors are governed by various quasiparticles like excitons, trions, bi-excitonsbesides free electrons and holes. There has been an avalanche of research interests on TMDCs because of the potential application viewpoint and the fact that quasiparticles encode intriguing fundamental physics at the nano-scale. The advent of femtosecond pump-probe spectroscopy has allowed directobservation of the formation and evolution of different quasiparticles during light-matter interactions. In particular, researchers have been fascinated by mono-layered TMDCs. Atomically thin (< 1 nm thick) single layers of TMDC possess around 15-20 % linear absorption and are direct bandgapsemiconductors contrary to few-layered or bulk materials. Also, excitons in mono-layered TMDCsdisplay binding energies from hundreds of meV up to 1 eV owing to strong Coulomb interactionsand reduced dielectric screening. Therefore, it is evident that research interests in these layeredsemiconductors have revolved around atomically thin single layers owing to their uniqueness, as soon as it was realized in 2010.

On the other hand, the bulk counterparts display significant Coulomb screening and weakly-bound excitons. An increase in layer numbers displays notable differences in optoelectronic properties. In between the sub-nm thick mono-layers and bulk crystals, few-layered counterparts display strongly- bound excitons, as well as sizable screening enabling understanding of quasiparticles interactions in the presence of enhanced dielectric and carrier screening.

In this thesis, the author explores exciton, Coulomb-correlated electron-hole plasma, free-carrier, and trion dynamics following ultrafast light-matter interactions in few-layered TMDCs, using molybdenum disulfide (MoS_2) as a prototypical system. As the technology inches toward the commercialization of atomically thin semiconductor-based devices, tunability in the optoelectronic properties is essential. From this viewpoint, few to multilayered semiconductors might be a unique combination of nm thickness, strong light-matter interaction and, yet sizable tunability stemming from controllable screening from multiple layers. Ultrafast light-matter interaction in another emerging class of layered semiconductors- III-VI metal chalcogenides are also explored. Here, the excitonic effects are much weaker as compared to TMDCs, and free carrier-induced dynamical processes are revealed.

This thesis has been organized into seven chapters.

Chapter 1 primarily provides the basic introduction, including relevant physical phenomena, motivation, and background for the studies.

Chapter 2 describes the relevant experimental methodologies and data analysis techniques formulated in this dissertation. A generalized discussion on modeling transient absorption spectra from scratch is also incorporated in this chapter.

Chapter 3 discusses dynamic screening of excitons. While optoelectronic technology is inching to- wards excitonic devices, external control and manipulation of these neutral

quasiparticles are essential to realize potential applications. Excitonic bandgap in TMDCs can be tuned by altering the Coulomb field strength between its constituents by modifying the surrounding cloud of charge-carrying quasi- particles and hence, the effective dielectric permittivity. As an approximation, static approaches are commonly used to comprehend the experimental outcomes of bandgap tuning through the injectionof free carriers, engineering of the dielectric environment, and photo-excitation. However, such an electrostatic framework overestimates the excitonic screening effect as screening is particularly sensitive to some 'characteristic frequencies' related to electron-hole bound pair formation, many-body interactions etc. The screening at other frequencies is too fast or too slow to affect the electron-hole attractive force in an exciton. Overall, an accurate solution to the long-sought problem of dynamic exciton screening concerning all other quasiparticles is pretty involved. One can find theoretical approaches from the early 70's as well as from the past few years, which mainly address the carrier screening of Coulomb correlations. This specific 'characteristic frequency' is an open question todate. Although some theoretical studies claim that $E_b/\hbar$ (E_b: exciton binding energy) is the characteristic frequency at which free carriers affect the screening, there is no theoretical or experimental discussion on exciton-induced Coulomb screening. The co-existence of different excitonic states in TMDCs leaves this problem extremely important. In this chapter, a ground (1s) and first excited exciton state (2s) in a multilayered transition metal dichalcogenide (MoS_2) is observed upon ultrafast photo-excitation. Despite the expected Pauli blocking and screening-induced reduction in excitonic ab- sorption, the excited state shows an anomalous population enhancement followed by photo-excitation. Empirical analysis, coupled with experimental data, confirms that the 1s exciton polarization eventually controls the effective dielectric permittivity at the excited state and, therefore, its absorption probability. Notably, the resonance energy of the excited state appears to be the characteristic frequency at which Coulomb screening from other excitons is efficient. Our study provides first-ever experimental evidence and hence, an initial stepping stone towards the perception of exciton-induced dynamic screening in TMDC. Notably, the observation of photo-induced enhanced exciton absorption along with simultaneous resonance renormalization opens up new opportunities to tailor the exciton resonance without losing its population, unlike the existing methods. Therefore, new approaches to excitonic device engineering in mono-to-few layered and hetero-structured TMDCs are envisaged.

Chapter 4 is dedicated to studying the uncorrelated free-carrier to Coulomb-correlated electron- hole plasma formation in multilayered MoS_2. Electron-hole plasma is a bunch of free charge carriers correlated via Coulomb interaction, creating local density fluctuations in metals or excited semiconductors. Interestingly, the formation of such a many-particle state is not instantaneous. A phenomenalstudy by Huber et al. finds that it takes about one whole oscillation period (of plasma oscillations)time after photo-excitation to form the plasma state. Electron-hole plasma acts as a ubiquitous tool for altering optical properties via exciton-plasma interactions and therefore is crucial for device engineering. Nevertheless, the evolution of electron-hole plasma following light-matter interaction in such a system remains unexplored. In this chapter, Coulomb-correlated electron-hole plasma formation *via* its interaction with excitons in multilayered MoS_2 is explored. It is observed that under intense photo-excitation $\sim 10^{19}$ per cm^3, huge damping destroys the Coulomb-correlation and hinders the plasma formation until a majority of the free-carriers recombine and plasma oscillation period be- comes sufficiently smaller than the damping time constant. Moreover, only 1-3% of the injected free carriers form Coulomb-correlated plasma. Our study sheds light on exciton-plasma interactions and quasi-static Coulomb screening, which play pivotal roles in device engineering.

Chapter 5 explores exciton and trion dynamics upon intense photo-excitation. Multilayered MoS_2 is perturbed with intense photo-excitation approaching Mott density; intriguing transient phenomena involving different quasiparticles alter the time-resolved optical spectrum. As the excitons become unstable and disintegrate into uncorrelated, free carriers, hot-carrier induced two-step trion formation through pump and probe excitation is identified. Pump excitation creates a hot carrier distribution that contributes a charged carrier (either electron or hole); following absorption of probe pulse creates two oppositely charged carriers, eventually forming the three-body quasiparticle- trion.A rapid temporal window of the non-thermal regime is identified following near Mott threshold photo-excitation. Interestingly, exciton linewidth narrows down, indicating reduced exciton-phonon scattering in this temporal regime.

Chapter 6 depicts intriguing photo-induced carrier dynamics in a newer class of layered semiconductors, metal monochalcogenides. Recently, atomically-thin III-VI metal monochalcogenides (MMC) of type MX (M = Ga, In, X = S, Se, Te) have appeared as successors in the family of layered semiconductors. These materials display excellent photo-responsivity, mobility, and several anisotropic optical properties that are competitive and often superior to the TMDCs. Unlike TMDCs, that are usually indirect bandgap semiconductor and display direct bandgap only at the monolayer limit, MMCs are direct bandgap in the few-layer to bulk and display indirect bands in mono-to-quad layers. These layered materials possess weakly bound excitons, and hence, the optical properties are dominated by unbound charge carriers. broadband optical and NIR transient absorption spectroscopy is utilized and photo-induced Pauli-blocking of the direct bands in the optical region is identified. Interestingly, it is found that free carriers relax through indirect relaxation pathway despite the direct bandgap nature of the material. In addition, as confirmed from transient studies in a bulk and a few-layered GaTe,the presence of high defect densities does not influence the carrier relaxation rate of the direct bands of this material. Slow, indirect and defect-tolerant carrier relaxation (~ tens of ps) in the direct bands in this multi-valley semiconductor explains the superior photo-responsivity. Moreover, mid-gap defect levels enable sub-bandgap linear absorption and mediate broadband excited state absorption.

Chapter 7 summarizes the work highlighting the novelty of the thesis and prospects. Despite some theoretical arguments on frequency-dependent exciton screening, there was no direct experimental evidence. Study presented in chapter 3 provides first-ever experimental evidence and hence, a first stepping stone towards the perception of exciton-induced dynamic screening of excitonic Coulomb potential. Notably, as opposed to existing methods for tuning exciton resonance through increased screening, where exciton oscillator strength inevitably drops, tunability of exciton resonance along withan enhanced exciton absorption due to “anti-screening” is observed. Therefore, new approaches to excitonic device engineering are envisaged. While excitons are sensitive to screening at their resonancefrequencies, the quasiparticle bandgap is influenced by the quasi-static screening from plasma. The electron-hole plasma (EHP) acts as a ubiquitous tool for altering optical properties, like- bandgap engineering via exciton-plasma interactions, and therefore is crucial for device engineering. Huber*et al.* have demonstrated that plasma formation is retarded by a timescale related to the inverse of the plasma frequency. Nevertheless, this time-resolved study was performed for a specific excitation
density (2×10^{18} per cm^3) in GaAs. It is unclear whether the entire free-carrier gas converts to Coulomb-correlated plasma in all semiconductors, irrespective of the magnitude of the input carrier
density. Recently, Steinhoff *et al.* have theoretically calculated the fraction of EHP for a range of carrier injection densities in transition metal dichalcogenides in thermal equilibrium. However, the experimental distinction between the carrier and electron-hole plasma and the transition of the formerto the latter remained unexplored in a wider

context. The author, along with her colleagues werefirst to experimentally demonstrate that a small fraction (1 − 3 %) of photo-injected carriers form the Coulomb-correlated electron-hole plasma. In addition, this study provides the first-ever experimental demonstration of electron-hole plasma formation in a TMDC that is hindered by fast carrier-carrier scattering.

Under intense photo-excitation, light-matter interactions lead to nontrivial quasiparticle dynamics that remain unexplored. As the pump intensity is tuned near the Mott threshold, excitonic quasiparticles become unstable, and enhanced trion formation is observed. In a photo-induced non-thermal regime, bandedge A exciton display linewidth narrowing. In stark contrast to available studies that observe photo-induced exciton linewidth broadening, this observation demonstrates reduced exciton-phonon coupling in the non-thermal regime. Such anomalous behavior has never been reported earlier in any transition metal dichalcogenides.

Light-matter interaction of layered semiconductors with weak exciton binding energies is dominated by free carriers. Chapter 6 explores photo-induced carrier dynamics in few-layered Gallium Telluride for the first time, where indirect carrier relaxation in the direct bandgap material is noted. Such unique carrier dynamics make this material ideal for photo-detection as direct bands ensure high absorption oscillator strength, and slow, indirect carrier recombination facilitates efficient carrier ex- traction leading to sizable light-to-electricity conversion. This work explains the physical origin behind the excellent photo-detection properties of GaTe reported in the literature. In addition, excitons in GaTe display surprisingly high coherence time (> 150 *fs*). This value is about an order higher thanthat found in TMDCs. Efficient, coherent control of the excitons in this 2D material at cryogenic temperatures would lead to applications in quantum information processing.

TH-13. IN-SITU PROBING OF INTERFACIAL MOLECULAR STRUCTURE OF POLYMERS AND NANOMATERIALS USING SUM FREQUENCY GENERATION VIBRATIONAL SPECTROSCOPY

Harpreet Kaur *Indian Institute of Technology Ropar,* ***Email:*** *harpreet.kaur@iitrpr.ac.in*

In-situ probing of material surfaces/interfaces at the molecular level is an exciting research area that helps to recognize many significant surface/interface-associated mechanisms, further benefiting modern science and engineering. The investigation of molecular structures at the interfaces and surfaces is under continuous development and has continuously attracted remarkable attention in different research areas, including biosensing, optoelectronics, microelectronics, biomedical, drug-delivery, coatings, etc. [1, 2] Our research work mainly focuses on realizing the interfacial molecular structures and dynamics at different solid and liquid interfaces for polymers and nanomaterials, respectively. Polymers and nanomaterials have huge potential applications in various areas of science and industry. Polymers are extensively utilized in every field of our modern life, from traditional materials to biomaterials. [3-7] The rapid progress in nanomaterials and nanotechnology has significantly impacted multiple disciplines of science and technology for worldwide research and development. Man-made nanomaterials are materials with at least one external dimension between 1 and 100 nm and possess unique properties and functions. [8] This field is growing quickly, and remarkable efforts are going on for their synthesis, characterization, and application. Thus, the highly advanced nanomaterials with better performance for a particular application are required to develop through controlling the shape and size within the nanometer range. For example, nowadays, nanomaterials are applied in water and treatment of wastewater due to their high reactivity and strong adsorption capacities along with high mobility in the aqueous medium. It has been reported that various nanomaterials are utilized to remove bacteria, heavy metals, inorganic anions, and organic pollutants due to their high mobility in the aqueous medium. [9-13] Our study

focuses on exploring the interfacial molecular structure of organic and inorganic nanomaterials with their simultaneous impact on the interfacial water structure for various aqueous systems for different applications in the present research work.

The molecular organization at the surface/interface is quite distinct and unique as compared to that of bulk phases, and the confined interfacial structure is adequately approximated in the nanometric length scale. This is a big challenge to achieve sufficient surface/interface specificity with the exclusion of the contribution from the bulk phase. The sum frequency generation (SFG) vibrational spectroscopy has shown excellent intrinsic interface-selectivity to probe molecules present at the surface/interface. [14-16] It is a second-order non-linear optical technique used to elucidate the molecular structure of aqueous surfaces and buried interfaces under different experimental conditions. We have applied SFG vibrational spectroscopy to explore various molecular systems based on polymer and nanomaterials in probing the molecular conformation and dynamics of the molecules residing at the air-polymer and air-aqueous interfaces.

We have used SFG spectrometer (Ekspla, Lithuania) to probe the interfacial molecular conformations and interactions. The experimental set-up of the SFG spectrometer includes a passively mode-locked Nd: YAG laser (Ekspla PL2231). The laser unit is generated an output beam with a pulse duration (at full width half maximum) of 30 picoseconds and pulse energy of 40 mJ at a wavelength of 1064 nm of diameter 6 mm approximately with a repetition rate of 50 Hz. The fundamental laser beam 1064 nm is directed towards the second-harmonic generation unit (SFGH500-2H) from the laser output port to generate two visible beams at frequency 532 nm, as shown in figure1. The SHG unit has three output ports, which provide two beams at the same frequency as 532 nm and one fundamental beam at frequency 1064 nm. The high energy 532 nm beam is used to feed the non-linear crystals BBO1 (β barium borate) and BBO2 in the parametric generator (Ekspla PG 501/DFG) and leads to the generation of radiation (idler) within the wavelength range from 1064 nm-2300 nm through optical parametric oscillation (OPO) and optical parametric amplification (OPA) processes. The idler radiation is mixed with fundamental 1064 nm wavelength in the non-linear crystal ($AgGaS_2$ or GaSe), which produces a tunable IR beam with a broad spectral range from 2300 nm to 16000 nm due to difference frequency generation (DFG). The tunable IR beam and second visible (532 nm) beam are overlapped spatially and temporally at the sample interface. As a result, the SFG signal is generated from the interfacial molecules. The incident angle of the IR and the visible beams is 56° and 63° with respect to the surface normal at the probing interface in co-propagating reflection geometry, respectively, as shown in figure 1.

In accordance with the electric dipole approximation, the sum frequency beam is induced in a reflected direction at an angle of 61° with respect to the surface normal following the phase-matching condition. The induced SFG signal is passed through the spatial filter and directed towards a detection unit composed of a monochromator (MS2001, SOL instruments Ltd., Belarus) and an ultraviolet-visible sensitive photomultiplier tube (Hamamatsu R7899). Data was collected by averaging 200 pulses with a step size variation of 2-5 cm^{-1} for the IR beam. The SFG experiments are carried out under various polarization combinations as ssp, ppp, and sps. LABVIEW software in the computer is used to control the functioning of all motorized optical components. The schematic illustration of the experimental set-up through ray-diagram for the SFG spectrometer, including picosecond Nd: YAG laser, SHG, OPG/OPA, DFG, and detection units, are shown in figure 1.

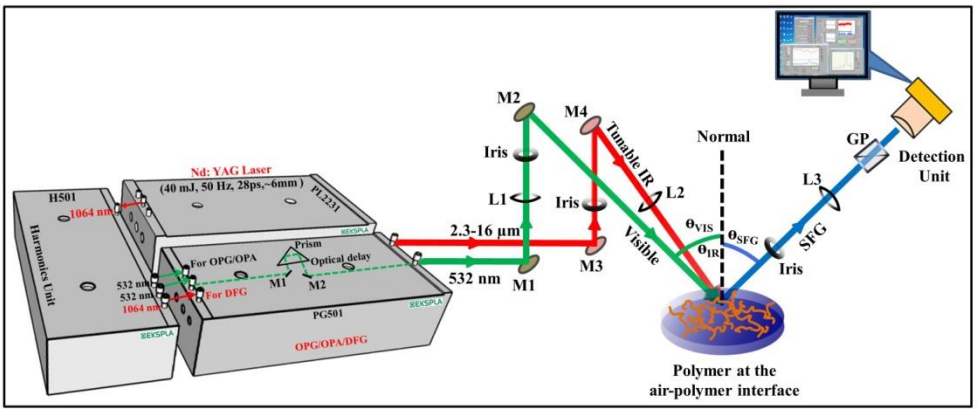

Figure 1: *Schematic representation of the experimental set-up through ray-diagram for the SFG spectrometer including picosecond Nd: YAG laser, SHG, OPA/DFG, and detection unit, applied to probe molecular structure of polymer at the air-polymer interface.*

All the experimental procedures and analysis of observed data with detailed explanation are presented in the thesis, which is divided into seven chapters as follows:

Chapter 1 briefly introduces the importance of probing the molecular arrangement at surfaces/interfaces of polymer and aqueous media. Also, the significance of probes to inspect various surfaces/interfaces and related mechanisms is discussed. We have given detailed information about the historical background and evolution of second-order non-linear vibrational spectroscopy to investigate and illustrate various intermolecular interactions at different interfaces. A brief literature review is given to provide insights about the utilization of surface-specific tools to probe polymer coatings and aqueous interfaces to recognize the conformation of interfacial molecules and impact on the interfacial water structure during interactions between different species present in the aqueous medium, respectively.

Chapter 2 comprises an overview of the experimental tools used and a detailed theory of the experimental procedures employed to reveal the interfacial molecular activities of various molecules residing at various interfacial regions. The detailed basic theory about non-linear optical processes, mainly theoretical facets of the SFG vibrational spectroscopy, is presented. The details about the experimental implementation of the spectroscopic tool are provided to probe the molecular behavior at the surface or interface. A complete description of experimental methods is illustrated with the preparation of samples, recording of the SFG spectrum, and its analysis to explore the structure of interfacial molecules and intermolecular interactions.

Chapter 3 presents the systematic investigation of the in-situ interfacial molecular structure of tetraethyl orthosilicate (TEOS) at the air-TEOS interface under different polarization combinations and its dynamics with varying concentrations at the air-aqueous interface using SFG vibrational spectroscopy. The results of our study demonstrated the occurrence of hydrolysis and condensation processes of TEOS in the presence of water at the air-aqueous interface. The observed alterations in the SFG signal in the CH-and OH-stretch regions with time are indicated the hydrolysis and condensation processes. The elimination of CH-stretch modes and overall increase and a further decrease in the SFG signal in the OH-stretch region demonstrated the role of hydrolysis and condensation processes of the TEOS molecules at the air-aqueous interface. The dynamic light scattering technique strongly supported the condensation mechanism of TEOS molecules in water by the size measurements of silica nanoparticles. This work can provide insights into the interfacial molecular mechanisms of TEOS and water structure to explore the various stages of the sol-gel process to form silica nanoparticles. Our pH studies also give the comparative role of hydrolysis of TEOS as confirmed from SFG vibrational spectroscopy and Zeta potential measurements.

Chapter 4, we observed and compared organic nanoparticles (ONPs) and carbon dots (CDs) sensing activities in the aqueous bulk media and at the air-aqueous interface using fluorescence spectroscopy and SFG vibrational spectroscopy respectively. Fluorescence spectroscopic results have illustrated that ONPs preferably sense the Cs (I) ions, whereas CDs have selective sensing towards Ag (I) ions in the bulk aqueous media. SFG results have demonstrated that the ONPs-Cs (I) binding might be a bulk phenomenon while the CDs-Ag (I) binding activities affect the molecular structure of water molecules and CDs at the interface. The present study provides a broad outlook of how temperature-modulated self-assemblies of the same material can exhibit tunable selectivity towards different cations.

Chapter 5, we have examined the impact of molecular weight on the surface structure of the PDMS using SFG vibrational spectroscopy, contact angle measurements, and atomic force microscopy (AFM). This study has provided detailed calculations of the Fresnel factor correction to the SFG spectra of polymer films as recorded in different polarization schemes of SFG spectroscopy. This can be further utilized to obtain true information about molecular conformation and orientation of the functional groups at the air-polymer interface. Along with this, the observed ordered alignment of surface methyl groups with variation in polymer molecular weights, as evident from the presence of sharp SFG peaks, finds an intriguing correlation with the macroscopic root mean squared surface roughness and hydrophobicity studies as performed on polymer films using AFM and contact angle measurements.

Chapter 6, we have performed a systematic study of drug-polymer interactions and aqueous drug solubility at the air-water interface from the perspective of probing the molecular-level interactions involved during the process. Rifaximain and albendazole are used as two model drug systems, while hydroxypropyl methylcellulose E15, Soluplus, polyvinyl pyrrolidone K30, and poly(vinyl alcohol) are taken as model polymer systems to study drug-polymer associations in relevant media. The SFG spectra are recorded for signatures of the drug in the CH-stretch region and the effect of drug molecules on the ordering of interfacial water molecules in the OH-stretch region with time under the ssp polarization combination. The molecular mechanism of drug-polymer interactions is extracted at the air-water interface using SFG spectroscopy through variations in the interfacial H-bonding environment of water molecules. The experimental findings and the understanding from these drug-polymer interactions using SFG are presented through detailed discussion in this chapter.

Chapter *7* summarizes and concludes the research work that was carried out for this thesis work about molecular-level investigations of organic-inorganic nanoparticles and polymeric materials at both air-aqueous and air-solid interfaces using non-linear vibrational spectroscopy.

References:

[1] B. D. Ratner, and D. G. Castner, *Surface modification of polymeric biomaterials* (Plenum Press, New York, 1997),

[2] W. J. Feast, and H. S. Munro, *Polymer surfaces and interfaces* (Wiley, New York, 1987),

[3] I. Wong, and C.-M. Ho, Microfluid. Nanofluid. ***7*** 291 (2009).

[4] Y. Xia, and G. M. Whitesides, Annu. Rev. Mater. Sci. **28** 153 (1998).

[5] J. H. So, J. Thelen, A. Qusba, G. J. Hayes, G. Lazzi, and M. D. Dickey, Adv. Funct. Mater. **19** 3632 (2009).

[6] S. Ahmed, H.-k. Yang, A. E. Ozcam, K. Efimenko, M. C. Weiger, J. Genzer, and J. M. Haugh, Biomacromolecules **12** 1265 (2011).

[7] P. Gorrn, M. Lehnhardt, W. Kowalsky, T. Riedl, and S. Wagner, Adv. Mater. **23** 869 (2011).

[8] C. Buzea, I. I. Pacheco, and K. Robbie, Biointerphases **2** MR17 (2007).

[9] R. S. Kalhapure, S. J. Sonawane, D. R. Sikwal, M. Jadhav, S. Rambharose, C. Mocktar, and T. Govender, Colloids Surf. B **136** 651 (2015).

[10] W.-W. Tang, G.-M. Zeng, J.-L. Gong, J. Liang, P. Xu, C. Zhang, and B.-B. Huang, Sci. Total Environ. **468** 1014 (2014).

[11] F. Liu, J. Yang, J. Zuo, D. Ma, L. Gan, B. Xie, P. Wang, and B. Yang, J. Environ. Sci. **26** 1751 (2014).

[12] J. Yan, L. Han, W. Gao, S. Xue, and M. Chen, Bioresour. Technol. **175** 269 (2015).
[13] M. M. Khin, A. S. Nair, V. J. Babu, R. Murugan, and S. Ramakrishna, Energy & Environmental Science **5** 8075 (2012).
[14] C. D. Bain, J. Chem. Soc., Faraday Trans. **91** 1281(1995).
[15] G. Kaur, H. Kaur, A. Singh, M. Chaudhary, N. Kaur, N. Singh, and K. C. Jena, Chem. Asian J. **15** 2160 (2020).
[16] S. A. Hall, K. C. Jena, T. G. Trudeau, and D. K. Hore, J. Phys. Chem. C **115** 11216 (2011).

TH-14. NANOSECOND, FEMTOSECOND (FS) AND FS FILAMENTATION LIBS STUDIES COMBINED WITH MACHINE LEARNING FOR THE IDENTIFICATION OF PLASTIC WASTE AND STANDOFF DETECTION OF HEMS

Rajendhar Junjuri, ACRHEM *University of Hyderabad Telangana, India-500046,* ***Email:*** *rajendhar.j2008@gmail.com*

Introdction:

Spectroscopy is a branch of physics that deals with the interaction of electromagnetic radiation (EM) with matter[1]. Spectroscopic studies provide deep insights into the properties of the analyte (samples/materials) considered for the investigation. It finds application in a wide range of interests such as medicine, chemistry, biology, nanotechnology, materials science, environmental studies, and physics. The invention of the laser in the early 1960s has opened up new avenues in the field of spectroscopy[2]. Laser-matter interaction has become exciting research filed which has revolutionized the different research areas like photonics, nanoengineering, semiconductor physics, plasma dynamics, chemistry, and optical physics, etc. The interaction of high-intensity laser pulse on the sample results in the formation of transient, inhomogeneous, hot, and luminous plasma also referred to as laser-induced plasma (LIP)[3, 4]. Instantly after the formation of LIP, it expands into the surrounding medium and cools down with the emission of intense EM radiation (in ~0.5 -1 μs) accompanied by the generation of a shock wave (in ~3-5 μs) which immediately decays to acoustic signal (in ~20-40 μs). The characteristic emission from the plasma (after ~ 0.5 μs) provides the atomic elemental information of the sample and this analytical spectroscopic technique called as the Laser-induced breakdown spectroscopy (LIBS)[5, 6].

The initial LIBS experiments were carried out by Cross and Brech in 1962[7]. Radziemski et al. have critically reviewed and presented the historical development as well as the significant progress achieved in the LIBS technique[8]. A single laser pulse is sufficient to create the plasma which acts as a rich source of spectral emissions resulting in the LIBS spectrum. A typical LIBS spectrum spans over 200-1000 nm which covers the characteristic emissions starting from UV to IR. The elemental assignment of the spectral peaks can be accomplished with the aid of the 'NIST Atomic Spectra Database' [9]. The measurement of spectral line emissions provides qualitative and quantitative information about the elemental constituents of the sample. As an analytical technique, it has many advantages over other conventional atomic spectroscopic methods such as in-situ multi-elemental detection in a single shot, rapid analysis, nearly non-destructive nature, and can analyze the samples regardless of their physical state i.e. solid or liquid or gas [10]. LIBS can detect all the elements in the periodic table as they emit light of characteristic frequencies when excited but limited only by the power of the laser as well as the sensitivity and wavelength range of the spectrograph. The unique features of LIBS are practically minimal sample preparation and the capability to perform real-time standoff/remote analysis by employing an intense pulsed laser beam on to the sample where the physical access to the sample is not possible albeit optical access can be envisaged. These key attributes make it as a promising cutting-edge technique for the concentration measurements and material identification applications.

The emission line intensity of a particular element in the LIBS spectra can be utilized for the concentration measurements with the aid of the calibration curve approach. In this method, a spectral line (at a characteristic wavelength) intensity is measured as a function of increasing the analyte concentration for preparing a 'standard calibration curve' which can be further utilized to find the concentration of the unknown sample. Alternatively, the calibration-free LIBS technique[11] can be employed to estimate the concentration of all the major and minor elements present in the sample [12, 13] which in principle avoids the pressing need for the matrix-matched standard samples. One of the most interesting uses of LIBS is the identification/classification of material from a collection of materials of interest[14][15] using various machine learning/ multivariate algorithms. It finds the applications in different fields namely, defence [16-19], space exploration [20, 21], archaeology [22, 23], biology [24, 25], nuclear materials[26], medical diagnosis[27, 28], soil analysis[29, 30], and forensic studies[31, 32], etc.

Motivation:

The present thesis mainly focuses on the identification of the high energy materials (HEMs)/explosives[33] in standoff mode and plastics waste [34, 35] in near filed using different machine learning/multivariate approaches for homeland security and environmental applications respectively. It also proposes a theoretical model for the kinetic evolution of the plasma and validates results with the experimental data in the initial chapters. Further, it discusses the exploration of fs LIBS application for the plastics identification. It also presents the spatial and temporal characterization of Cu plasma produced by fs filaments in ambient air aiming at futuristic standoff measurements for the HEMs identification.

Over the decades, various HEMs and improvised explosive devices (IED) are being used for the bomb blasts which is a major threat from the anti-social elements[33]. Thus the discrimination of HEMs and their labelling is a primary concern to every country for the safeguard of their citizens. Further, their identification also avoids illegal transport which is an immediate requirement for minimising the terrorist activities around the globe [36, 37]. Moreover, identification of HEMs is a prior task at transport checkpoints and public meetings to avoid unwanted incidents which mitigate the damage to the public and their property. Post bomb analysis for the HEMs trace identification helps the forensic interrogation. LIBS can serve as an efficient labelling tool for this application owing to its intrinsic unique capability of probing the samples in standoff mode which is an immediate and primary requirement. Few research groups around the world are working towards the in situ identification of the HEM's[19, 38] as well as the standoff detection[18, 39, 40]. However, only very few works have been devoted for the standoff identification of HEMs. To the best of my knowledge, only double-pulse LIBS (DP-LIBS) configurations with big telescopic arrangements have been deployed for the standoff measurements. The utilization of the DP LIBS systems for the standoff investigation has enhanced the signal strength [41] however, the total system size is huge [42]. Hence in this thesis, a compact single-shot standoff LIBS (ST-LIBS) detection system has been developed. The preliminary studies were performed at 1 m[33] and further, it extended to a standoff distance of 6.5 m. The overall size of the developed ST-LIBS system is reduced because of the use of a single pulse laser system and a just a convex lens. Further, the cost also greatly reduces due to the usage of a non-gated compact CCD spectrometer, which is an essential factor in making a low-cost portable LIBS system. The first task of the HEMs identification is to identify whether the given sample is a HEM or not, later to label it as a specific HEM. Explosive identification poses challenges due to the wide variety of the interferent organic non HEMs. Besides that the nitro rich ambient environment leads to complex formation however it is inevitable for the standoff measurements. Hence, in the current thesis, five HEMs and nineteen organic non-HEMs were considered for the analysis and identified utilizing machine learning algorithms. Among all non-HEMs, plastics can be considered to be potentially interfering agents for the identification of HEMs as they are commonly used as transport containers/boxes in airports and public transport systems [43].

Further, the recognition of plastics waste is demonstrated as their identification is a crucial and primary step in the recycling process. Most of the LIBS studies reported in the literature have investigated the standard plastics purchased from the companies with the aid of Echelle based ICCD spectrometers and multichannel gated CCD spectrometers [44-47]. However, single-shot identification of post-consumer plastics with low-cost CCD detection systems are not explored[46]. Hence in the thesis, the performance of LIBS evaluated for the identification of post-consumer plastic waste obtained from local recycling as their identification is more relevant to the actual scenario instead of considering standard plastics purchased from the company/industry[34]. A systematic investigation has been performed with the CCD and ICCD based LIBS detection system and evaluated their performance with different machine learning algorithms in single-shot and ten shot average mode. Further, the fs LIBS is explored for the identification of plastic waste[34]. The fs filaments can propagate and deliver energies over very long distances without any diffraction effects, demonstrates it as a potential candidate for the remote sensing applications compared to the conventional ns laser pulses. Hence, the basic characterization of the fs filaments produced by different lenses has been performed.

References:

1. W. Demtröder, "Atoms, molecules and photons", Springer**2010**.
2. W.T. Silfvast, "Laser fundamentals", Cambridge university press**2004**.
3. D.A. Cremers, and A.K. Knight, "Laser-Induced Breakdown Spectroscopy", Wiley Online Library**2006**.
4. V. Unnikrishnan, K. Alti, V. Kartha *et al*., "Measurements of plasma temperature and electron density in laser-induced copper plasma by time-resolved spectroscopy of neutral atom and ion emissions", Pramana, *74*, **2010**.
5. H.R. Griem, "Principles of plasma spectroscopy", Cambridge University Press**2005**.
6. J.P. Singh, and S.N. Thakur, "Laser-induced breakdown spectroscopy", Elsevier**2007**.
7. F. Brech, and L. Cross, "Optical microemission stimulated by a ruby laser", Appl. Spectrosc, 16, **1962**.
8. L.J. Radziemski, "From LASER to LIBS, the path of technology development", Spectrochimica Acta Part B: Atomic Spectroscopy, *57*, **2002**.
9. R. Junjuri, M.K. Gundawar, and A.K. Myakalwar, "Standoff Detection of Explosives at 1 m using Laser Induced Breakdown Spectroscopy", Defence Science Journal, 67, **2017**.
10. A.W. Miziolek, V. Palleschi, and I. Schechter, "Laser induced breakdown spectroscopy", Cambridge university press**2006**.
11. E. Tognoni, G. Cristoforetti, S. Legnaioli *et al*., "Calibration-free laser-induced breakdown spectroscopy: state of the art", Spectrochimica Acta Part B: Atomic Spectroscopy, 65, **2010**.
12. Z. Hao, L. Liu, R. Zhou *et al*., "One-point and multi-line calibration method in laser-induced breakdown spectroscopy", Optics express, 26, **2018**.
13. H. Shakeel, S. Haq, G. Aisha *et al*., "Quantitative analysis of Al-Si alloy using calibration free laser induced breakdown spectroscopy (CF-LIBS)", Physics of Plasmas, 24, **2017**.
14. A.K. Myakalwar, S.K. Anubham, S.K. Paidi *et al*., "Real-time fingerprinting of structural isomers using laser induced breakdown spectroscopy", Analyst, 141, **2016**.
15. L. Radziemski, and D. Cremers, "A brief history of LIBS: from the concept of atoms to LIBS 2012", Spectrochimica Acta Part B: Atomic Spectroscopy, 87, **2013**.
16. J.L. Gottfried, F.C. De Lucia, C.A. Munson *et al*., "LIBS for detection of explosives residues: a review of recent advances, challenges, and future prospects", Analytical and bioanalytical chemistry, 395, **2009**.
17. R. Junjuri, A.K. Myakalwar, and M.K. Gundawar, "Standoff Detection of Explosives at 1 m using Laser Induced Breakdown Spectroscopy", Def. Sci. J., 67, **2017**.
18. J. Laserna, R.F. Reyes, R. González *et al*., "Study on the effect of beam propagation through atmospheric turbulence on standoff nanosecond LIBS measurements", Optics express, 17, **2009**.
19. A.K. Myakalwar, N. Spegazzini, C. Zhang *et al*., "Less is more: Avoiding the LIBS dimensionality curse through judicious feature selection for explosive detection", Scientific reports, *5*, **2015**.

20. A.K. Knight, N.L. Scherbarth, D.A. Cremers *et al.*, "Characterization of LIBS for Application to Space Exploration", Appl. Spectrosc., 54, **2000**.
21. S. Sharma, A. Misra, P. Lucey *et al.*, "Combined remote LIBS and Raman spectroscopy at 8.6 m of sulfur-containing minerals, and minerals coated with hematite or covered with basaltic dust", Spectrochimica Acta Part A: Molecular and Biomolecular Spectroscopy, 68, **2007**.
22. I. Gaona, P. Lucena, J. Moros *et al.*, "Evaluating the use of standoff LIBS in architectural heritage: surveying the Cathedral of Málaga", Journal of Analytical Atomic Spectrometry, 28, **2013**.
23. A. Giakoumaki, K. Melessanaki, and D. Anglos, "LIBS in archaeological science—applications and prospects", Analytical and bioanalytical chemistry, 387, **2007**.
24. V.K. Singh, and A.K. Rai, "Prospects for laser-induced breakdown spectroscopy for biomedical applications: a review", Lasers in medical science, 26, **2011**.
25. D. Thomas, S. Surendran, and N. Vasa, "Nanosecond laser induced breakdown spectroscopy for biofouling analysis and classification of fouling constituents", Spectrochimica Acta Part B: Atomic Spectroscopy, **2020**.
26. A. Sarkar, D. Alamelu, and S.K. Aggarwal, "Determination of trace constituents in thoria by laser induced breakdown spectrometry", Journal of Nuclear Materials, 384, **2009**.
27. D. Marcos-Martinez, J. Ayala, R. Izquierdo-Hornillos *et al.*, "Identification and discrimination of bacterial strains by LIBS and neural networks", Talanta, 84, **2011**.
28. M. Bonta, J.J. Gonzalez, C.D. Quarles *et al.*, "Elemental mapping of biological samples by the combined use of LIBS and LA-ICP-MS", Journal of Analytical Atomic Spectrometry, 31, **2016**.
29. J. El Haddad, M. Villot-Kadri, A. Ismaël *et al.*, "Artificial neural network for on-site quantitative analysis of soils using LIBS", Spectrochimica Acta Part B: Atomic Spectroscopy, 79-80, **2013**.
30. M.J.C. Pontes, J. Cortez, R.K.H. Galvão *et al.*, "Classification of Brazilian soils by using LIBS and variable selection in the wavelet domain", Analytica Chimica Acta, 642, **2009**.
31. M.M. El-Deftar, N. Speers, S. Eggins *et al.*, "Assessment and forensic application of laser-induced breakdown spectroscopy (LIBS) for the discrimination of Australian window glass", Forensic science international, 241, **2014**.
32. E. Rodriguez-Celis, I. Gornushkin, U. Heitmann *et al.*, "LIBS as a tool for discrimination of glass for forensic applications", Analytical and bioanalytical chemistry, 391, **2008**.
33. M.K. Gundawar, R. Junjuri, and A.K. Myakalwar, "Standoff Detection of Explosives at 1 m using Laser Induced Breakdown Spectroscopy", Defence Science Journal, 67, **2017**.
34. R. Junjuri, C. Zhang, I. Barman *et al.*, "Identification of post-consumer plastics using laser-induced breakdown spectroscopy", Polymer Testing, 76, **2019**.
35. R. Junjuri, and M.K.K. Gundawar, "Femtosecond laser induced breakdown spectroscopy studies for the identification of the plastics", Journal of Analytical Atomic Spectrometry, **2019**.
36. S. Almaviva, A. Palucci, V. Lazic *et al.*, "LIBS for the remote detection of explosives at level of fingerprints", Optical Sensing and Detection IV, International Society for Optics and Photonics, **2016**.
37. F.C. De Lucia, and J.L. Gottfried, "Classification of explosive residues on organic substrates using LIBS", Applied optics, 51, **2012**.38. J.S. Caygill, F. Davis, and S.P. Higson, "Current trends in explosive detection techniques", Talanta, 88, **2012**.
39. P.D. Barnett, N. Lamsal, and S.M. Angel, "Standoff Laser-Induced Breakdown Spectroscopy (LIBS) Using a Miniature Wide Field of View Spatial Heterodyne Spectrometer with Sub-Microsteradian Collection Optics", Appl. Spectrosc., 71, **2017**.
40. S. Wallin, A. Pettersson, H. Östmark *et al.*, "Laser-based standoff detection of explosives: a critical review", Anal. Bioanal. Chem., 395, **2009**.
41. R. Ahmed, and M. Baig, "A comparative study of enhanced emission in double pulse laser induced breakdown spectroscopy", Optics & Laser Technology, 65, **2015**.
42. J.L. Gottfried, F.C. De Lucia, C.A. Munson *et al.*, "Double-pulse standoff LIBS for versatile hazardous materials detection", Spectrochimica Acta Part B: Atomic Spectroscopy, 62, **2007**.

43. Q. Wang, G. Teng, C. Li *et al*., "Identification and classification of explosives using semi-supervised learning and LIBS", Journal of Hazardous Materials, **2019**.
44. J. Anzano, I. Gornushkin, B. Smith *et al*., "Laser-induced plasma spectroscopy for plastic identification", Polymer engineering & science, 40, **2000**.
45. S. Grégoire, M. Boudinet, F. Pelascini *et al*., "Laser-induced breakdown spectroscopy for polymer identification", Analytical and bioanalytical chemistry, 400, **2011**.
46. K. Liu, D. Tian, C. Li *et al*., "A review of laser-induced breakdown spectroscopy for plastic analysis", TrAC Trends in Analytical Chemistry, 110, **2019**.
47. V. Unnikrishnan, K. Choudhari, S.D. Kulkarni *et al*., "Analytical predictive capabilities of LIBS with PCA for plastic classification", RSC Advances, 3, **2013**.

TH-15. EXPERIMENTAL STUDIES AND PARAMETRIC INVESTIGATION ON LASER DIRECTED ENERGY DEPOSITION BASED ADDITIVE MANUFACTURING OF HASTELLOY-X THIN WALLS AND BULK STRUCTURE

.

Jinoop A N, Raja Ramanna Centre for Advanced Technology, Indore, Homi Bhabha National Institute, Mumbai, Email: anjinoop@gmail.com

1. Introduction

Additive Manufacturing (AM) is a "process of joining materials to make parts from 3D model data, usually layer upon layer, as opposed to subtractive manufacturing and formative manufacturing methodologies" [1]. As metals are most commonly used material in the industries, AM evolved to build metallic components by transforming itself from a process for "design validation and prototyping" to a process for building "near-net shaped components" [2]. Being the tool of power and precision, lasers are also used for these applications and laser based AM process is called Laser Additive Manufacturing (LAM). It provides freedom of shape design, material design, post-processing and logistics, which attracts its deployment in several sectors including aerospace, power, medical and automotive, with rising demand in aerospace [3] and power sector [4] to build high-performance components subjected to extreme duty conditions. These extreme duty conditions require the materials with high strength, oxidation resistance and corrosion resistance at elevated temperatures [5], for which nickel based superalloys are preferred choice. Hastelloy-X (Hast-X) is one of the nickel-based superalloys suitable for high-temperature applications due to the excellent blend of high-temperature strength, toughness and resistance to degradation in a corrosive or oxidizing environment. The application of Hast-X includes components for various advanced power generation cycles (like - supercritical cycles and concentrated solar power plants [6]), combustion zone components (such as transition ducts, combustor cans, spray bars and flame holders) in gas turbine engines [6], and intermediate heat exchanger for high temperature reactor applications [7]. Some of these applications use advanced designs and materials for improved performance, which cannot be built using conventional manufacturing processes due to inherent process limitations. These limitations motivated to take up an assignment in this direction and the present thesis is focused on investigation and deployment of the versatile Laser Directed Energy Deposition (LDED) based LAM technique to deposit defect free Hast-X for building thin-wall and bulk structures and subsequently investigate their behavior at different process and service conditions to build printed circuit heat exchanger.

2. Gap areas

The literature review indicates that only limited number of nickel-based superalloys are explored by LDED. The literature indicates that the material specific LDED processing strategies and parameters are essential for defect free deposition and the mechanical properties are a function of processing strategies, parameters and the resultant microstructure [8]. In case of Hast-X, the major challenge in the processing is its susceptibility to hot cracking or solidification cracking. The Solidification Cracking Temperature Range (SCTR) of Hast-X is 190 °C, which

indicates that the material has moderate to high crack susceptibility [9]. Based on the extensive literature survey, the following gap areas are identified:
a) There is limited published literature on LDED of Hastelloy grade materials, like - Hast-X, showing a knowledge gap especially on the effect of process parameters on the track geometry and track quality.
b) LDED built thin-wall structures (multi-layer deposition) are basic blocks for building complex engineering components and thus, it is necessary to understand the characteristics of thin walls. There is a lack of comprehensive studies on the effect of process parameters and interlayer delay conditions on the geometry, microstructure and mechanical properties of LDED built nickel-based superalloy wall structures.
c) Bulk structures (multiple overlapped tracks and multi-layer deposition) are necessary to build complex shaped engineering components with higher build rate. There is no literature available on the microstructure and mechanical properties of LDED built Hast-X bulk structures.
d) LDED built bulk structures are generally subjected to several in-situ and ex-situ treatments for defect rectification and tailoring its properties [8]. In-situ Sequential Layer-by-layer Laser Remelting (SLLR) can be deployed for reducing the porosity, grain refinement and improving surface finish of LDED built components. Hast-X, being a solid solution strengthened superalloy, requires probing into the microstructural and mechanical characteristics of LDED built Hast-X in solution treated condition. There is no study available in open literature on the effect of in-situ SLLR and solution treatment on the behavior of LDED built Hast-X components.
e) Literature confirms the suitability of Hast-X for building heat exchangers [7]. However, there is no study available in public domain on the development of Hast-X heat exchanger using LDED.

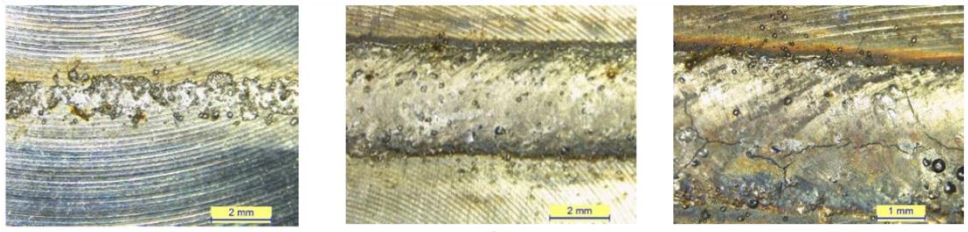

Figure 1: Single track morphology (a) Dis-continuous (b) Continuous (c) Cracked

Summary of Research Work

3.1 Experimental Analysis and Modelling of LDED built Hast-X Single Tracks: The geometry of LDED built Hast-X single tracks are analyzed using analytical modelling and verified by experimental analysis. In general, the geometry of the single track is a function of the LDED process parameters and the major LDED process parameters governing the single track characteristics are laser power, scan speed and powder feed rate at a particular laser beam diameter. The analytical modelling is an extension of Rosenthal point source heat equation with a Gaussian laser source by considering multiple point heat sources to predict the track width and track height. Track width is predicted by estimating the melt-pool limited to the substrate melting point by calculating the temperature distribution, while track height is estimated by using a combination of excess enthalpy and mass-balance approach. Experimental analysis shows that the track width and track height increases with an increase in laser power, reduction in scan speed and increase in powder feed rate. However, it is observed that the track width is highly influenced by the laser power, while the effect of powder feed rate is more significant on track height. Comparisons between experimental and modelling results show a good

agreement. Investigations on the process window identification show that deposits are irregular at Laser Energy
per unit Powder Feed (LEPF) of 4.5 kJ/g and 7.2 kJ/g, while cracked deposits are observed at higher LEPF of 19.2 kJ/g. Uniform deposits without cracks are observed for moderate LEPF in the range of 8.25 kJ/g to 13.2 kJ/g at all scan speeds (0.3 m/min to 0.7 m/min). When the LEPF is lower than 4.5 kJ/g, the requisite amount of energy for continuous deposition of material is not available, which yielded in irregular deposition (refer Figure 1). The cracking at higher LEPF can be due to a combination of higher thermal stresses in the solidifying deposit caused by large thermal strain and elemental segregations. Elemental mapping of the crack confirms the segregation of carbon and silicon along the length of the crack. Porosity analysis of the tracks performed using area fraction technique show that the area fraction density of the continuous tracks is found to be greater than 99.5%. Further, a combination of the build rate analysis and porosity analysis is used to select process parameter combination for multiple overlapped track deposition. The multiple overlapped track depositions are analyzed and observed to be defect free in the macro and micro scale.

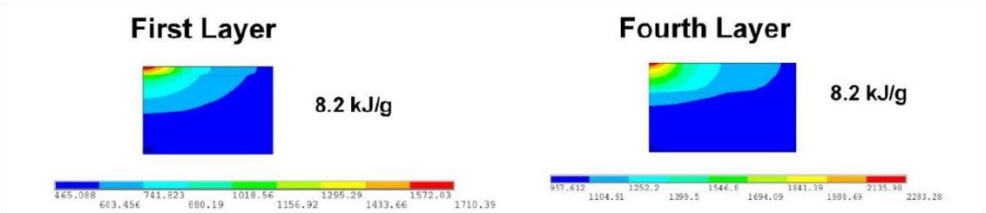

Figure 2: Effect of layer number on the temperature profile

Effect of Laser Energy per unit Powder Feed and interlayer delay period on LDED built Hast-X thin walls: A detailed investigation is carried out to understand the effect of LEPF and interlayer delay on the wall geometry and Hast-X material property. Finite element based numerical simulation tool is deployed to understand the experimental results. For the walls built at different LEPF, it is observed that the variation in wall height increases with an increase in LEPF due to relatively higher melt-pool flow at higher LEPF, while the variation in wall width decreases with an increase in LEPF due to reduction in necking phenomenon near the base of the thin wall. The geometry analysis along the build direction shows the maximum deviation for 8.2 kJ/g at lower layers primarily due to necking and presence of partially melted powders, while the maximum deviation for 13.2 kJ/g at the top layer can be due to excessive melt-pool flow. Cellular/ dendritic growth at all conditions during microstructural analysis and a marginal reduction in mechanical properties, i.e., average microhardness (~ 10 %), yield strength (~ 3.7 %) and ultimate tensile strength (~ 4 %) are observed with an increase in LEPF due to reduction in the cooling rate. Numerical simulation shows that the preheat temperature on the previously built layers increases with an increase in LEPF and number of layers (refer Figure 2). In case of walls built with different interlayer delay, it is observed that the average wall height is slightly higher for walls built with higher interlayer delay. This is attributed to reduction in preheat temperature (reaching closer to initial temperature) and relatively lower outward flow of the melt-pool with an increase in interlayer delay. The width and variation in wall width decrease with an increase in interlayer delay. Microstructural studies show the presence of cellular and dendritic growth at all conditions with relatively fine grain structure at higher interlayer delay period due to less heat accumulation. The increased interlayer delay yields higher cooling rate and leads to the reduction in elemental segregation along with improved mechanical properties.

3.3 Elucidating the microstructural and mechanical behavior of LDED built bulk structures: The as-built samples deposited at identified parameters presented in chapter 4 are analyzed for macro-defects. The as-built structures are observed to be defect free in the macro-scale.

However, porosity analysis using area fraction technique revealed a relative density of ~ 99.5% due to circular and irregular shaped micro-pores generated as
gas and lack of fusion porosity, respectively. Optical microscopy and Scanning Electron Microscopy shows that the microstructure is a mix of fine cellular and dendritic growth and the presence of FCC matrix is revealed during X-ray diffraction studies. The as-built samples revealed random grain orientation with slightly preferred texture along the <100> plane. The elemental mapping revealed the presence of elemental segregations of C, Mo, and Si during the non-equilibrium solidification in LDED. In addition, the presence of Mo rich carbides is also detected, which can be due to the continuous thermal cycling during LDED leading to higher bulk temperature, remelting and carbide formation. Residual stress measurement reveals predominantly tensile stress on the deposited surface with a maximum value of 252 MPa. The measured average micro-hardness is 239 HV1.96N, which is higher than hardness of conventional counterparts (180 HV) [6]. The mechanical properties are analyzed at the room temperature and elevated temperature (up to 600 °C) using Automated Ball Indentation (ABI). It is revealed that the yield strength of LDED built Hast-X structures are higher than the conventionally built Hast-X at room temperature and elevated temperature. The higher strength values of LDED built structures can be primarily due to the higher cooling rate resulting in finer grain structure and higher dislocation density in LDED as compared to conventional counterparts. It is also observed that the mechanical strength of bulk structures is higher than that of wall structures built at the same process parameters due to higher cooling rates in bulk structures as compared to that in thin walls.

3.4 Understanding the effect of In-situ Sequential Layer by Layer Re-melting (SLLR) and post heat-treatment of Hast-X bulk structures: SLLR, a process involving laser remelting after LDED of each layer, is used to improve the surface and bulk properties of LDED components. SLLR of bulk structures shows a significant reduction in surface roughness and porosity. The relative density increased from 99.5% in as-built samples to 99.99% after SLLR and average surface roughness reduced by 71.4% after SLLR. Microstructure is found to be relatively fine after SLLR without preferential growth along <100> direction as opposed to that without SLLR due to thermal effect. Mo, Si and C segregations and presence of Mo rich carbides are present in LDED and SLLR samples. The finer dendritic microstructures in SLLR samples led to an increase in the microhardness by 12% and yield strength by 7 % along the build direction as compared to samples without SLLR.

Further, the microstructure and elevated temperature mechanical properties of Hast-X bulk structures built using LDED is investigated in as-built and post heat-treated conditions. Hast-X, being a solid solution strengthened alloy, solution treatment is carried out at 1177 °C followed by water quenching [6]. Microscopic analysis shows the presence of recrystallized and coarsened equiaxed grains in solution treated samples as opposed to fine cellular and dendritic growth in as-built samples. The solution treated samples revealed random grain orientation as opposed to slightly preferred texture along the <100> plane in the as-built samples. Further, the elemental segregation of Mo, Si and C and precipitation of Mo-rich carbides revealed in the as-built samples are not observed in the solution treated samples. X-ray diffraction studies reveal the presence of nickel γ-matrix and a peak shift is observed after solution treatment, primarily due to change in surface residual stress. The average micro-hardness changed from 239 HV1.96N to 208 HV1.96N after solution treatment, which is similar to microhardness of conventional Hast-X. ABI tests are used to evaluate the mechanical properties in as-built and solution treated conditions from ambient temperature to 873 K. It is observed that the strength and ABI hardness decreases with an increase in test temperature. The yield strength of solution treated sample is similar to that of conventionally processed wrought Hast-X taken from literature at all test temperatures.

3.5 Process methodology for LDED of Printed Circuit Heat Exchanger (PCHE) using wall and bulk structures: Overhang walls are deposited using LDED to understand the effect on the angle and uniformity of deposition by varying the process parameters such as percentage

overlap (x-shift) and a fraction of layer height (z-increment). It is observed that for all other process parameters kept constant, the maximum x-shift that can be deployed for fabricating overhang walls without failure is 15%. This may be due to the dominance of gravitational force over surface and viscous forces in overhang portion of the wall. The angle made by the wall with the horizontal plane decreases with increased value of x-shift for the same z-increment. It can also be observed that the angle made by the walls reduces as z-increment decreases. LEPF of 10 kJ/g is used for wall deposition and 12 kJ/g is used for bulk deposition. Remelting of the bulk deposition is also carried out to control surface quality and density. Figure 3a presents one of the typical channels built using LDED and Figure 3b presents the photographic view of prototype PCHE of size 200 mm x 200 mm x 170 mm built using LDED.

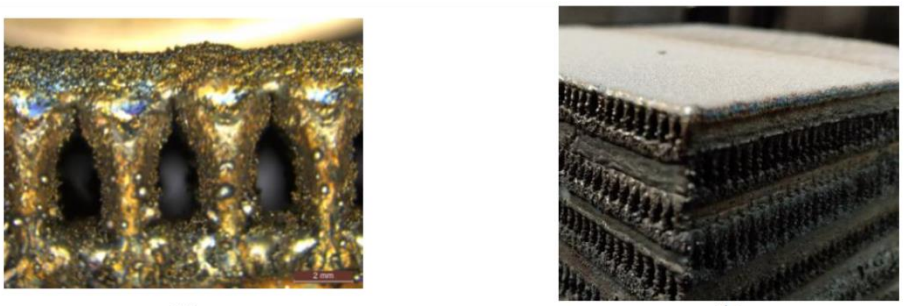

(a) (b)

Figure 3: Photographic view of (a) Channels (b) Prototype PCHE

References

1. International Organization for Standardization – American Society for Testing and Materials International, ISO/ASTM52900:2015: Additive Manufacturing. General principles - Terminology, 2015.

2. C.P. Paul, P. Bhargava, A. Kumar, A. K. Pathak, L. M. Kukreja, Laser Rapid Manufacturing: Technology, Applications, Modeling and Future Prospects. J. Paulo Davim, editor. Lasers in Manufacturing, UK: ISTE-Wiley; 2012, pp.1-60.

3. M. Brandt, Laser Additive Manufacturing: Materials, Design, Technologies, and Applications, 1st ed., Woodhead Publishing, Cambridge, 2016.

4. M. Brandt, S.Sun, N.Alam, P. Bendeich, A. Bishop, Int. Heat Treat. Surf. Eng. 3(3), 105–114 (2009).

5. M.Perrut, P. Caron, M. Thomas, A. Couret., Comptes Rendus Physique 19 (8), 657 – 661(2018).

6. Haynes International, http://www.haynesintl.com/alloys/alloy-portfolio_/High-temperature-Alloys/HASTELLOY-X-alloy/HASTELLOY-X-principal-features.aspx (accessed 14 November 2021)

7. H. E. McCoy, J. P. Strizak, J. F. King, Nucl. Technol. 66(1), 161-174 (1984).

8. W. J. Sames, F. A. List, S. Pannala, R. R. Dehoff & S. S. Babu, Int. Mater. Rev., 61, 315-360 (2016).

9. J.N. DuPont, J.C. Lippold, S. D. Kiser, Welding Metallurgy and Weldability of Nickel-Base Alloys, Wiley, Hoboken, New Jersey, 2009.

LIST OF EXHIBITORS

Sr. No	Company	Place
1	Ms Anatech Instruments Pvt. Ltd.,	Mumbai
2	Ms Applied Optical Technologies Pvt. Ltd.,	Ambernath
3	Ms ATOS	Bangaluru
4	Ms D B Solutions Ms New	Mumbai
5	Ms Dyanotech Instruements	Mumbai
6	Ms Holmarc Optomechtronics Pvt. Ltd.	Cochin
7	Ms Infrared Optics	Gurugram
8.	Ms Laser Science (I) Pvt. Ltd.,	Navi Mumbai
9.	Ms Light Guide Optics	Indore
10.	Ms New Age Instruments and Materails Pvt. Ltd.	Gurugram
11.	Ms Photonics Marketing Companey	Mumbai
12.	Ms SIMCO Globle Technologies Systems Ltd.,	New Delhi
13.	Ms Specilise Instruments	Mumbai
14.	Ms Tech Éclair Scientific Pvt. Ltd,	Cochin

AUTHOR INDEX

ATOS

ATOSCOPE

Sona sCMOS
Large Format – 95% Quantum Efficiency – Cooled to -45^{0}C

ANDOR

Kymera Multimodal Spectroscopy Platform - Adaptive Focus – True Res – Quad Grating Turret - µManager

Sacher Lasertechnik

Tunable Diode Lasers – Littrow & Littman
External & Vertical Cavity Surface Emitting
Tera Hertz & Quantum Cascade Lasers

FLIR

Cooled & Uncooled IR cameras
Portable and fixed cameras

BENTHAM

Solar cell QE measurement, photobiological safety, light/display characterisation & spectroradiometers

specim
SPECTRAL IMAGING

Hyperspectral Imaging cameras for field, lab and airborne applications

OXFORD INSTRUMENTS

Flow Cryostats for 3K and 77K measurements with ultra-low vibration system. Cryogen free cryostats for 4K measurements.

aspectimaging

Compact MRI and NMR systems, 1m X 1m Footprint, Preclinical and clinical imaging.

ATOS Instruments Marketing Services

ATOSCOPE Instruments Pvt. Ltd.

www.atosindia.com

atos@atosindia.com

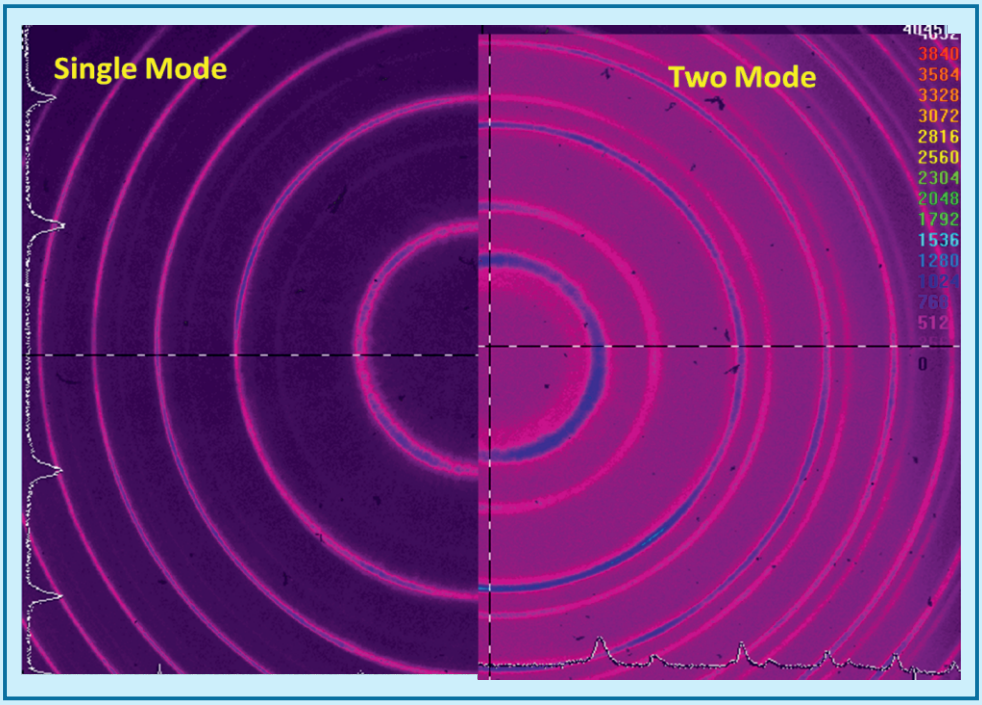

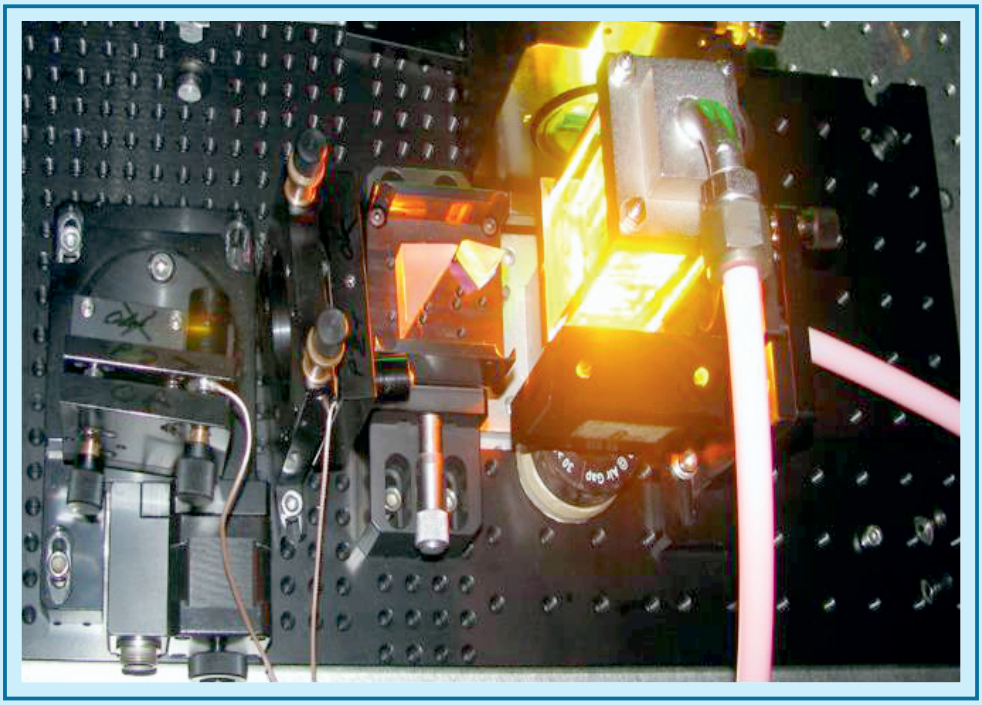

आज़ादी का अमृत महोत्सव